US 20250262167A1

(19) United States
(12) Patent Application Publication
Chen et al.
(10) Pub. No.: US 2025/0262167 A1
(43) Pub. Date: Aug. 21, 2025

(54) **COMPOUNDS, TARGETS AND PATHWAYS FOR MACROPHAGE MODULATION**

(71) Applicant: **Massachusetts Institute of Technology**, Cambridge, MA (US)

(72) Inventors: **Jianzhu Chen**, Lexington, MA (US); **Guangan Hu**, Westwood, MA (US)

(21) Appl. No.: **19/035,427**

(22) Filed: **Jan. 23, 2025**

Related U.S. Application Data

(62) Division of application No. 17/381,857, filed on Jul. 21, 2021, now abandoned.

(60) Provisional application No. 63/080,988, filed on Sep. 21, 2020.

Publication Classification

(51) **Int. Cl.**
A61K 31/03 (2006.01)
G01N 33/50 (2006.01)

(52) **U.S. Cl.**
CPC ***A61K 31/03*** (2013.01); ***G01N 33/5026*** (2013.01)

(57) **ABSTRACT**

Disclosed are methods of modulating macrophage activation to treat various diseases, such as cancer, fibrosis, infectious diseases, inflammatory diseases, metabolic diseases, or autoimmune diseases. Also disclosed are methods of identifying compounds useful for modulating macrophage activation as means to treat cancer, fibrosis, infectious diseases, inflammatory diseases, metabolic diseases, or autoimmune diseases.

Specification includes a Sequence Listing.

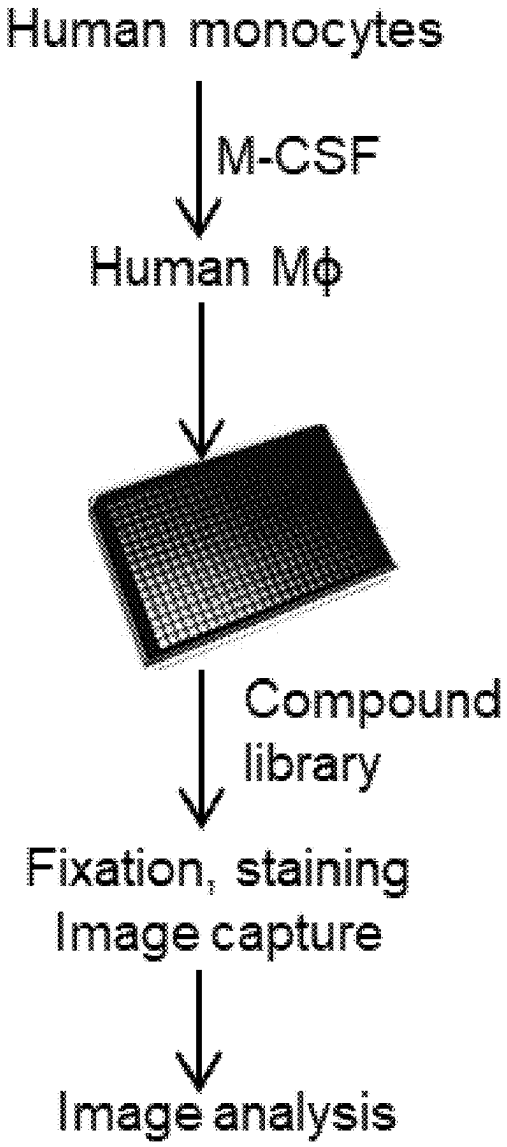

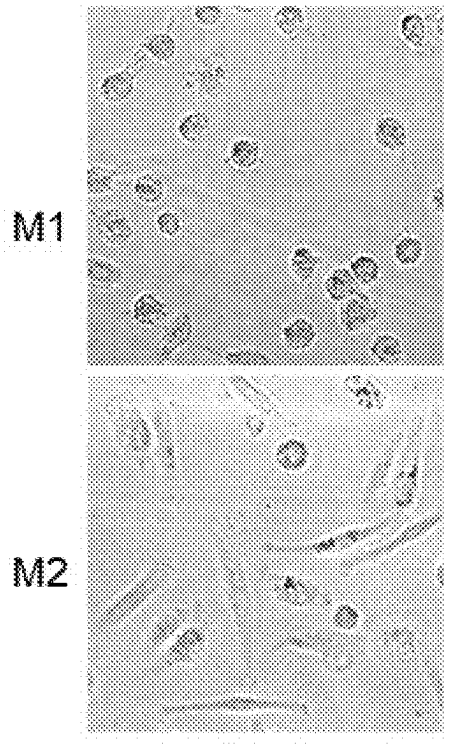

Figure 1A

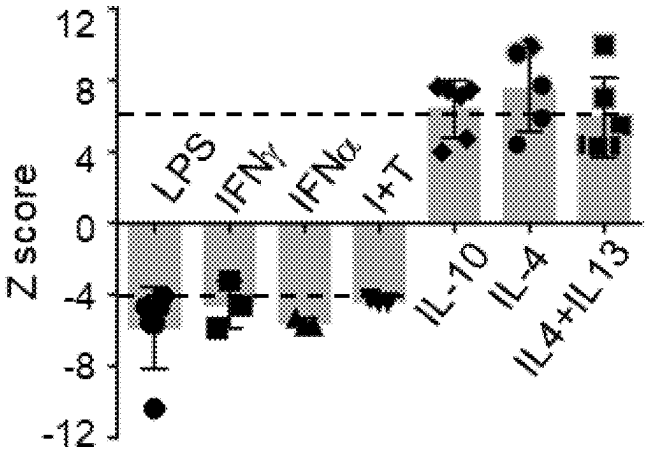

Figure 1B

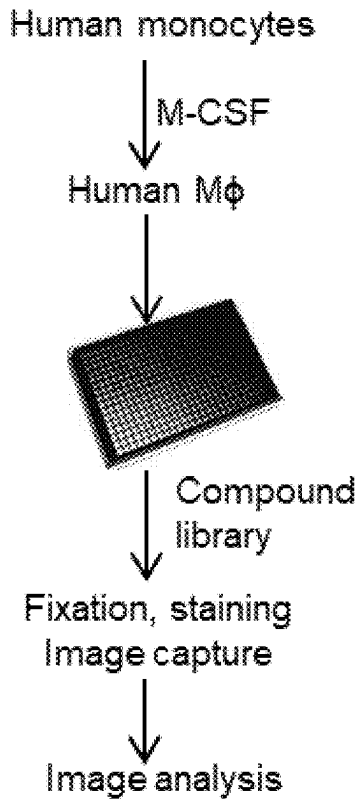

Figure 1C

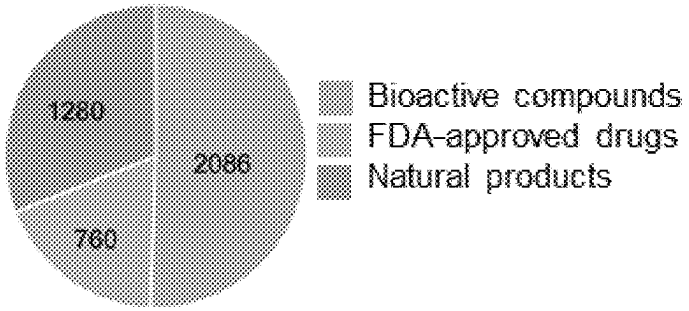

Figure 1D

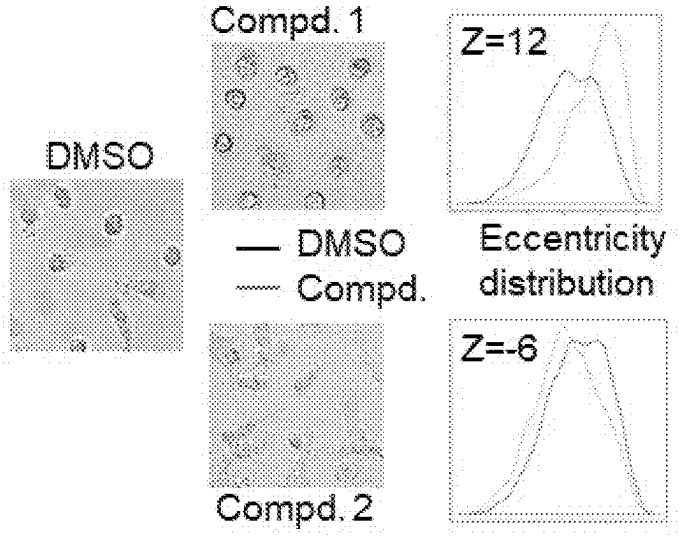

Figure 1E

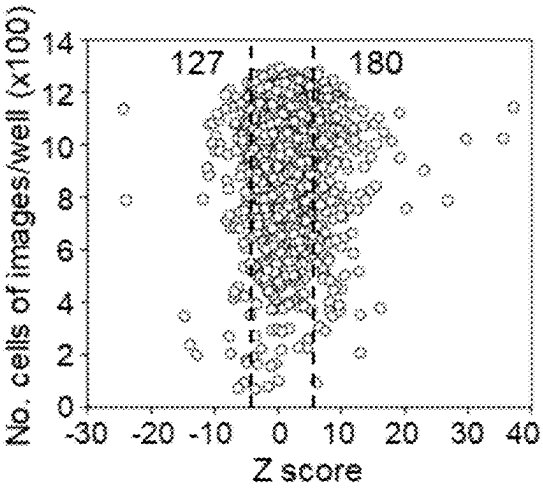

Figure 1F

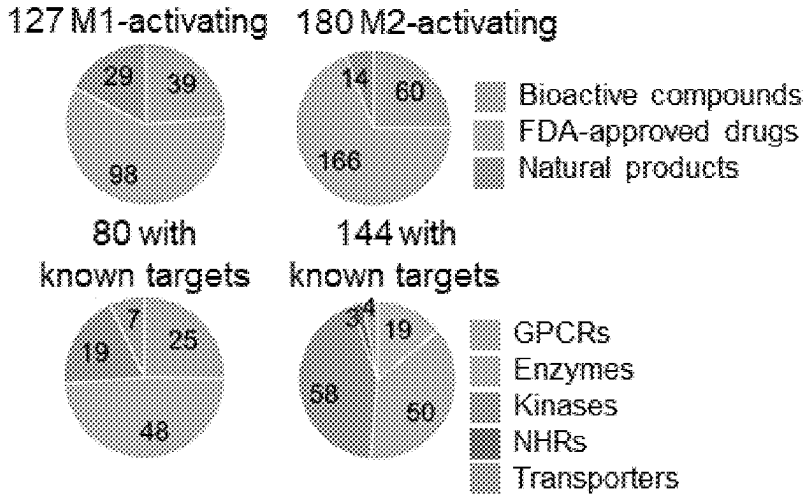

Figure 1G

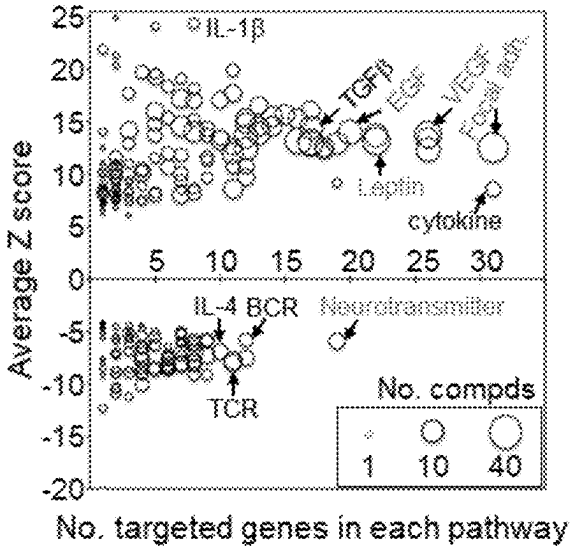

Figure 1H

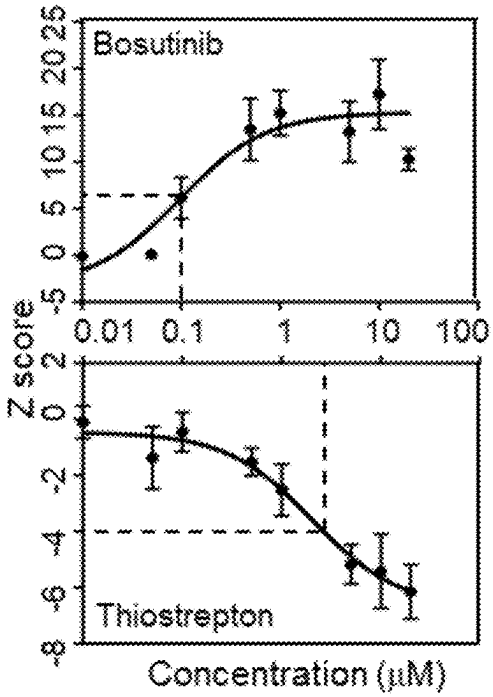

Figure 2A

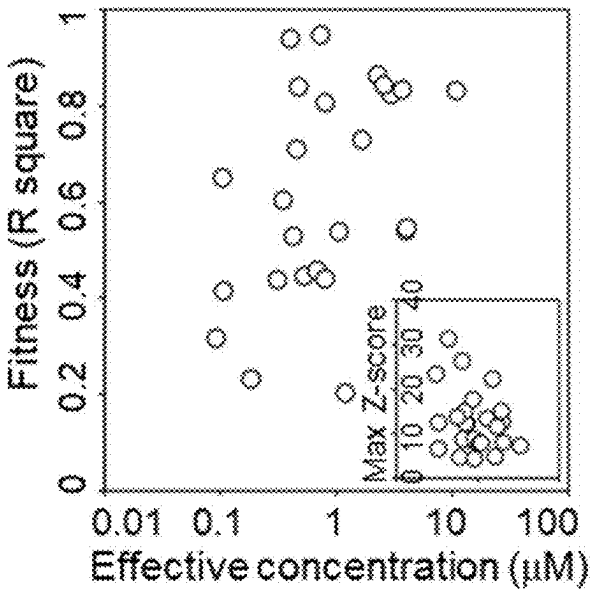

Figure 2B

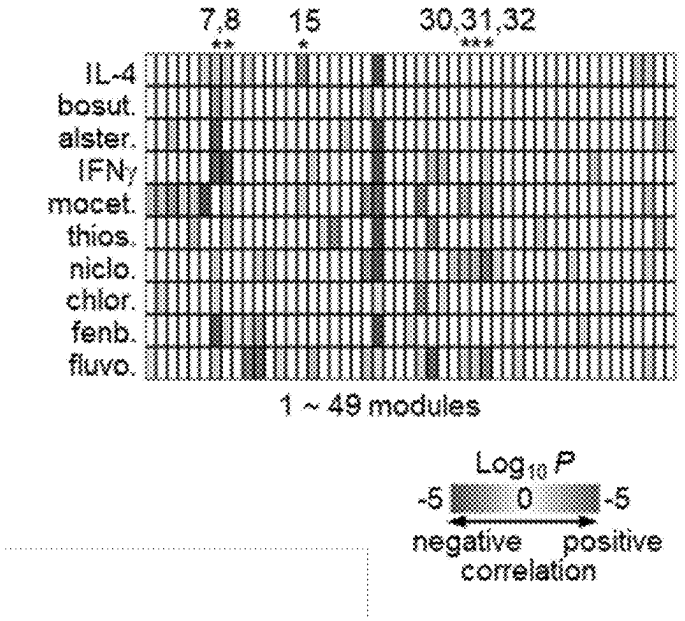
7,8
15
30,31,32
IL-4
bosut.
alster.
IFNγ
macet.
thios.
niclo.
chlor.
fenb.
fluvo.
1 ~ 49 modules
Log10 P
-5
0
-5
negative
positive
correlation

Figure 2C

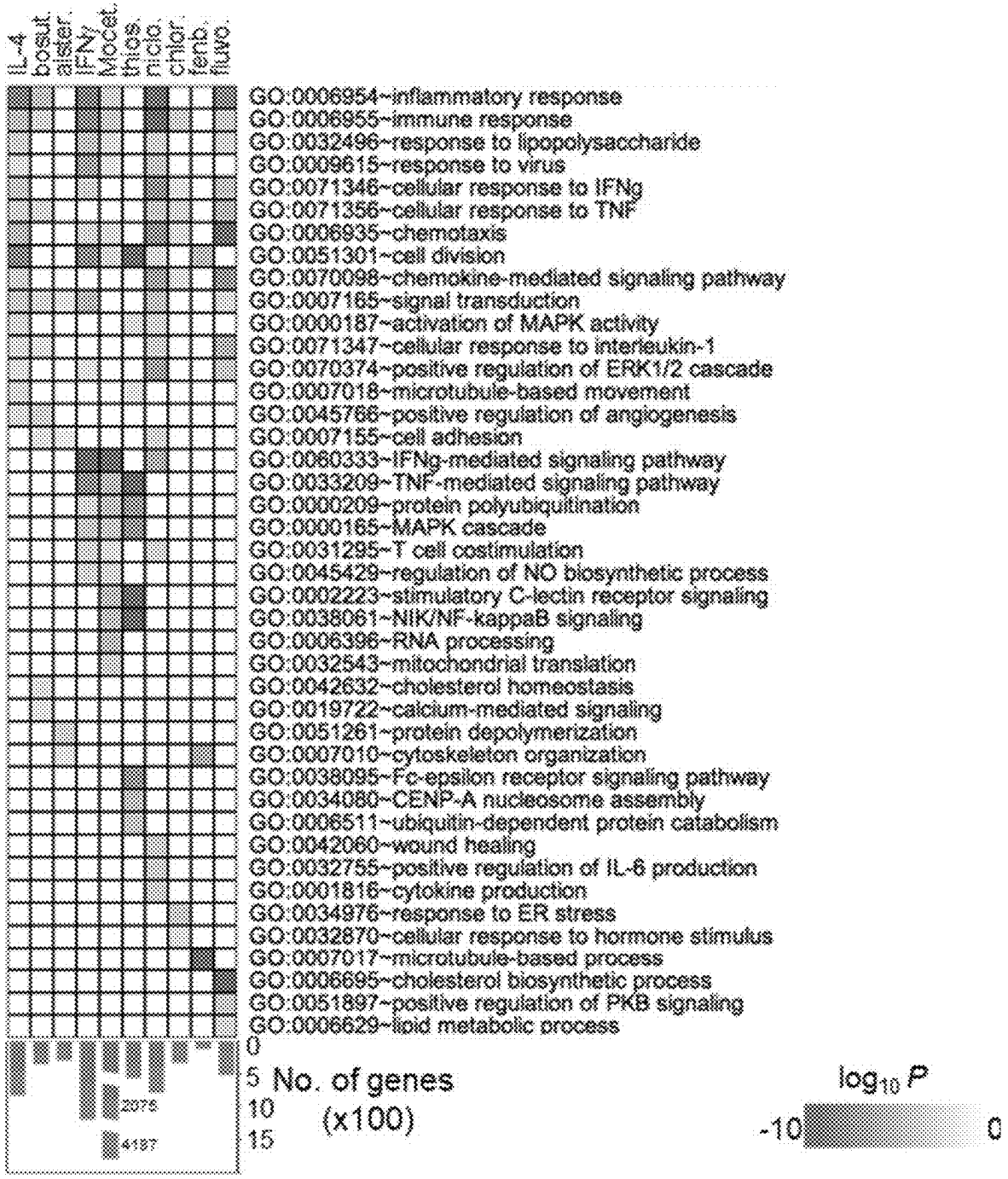
IL-4
bosut.
alster.
IFNγ
Mocet.
thios.
nicto.
chlor.
fenb.
fluvo.
GO:0006954~inflammatory response
GO:0006955~immune response
GO:0032496~response to lipopolysaccharide
GO:0009615~response to virus
GO:0071346~cellular response to IFNg
GO:0071356~cellular response to TNF
GO:0006935~chemotaxis
GO:0051301~cell division
GO:0070098~chemokine-mediated signaling pathway
GO:0007165~signal transduction
GO:0000187~activation of MAPK activity
GO:0071347~cellular response to interleukin-1
GO:0070374~positive regulation of ERK1/2 cascade
GO:0007018~microtubule-based movement
GO:0045766~positive regulation of angiogenesis
GO:0007155~cell adhesion
GO:0060333~IFNg-mediated signaling pathway
GO:0033209~TNF-mediated signaling pathway
GO:0000209~protein polyubiquitination
GO:0000165~MAPK cascade
GO:0031295~T cell costimulation
GO:0045429~regulation of NO biosynthetic process
GO:0002223~stimulatory C-lectin receptor signaling
GO:0038061~NIK/NF-kappaB signaling
GO:0006396~RNA processing
GO:0032543~mitochondrial translation
GO:0042632~cholesterol homeostasis
GO:0019722~calcium-mediated signaling
GO:0051261~protein depolymerization
GO:0007010~cytoskeleton organization
GO:0038095~Fc-epsilon receptor signaling pathway
GO:0034080~CENP-A nucleosome assembly
GO:0006511~ubiquitin-dependent protein catabolism
GO:0042060~wound healing
GO:0032755~positive regulation of IL-6 production
GO:0001816~cytokine production
GO:0034976~response to ER stress
GO:0032870~cellular response to hormone stimulus
GO:0007017~microtubule-based process
GO:0006695~cholesterol biosynthetic process
GO:0051897~positive regulation of PKB signaling
GO:0006629~lipid metabolic process
0
5
10
15
No. of genes
(x100)
2075
4197
log10 P
-10
0

Figure 2D

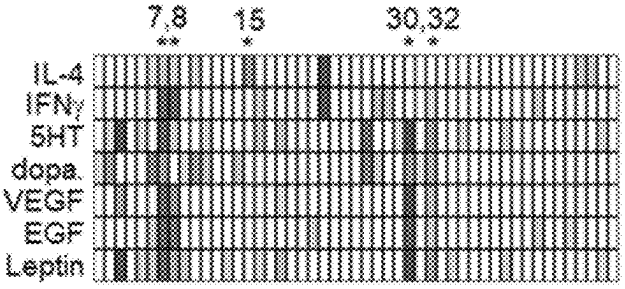

Figure 2E

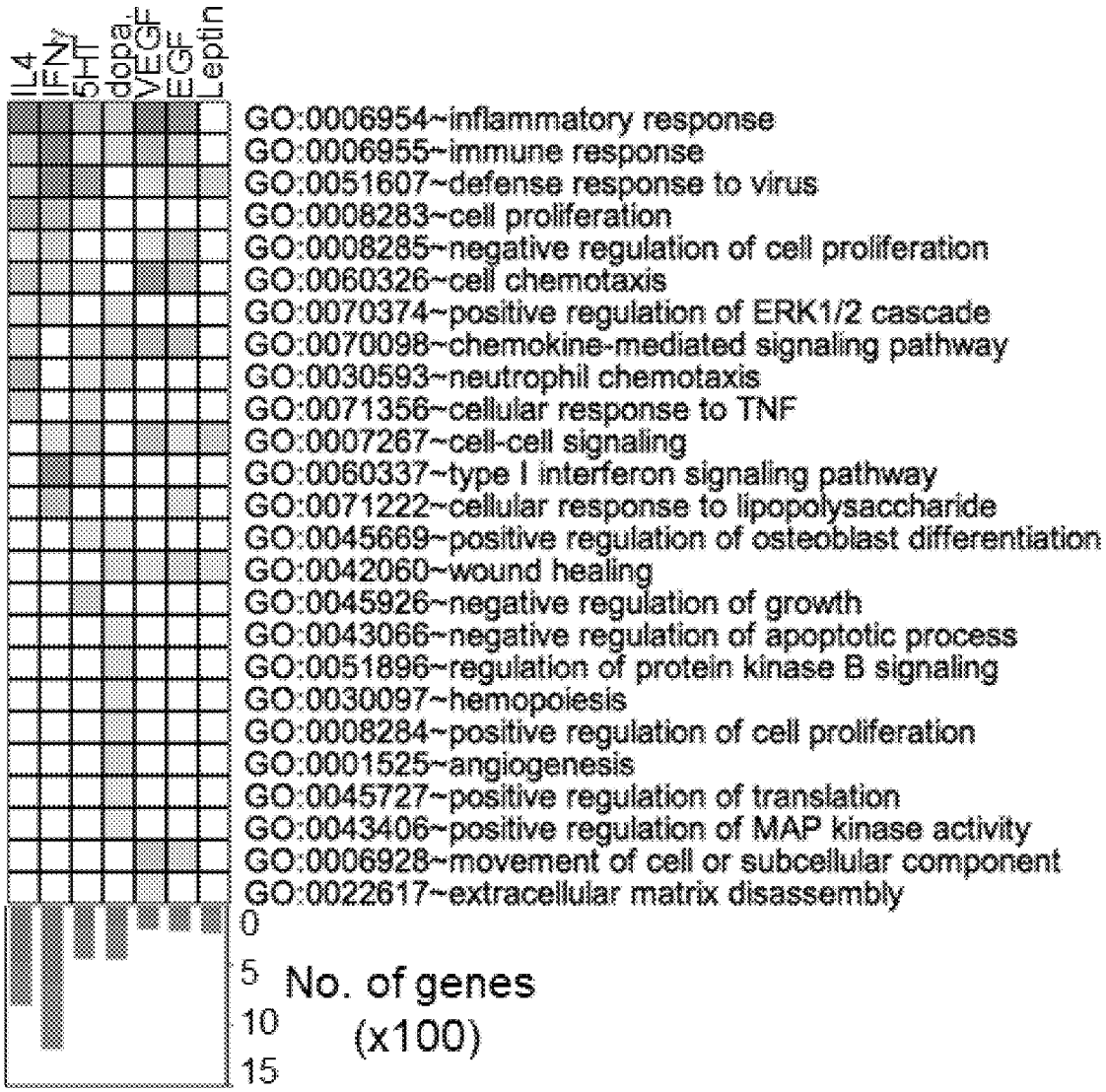

Figure 2F

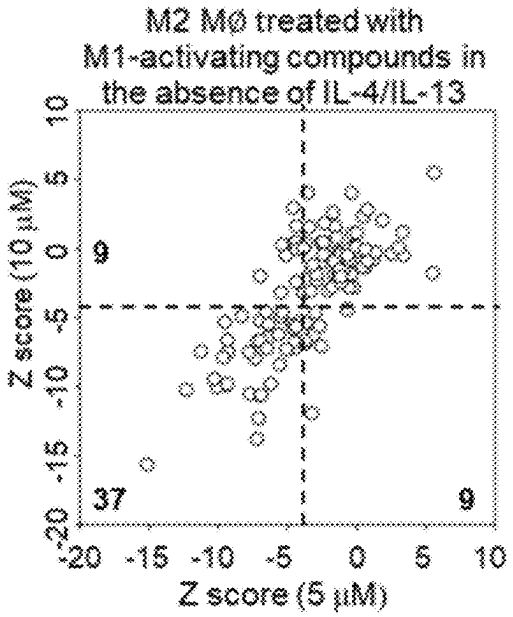

Figure 3A

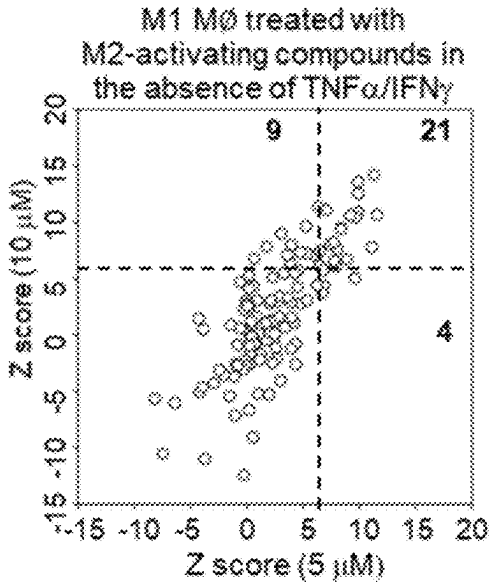

Figure 3B

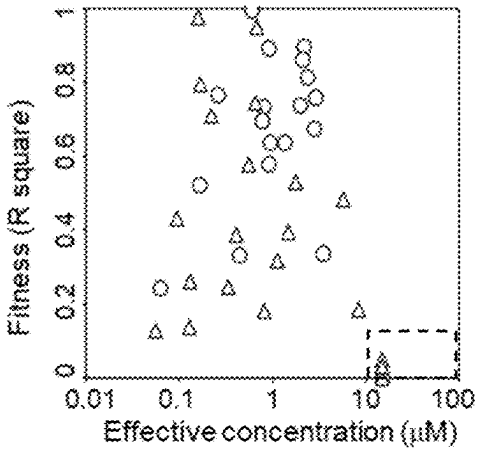

Figure 3C

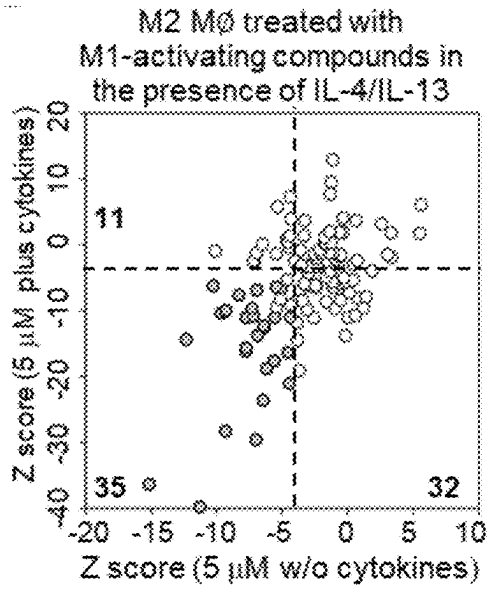

Figure 3D

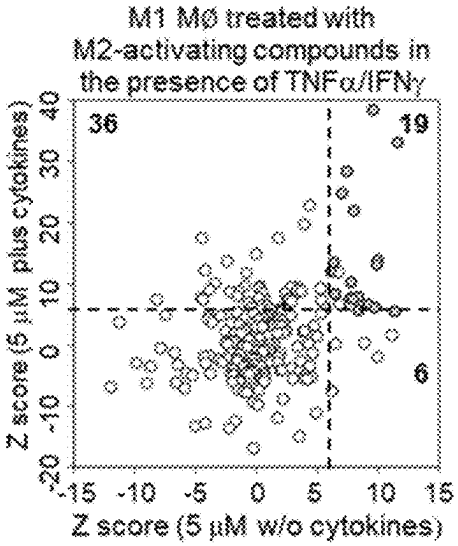
M1 MØ treated with
M2-activating compounds in
the presence of TNFα/IFNγ
36
19
6
6
Z score (5 μM plus cytokines)
40
30
20
10
0
-10
-20
-15
-10
-5
0
5
10
15
Z score (5 μM w/o cytokines)

Figure 3E

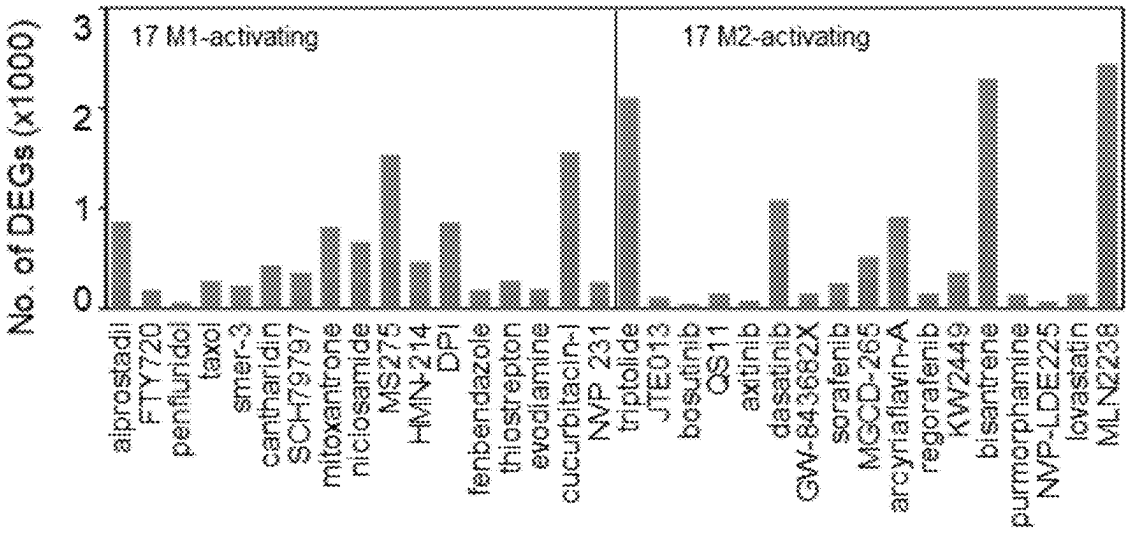

Figure 4A

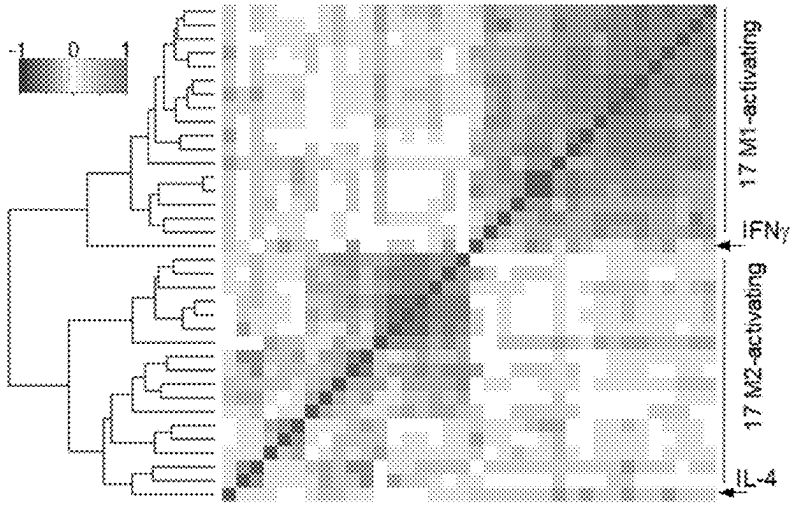

Figure 4B

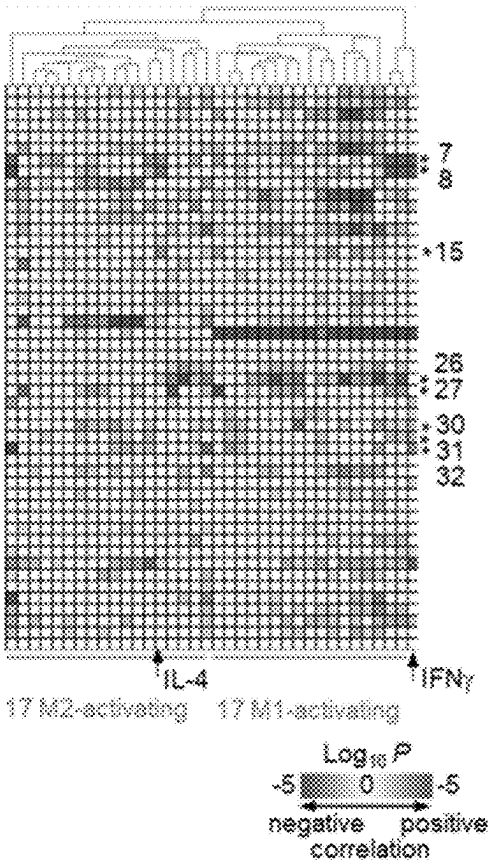
7
8
15
26
27
30
31
32
IL-4
IFNγ
17 M2-activating
17 M1-activating
Log10 P
-5
0
-5
negative
positive
correlation

Figure 4C

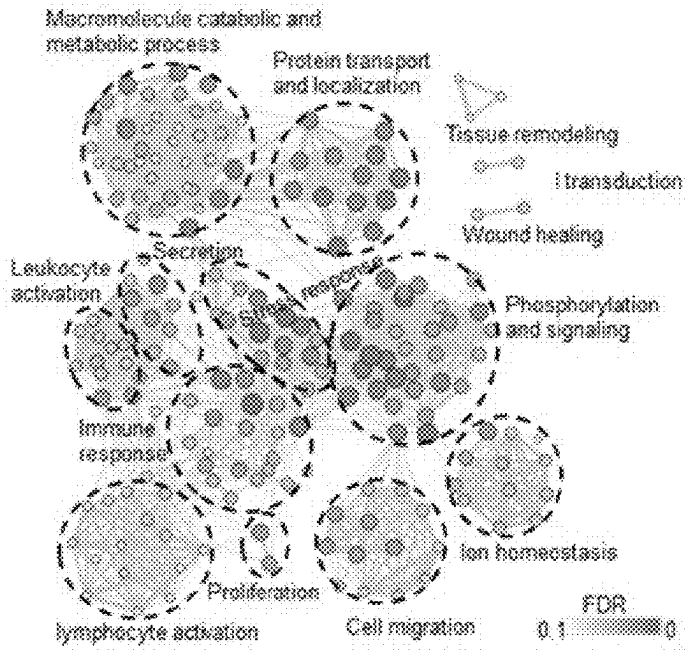

Figure 4D

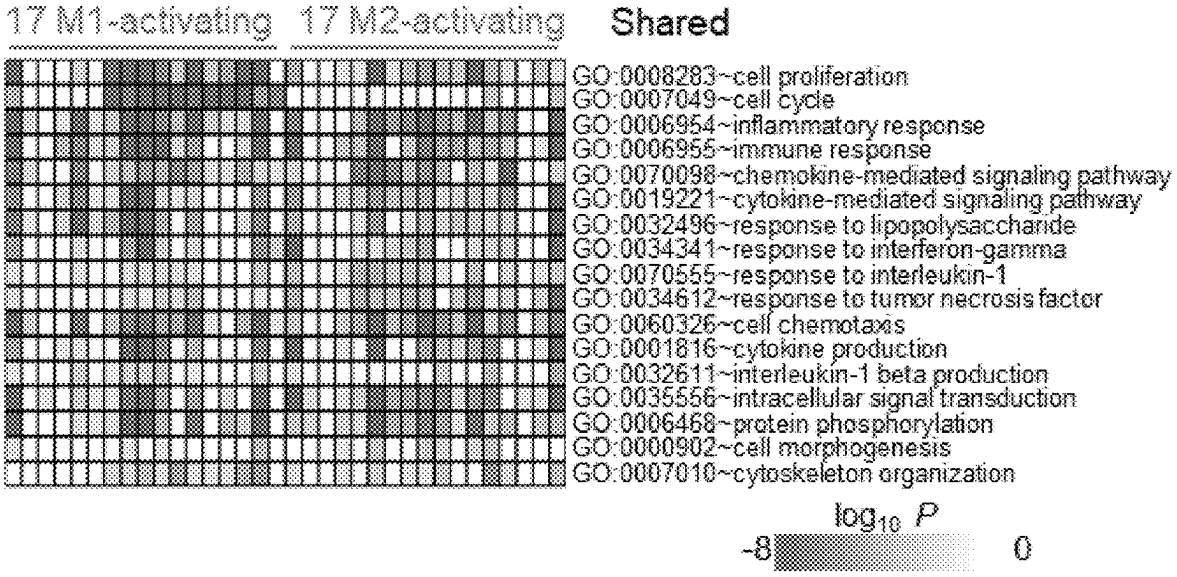

Figure 4E

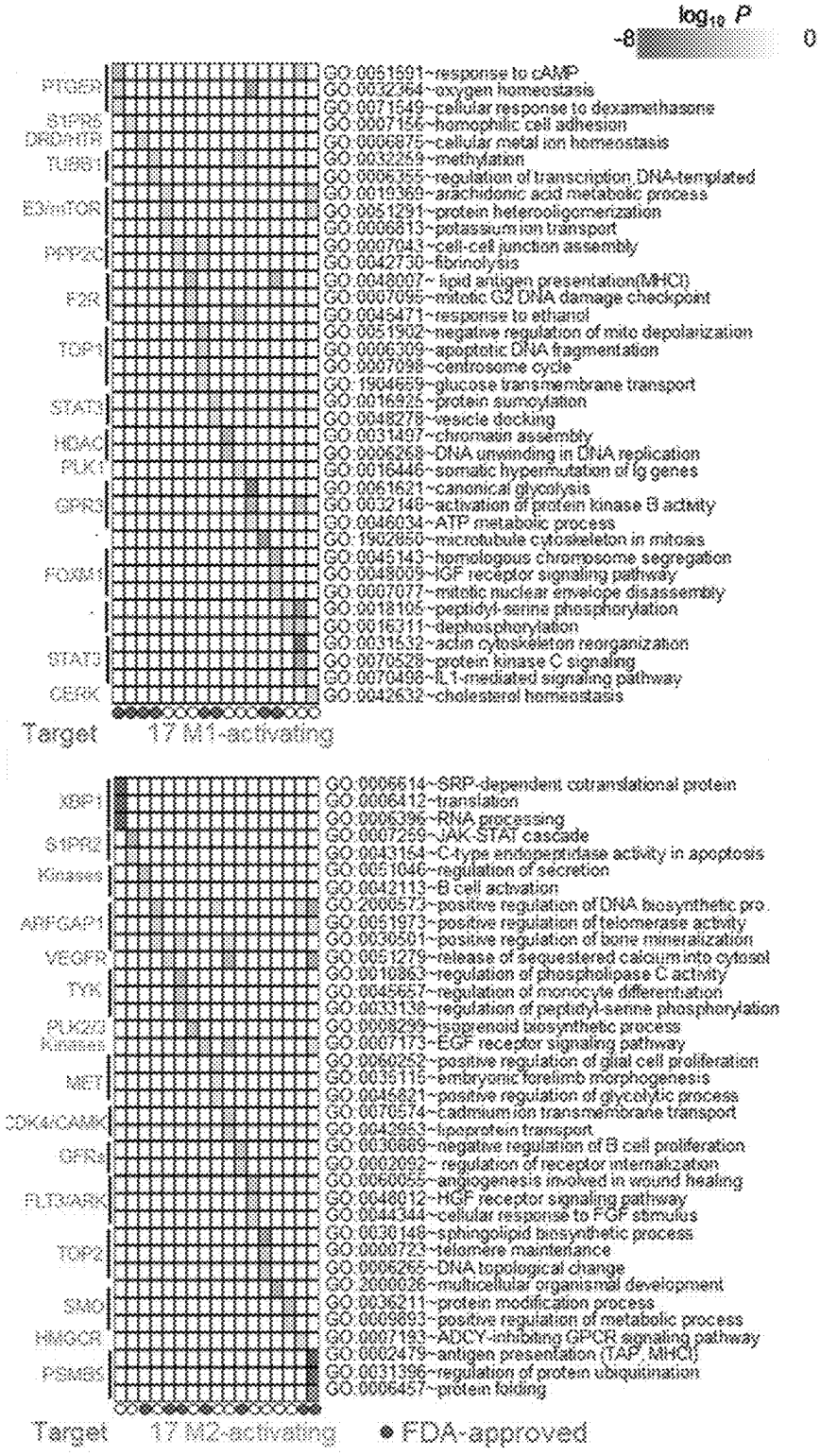
log10 P
-8
0
PTGER
S1PR5
DRD1/HTR
TUBB1
EDN/mTOR
PPP2C
F2R
TGF1
STAT3
NGAC
PLK1
GPR3
FOXM1
STAT3
CERK
GO:0051591~response to cAMP
GO:0032364~oxygen homeostasis
GO:0071549~cellular response to dexamethasone
GO:0007156~homophilic cell adhesion
GO:0006875~cellular metal ion homeostasis
GO:0032259~methylation
GO:0006355~regulation of transcription,DNA-templated
GO:0019369~arachidonic acid metabolic process
GO:0051291~protein heterooligomerization
GO:0006813~potassium ion transport
GO:0007043~cell-cell junction assembly
GO:0042730~fibrinolysis
GO:0048007~ lipid antigen presentation(MHCI)
GO:0007095~mitotic G2 DNA damage checkpoint
GO:0045471~response to ethanol
GO:0051902~negative regulation of mito depolarization
GO:0006309~apoptotic DNA fragmentation
GO:0007098~centrosome cycle
GO:1904659~glucose transmembrane transport
GO:0016925~protein sumoylation
GO:0048278~vesicle docking
GO:0031497~chromatin assembly
GO:0006268~DNA unwinding in DNA replication
GO:0016446~somatic hypermutation of Ig genes
GO:0061621~canonical glycolysis
GO:0032148~activation of protein kinase B activity
GO:0046034~ATP metabolic process
GO:1902850~microtubule cytoskeleton in mitosis
GO:0045143~homologous chromosome segregation
GO:0048009~IGF receptor signaling pathway
GO:0007077~mitotic nuclear envelope disassembly
GO:0018105~peptidyl-serine phosphorylation
GO:0016311~dephosphorylation
GO:0031532~actin cytoskeleton reorganization
GO:0070528~protein kinase C signaling
GO:0070498~IL1-mediated signaling pathway
GO:0042632~cholesterol homeostasis
Target
17 M1-activating
KSP1
S1PR2
Kinases
ARFGAP1
VEGFR
TYK
PLK2/3
Kinases
MET
CDK4/CAMK
GFR4
PLT3/ARK
TGF2
SMO
HMGCR
PSMB5
GO:0006614~SRP-dependent cotranslational protein
GO:0006412~translation
GO:0006396~RNA processing
GO:0007259~JAK-STAT cascade
GO:0043154~C-type endopeptidase activity in apoptosis
GO:0051046~regulation of secretion
GO:0042113~B cell activation
GO:2000573~positive regulation of DNA biosynthetic pro.
GO:0051973~positive regulation of telomerase activity
GO:0030501~positive regulation of bone mineralization
GO:0051279~release of sequestered calcium into cytosol
GO:0010863~regulation of phospholipase C activity
GO:0045657~regulation of monocyte differentiation
GO:0033138~regulation of peptidyl-serine phosphorylation
GO:0008299~isoprenoid biosynthetic process
GO:0007173~EGF receptor signaling pathway
GO:0060252~positive regulation of glial cell proliferation
GO:0035115~embryonic forelimb morphogenesis
GO:0046821~positive regulation of glycolytic process
GO:0070574~cadmium ion transmembrane transport
GO:0042953~lipoprotein transport
GO:0030889~negative regulation of B cell proliferation
GO:0002092~ regulation of receptor internalization
GO:0060055~angiogenesis involved in wound healing
GO:0048012~HGF receptor signaling pathway
GO:0044344~cellular response to FGF stimulus
GO:0030149~sphingolipid biosynthetic process
GO:0000723~telomere maintenance
GO:0006265~DNA topological change
GO:2000026~multicellular organismal development
GO:0036211~protein modification process
GO:0009893~positive regulation of metabolic process
GO:0007193~ADCY-inhibiting GPCR signaling pathway
GO:0002479~antigen presentation (TAP, MHCI)
GO:0031396~regulation of protein ubiquitination
GO:0006457~protein folding
Target
17 M2-activating
FDA-approved

Figure 4F

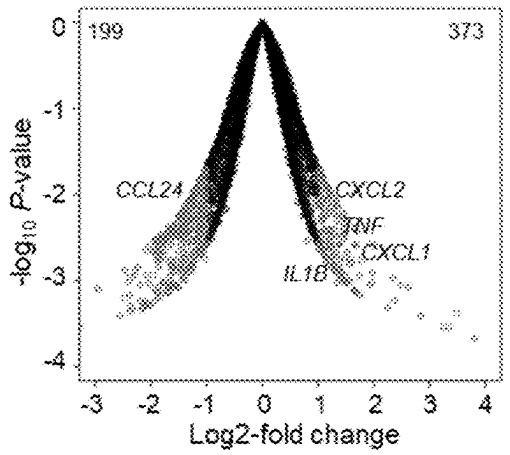

Figure 5A

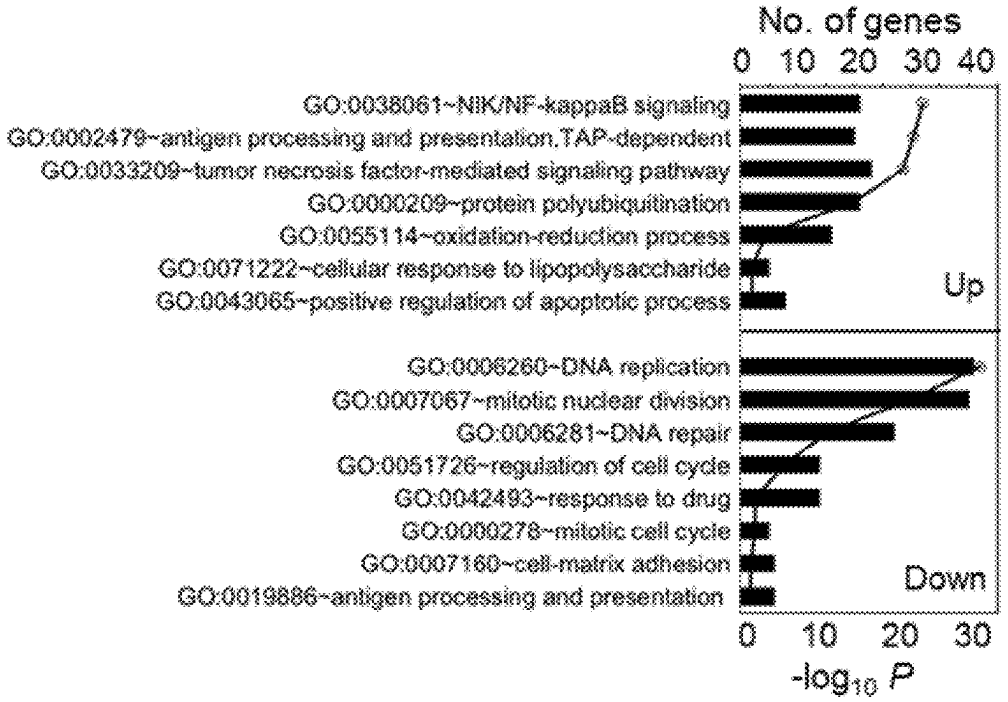

Figure 5B

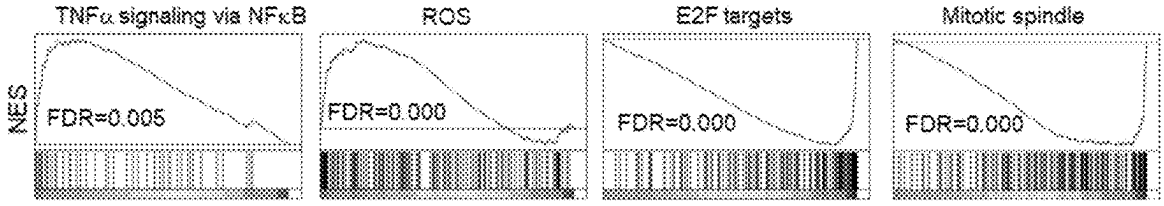

Figure 5C

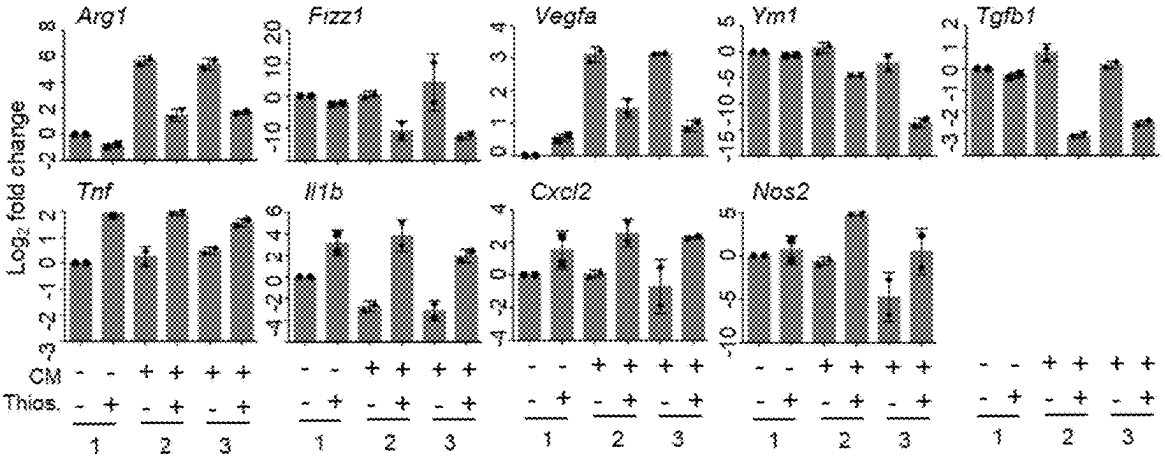

Figure 5D

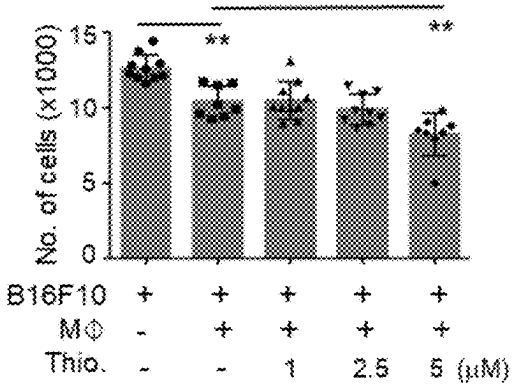

Figure 5E

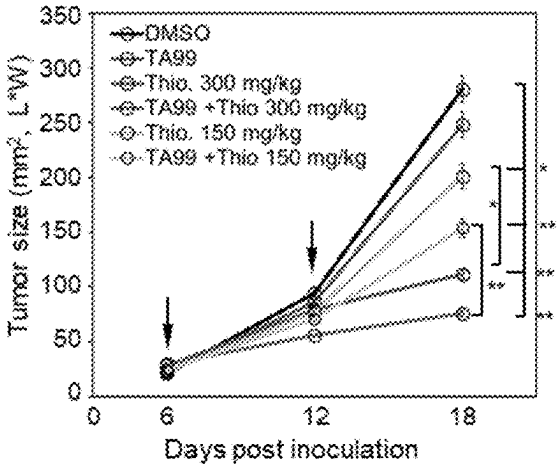

Figure 6A

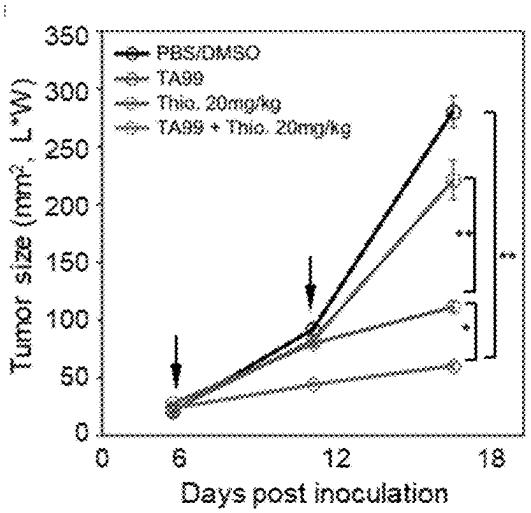

Figure 6B

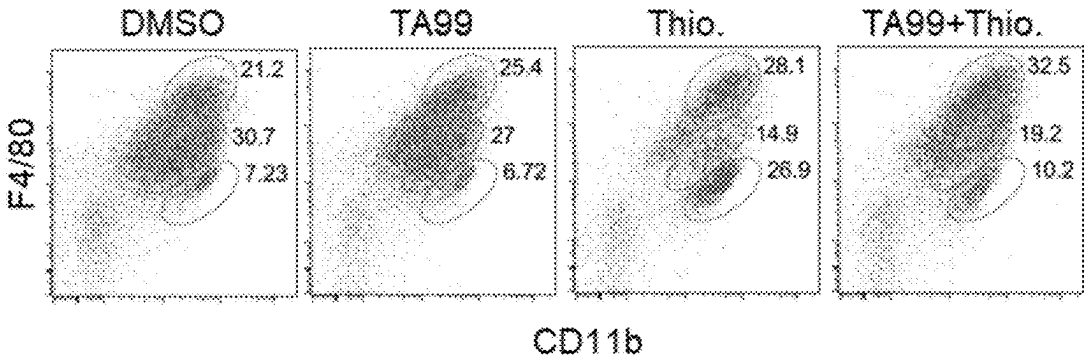

Figure 6C

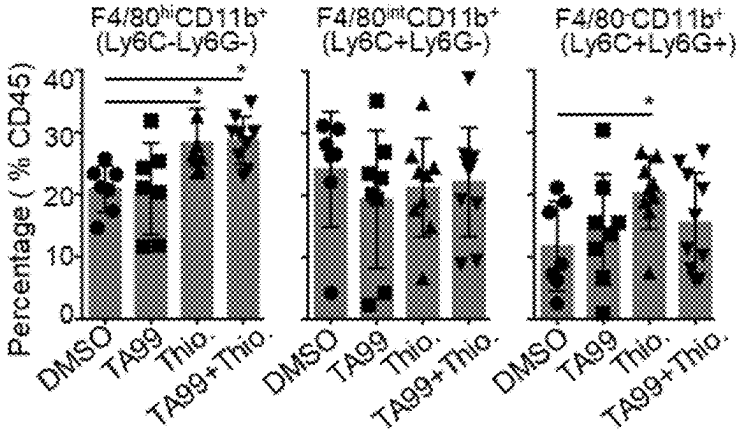

Figure 6D

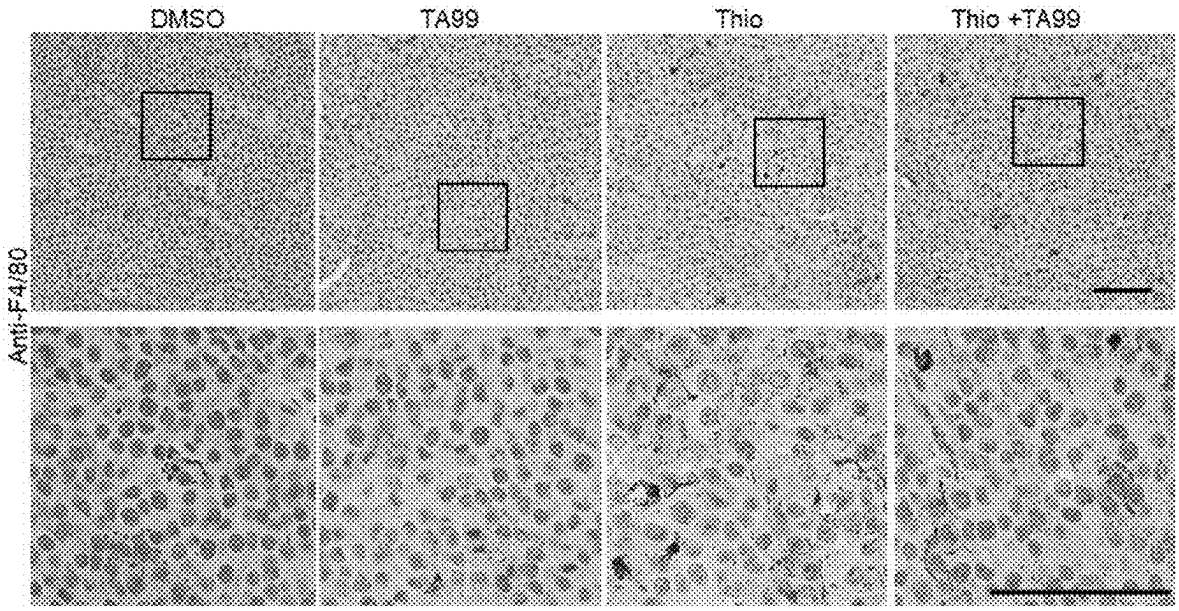

Figure 6E

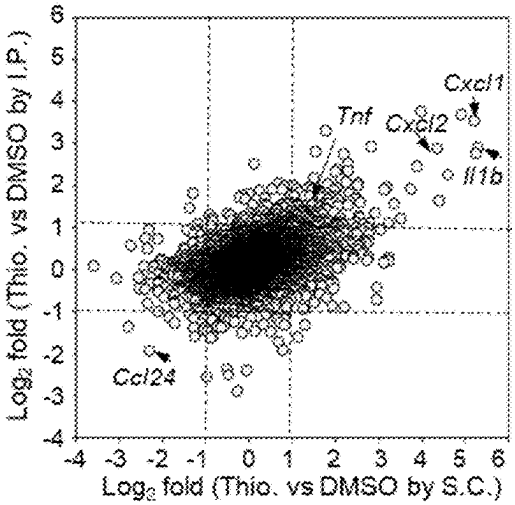

Figure 6F

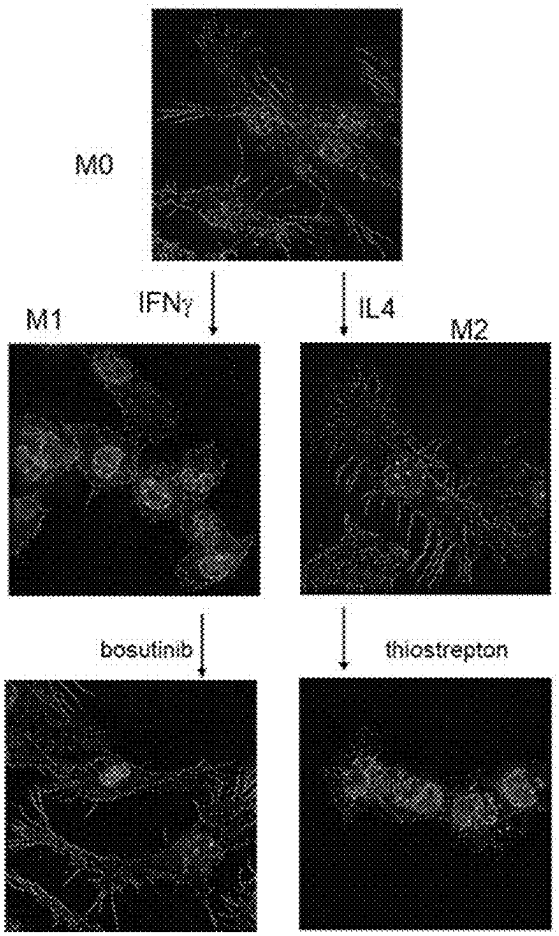

Figure 7A

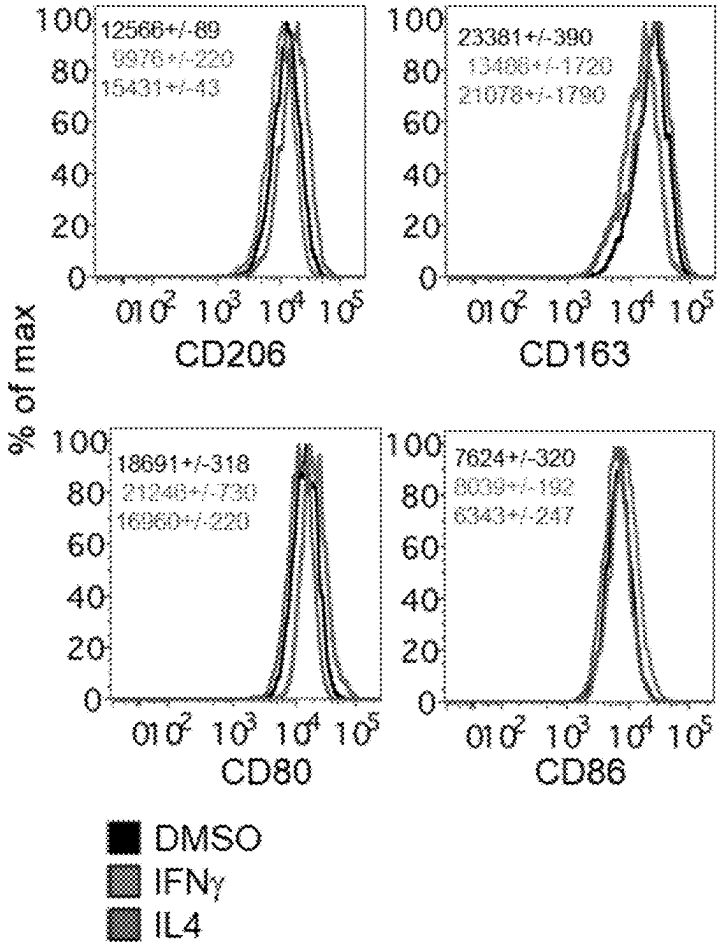
% of max
12566+/-89
9976+/-220
15431+/-43
CD206
23381+/-390
13466+/-1720
21078+/-1790
CD163
18691+/-318
21246+/-730
16960+/-220
CD80
7624+/-320
8039+/-192
6343+/-247
CD86
DMSO
IFNγ
IL4

Figure 7B

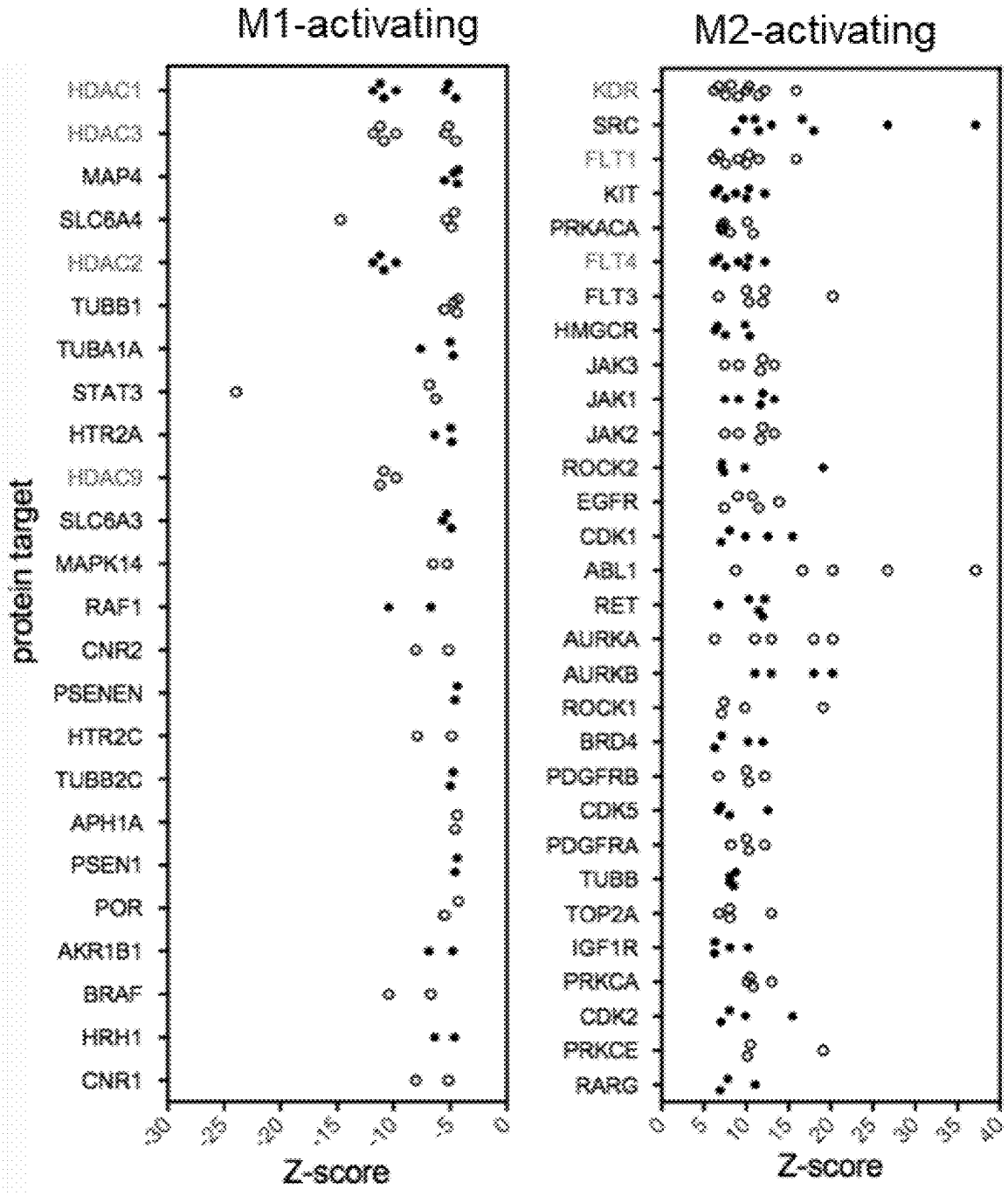
M1-activating
M2-activating
protein target
HDAC1
HDAC3
MAP4
SLC6A4
HDAC2
TUBB1
TUBA1A
STAT3
HTR2A
HDAC9
SLC6A3
MAPK14
RAF1
CNR2
PSENEN
HTR2C
TUBB2C
APH1A
PSEN1
POR
AKR1B1
BRAF
HRH1
CNR1
-30
-25
-20
-15
-10
-5
0
Z-score
KDR
SRC
FLT1
KIT
PRKACA
FLT4
FLT3
HMGCR
JAK3
JAK1
JAK2
ROCK2
EGFR
CDK1
ABL1
RET
AURKA
AURKB
ROCK1
BRD4
PDGFRB
CDK5
PDGFRA
TUBB
TOP2A
IGF1R
PRKCA
CDK2
PRKCE
RARG
0
5
10
15
20
25
30
35
40
Z-score

Figure 8

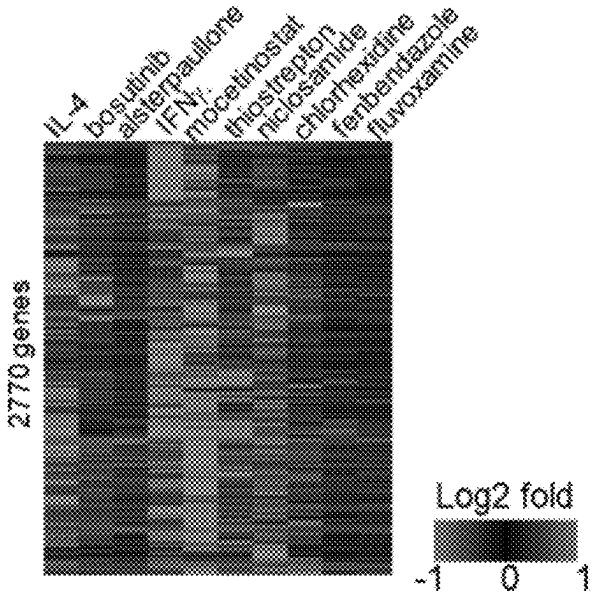

Figure 9A

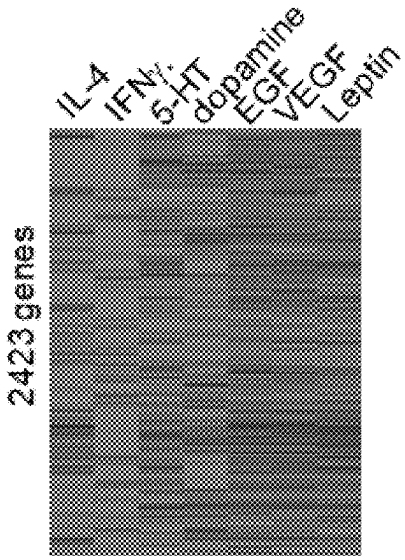

Figure 9B

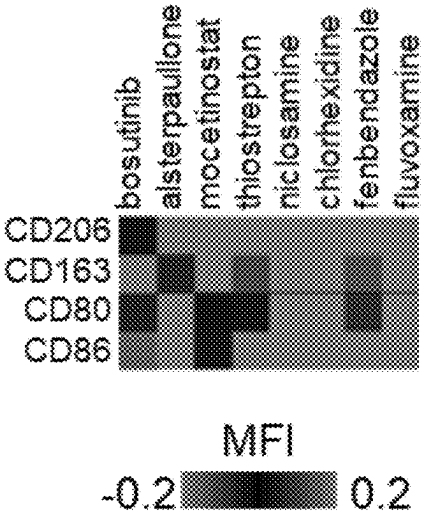
bosutinib
alsterpaullone
mocetinostat
thiostrepton
niclosamine
chlorhexidine
fenbendazole
fluvoxamine
CD206
CD163
CD80
CD86
MFI
-0.2
0.2

Figure 9C

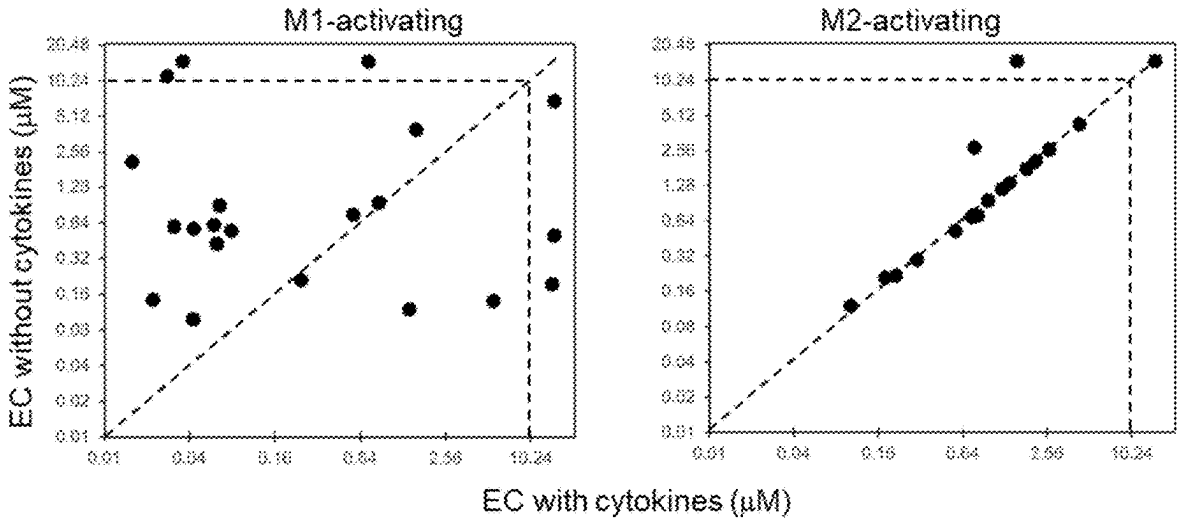
M1-activating
M2-activating
EC without cytokines (μM)
EC with cytokines (μM)
20.48
10.24
5.12
2.56
1.28
0.64
0.32
0.16
0.08
0.04
0.02
0.01
0.01
0.04
0.16
0.64
2.56
10.24

Figure 10

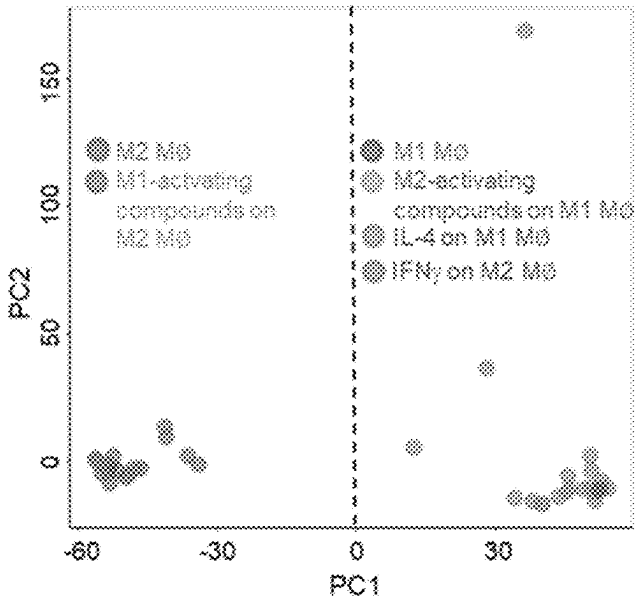

Figure 11A

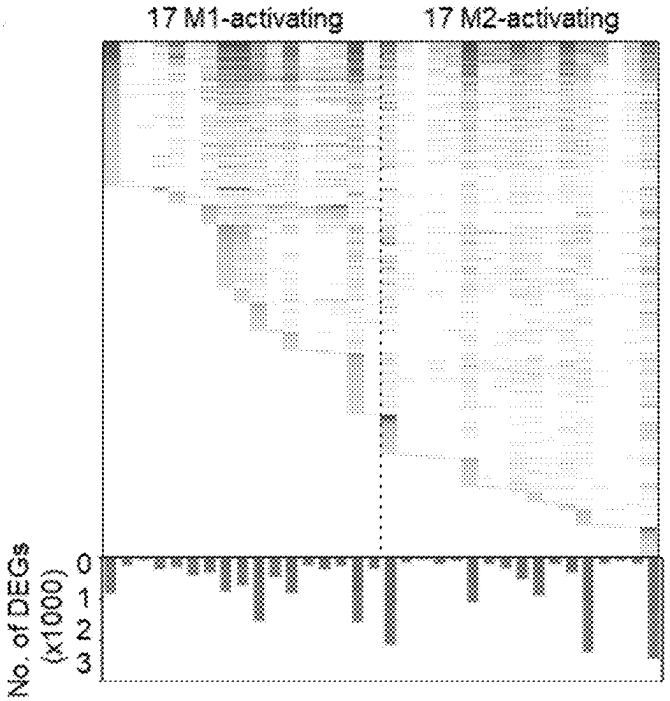

Figure 11B

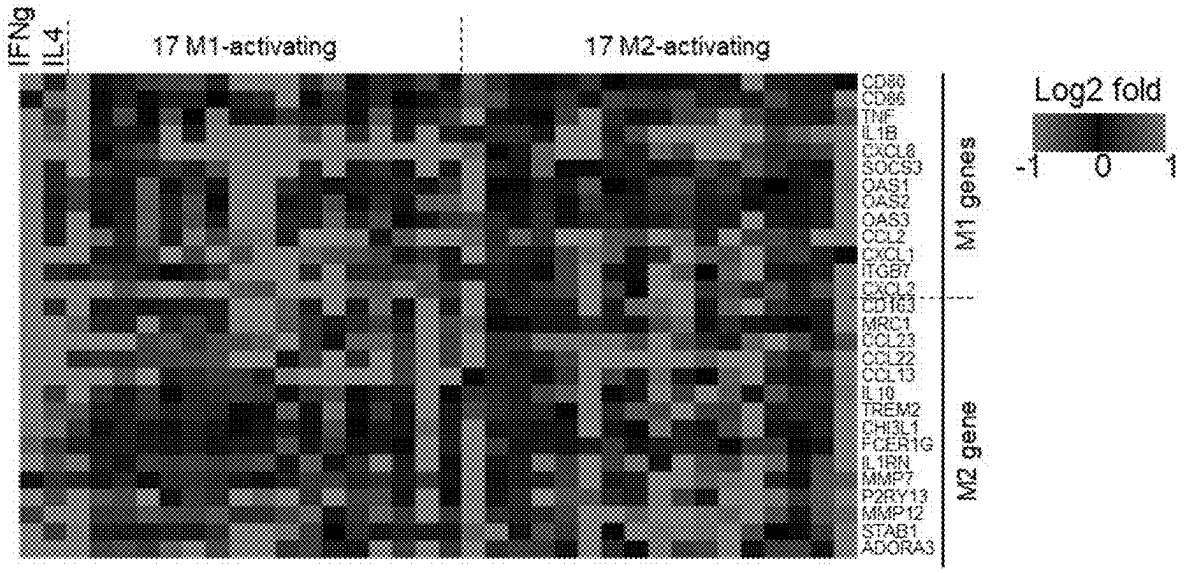

Figure 11C

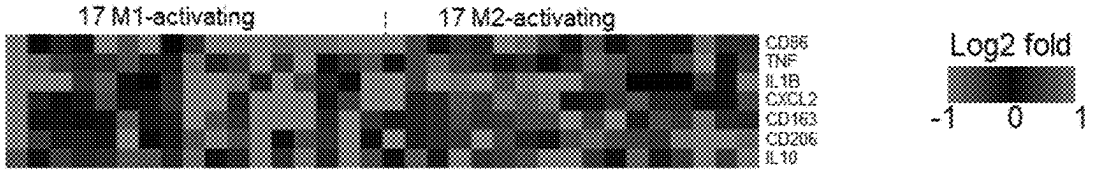

Figure 11D

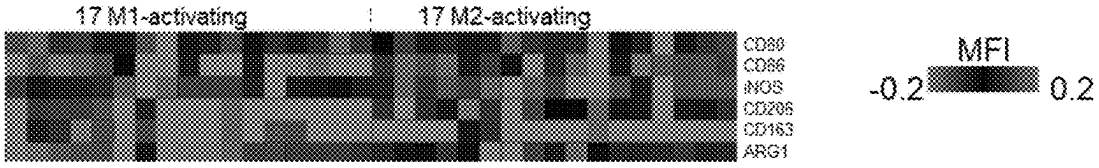

Figure 11E

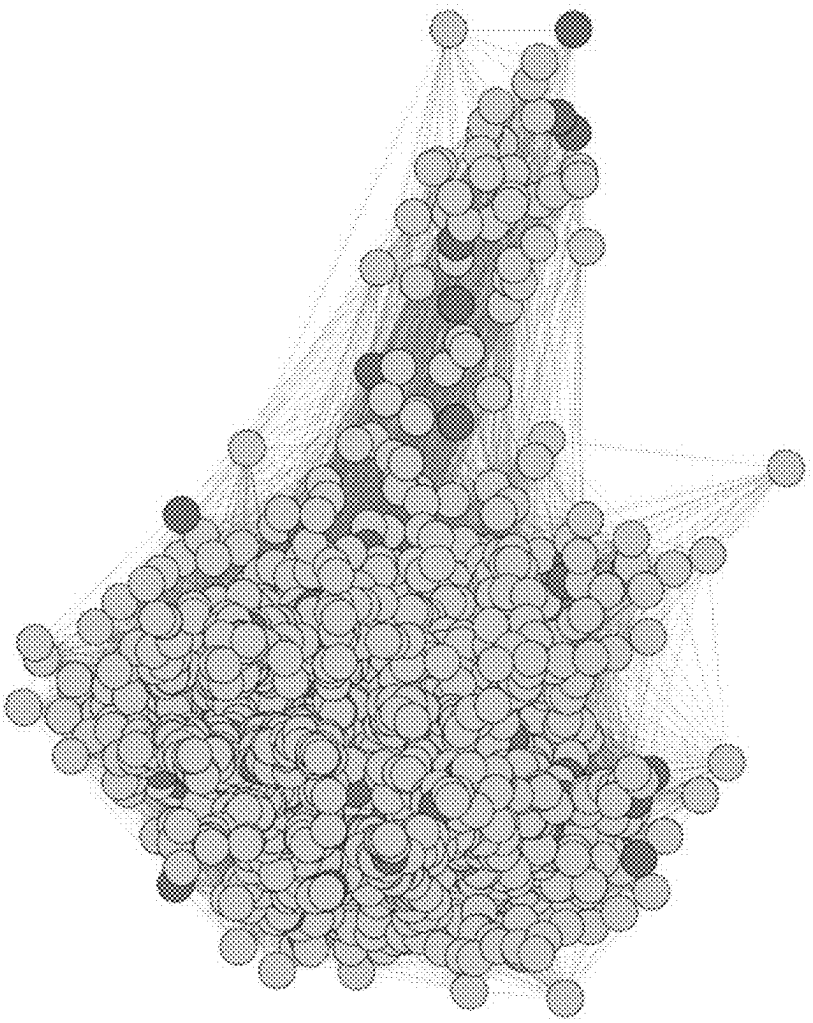

Hub genes

Gene	Degree
GBP1	689
KIAA1244	659
FAM26F	617
COLEC12	596
GBP4	582
MYO1G	554
TYMP	546
GCH1	528
SNX10	514
CNIH4	508
STAT1	498
MCOLN1	491
NISCH	486

Hub TF

Gene	Degree
STAT1	498
MXD4	456
TSC22D1	427
ZNF814	413
BNC2	413
ZNF331	383
IRF1	373
ZNF440	347
HES2	345
ZBTB8A	325
BATF2	319
MAX	319
NFIX	305

Figure 12

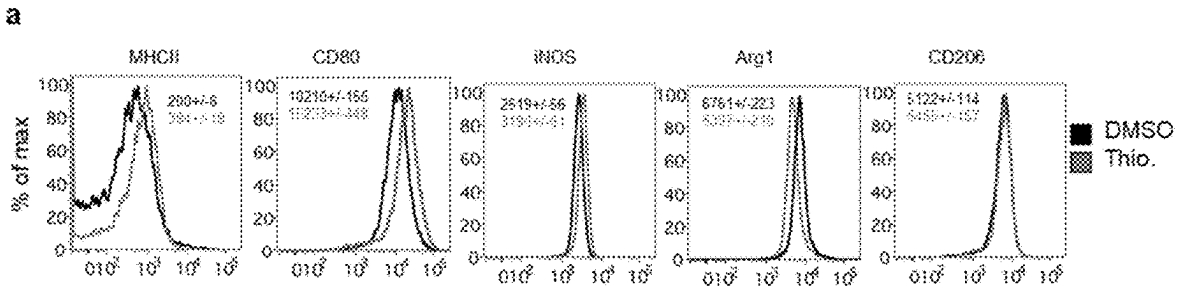

Figure 13A

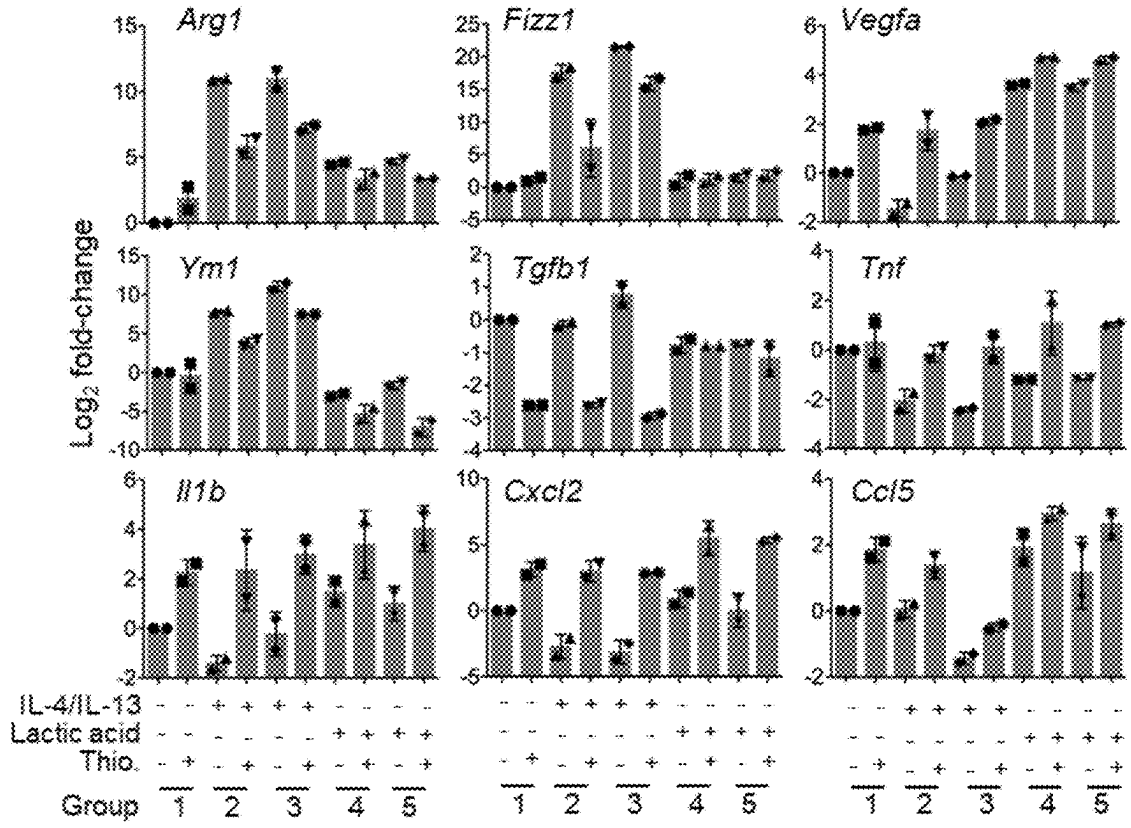

Figure 13B

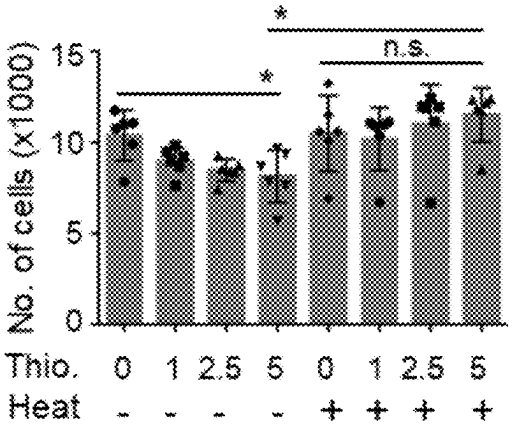

Figure 14A

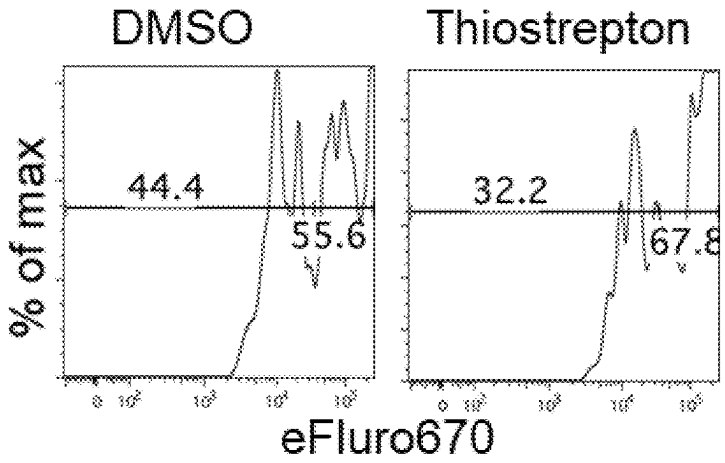

Figure 14B

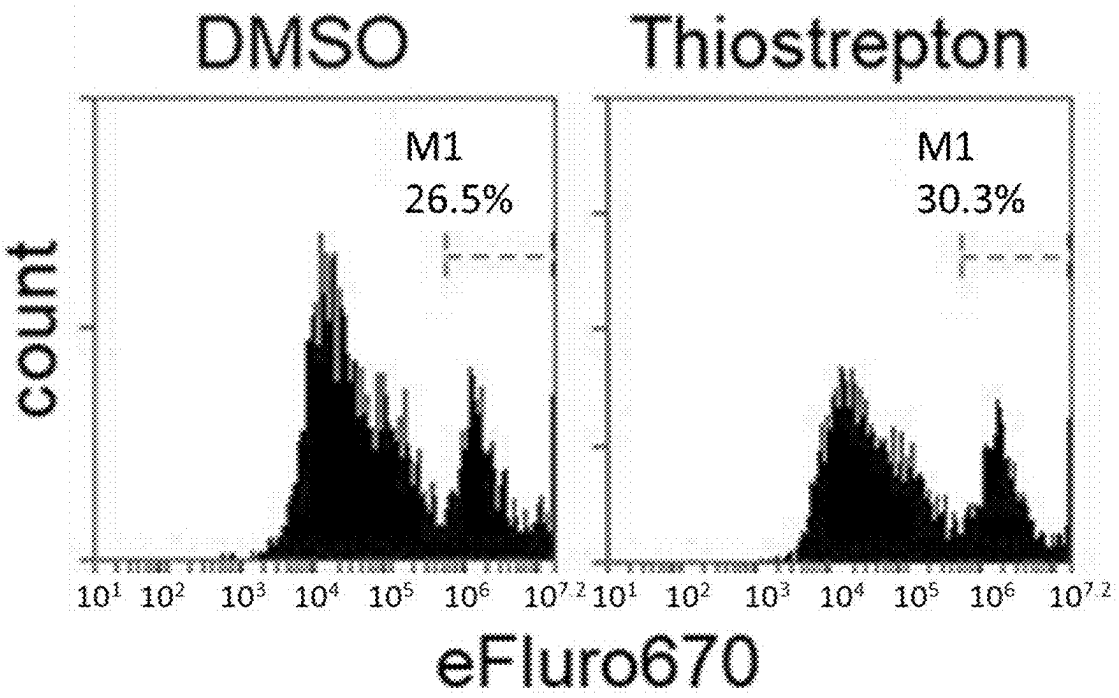
DMSO
Thiostrepton
M1
26.5%
M1
30.3%
count
10^1 10^2 10^3 10^4 10^5 10^6 $10^{7.2}$
10^1 10^2 10^3 10^4 10^5 10^6 $10^{7.2}$
eFluro670

Figure 14C

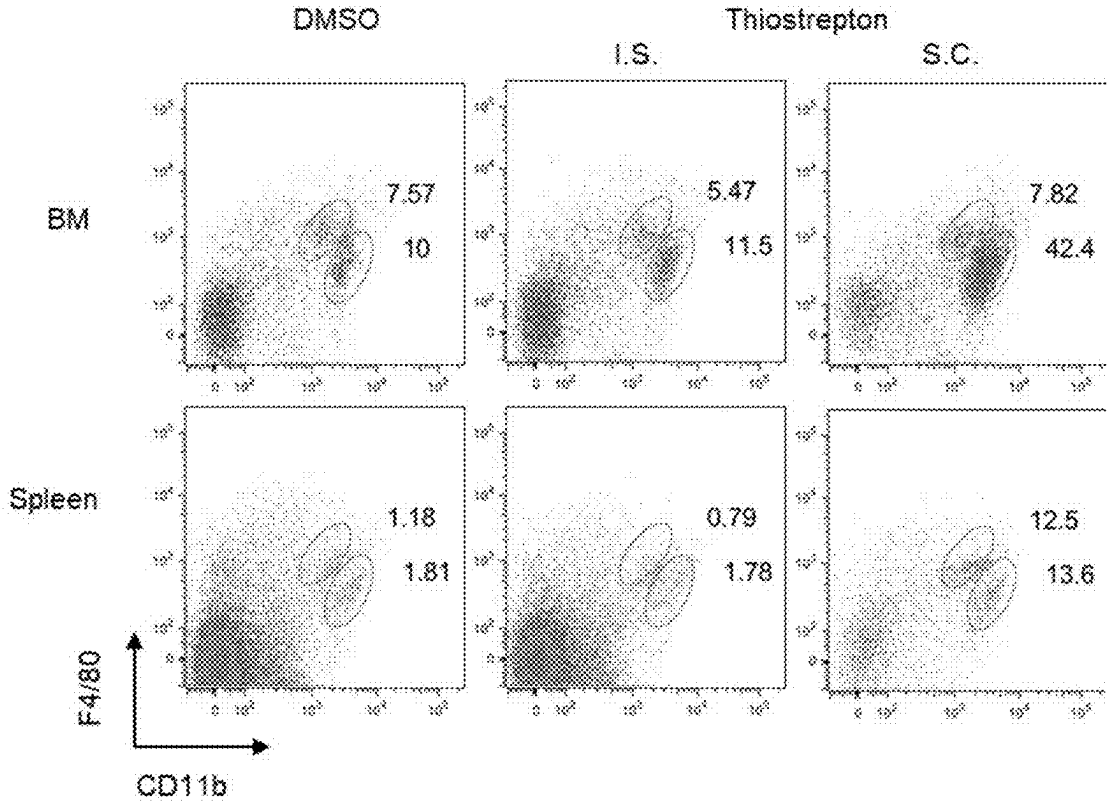

Figure 15A

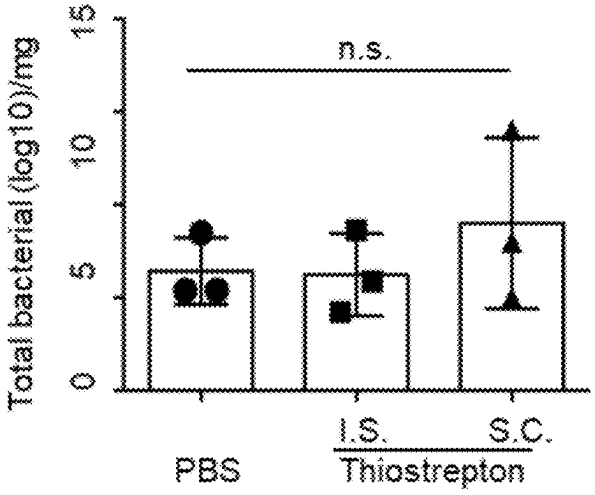

Figure 15B

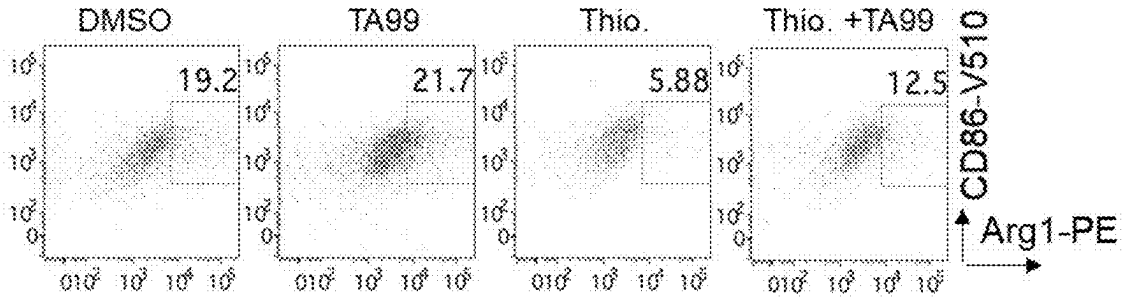

Figure 16A

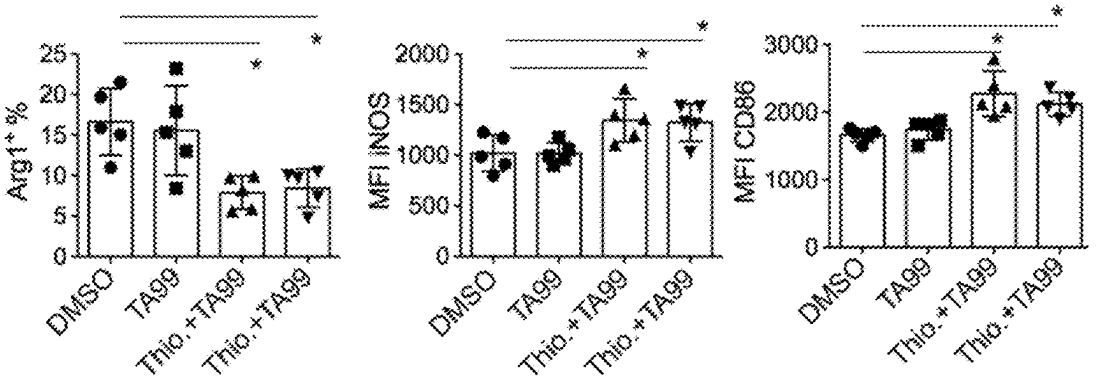

Figure 16B

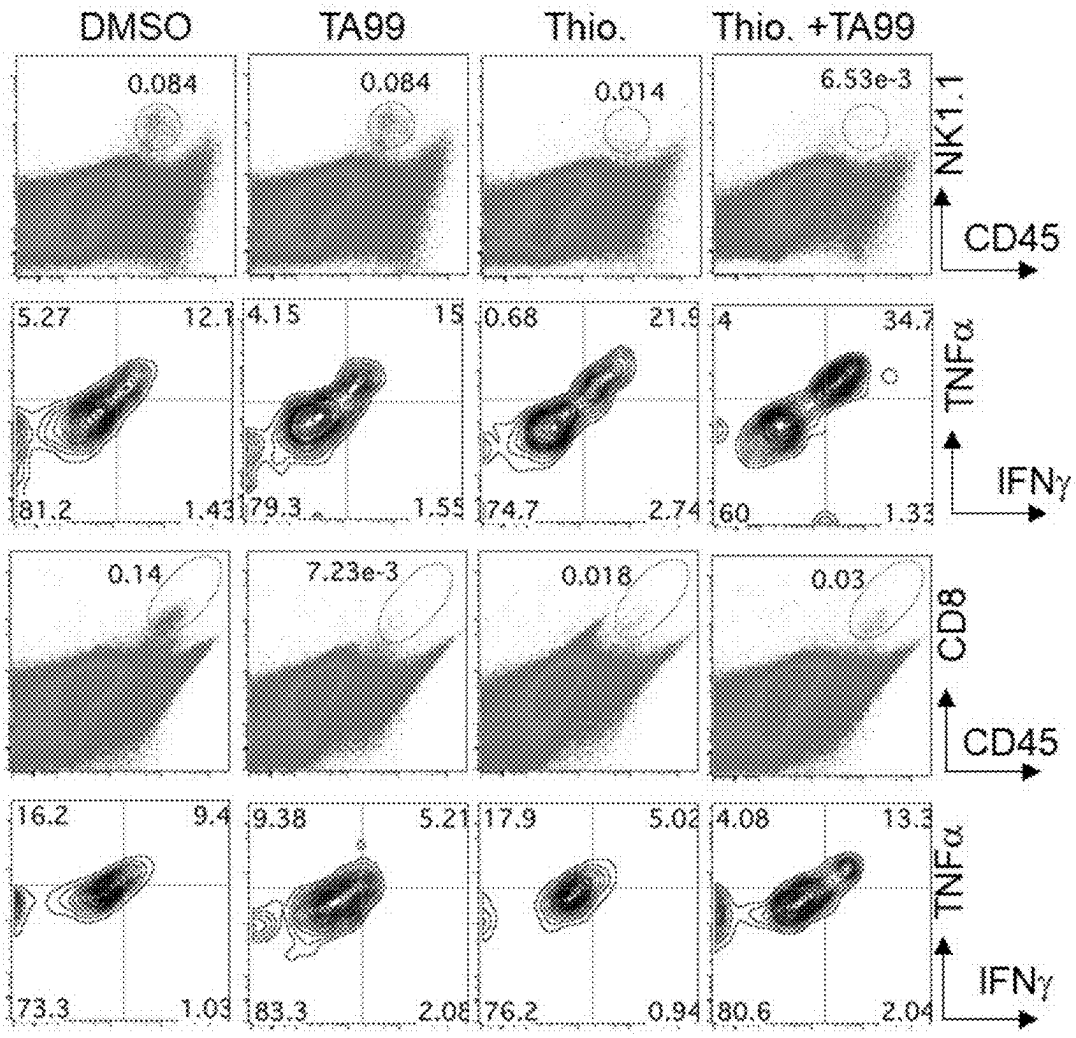
DMSO
TA99
Thio.
Thio. +TA99
0.084
0.084
0.014
6.53e-3
NK1.1
CD45
5.27
12.1
4.15
15
0.68
21.9
4
34.7
TNFα
IFNγ
81.2
1.43
79.3
1.55
74.7
2.74
60
1.33
0.14
7.23e-3
0.018
0.03
CD8
CD45
16.2
9.4
9.38
5.21
17.9
5.02
4.08
13.3
TNFα
IFNγ
73.3
1.03
83.3
2.08
76.2
0.94
80.6
2.04

Figure 16C

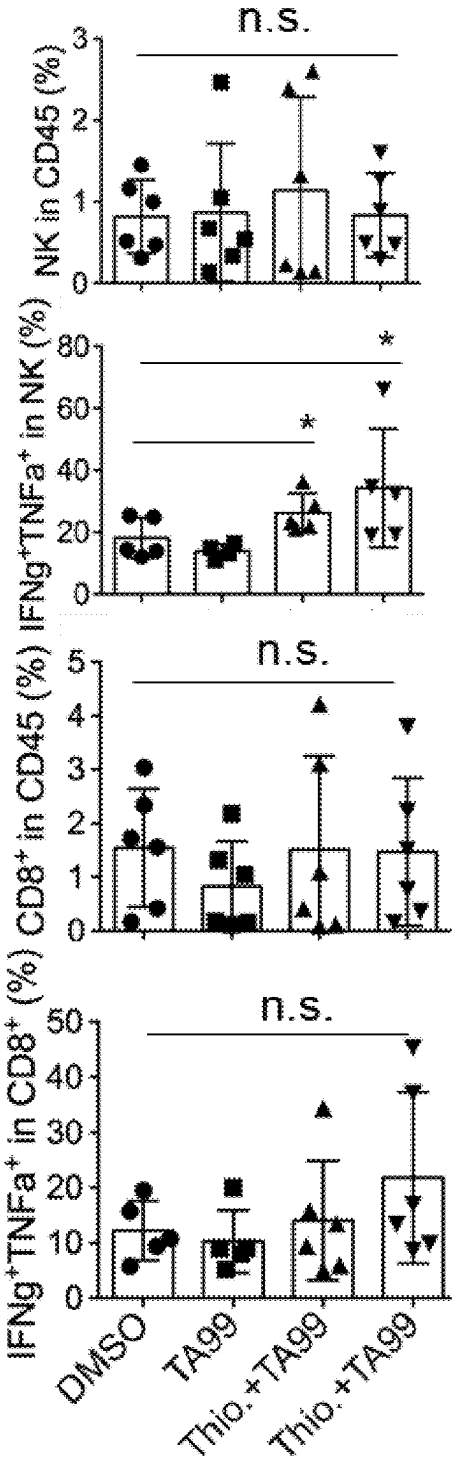
n.s.
NK in CD45 (%)
0
1
2
3
IFNg+TNFa+ in NK (%)
0
20
40
60
80
*
*
n.s.
CD8+ in CD45 (%)
0
1
2
3
4
5
n.s.
IFNg+TNFa+ in CD8+ (%)
0
10
20
30
40
50
DMSO
TA99
Thio.+TA99
Thio.+TA99

Figure 16D

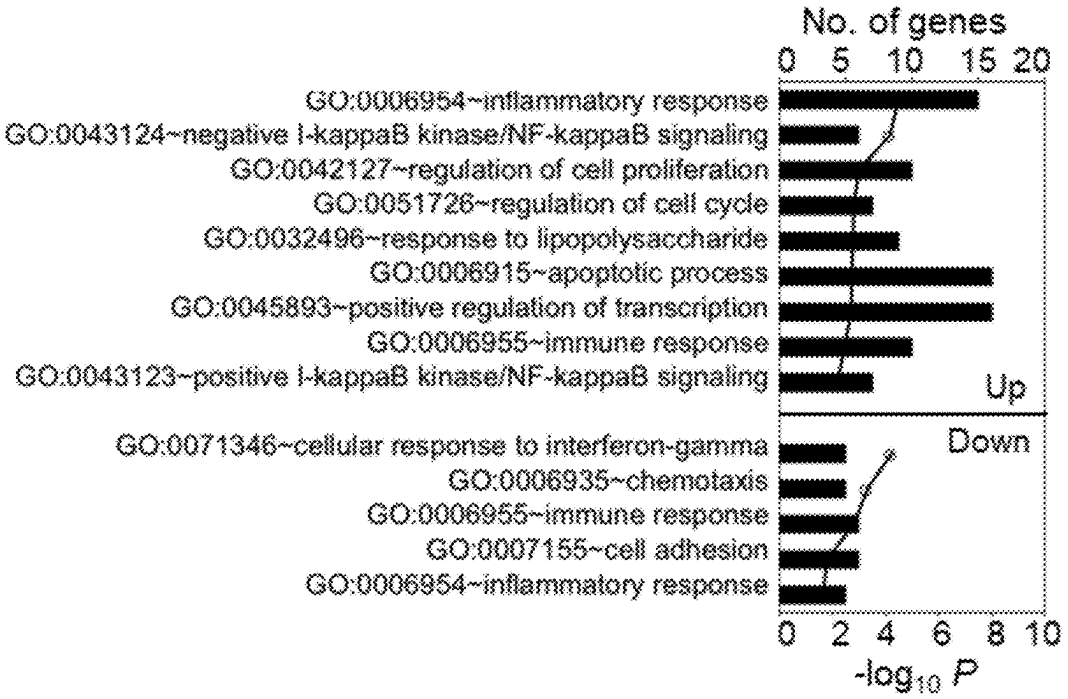
No. of genes
0 5 10 15 20
GO:0006954~inflammatory response
GO:0043124~negative I-kappaB kinase/NF-kappaB signaling
GO:0042127~regulation of cell proliferation
GO:0051726~regulation of cell cycle
GO:0032496~response to lipopolysaccharide
GO:0006915~apoptotic process
GO:0045893~positive regulation of transcription
GO:0006955~immune response
GO:0043123~positive I-kappaB kinase/NF-kappaB signaling
Up
Down
GO:0071346~cellular response to interferon-gamma
GO:0006935~chemotaxis
GO:0006955~immune response
GO:0007155~cell adhesion
GO:0006954~inflammatory response
0 2 4 6 8 10
-log10 P

Figure 17A

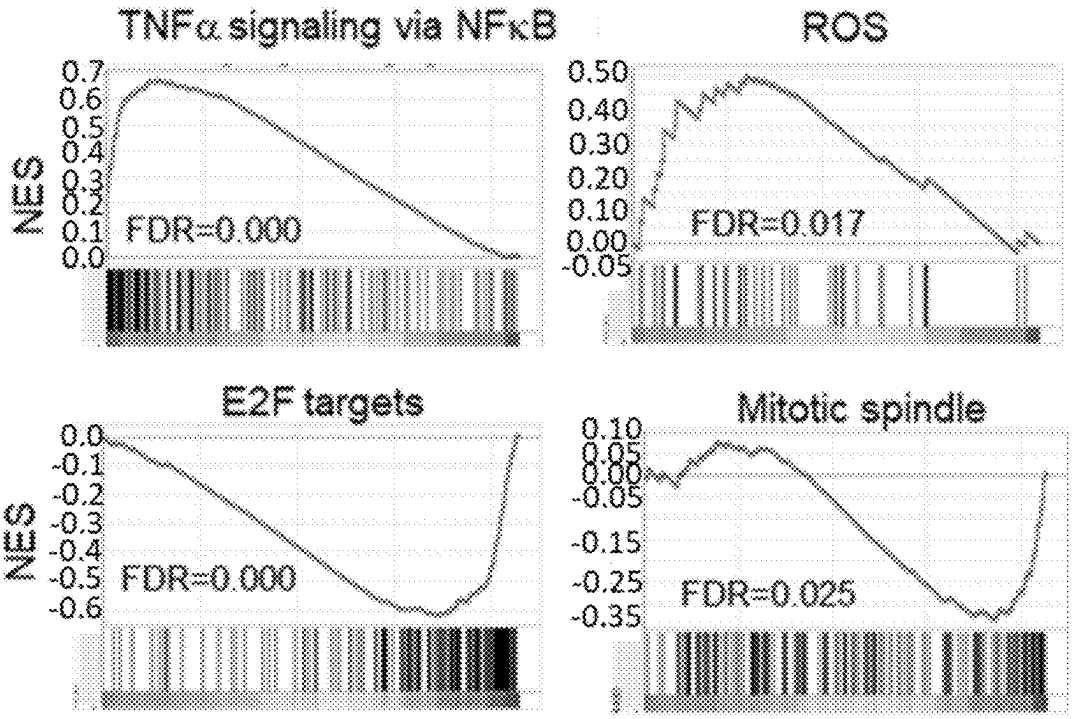
TNFα signaling via NFκB
NES
0.7
0.6
0.5
0.4
0.3
0.2
0.1
0.0
FDR=0.000
ROS
0.50
0.40
0.30
0.20
0.10
0.00
-0.05
FDR=0.017
E2F targets
NES
0.0
-0.1
-0.2
-0.3
-0.4
-0.5
-0.6
FDR=0.000
Mitotic spindle
0.10
0.05
0.00
-0.05
-0.15
-0.25
-0.35
FDR=0.025

Figure 17B

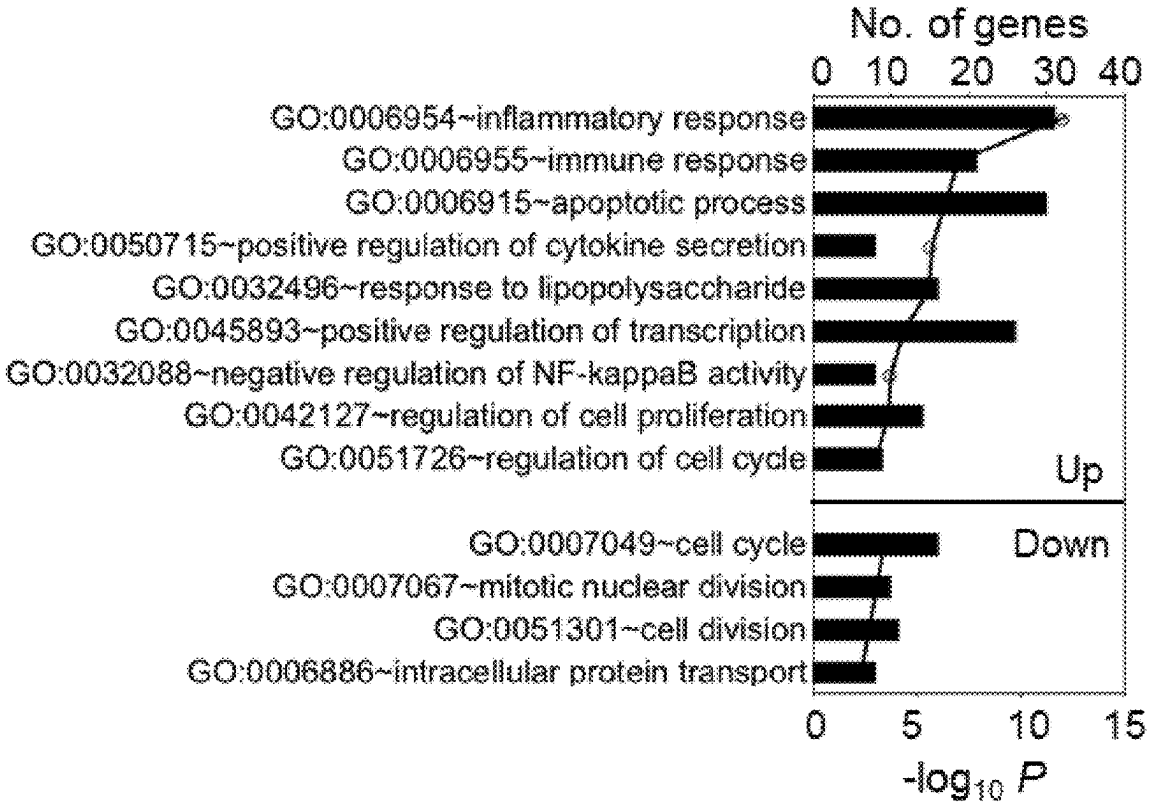

Figure 17C

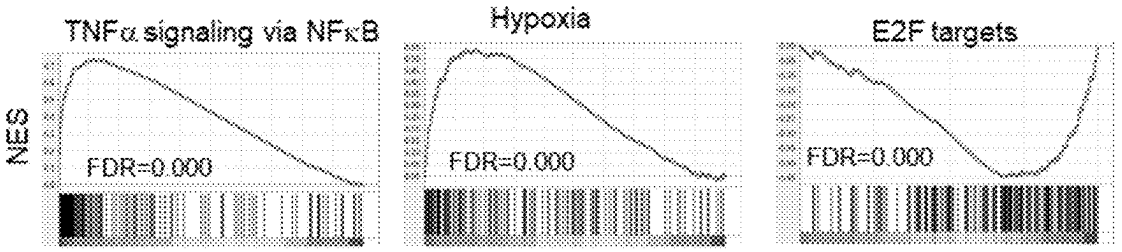

Figure 17D

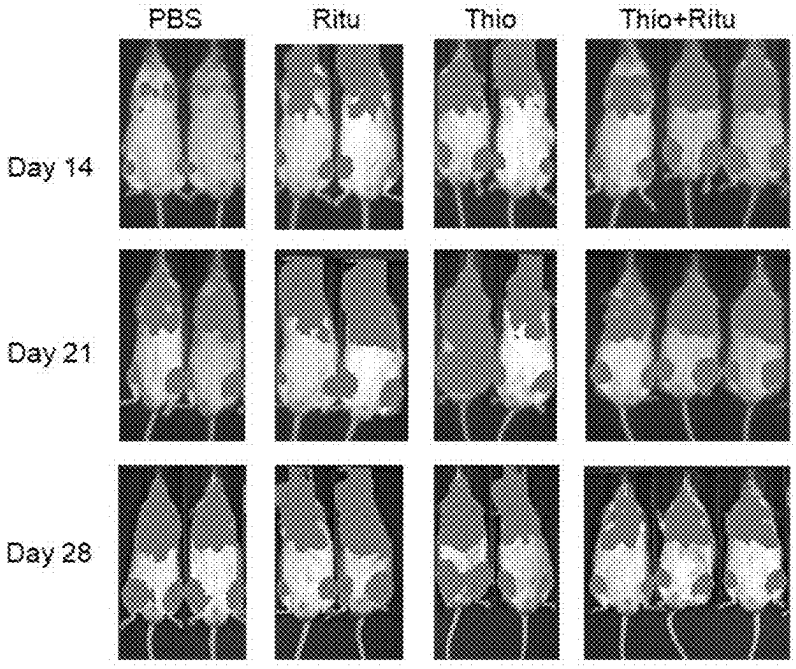

Figure 18A

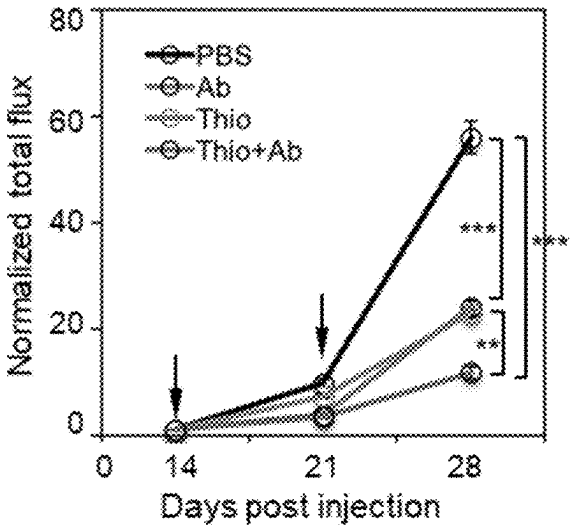

Figure 18B

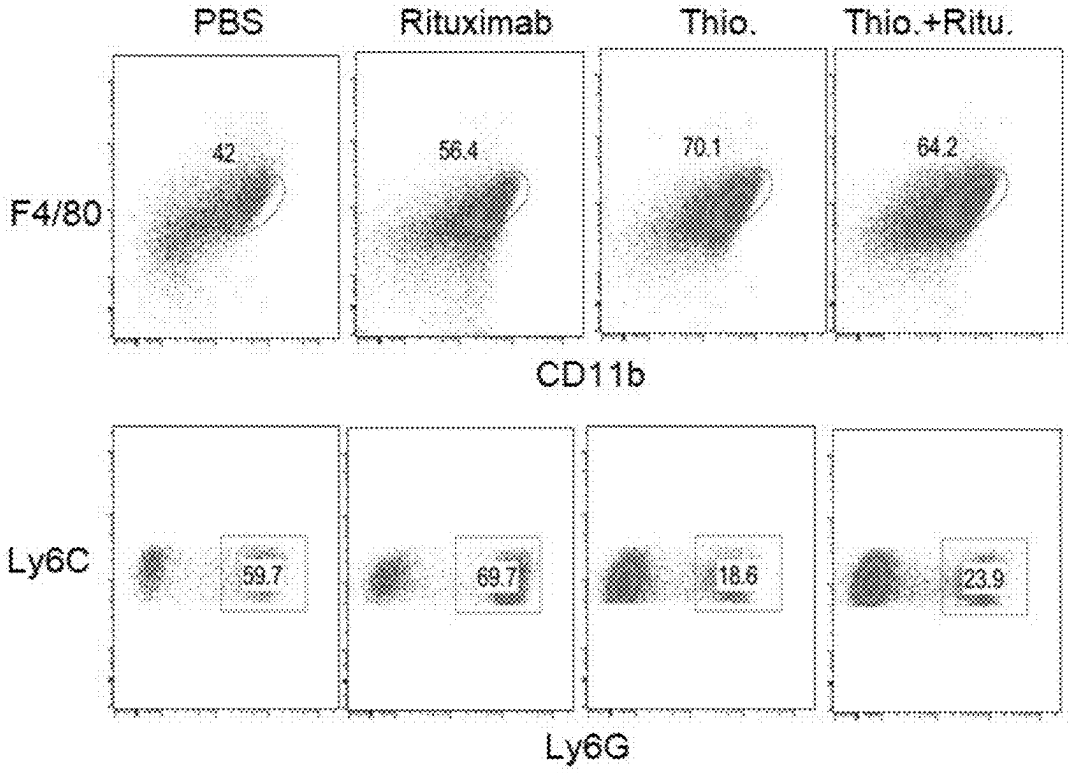

Figure 18C

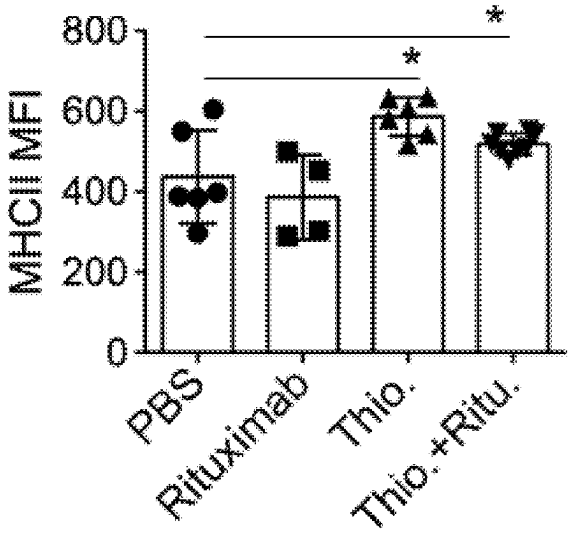

Figure 18D

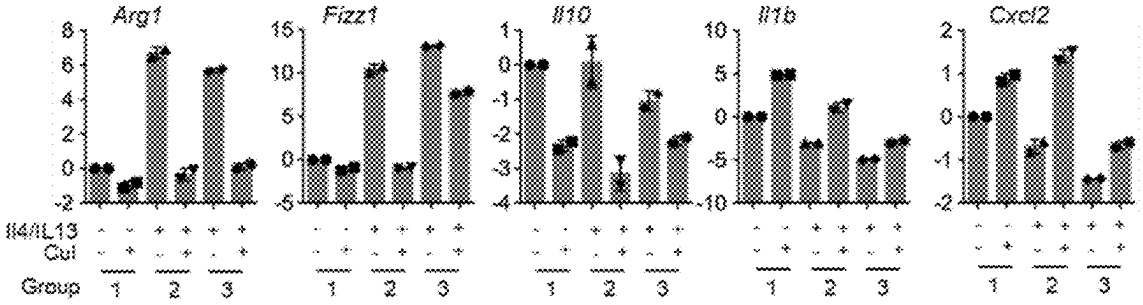

Figure 19A

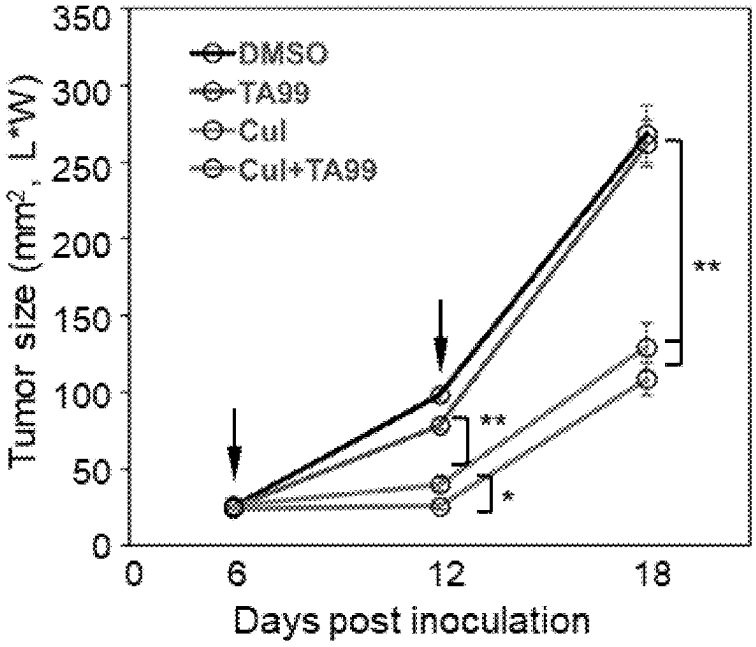

Figure 19B

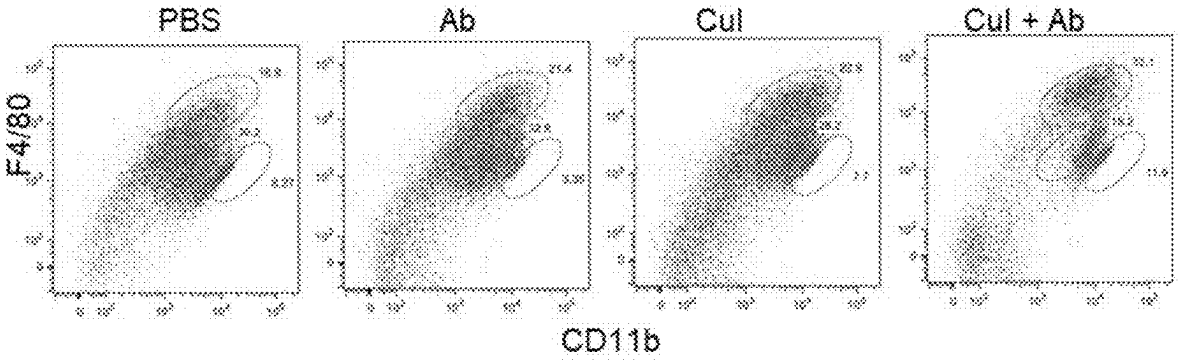

Figure 19C

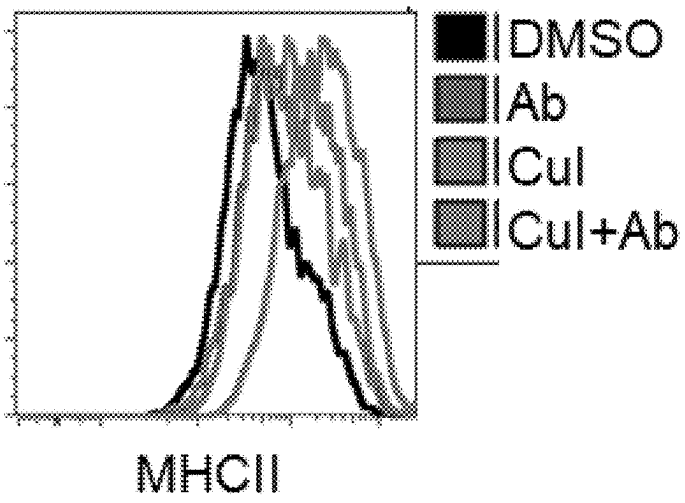

Figure 19D

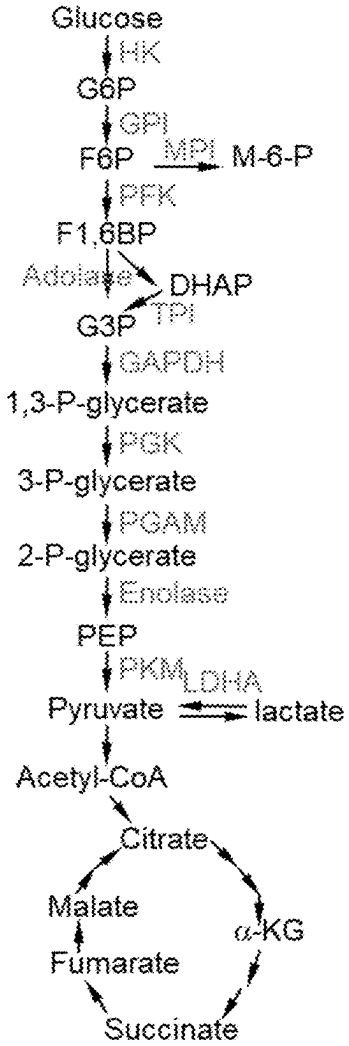

Figure 20A

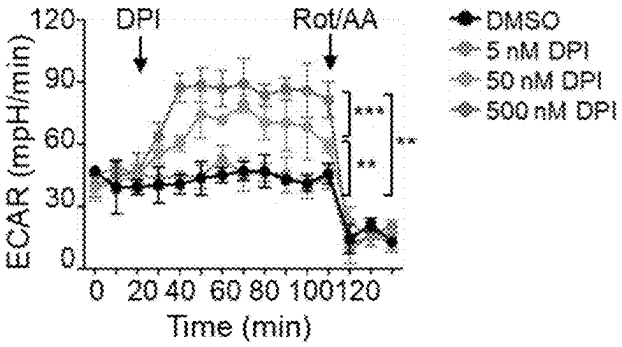

Figure 20B

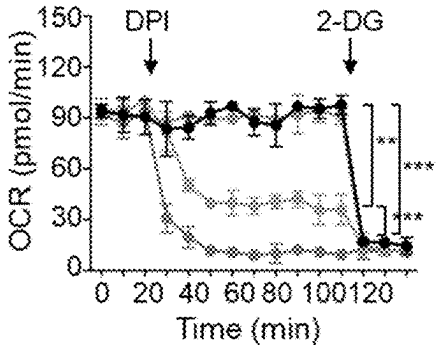

Figure 20C

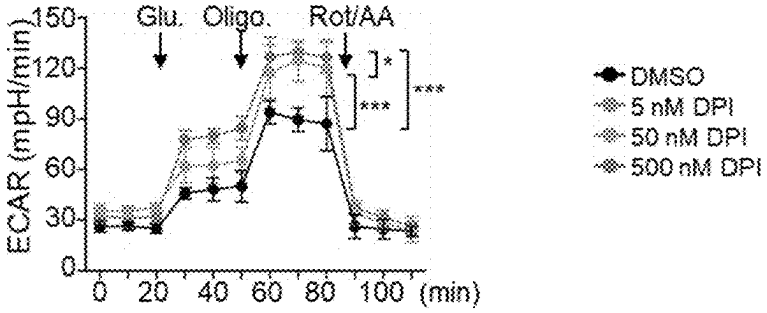

Figure 20D

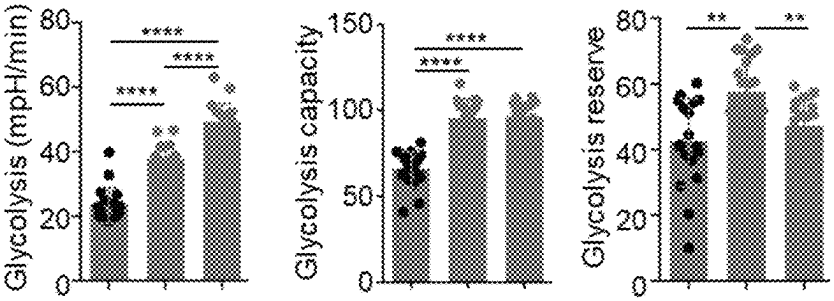

Figure 20E

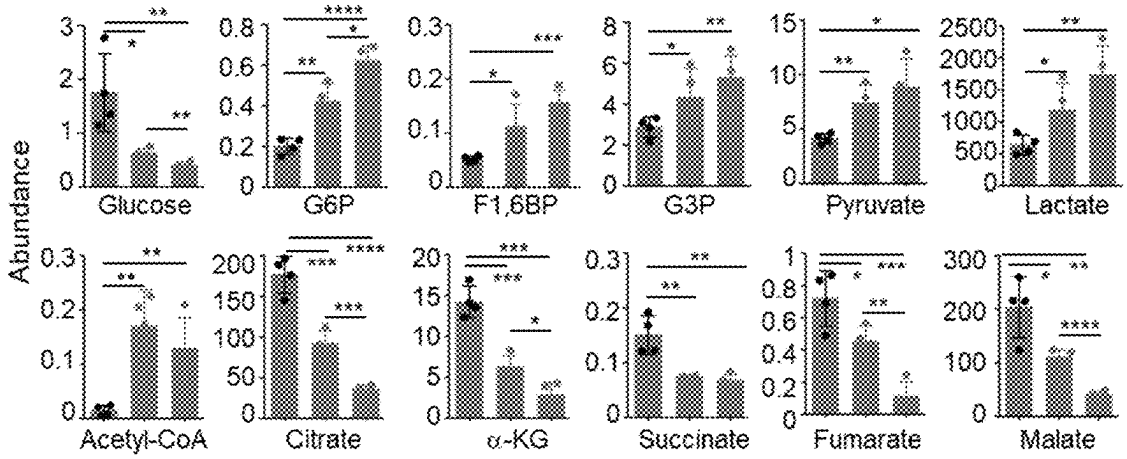

Figure 20F

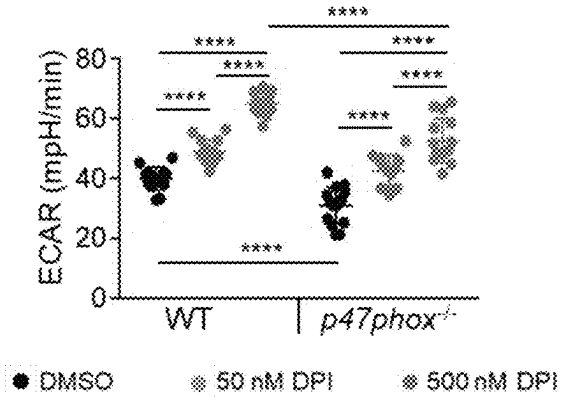

Figure 21A

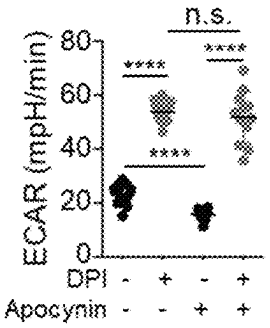

Figure 21B

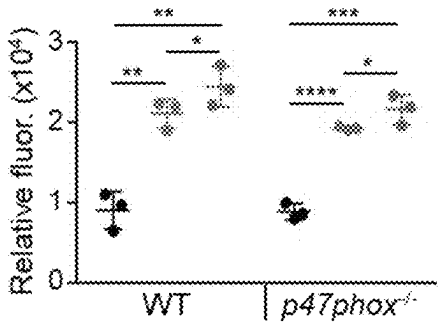

Figure 21C

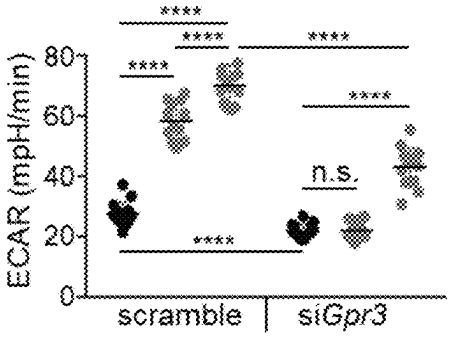

Figure 21D

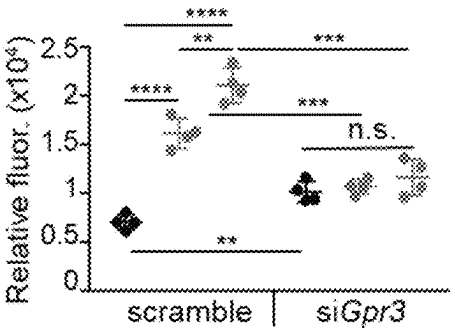

Figure 21E

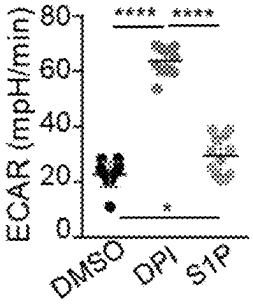

Figure 21F

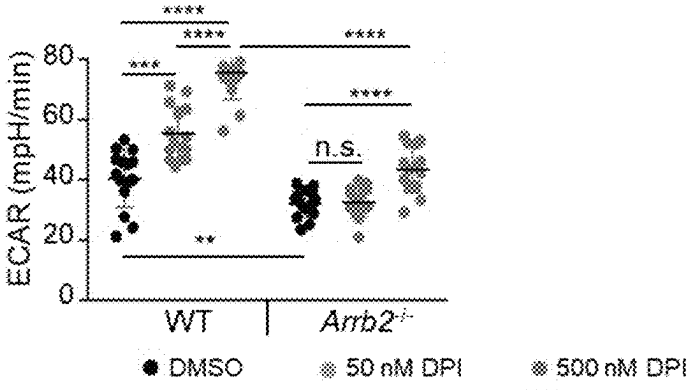

Figure 21G

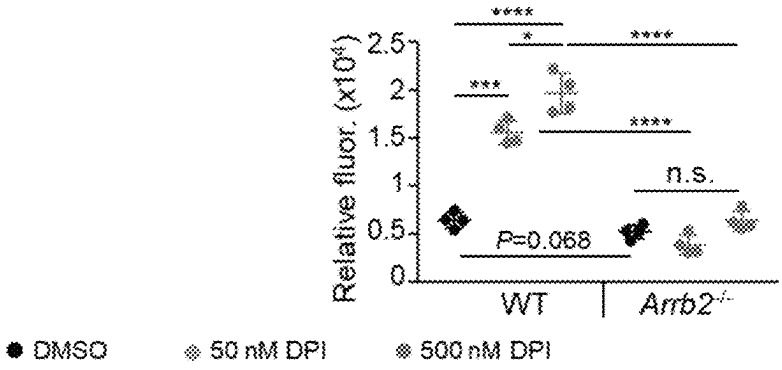

Figure 21H

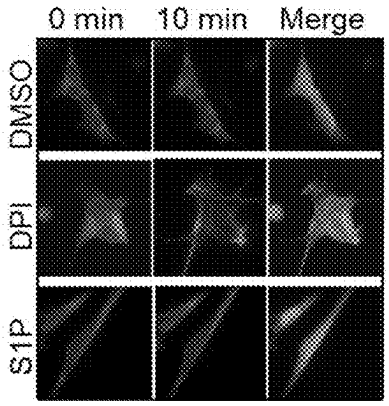

Figure 21I

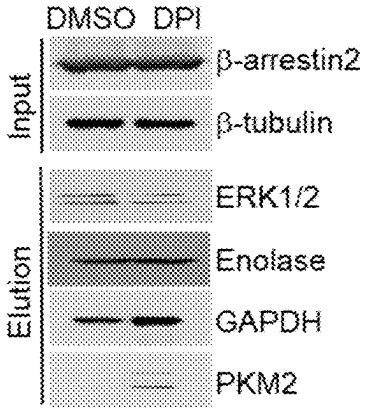

Figure 22A

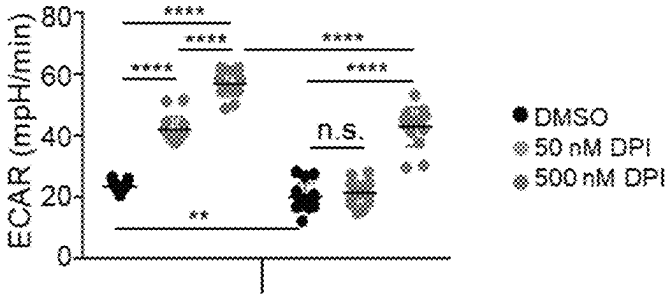

Figure 22B

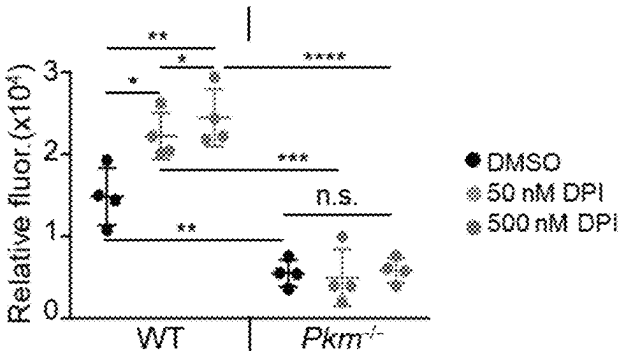

Figure 22C

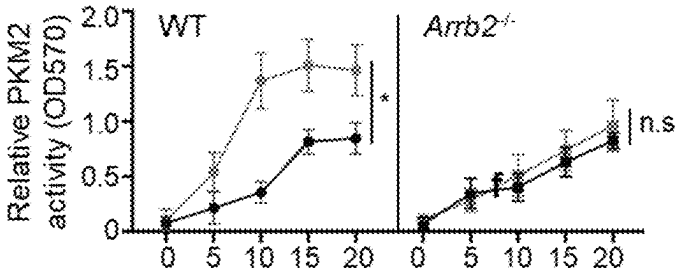

Figure 22D

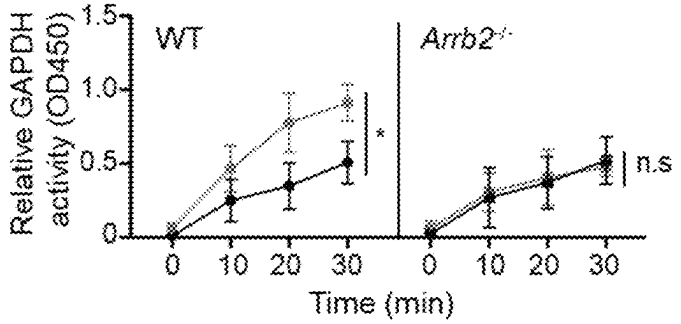

Figure 22E

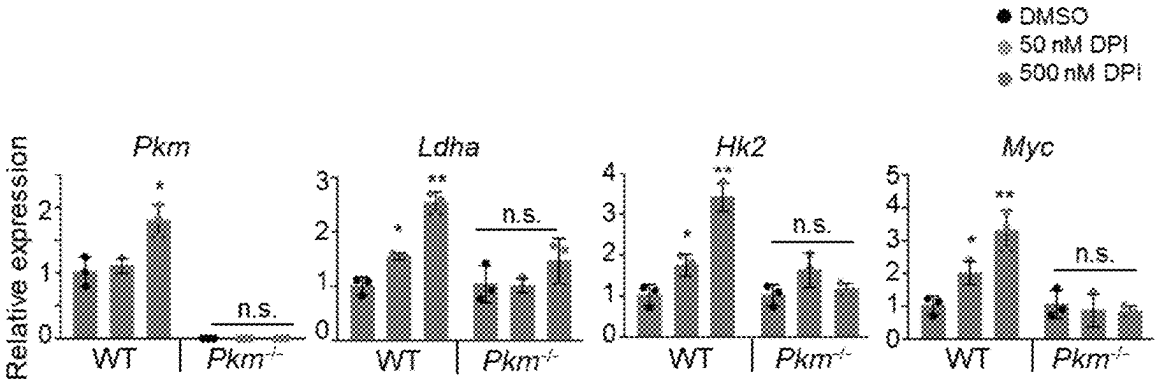

Figure 23A

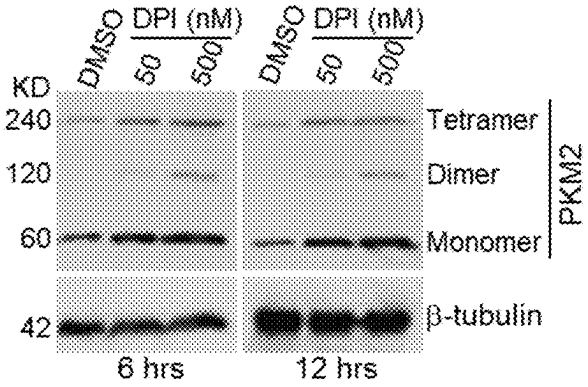

Figure 23B

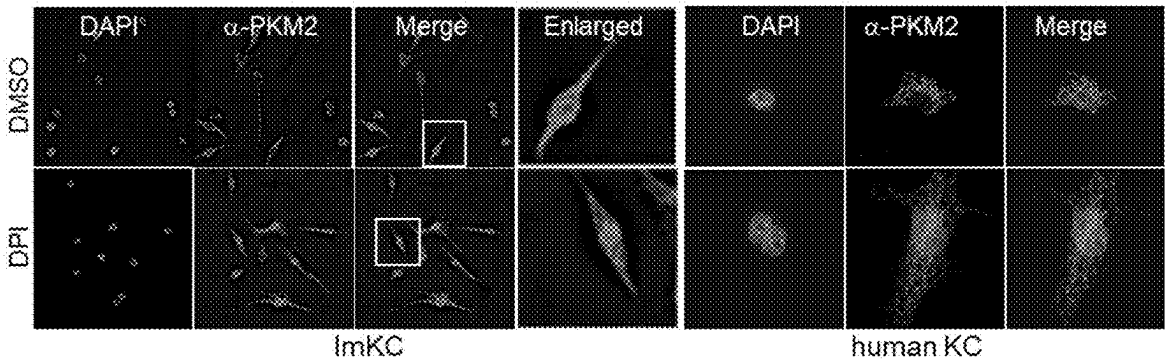

Figure 23C

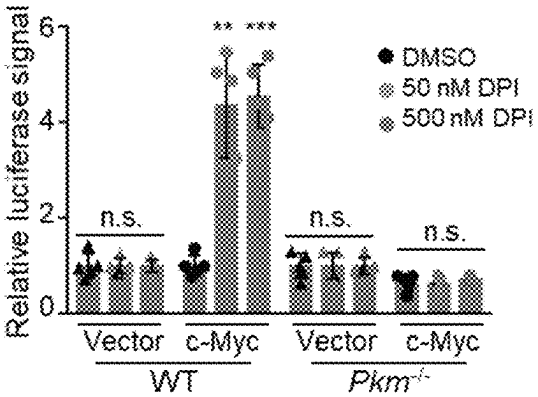

Figure 23D

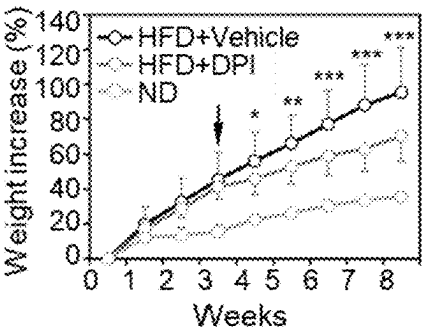

Figure 24A

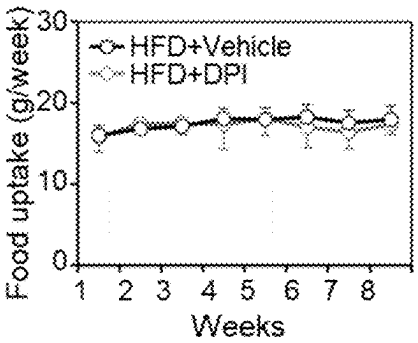

Figure 24B

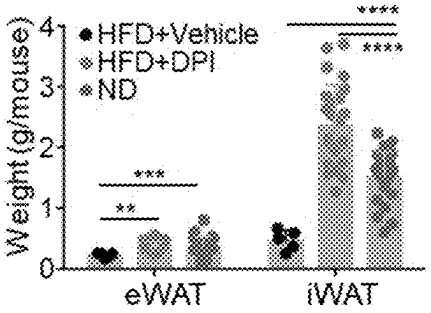

Figure 24C

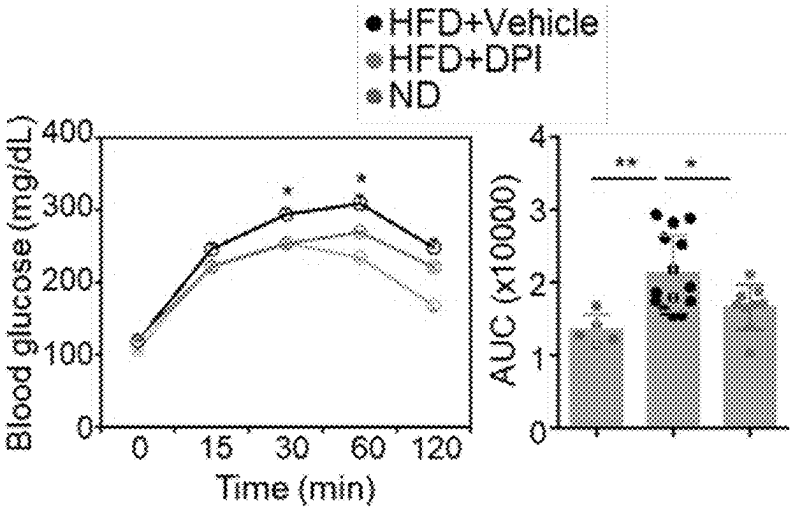

Figure 24D

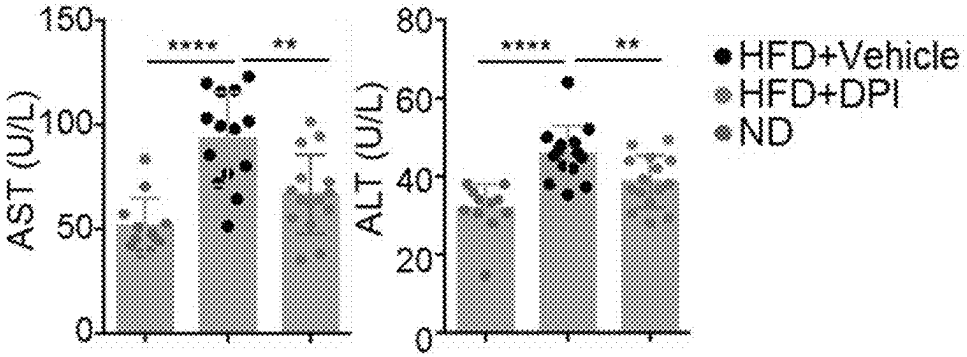

Figure 24E

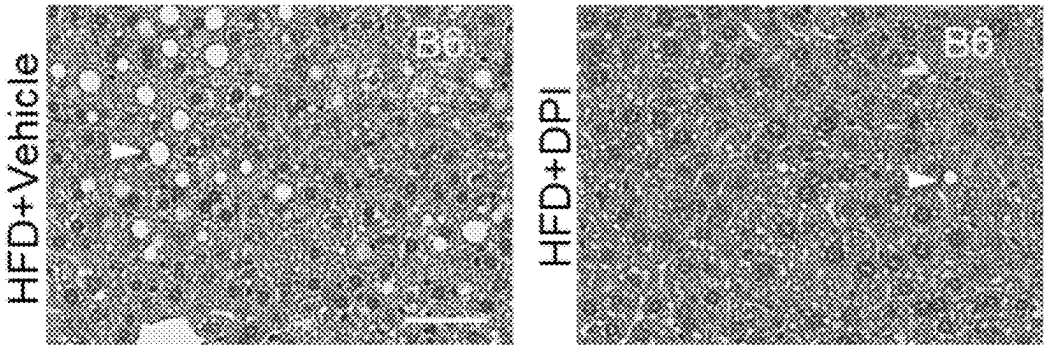

Figure 24F

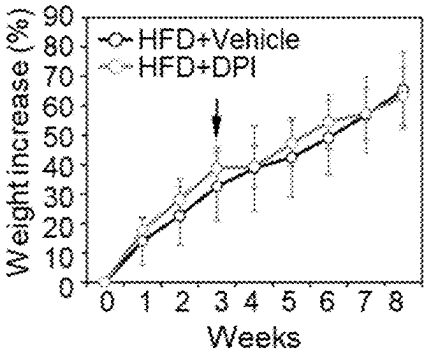

Figure 24G

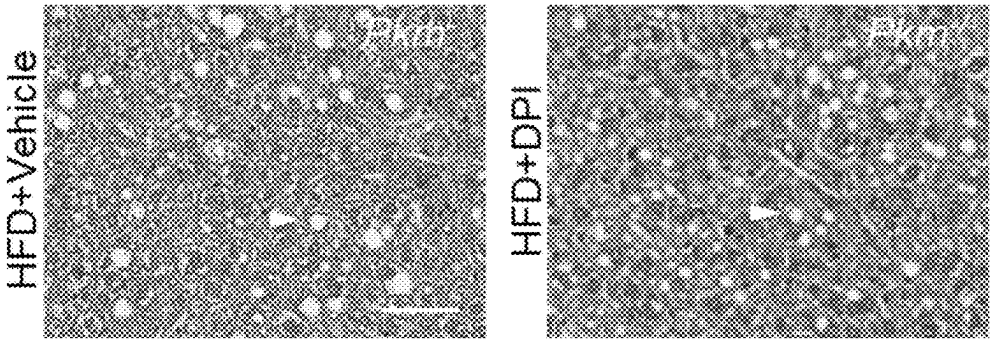

Figure 24H

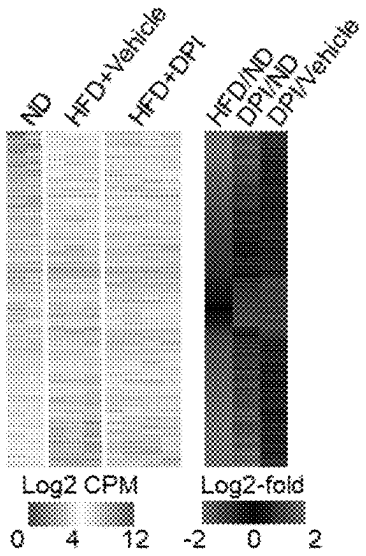

Figure 25A

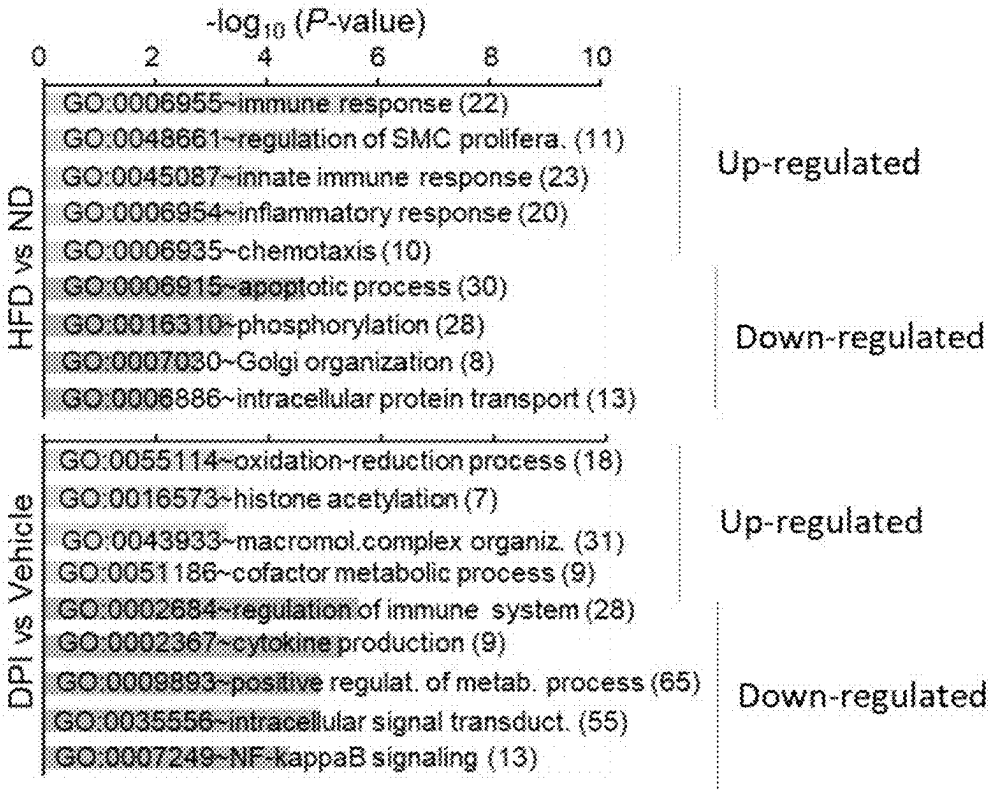

Figure 25B

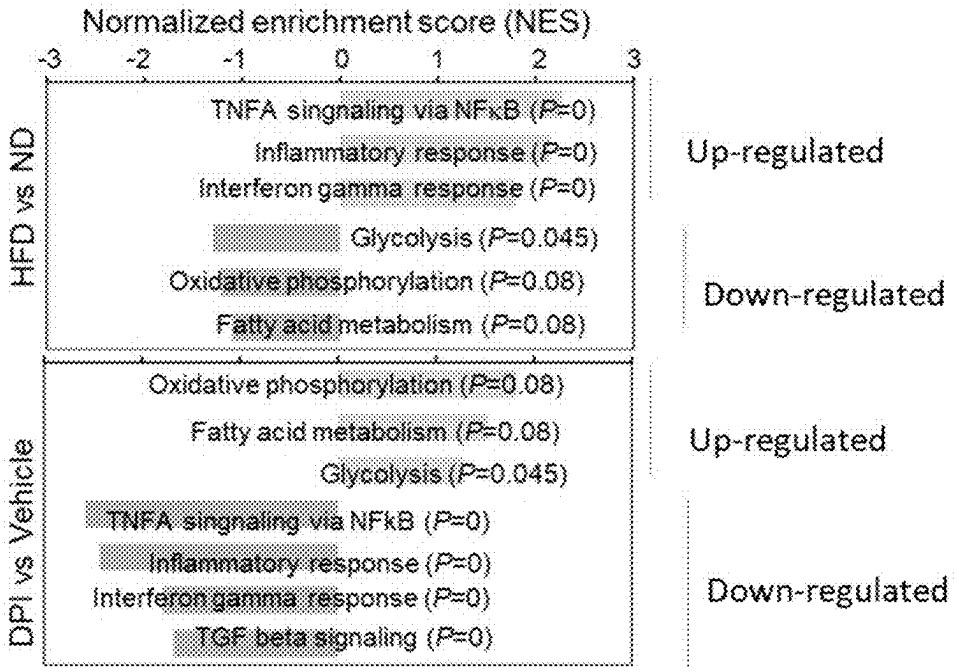

Figure 25C

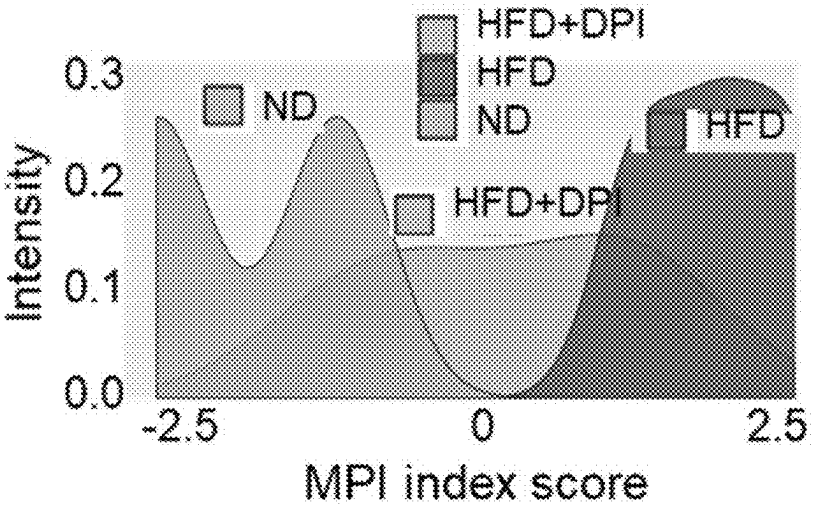

Figure 25D

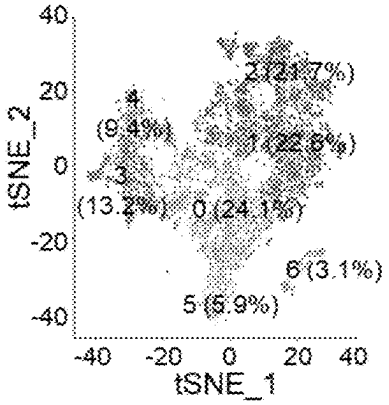

Figure 26A

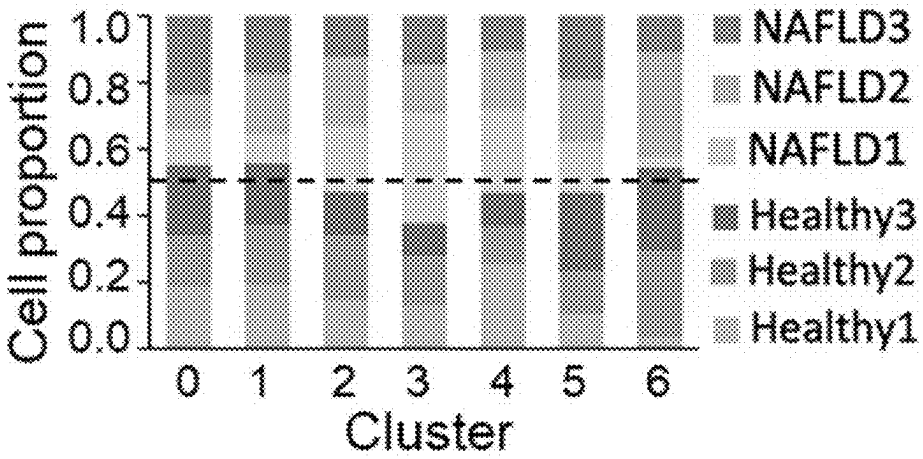

Figure 26B

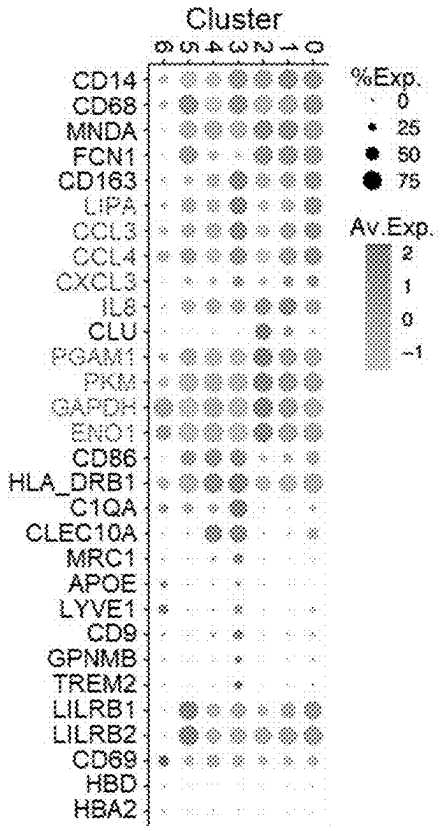

Figure 26C

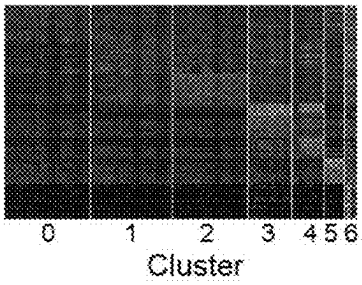

Figure 26D

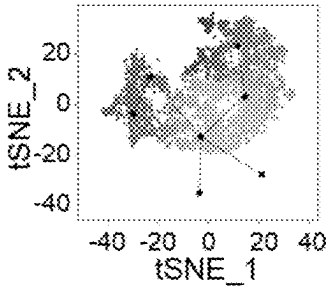

Figure 26E

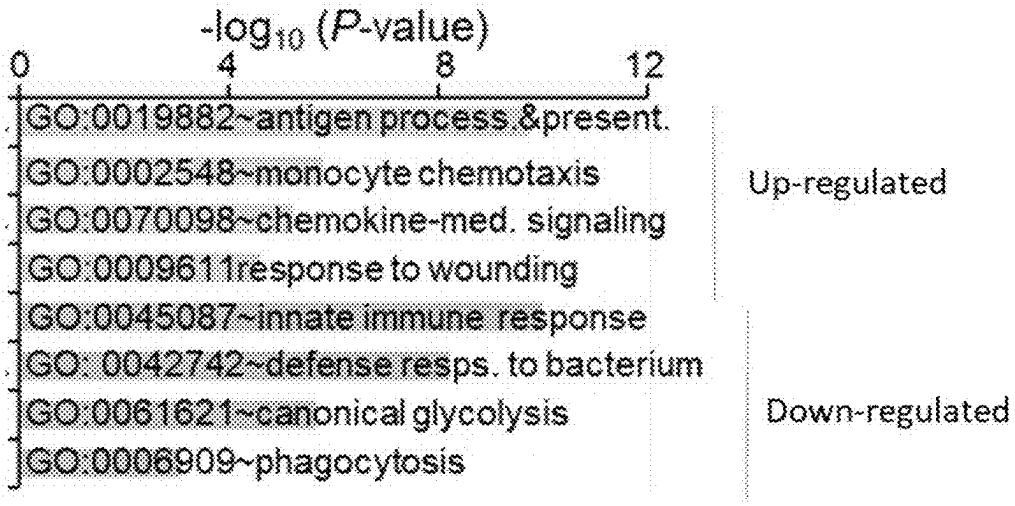

Figure 26F

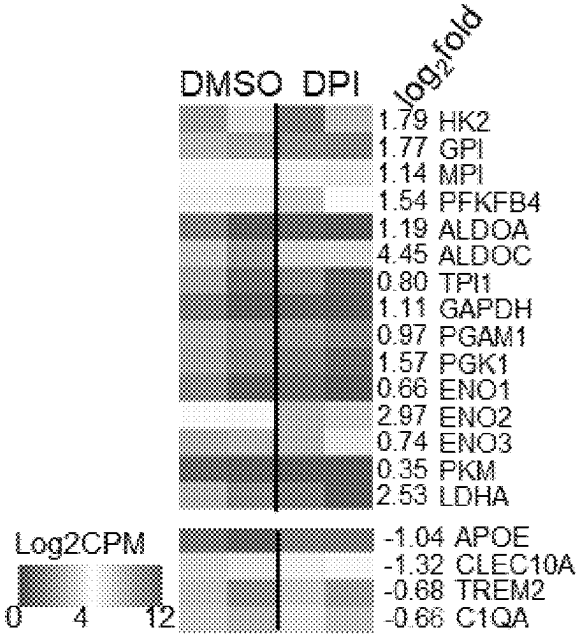

Figure 26G

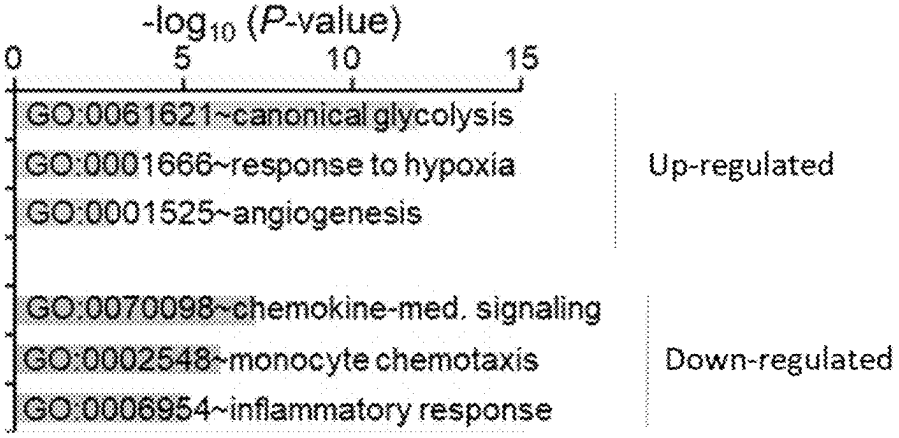

Figure 26H

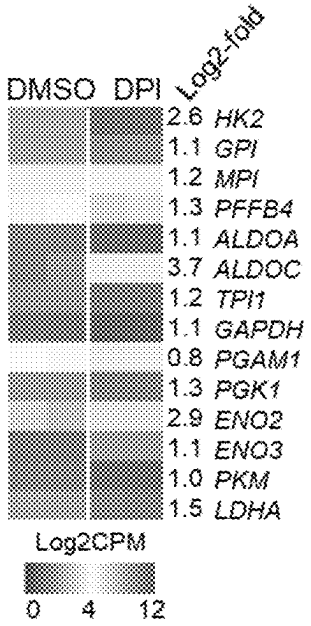

Figure 27A

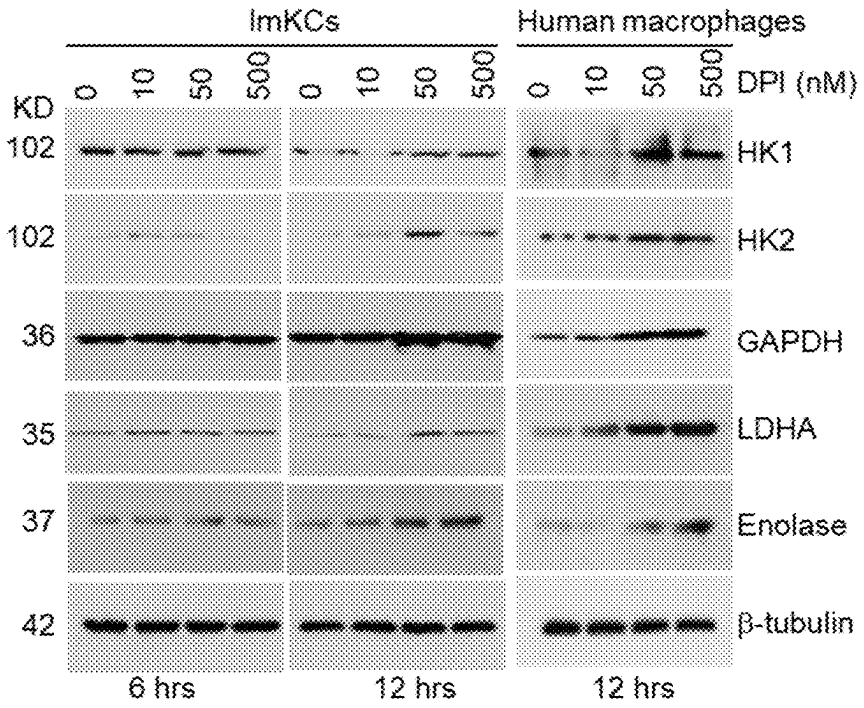

Figure 27B

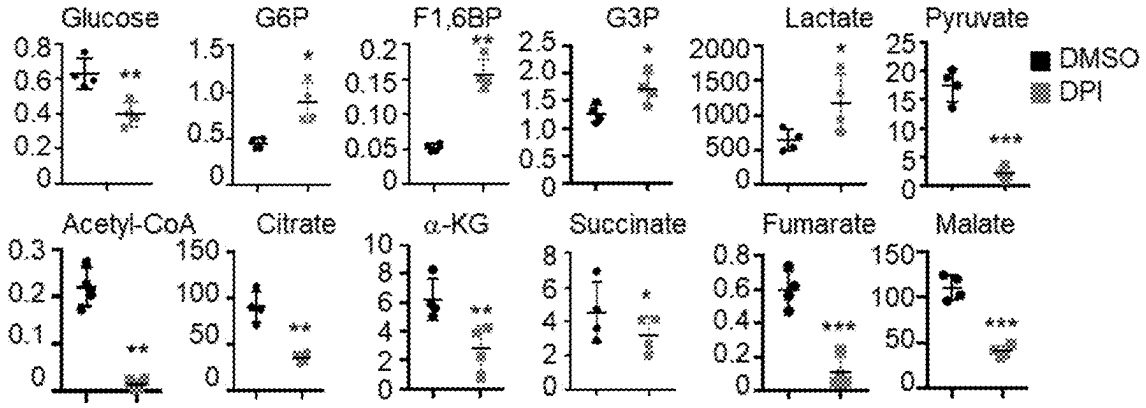

Figure 27C

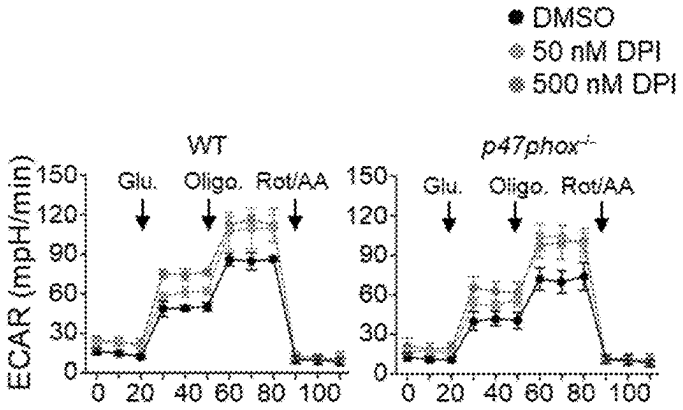

Figure 28A

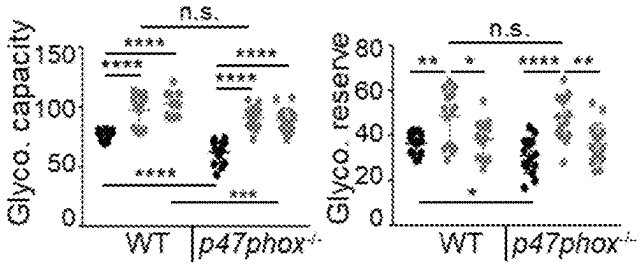

Figure 28B

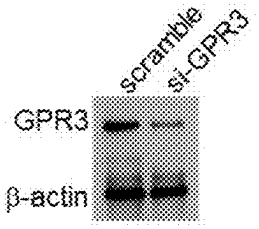

Figure 28C

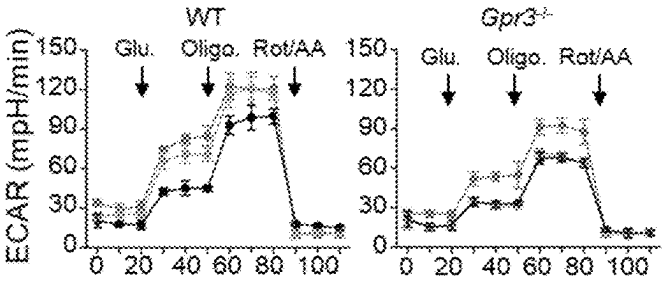

Figure 28D

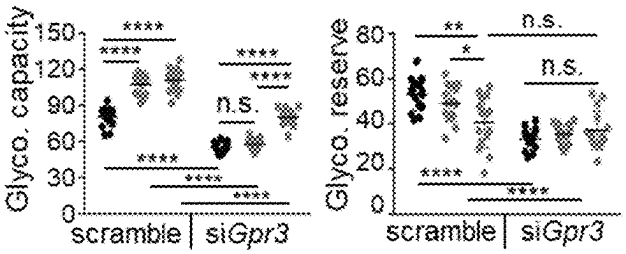

Figure 28E

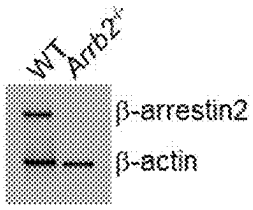

Figure 28F

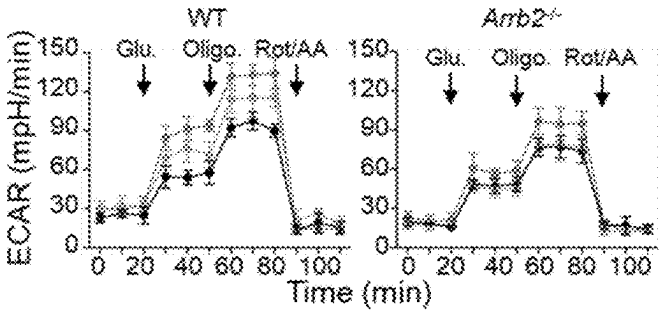

Figure 28G

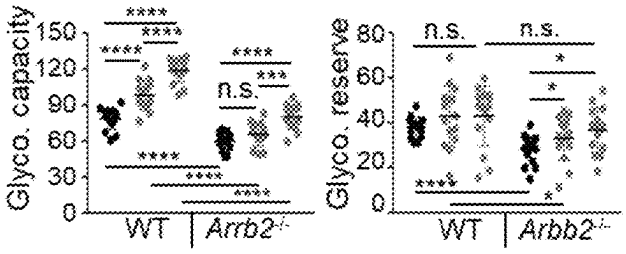

Figure 28H

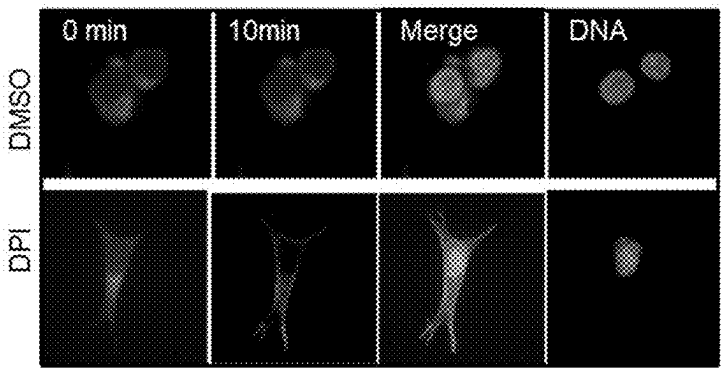

Figure 28I

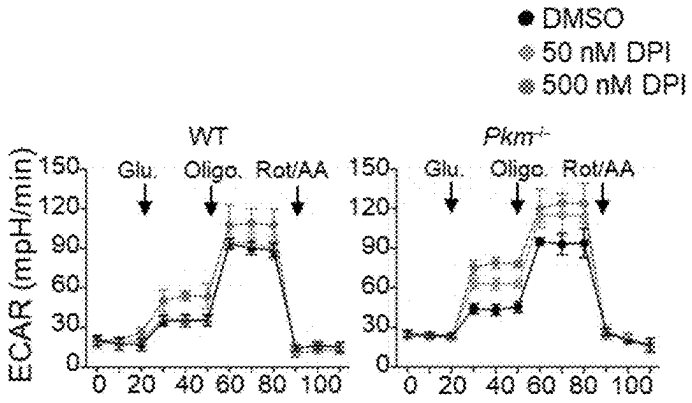

Figure 29A

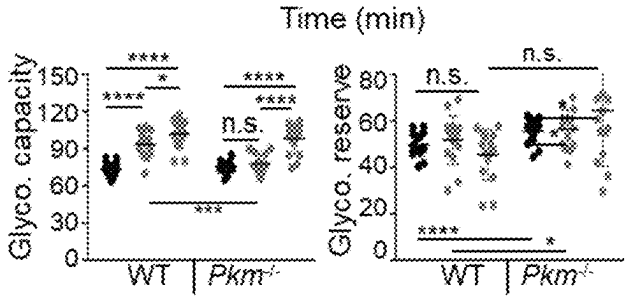

Figure 29B

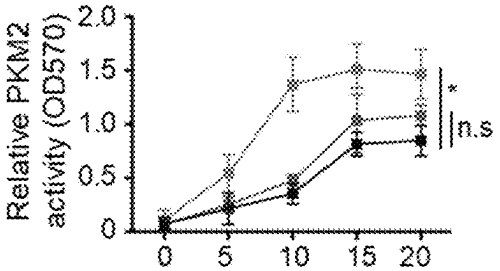

Figure 29C

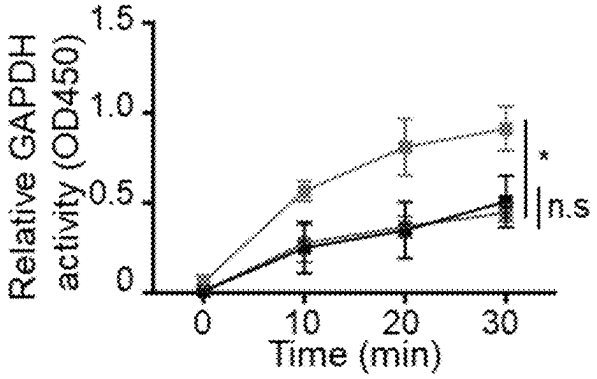

Figure 29D

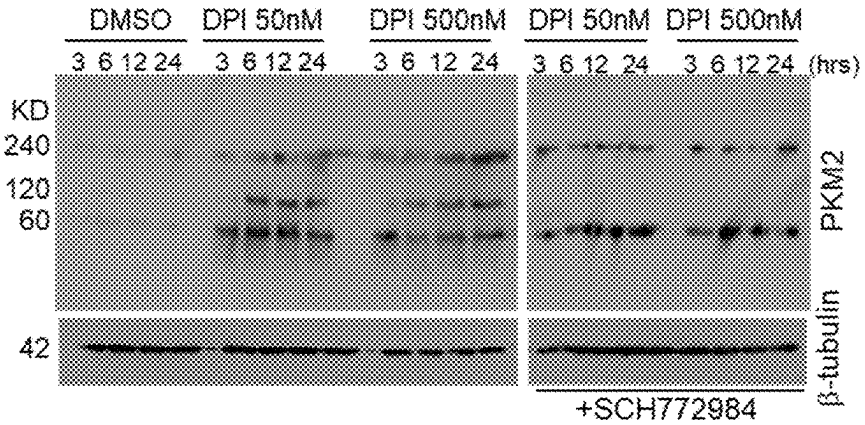

Figure 30A

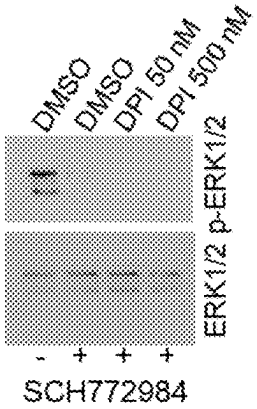

Figure 30B

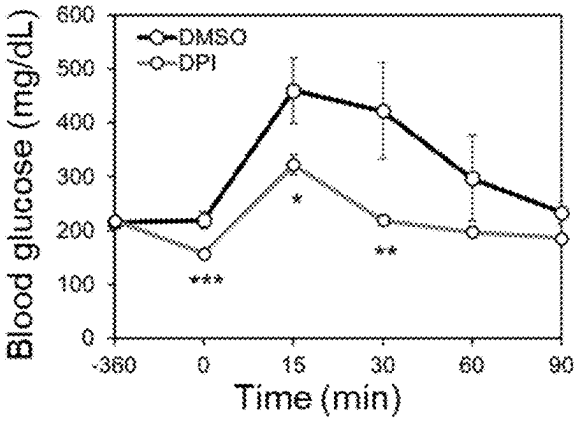

Figure 31

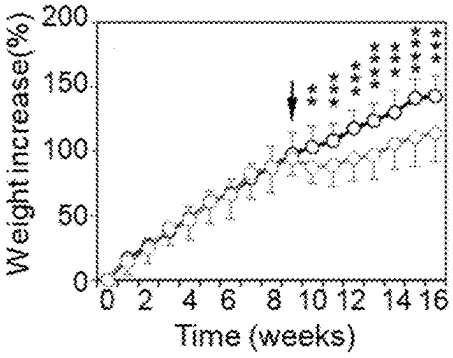

Figure 32A

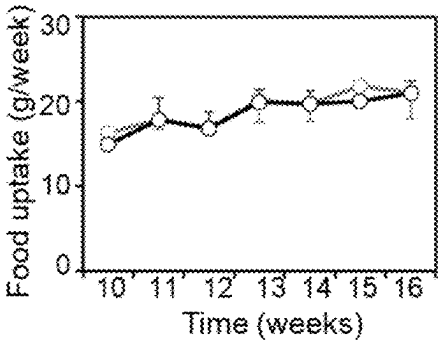

Figure 32B

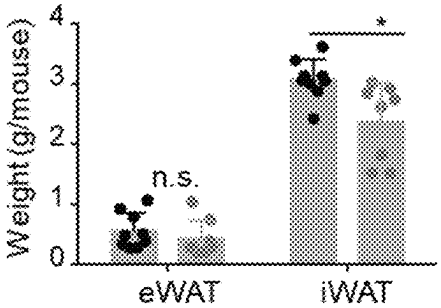

Figure 32C

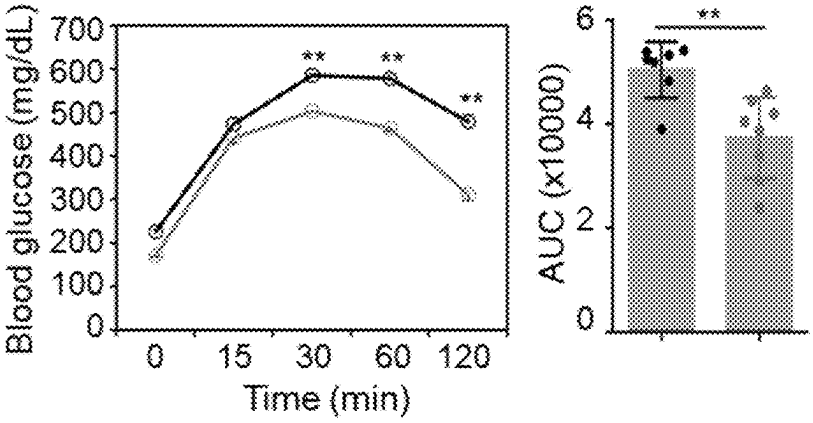

Figure 32D

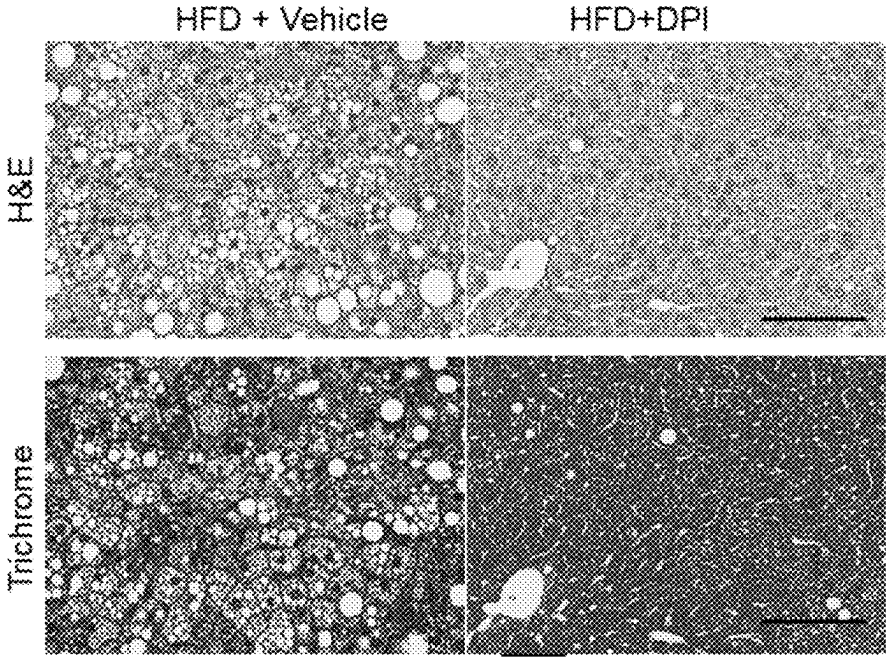

Figure 32E

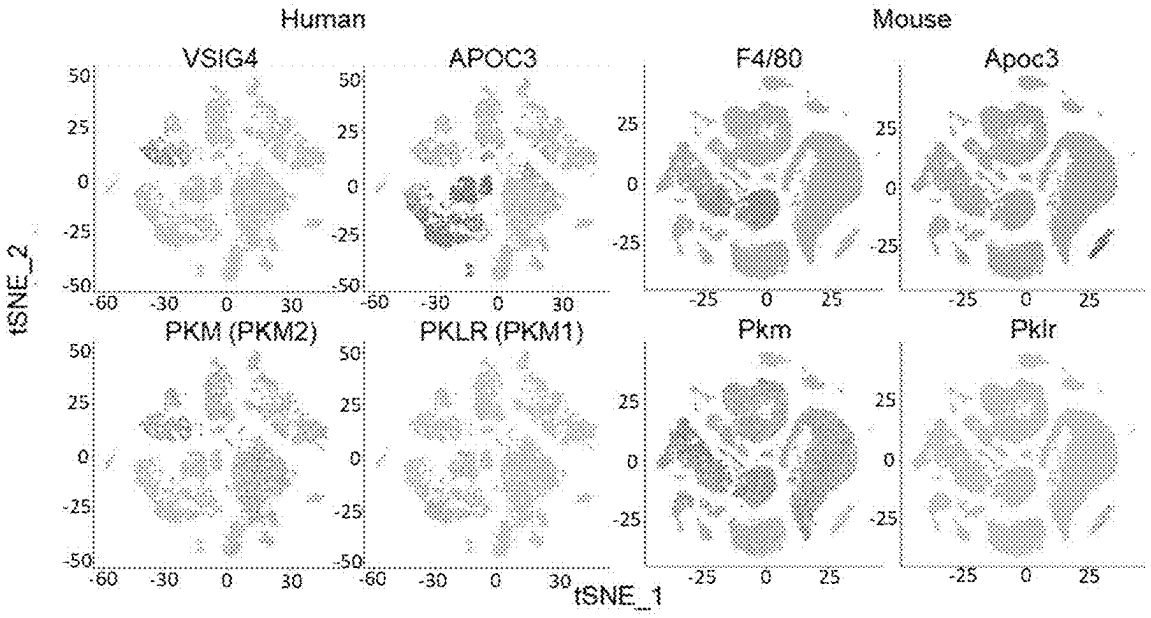

Figure 33

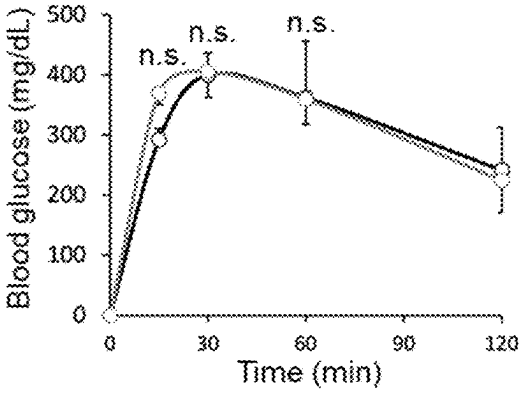

Figure 34A

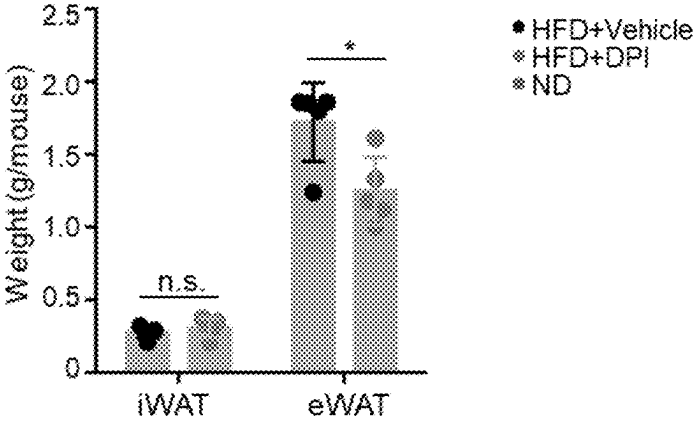

Figure 34B

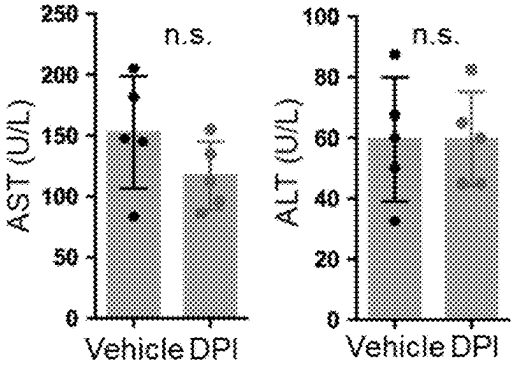

Figure 34C

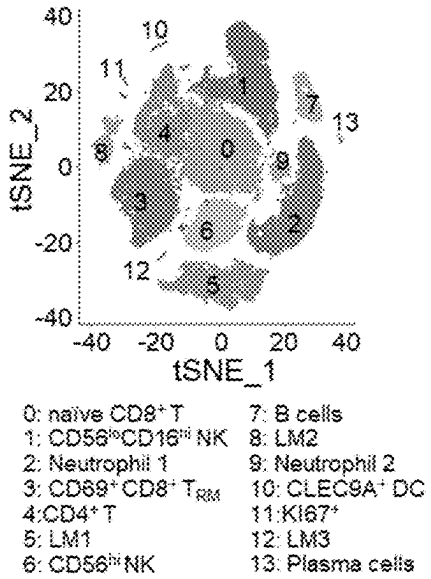

Figure 35A

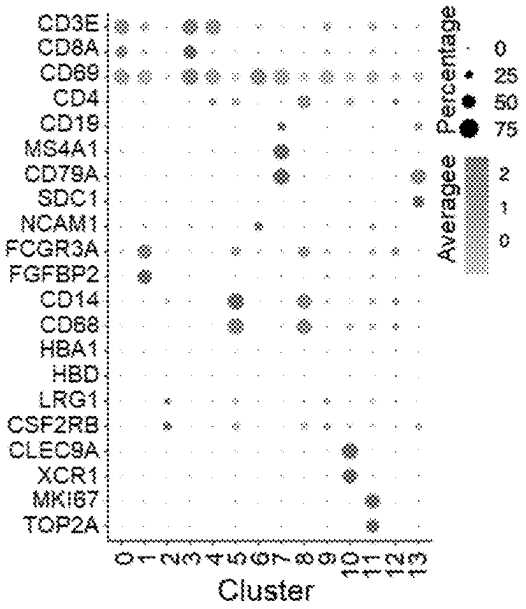

Figure 35B

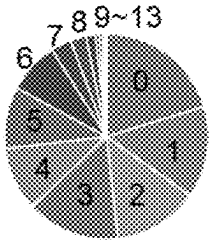

Figure 35C

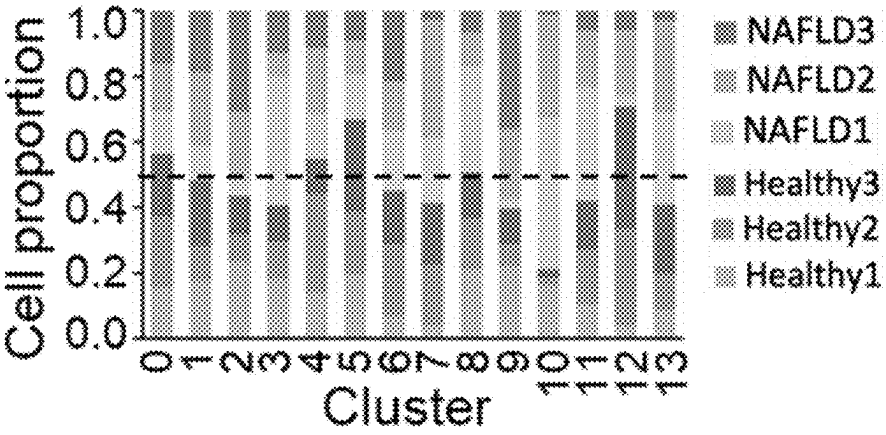

Figure 35D

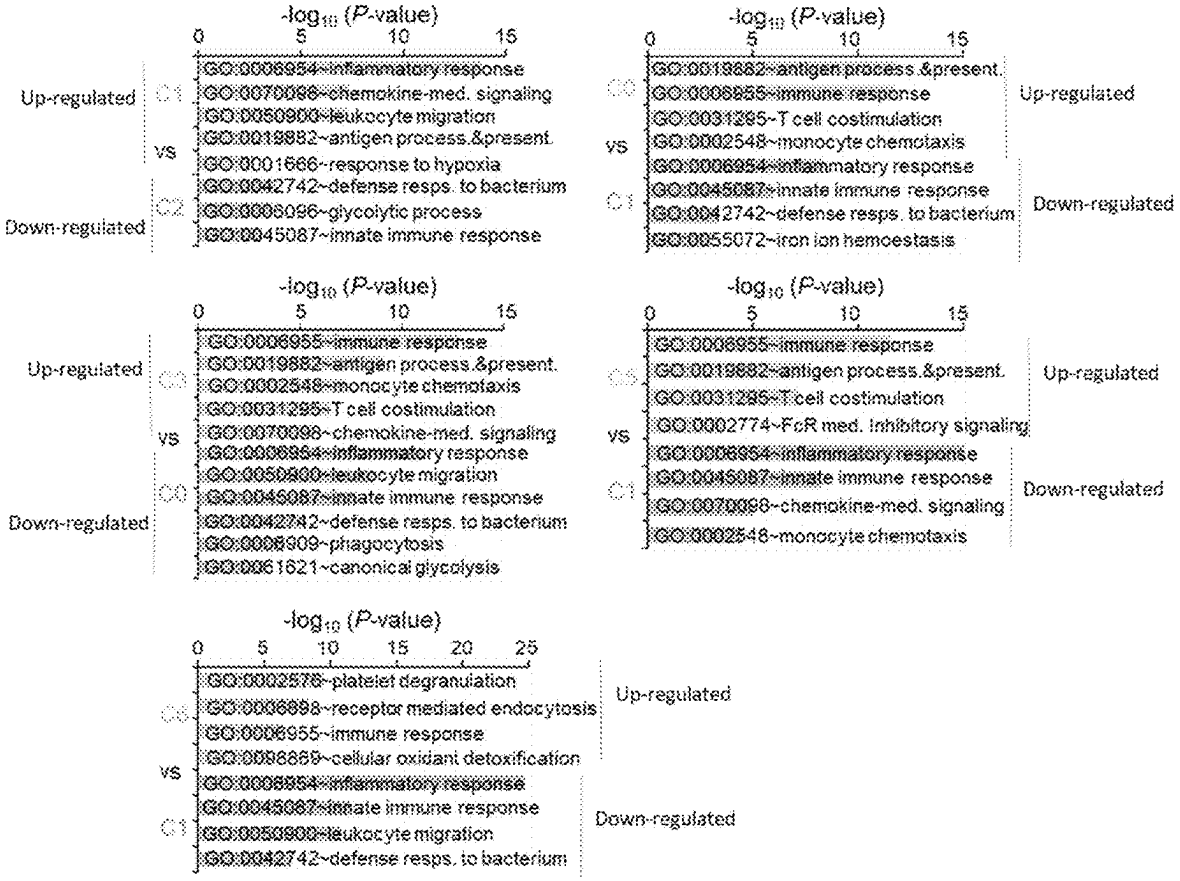
-log10 (P-value)
0 5 10 15
Up-regulated
C1
vs
C2
Down-regulated
GO:0006954~inflammatory response
GO:0070098~chemokine-med. signaling
GO:0050900~leukocyte migration
GO:0019882~antigen process.&present.
GO:0001666~response to hypoxia
GO:0042742~defense resps. to bacterium
GO:0006096~glycolytic process
GO:0045087~innate immune response
-log10 (P-value)
0 5 10 15
C3
vs
C1
Up-regulated
Down-regulated
GO:0019882~antigen process.&present.
GO:0006955~immune response
GO:0031295~T cell costimulation
GO:0002548~monocyte chemotaxis
GO:0006954~inflammatory response
GO:0045087~innate immune response
GO:0042742~defense resps. to bacterium
GO:0055072~iron ion hemoestasis
-log10 (P-value)
0 5 10 15
C3
vs
C2
Up-regulated
Down-regulated
GO:0006955~immune response
GO:0019882~antigen process.&present.
GO:0002548~monocyte chemotaxis
GO:0031295~T cell costimulation
GO:0070098~chemokine-med. signaling
GO:0006954~inflammatory response
GO:0050900~leukocyte migration
GO:0045087~innate immune response
GO:0042742~defense resps. to bacterium
GO:0006909~phagocytosis
GO:0061621~canonical glycolysis
-log10 (P-value)
0 5 10 15
C3
vs
C1
Up-regulated
Down-regulated
GO:0006955~immune response
GO:0019882~antigen process.&present.
GO:0031295~T cell costimulation
GO:0002774~FcR med. inhibitory signaling
GO:0006954~inflammatory response
GO:0045087~innate immune response
GO:0070098~chemokine-med. signaling
GO:0002548~monocyte chemotaxis
-log10 (P-value)
0 5 10 15 20 25
C3
vs
C1
Up-regulated
Down-regulated
GO:0002576~platelet degranulation
GO:0006898~receptor mediated endocytosis
GO:0006955~immune response
GO:0098869~cellular oxidant detoxification
GO:0006954~inflammatory response
GO:0045087~innate immune response
GO:0050900~leukocyte migration
GO:0042742~defense resps. to bacterium

Figure 36

COMPOUNDS, TARGETS AND PATHWAYS FOR MACROPHAGE MODULATION

RELATED APPLICATIONS

[0001] This application is a division of application Ser. No. 17/381,857, filed Jul. 21, 2021; which claims the benefit of priority to U.S. Provisional Patent Application Ser. No. 63/080,988, filed Sep. 21, 2020; the contents of each of said applications are hereby incorporated herein by reference in their entirety.

GOVERNMENT SUPPORT

[0002] This invention was made with Government support under Grant No. R35 CA197605 awarded by the National Institutes of Health (NIH). The Government has certain rights in the invention.

REFERENCE TO A SEQUENCE LISTING XML

[0003] This application contains a Sequence Listing which has been submitted electronically in XML format. The Sequence Listing XML is incorporated herein by reference. Said XML file, created on Apr. 14, 2025, is named MTV-19202_SL.xml and is 36,310 bytes in size.

BACKGROUND

[0004] Macrophages play an essential role in development, tissue homeostasis and repair, and immunity. Most macrophages exhibit multi-dimensional spectrum of phenotypes in response to various physiological and pathological signals. Because of their critical function in maintaining tissue homeostasis and repair, dysregulation of macrophage polarization has been implicated in contributing to many human diseases including cancer, fibrosis, obesity, diabetes, and infectious, cardiovascular, inflammatory and neurodegenerative diseases. Accordingly, there is a great need to identify modulators of macrophage activation for disease intervention.

SUMMARY OF THE INVENTION

[0005] In one aspect, described herein is a method of identifying a modulator of macrophage activation. The method comprises contacting a primary macrophage cell with a candidate agent; monitoring or photographing the morphology of the cell contacted with the candidate agent; and optionally comparing the cell's morphology in the presence of the candidate agent with the cell's morphology in the absence of the candidate agent; wherein a change in morphology in the presence of the candidate agent is indicative of modulation of macrophage activation. Numerous embodiments are further provided that can be applied to any aspect of the present invention described herein. For example, in some embodiments, the primary macrophage cell is a bone marrow-derived macrophage or a monocyte-derived macrophage. In some embodiments, the morphology of the cell is monitored or photographed by a microscope, such as a fluorescence microscope. In some embodiments, the morphology of the cell is monitored or photographed by Opera Phenix high content screening system or CellProfiler. In some embodiments, the morphology of the cell is changed from elongated shape to round shape. In some embodiments, the modulator activates a M1-like macrophage, deactivates a M2-like macrophage, changes a tumor-associated macrophage (TAM) to M1-like macrophage, changes a M2-like macrophage to a M1-like macrophage, changes a M-CSF macrophage to a M1-like macrophage, changes a GM-CSF macrophage to a M1-like macrophage, changes a primary macrophage to a M1-like macrophage, induces LPS, IFNγ or TNFα, or activates a serotonin transporter or receptor, a histamine transporter or receptor, a dopamine transporter or receptor, an adrenoceptor, VEGF, EGF and/or leptin. In some embodiments, the modulator is a M1-activating compound. In some embodiments, the modulator is cytochalasin-B, fenbendazole, parbendazole, methiazole, alprostadil, FTY720, penfluridol, taxol, smer-3, cantharidin, SCH79797, mitoxantrone, niclosamide, MS275, HMN-214, DPI, thiostrepton, evodiamine, cucurbitacin-I, NVP 231, Chlorhexidine, Diphenyleneiodonium, LE135, Fluvoxamine, Mocetinostat, Pimozide, NP-010176, Celastrol, FTY720, WP1130, Prulifloxacin, dihydrocelastryl diacetate, or Quinolinium. In some embodiments, the M1-like macrophage mediates a pro-inflammatory response, an anti-microbial response, and/or an anti-tumor response. In some embodiments, the modulator treats cancer, fibrosis, and/or an infectious disease. In some embodiments, the cancer is hematological malignancy, acute nonlymphocytic leukemia, chronic lymphocytic leukemia, acute granulocytic leukemia, chronic granulocytic leukemia, acute promyelocytic leukemia, adult T-cell leukemia, aleukemic leukemia, a leukocythemic leukemia, basophilic leukemia, blast cell leukemia, bovine leukemia, chronic myelocytic leukemia, leukemia cutis, embryonal leukemia, eosinophilic leukemia, Gross' leukemia, Rieder cell leukemia, Schilling's leukemia, stem cell leukemia, subleukemic leukemia, undifferentiated cell leukemia, hairy-cell leukemia, hemoblastic leukemia, hemocytoblastic leukemia, histiocytic leukemia, stem cell leukemia, acute monocytic leukemia, leukopenic leukemia, lymphatic leukemia, lymphoblastic leukemia, lymphocytic leukemia, lymphogenous leukemia, lymphoid leukemia, lymphosarcoma cell leukemia, mast cell leukemia, megakaryocytic leukemia, micromyeloblastic leukemia, monocytic leukemia, myeloblastic leukemia, myelocytic leukemia, myeloid granulocytic leukemia, myelomonocytic leukemia, Naegeli leukemia, plasma cell leukemia, plasmacytic leukemia, promyelocytic leukemia, acinar carcinoma, acinous carcinoma, adenocystic carcinoma, adenoid cystic carcinoma, carcinoma adenomatosum, carcinoma of adrenal cortex, alveolar carcinoma, alveolar cell carcinoma, basal cell carcinoma, carcinoma basocellulare, basaloid carcinoma, basosquamous cell carcinoma, bronchioalveolar carcinoma, bronchiolar carcinoma, bronchogenic carcinoma, cerebriform carcinoma, cholangiocellular carcinoma, chorionic carcinoma, colloid carcinoma, comedo carcinoma, corpus carcinoma, cribriform carcinoma, carcinoma en cuirasse, carcinoma cutaneum, cylindrical carcinoma, cylindrical cell carcinoma, duct carcinoma, carcinoma durum, embryonal carcinoma, encephaloid carcinoma, epiennoid carcinoma, carcinoma epitheliale adenoides, exophytic carcinoma, carcinoma ex ulcere, carcinoma fibrosum, gelatiniform carcinoma, gelatinous carcinoma, giant cell carcinoma, signet-ring cell carcinoma, carcinoma simplex, small-cell carcinoma, solanoid carcinoma, spheroidal cell carcinoma, spindle cell carcinoma, carcinoma spongiosum, squamous carcinoma, squamous cell carcinoma, string carcinoma, carcinoma telangiectaticum, carcinoma telangiectodes, transitional cell carcinoma, carcinoma tuberosum, tuberous carcinoma, ver-

rucous carcinoma, carcinoma villosum, carcinoma gigantocellulare, glandular carcinoma, granulosa cell carcinoma, hair-matrix carcinoma, hematoid carcinoma, hepatocellular carcinoma, Hurthle cell carcinoma, hyaline carcinoma, hypernephroid carcinoma, infantile embryonal carcinoma, carcinoma in situ, intraepidermal carcinoma, intraepithelial carcinoma, Krompecher's carcinoma, Kulchitzky-cell carcinoma, large-cell carcinoma, lenticular carcinoma, carcinoma lenticulare, lipomatous carcinoma, lymphoepithelial carcinoma, carcinoma medullare, medullary carcinoma, melanotic carcinoma, carcinoma molle, mucinous carcinoma, carcinoma muciparum, carcinoma mucocellulare, mucoepidermoid carcinoma, carcinoma mucosum, mucous carcinoma, carcinoma myxomatodes, naspharyngeal carcinoma, oat cell carcinoma, carcinoma ossificans, osteoid carcinoma, papillary carcinoma, periportal carcinoma, preinvasive carcinoma, prickle cell carcinoma, pultaceous carcinoma, renal cell carcinoma of kidney, reserve cell carcinoma, carcinoma sarcomatodes, schneiderian carcinoma, scirrhous carcinoma, carcinoma scroti, chondrosarcoma, fibrosarcoma, lymphosarcoma, melanosarcoma, myxosarcoma, osteosarcoma, endometrial sarcoma, stromal sarcoma, Ewing's sarcoma, fascial sarcoma, fibroblastic sarcoma, giant cell sarcoma, Abemethy's sarcoma, adipose sarcoma, liposarcoma, alveolar soft part sarcoma, ameloblastic sarcoma, botryoid sarcoma, chloroma sarcoma, chorio carcinoma, embryonal sarcoma, Wilms' tumor sarcoma, granulocytic sarcoma, Hodgkin's sarcoma, idiopathic multiple pigmented hemorrhagic sarcoma, immunoblastic sarcoma of B cells, lymphoma, immunoblastic sarcoma of T-cells, Jensen's sarcoma, Kaposi's sarcoma, Kupffer cell sarcoma, angiosarcoma, leukosarcoma, malignant mesenchymoma sarcoma, parosteal sarcoma, reticulocytic sarcoma, Rous sarcoma, serocystic sarcoma, synovial sarcoma, telangiectaltic sarcoma, Hodgkin's Disease, Non-Hodgkin's Lymphoma, multiple myeloma, neuroblastoma, bladder cancer, breast cancer, ovarian cancer, lung cancer, rhabdomyosarcoma, primary thrombocytosis, primary macroglobulinemia, small-cell lung tumors, primary brain tumors, stomach cancer, colon cancer, malignant pancreatic insulanoma, malignant carcinoid, premalignant skin lesions, testicular cancer, lymphomas, thyroid cancer, neuroblastoma, esophageal cancer, genitourinary tract cancer, malignant hypercalcemia, cervical cancer, endometrial cancer, adrenal cortical cancer, Harding-Passey melanoma, juvenile melanoma, lentigo maligna melanoma, malignant melanoma, acral-lentiginous melanoma, amelanotic melanoma, benign juvenile melanoma, Cloudman's melanoma, S91 melanoma, nodular melanoma subungal melanoma, or superficial spreading melanoma. In some embodiments, the infectious disease is a viral infection, or a bacterial infection. The infection may be associated with COVID-19 (SARS-CoV-2), SARS-CoV, MERS-CoV, Ebola virus, influenza, cytomegalovirus, variola and group A *Streptococcus*, or sepsis.

[0006] In some embodiments, the morphology of the cell is changed from round shape to elongated shape. In some embodiments, the modulator activates a M2-like macrophage, deactivates a M1-like macrophage, changes a M1-like macrophage to a M2-like macrophage, changes a M-CSF macrophage to a M2-like macrophage, changes a GM-CSF macrophage to a M2-like macrophage, changes a primary macrophage to a M2-like macrophage, modulator induces a M2-activating stimuli selected from IL4, IL13 and IL10, or inhibits a serotonin transporter or receptor, a histamine transporter or receptor, a dopamine transporter or receptor, an adrenoceptor, VEGF, EGF and/or leptin. In some embodiments, the modulator is a M2-activating compound. In some embodiments, the modulator is Bostunib, Su11274, Alsterpaullone, Alrestatin, Bisantrene, triptolide, lovastatin, QS 11, Regorafenib, Sorafenib, MLN2238, GW-843682X, KW 2449, Axitinib, JTE 013, Purmorphamine, Arcyriaflavin A, Dasatinib, NVP-LDE225, 1-Naphthyl PP1, Selamectin, MGCD-265, podofilox, colchicine, or vinblastine sulfate. In some embodiments, the M2-like macrophage mediates an anti-inflammatory or a tissue repair response. In some embodiments, the modulator treats an inflammatory disease, a metabolic disease, an autoimmune disease, or a neurodegenerative disease. In some embodiments, the inflammatory disease, the metabolic disease, or the autoimmune disease is diabetes, obesity, non-alcoholic fatty liver disease (NAFLD), hepatic steatosis, non-alcoholic steatohepatitis, cirrhosis, rheumatoid arthritis (RA), acute respiratory distress syndrome (ARDS), cardiovascular disease, remote tissue injury after ischemia and reperfusion, dermatomyositis, pemphigus, lupus nephritis and resultant glomerulonephritis and vasculitis, cardiopulmonary bypass, cardioplegia-induced coronary endothelial dysfunction, type II membranoproliferative glomerulonephritis, IgA nephropathy, acute renal failure, cryoglobulinemia, antiphospholipid syndrome, Chronic open-angle glaucoma, acute closed angle glaucoma, macular degenerative diseases, age-related macular degeneration (AMD), choroidal neovascularization (CNV), uveitis, diabetic retinopathy, ischemia-related retinopathy, endophthalmitis, intraocular neovascular disease, diabetic macular edema, pathological myopia, von Hippel-Lindau disease, histoplasmosis of the eye, Neuromyelitis Optica (NMO), Central Retinal Vein Occlusion (CRVO), corneal neovascularization, retinal neovascularization, Leber's hereditary optic neuropathy, optic neuritis, Behcet's retinopathy, ischemic optic neuropathy, retinal vasculitis, Anti-Neutrophilic Cytoplasmic Autoantibody vasculitis, Purtscher retinopathy, Sjogren's dry eye disease, dry AMD, sarcoidosis, temporal arteritis, polyarteritis nodosa, multiple sclerosis, hyperacute rejection, hemodialysis, chronic occlusive pulmonary distress syndrome (COPD), asthma, aspiration pneumonia, multiple sclerosis, Guillain-Barre syndrome, Myasthenia Gravis, Bullous Pemphigoid, or myositis. In some embodiments, the neurodegenerative disease is Alzheimer's disease, amyotrophic lateral sclerosis, multiple sclerosis, glaucoma, myotonic dystrophy, Guillain-Barre' syndrome (GBS), Myasthenia Gravis, Bullous Pemphigoid, spinal muscular atrophy, Down syndrome, Parkinson's disease, or Huntington's disease.

[0007] In one aspect, described herein is a method of treating cancer, fibrosis, or an infectious disease. The method comprises administering to a subject in need thereof an effective amount of a modulator of macrophage activation; wherein the modulator changes the morphology of a macrophage cell from elongated shape to round shape. Numerous embodiments are further provided that can be applied to any aspect of the present invention described herein. For example, in some embodiments, the modulator activates a M1-like macrophage, deactivates a M2-like macrophage, changes a tumor-associated macrophage (TAM) to M1-like macrophage, changes a M2-like macrophage to a M1-like macrophage, changes a M-CSF macrophage to a M1-like macrophage, changes a GM-CSF macrophage to a

M1-like macrophage, changes a primary macrophage to a M1-like macrophage, induces a M1-activating stimuli selected from LPS, IFNγ and TNFα, or activates a serotonin transporter or receptor, a histamine transporter or receptor, a dopamine transporter or receptor, an adrenoceptor, VEGF, EGF and/or leptin. In some embodiments, the modulator is a M1-activating compound. In some embodiments, the modulator is cytochalasin-B, fenbendazole, parbendazole, methiazole, alprostadil, FTY720, penfluridol, taxol, smer-3, cantharidin, SCH79797, mitoxantrone, niclosamide, MS275, HMN-214, DPI, thiostrepton, evodiamine, cucurbitacin-I, NVP 231, Chlorhexidine, Diphenyleneiodonium, LE135, Fluvoxamine, Mocetinostat, Pimozide, NP-010176, Celastrol, FTY720, WP1130, Prulifloxacin, dihydrocelastryl diacetate, or Quinolinium. In some embodiments, the M1-like macrophage mediates a pro-inflammatory response, an anti-microbial response, and/or an anti-tumor response. In some embodiments, the cancer is hematological malignancy, acute nonlymphocytic leukemia, chronic lymphocytic leukemia, acute granulocytic leukemia, chronic granulocytic leukemia, acute promyelocytic leukemia, adult T-cell leukemia, aleukemic leukemia, a leukocythemic leukemia, basophilic leukemia, blast cell leukemia, bovine leukemia, chronic myelocytic leukemia, leukemia cutis, embryonal leukemia, eosinophilic leukemia, Gross' leukemia, Rieder cell leukemia, Schilling's leukemia, stem cell leukemia, subleukemic leukemia, undifferentiated cell leukemia, hairy-cell leukemia, hemoblastic leukemia, hemocytoblastic leukemia, histiocytic leukemia, stem cell leukemia, acute monocytic leukemia, leukopenic leukemia, lymphatic leukemia, lymphoblastic leukemia, lymphocytic leukemia, lymphogenous leukemia, lymphoid leukemia, lymphosarcoma cell leukemia, mast cell leukemia, megakaryocytic leukemia, micromyeloblastic leukemia, monocytic leukemia, myeloblastic leukemia, myelocytic leukemia, myeloid granulocytic leukemia, myelomonocytic leukemia, Naegeli leukemia, plasma cell leukemia, plasmacytic leukemia, promyelocytic leukemia, acinar carcinoma, acinous carcinoma, adenocystic carcinoma, adenoid cystic carcinoma, carcinoma adenomatosum, carcinoma of adrenal cortex, alveolar carcinoma, alveolar cell carcinoma, basal cell carcinoma, carcinoma basocellulare, basaloid carcinoma, basosquamous cell carcinoma, bronchioalveolar carcinoma, bronchiolar carcinoma, bronchogenic carcinoma, cerebriform carcinoma, cholangiocellular carcinoma, chorionic carcinoma, colloid carcinoma, comedo carcinoma, corpus carcinoma, cribriform carcinoma, carcinoma en cuirasse, carcinoma cutaneum, cylindrical carcinoma, cylindrical cell carcinoma, duct carcinoma, carcinoma durum, embryonal carcinoma, encephaloid carcinoma, epiennoid carcinoma, carcinoma epitheliale adenoides, exophytic carcinoma, carcinoma ex ulcere, carcinoma fibrosum, gelatiniform carcinoma, gelatinous carcinoma, giant cell carcinoma, signet-ring cell carcinoma, carcinoma simplex, small-cell carcinoma, solanoid carcinoma, spheroidal cell carcinoma, spindle cell carcinoma, carcinoma spongiosum, squamous carcinoma, squamous cell carcinoma, string carcinoma, carcinoma telangiectaticum, carcinoma telangiectodes, transitional cell carcinoma, carcinoma tuberosum, tuberous carcinoma, verrucous carcinoma, carcinoma villosum, carcinoma gigantocellulare, glandular carcinoma, granulosa cell carcinoma, hair-matrix carcinoma, hematoid carcinoma, hepatocellular carcinoma, Hurthle cell carcinoma, hyaline carcinoma, hypernephroid carcinoma, infantile embryonal carcinoma, carcinoma in situ, intraepidermal carcinoma, intraepithelial carcinoma, Krompecher's carcinoma, Kulchitzky-cell carcinoma, large-cell carcinoma, lenticular carcinoma, carcinoma lenticulare, lipomatous carcinoma, lymphoepithelial carcinoma, carcinoma medullare, medullary carcinoma, melanotic carcinoma, carcinoma molle, mucinous carcinoma, carcinoma muciparum, carcinoma mucocellulare, mucoepidermoid carcinoma, carcinoma mucosum, mucous carcinoma, carcinoma myxomatodes, naspharyngeal carcinoma, oat cell carcinoma, carcinoma ossificans, osteoid carcinoma, papillary carcinoma, periportal carcinoma, preinvasive carcinoma, prickle cell carcinoma, pultaceous carcinoma, renal cell carcinoma of kidney, reserve cell carcinoma, carcinoma sarcomatodes, schneiderian carcinoma, scirrhous carcinoma, carcinoma scroti, chondrosarcoma, fibrosarcoma, lymphosarcoma, melanosarcoma, myxosarcoma, osteosarcoma, endometrial sarcoma, stromal sarcoma, Ewing's sarcoma, fascial sarcoma, fibroblastic sarcoma, giant cell sarcoma, Abemethy's sarcoma, adipose sarcoma, liposarcoma, alveolar soft part sarcoma, ameloblastic sarcoma, botryoid sarcoma, chloroma sarcoma, chorio carcinoma, embryonal sarcoma, Wilms' tumor sarcoma, granulocytic sarcoma, Hodgkin's sarcoma, idiopathic multiple pigmented hemorrhagic sarcoma, immunoblastic sarcoma of B cells, lymphoma, immunoblastic sarcoma of T-cells, Jensen's sarcoma, Kaposi's sarcoma, Kupffer cell sarcoma, angiosarcoma, leukosarcoma, malignant mesenchymoma sarcoma, parosteal sarcoma, reticulocytic sarcoma, Rous sarcoma, serocystic sarcoma, synovial sarcoma, telangiectaltic sarcoma, Hodgkin's Disease, Non-Hodgkin's Lymphoma, multiple myeloma, neuroblastoma, bladder cancer, breast cancer, ovarian cancer, lung cancer, rhabdomyosarcoma, primary thrombocytosis, primary macroglobulinemia, small-cell lung tumors, primary brain tumors, stomach cancer, colon cancer, malignant pancreatic insulanoma, malignant carcinoid, premalignant skin lesions, testicular cancer, lymphomas, thyroid cancer, neuroblastoma, esophageal cancer, genitourinary tract cancer, malignant hypercalcemia, cervical cancer, endometrial cancer, adrenal cortical cancer, Harding-Passey melanoma, juvenile melanoma, lentigo maligna melanoma, malignant melanoma, acral-lentiginous melanoma, amelanotic melanoma, benign juvenile melanoma, Cloudman's melanoma, S91 melanoma, nodular melanoma subungal melanoma, or superficial spreading melanoma. In some embodiments, the method further comprises administering to the subject an effective amount of a second cancer therapy. In some embodiments, the second cancer therapy comprises cancer immunotherapy. In some embodiments, the cancer immunotherapy comprises administering an immune checkpoint inhibitor, such as an antibody or antigen-binding fragment thereof that specifically binds to an immune checkpoint protein. The immune checkpoint protein may be CTLA4, PD-1, PD-L1, PD-L2, A2AR, B7-H3, B7-H4, BTLA, KIR, LAG3, TIM-3 or VISTA. The immune checkpoint inhibitor may be atezolizumab, avelumab, durvalumab, ipilimumab, nivolumab, pembrolizumab, pidilizumab, AMP-224, AMP-514, BGB-A317, STI-A1110, TSR-042, RG-7446, BMS-936559, MEDI-4736, MSB-0020718C, AUR-012 or STI-A1010. In some embodiments, the second cancer therapy comprises the administration of a chemotherapy agent, such as rituxumab, thiotepa, cyclosphosphamide, busulfan, improsulfan, piposulfan, benzodopa, carboquone, meturedopa, uredopa, altretamine, triethylenemelamine, trietylenephosphoramide,

triethiylenethiophosphoramide, trimethylolomelamine, bullatacin, bullatacinone, camptothecin, topotecan, bryostatin, callystatin, CC-1065, cryptophycin 1, cryptophycin 8, dolastatin, duocarmycin, eleutherobin, pancratistatin, sarcodictyin, spongistatin, chlorambucil, chlornaphazine, cholophosphamide, estramustine, ifosfamide, mechlorethamine, mechlorethamine oxide hydrochloride, melphalan, novembichin, phenesterine, prednimustine, trofosfamide, uracil mustard, carmustine, chlorozotocin, fotemustine, lomustine, nimustine, ranimnustine, calicheamicin, dynemicin, clodronate, esperamicin; neocarzinostatin chromophore, aclacinomysins, actinomycin, authrarnycin, azaserine, bleomycins, cactinomycin, carabicin, caminomycin, carzinophilin, chromomycinis, dactinomycin, daunorubicin, detorubicin, 6-diazo-5-oxo-L-norleucine, doxorubicin, epirubicin, esorubicin, idarubicin, marcellomycin, mitomycin, mitomycin C, mycophenolic acid, nogalamycin, olivomycin, peplomycin, potfiromycin, puromycin, quelamycin, rodorubicin, streptonigrin, streptozocin, tubercidin, ubenimex, zinostatin, zorubicin, methotrexate, 5-fluorouracil (5-FU), denopterin, methotrexate, pteropterin, trimetrexate, fludarabine, 6-mercaptopurine, thiamiprine, thioguanine, ancitabine, azacitidine, 6-azauridine, carmofur, cytarabine, dideoxyuridine, doxifluridine, enocitabine, floxuridine, calusterone, dromostanolone propionate, epitiostanol, mepitiostane, testolactone, aminoglutethimide, mitotane, trilostane, frolinic acid, aceglatone, aldophosphamide glycoside, aminolevulinic acid, eniluracil, amsacrine, bestrabucil, bisantrene, edatraxate, defofamine, demecolcine, diaziquone, elformithine, elliptinium acetate, epothilone, etoglucid, gallium nitrate, hydroxyurea, lentinan, lonidainine, maytansine, ansamitocins, mitoguazone, mitoxantrone, mopidanmol, nitraerine, pentostatin, phenamet, pirarubicin, losoxantrone, podophyllinic acid, 2-ethylhydrazide, procarbazine, PSK polysaccharide complex, razoxane, rhizoxin, sizofuran, spirogermanium, tenuazonic acid, triaziquone; 2,2',2"-trichlorotriethylamine, trichothecene, T-2 toxin, verracurin A, roridin A, anguidine, urethane, vindesine, dacarbazine, mannomustine, mitobronitol, mitolactol, pipobroman, gacytosine, arabinoside, cyclophosphamide, thiotepa, paclitaxel, doxetaxel, chlorambucil, gemcitabine, 6-thioguanine, mercaptopurine, methotrexate, cisplatin, oxaliplatin, carboplatin, vinblastine, platinum, etoposide, ifosfamide, mitoxantrone, vincristine, vinorelbine, novantrone, teniposide, edatrexate, daunomycin, aminopterin, xeloda, ibandronate, irinotecan, RFS 2000, difluoromethylomithine, retinoic acid or capecitabine. In some embodiments, the infectious disease is a viral infection, or a bacterial infection. In some embodiments, the infection is associated with COVID-19 (SARS-CoV-2), SARS-CoV, MERS-CoV, Ebola virus, influenza, cytomegalovirus, variola and group A *Streptococcus*, or sepsis.

[0008] In one aspect, described herein is a method of treating an inflammatory disease, a metabolic disease, an autoimmune disease, or a neurodegenerative disease. The method comprises administering to a subject in need thereof an effective amount of a modulator of macrophage activation; wherein the modulator changes the morphology of a macrophage cell from round shape to elongated shape. Numerous embodiments are further provided that can be applied to any aspect of the present invention described herein. For example, in some embodiments, the modulator activates a M2-like macrophage, deactivates a M1-like macrophage, changes a M1-like macrophage to a M2-like macrophage, changes a M-CSF macrophage to a M2-like macrophage, changes a GM-CSF macrophage to a M2-like macrophage, changes a primary macrophage to a M2-like macrophage, induces a M2-activating stimuli selected from IL4, IL13 and IL10, or inhibits a serotonin transporter or receptor, a histamine transporter or receptor, a dopamine transporter or receptor, an adrenoceptor, VEGF, EGF and/or leptin. In some embodiments, the modulator is a M2-activating compound. In some embodiments, the modulator is Bostunib, Su11274, Alsterpaullone, Alrestatin, Bisantrene, triptolide, lovastatin, QS 11, Regorafenib, Sorafenib, MLN2238, GW-843682X, KW 2449, Axitinib, JTE 013, Purmorphamine, Arcyriaflavin A, Dasatinib, NVP-LDE225, 1-Naphthyl PP1, Selamectin, MGCD-265, podofilox, colchicine, or vinblastine sulfate. In some embodiments, the M2-like macrophage mediates an anti-inflammatory or a tissue repair response. In some embodiments, the inflammatory disease, the metabolic disease, or the autoimmune disease is diabetes, obesity, non-alcoholic fatty liver disease (NAFLD), hepatic steatosis, non-alcoholic steatohepatitis, cirrhosis, rheumatoid arthritis (RA), acute respiratory distress syndrome (ARDS), cardiovascular disease, remote tissue injury after ischemia and reperfusion, dermatomyositis, pemphigus, lupus nephritis and resultant glomerulonephritis and vasculitis, cardiopulmonary bypass, cardioplegia-induced coronary endothelial dysfunction, type II membranoproliferative glomerulonephritis, IgA nephropathy, acute renal failure, cryoglobulinemia, antiphospholipid syndrome, Chronic open-angle glaucoma, acute closed angle glaucoma, macular degenerative diseases, age-related macular degeneration (AMD), choroidal neovascularization (CNV), uveitis, diabetic retinopathy, ischemia-related retinopathy, endophthalmitis, intraocular neovascular disease, diabetic macular edema, pathological myopia, von Hippel-Lindau disease, histoplasmosis of the eye, Neuromyelitis Optica (NMO), Central Retinal Vein Occlusion (CRVO), corneal neovascularization, retinal neovascularization, Leber's hereditary optic neuropathy, optic neuritis, Behcet's retinopathy, ischemic optic neuropathy, retinal vasculitis, Anti-Neutrophilic Cytoplasmic Autoantibody vasculitis, Purtscher retinopathy, Sjogren's dry eye disease, dry AMD, sarcoidosis, temporal arteritis, polyarteritis nodosa, multiple sclerosis, hyperacute rejection, hemodialysis, chronic occlusive pulmonary distress syndrome (COPD), asthma, aspiration pneumonia, multiple sclerosis, Guillain-Barre syndrome, Myasthenia Gravis, Bullous Pemphigoid, or myositis. In some embodiments, the neurodegenerative disease is Alzheimer's disease, amyotrophic lateral sclerosis, multiple sclerosis, glaucoma, myotonic dystrophy, Guillain-Barre' syndrome (GBS), Myasthenia Gravis, Bullous Pemphigoid, spinal muscular atrophy, Down syndrome, Parkinson's disease, or Huntington's disease.

[0009] In one aspect, described herein is a method of treating cancer, fibrosis, or an infectious disease. The method comprises administering to a subject in need thereof an effective amount of a modulator of macrophage activation; wherein the modulator activates a serotonin transporter or receptor, a histamine transporter or receptor, a dopamine transporter or receptor, an adrenoceptor, VEGF, EGF and/or leptin. Numerous embodiments are further provided that can be applied to any aspect of the present invention described herein. For example, in some embodiments, the modulator is cytochalasin-B, fenbendazole, parbendazole, methiazole, alprostadil, FTY720, penfluridol, taxol, smer-3, cantharidin,

SCH79797, mitoxantrone, niclosamide, MS275, HMN-214, DPI, thiostrepton, evodiamine, cucurbitacin-I, NVP 231, Chlorhexidine, Diphenyleneiodonium, LE135, Fluvoxamine, Mocetinostat, Pimozide, NP-010176, Celastrol, FTY720, WP1130, Prulifloxacin, dihydrocelastryl diacetate, or Quinolinium. In some embodiments, the cancer is hematological malignancy, acute nonlymphocytic leukemia, chronic lymphocytic leukemia, acute granulocytic leukemia, chronic granulocytic leukemia, acute promyelocytic leukemia, adult T-cell leukemia, aleukemic leukemia, a leukocythemic leukemia, basophilic leukemia, blast cell leukemia, bovine leukemia, chronic myelocytic leukemia, leukemia cutis, embryonal leukemia, eosinophilic leukemia, Gross' leukemia, Rieder cell leukemia, Schilling's leukemia, stem cell leukemia, subleukemic leukemia, undifferentiated cell leukemia, hairy-cell leukemia, hemoblastic leukemia, hemocytoblastic leukemia, histiocytic leukemia, stem cell leukemia, acute monocytic leukemia, leukopenic leukemia, lymphatic leukemia, lymphoblastic leukemia, lymphocytic leukemia, lymphogenous leukemia, lymphoid leukemia, lymphosarcoma cell leukemia, mast cell leukemia, megakaryocytic leukemia, micromyeloblastic leukemia, monocytic leukemia, myeloblastic leukemia, myelocytic leukemia, myeloid granulocytic leukemia, myelomonocytic leukemia, Naegeli leukemia, plasma cell leukemia, plasmacytic leukemia, promyelocytic leukemia, acinar carcinoma, acinous carcinoma, adenocystic carcinoma, adenoid cystic carcinoma, carcinoma adenomatosum, carcinoma of adrenal cortex, alveolar carcinoma, alveolar cell carcinoma, basal cell carcinoma, carcinoma basocellulare, basaloid carcinoma, basosquamous cell carcinoma, bronchioalveolar carcinoma, bronchiolar carcinoma, bronchogenic carcinoma, cerebriform carcinoma, cholangiocellular carcinoma, chorionic carcinoma, colloid carcinoma, comedo carcinoma, corpus carcinoma, cribriform carcinoma, carcinoma en cuirasse, carcinoma cutaneum, cylindrical carcinoma, cylindrical cell carcinoma, duct carcinoma, carcinoma durum, embryonal carcinoma, encephaloid carcinoma, epiennoid carcinoma, carcinoma epitheliale adenoides, exophytic carcinoma, carcinoma ex ulcere, carcinoma fibrosum, gelatiniform carcinoma, gelatinous carcinoma, giant cell carcinoma, signet-ring cell carcinoma, carcinoma simplex, small-cell carcinoma, solanoid carcinoma, spheroidal cell carcinoma, spindle cell carcinoma, carcinoma spongiosum, squamous carcinoma, squamous cell carcinoma, string carcinoma, carcinoma telangiectaticum, carcinoma telangiectodes, transitional cell carcinoma, carcinoma tuberosum, tuberous carcinoma, verrucous carcinoma, carcinoma villosum, carcinoma gigantocellulare, glandular carcinoma, granulosa cell carcinoma, hair-matrix carcinoma, hematoid carcinoma, hepatocellular carcinoma, Hurthle cell carcinoma, hyaline carcinoma, hypernephroid carcinoma, infantile embryonal carcinoma, carcinoma in situ, intraepidermal carcinoma, intraepithelial carcinoma, Krompecher's carcinoma, Kulchitzky-cell carcinoma, large-cell carcinoma, lenticular carcinoma, carcinoma lenticulare, lipomatous carcinoma, lymphoepithelial carcinoma, carcinoma medullare, medullary carcinoma, melanotic carcinoma, carcinoma molle, mucinous carcinoma, carcinoma muciparum, carcinoma mucocellulare, mucoepidermoid carcinoma, carcinoma mucosum, mucous carcinoma, carcinoma myxomatodes, naspharyngeal carcinoma, oat cell carcinoma, carcinoma ossificans, osteoid carcinoma, papillary carcinoma, periportal carcinoma, preinvasive carcinoma, prickle cell carcinoma, pultaceous carcinoma, renal cell carcinoma of kidney, reserve cell carcinoma, carcinoma sarcomatodes, schneiderian carcinoma, scirrhous carcinoma, carcinoma scroti, chondrosarcoma, fibrosarcoma, lymphosarcoma, melanosarcoma, myxosarcoma, osteosarcoma, endometrial sarcoma, stromal sarcoma, Ewing's sarcoma, fascial sarcoma, fibroblastic sarcoma, giant cell sarcoma, Abemethy's sarcoma, adipose sarcoma, liposarcoma, alveolar soft part sarcoma, ameloblastic sarcoma, botryoid sarcoma, chloroma sarcoma, chorio carcinoma, embryonal sarcoma, Wilms' tumor sarcoma, granulocytic sarcoma, Hodgkin's sarcoma, idiopathic multiple pigmented hemorrhagic sarcoma, immunoblastic sarcoma of B cells, lymphoma, immunoblastic sarcoma of T-cells, Jensen's sarcoma, Kaposi's sarcoma, Kupffer cell sarcoma, angiosarcoma, leukosarcoma, malignant mesenchymoma sarcoma, parosteal sarcoma, reticulocytic sarcoma, Rous sarcoma, serocystic sarcoma, synovial sarcoma, telangiectaltic sarcoma, Hodgkin's Disease, Non-Hodgkin's Lymphoma, multiple myeloma, neuroblastoma, bladder cancer, breast cancer, ovarian cancer, lung cancer, rhabdomyosarcoma, primary thrombocytosis, primary macroglobulinemia, small-cell lung tumors, primary brain tumors, stomach cancer, colon cancer, malignant pancreatic insulanoma, malignant carcinoid, premalignant skin lesions, testicular cancer, lymphomas, thyroid cancer, neuroblastoma, esophageal cancer, genitourinary tract cancer, malignant hypercalcemia, cervical cancer, endometrial cancer, adrenal cortical cancer, Harding-Passey melanoma, juvenile melanoma, lentigo maligna melanoma, malignant melanoma, acral-lentiginous melanoma, amelanotic melanoma, benign juvenile melanoma, Cloudman's melanoma, S91 melanoma, nodular melanoma subungal melanoma, or superficial spreading melanoma. In some embodiments, the method further comprises administering to the subject an effective amount of a second cancer therapy. In some embodiments, the second cancer therapy is cancer immunotherapy, such as an immune checkpoint inhibitor, for example, an antibody or antigen-binding fragment thereof that specifically binds to an immune checkpoint protein. In some embodiments, the immune checkpoint protein is CTLA4, PD-1, PD-L1, PD-L2, A2AR, B7-H3, B7-H4, BTLA, KIR, LAG3, TIM-3 or VISTA. In some embodiments, the immune checkpoint inhibitor is atezolizumab, avelumab, durvalumab, ipilimumab, nivolumab, pembrolizumab, pidilizumab, AMP-224, AMP-514, BGB-A317, STI-A1110, TSR-042, RG-7446, BMS-936559, MEDI-4736, MSB-0020718C, AUR-012 or STI-A1010. In some embodiments, the second cancer therapy is a chemotherapy agent, such as rituxumab, thiotepa, cyclosphosphamide, busulfan, improsulfan, piposulfan, benzodopa, carboquone, meturedopa, uredopa, altretamine, triethylenemelamine, trietylenephosphoramide, triethiylenethiophosphoramide, trimethylolomelamine, bullatacin, bullatacinone, camptothecin, topotecan, bryostatin, callystatin, CC-1065, cryptophycin 1, cryptophycin 8, dolastatin, duocarmycin, eleutherobin, pancratistatin, sarcodictyin, spongistatin, chlorambucil, chlornaphazine, cholophosphamide, estramustine, ifosfamide, mechlorethamine, mechlorethamine oxide hydrochloride, melphalan, novembichin, phenesterine, prednimustine, trofosfamide, uracil mustard, carmustine, chlorozotocin, fotemustine, lomustine, nimustine, ranimnustine, calicheamicin, dynemicin, clodronate, esperamicin; neocarzinostatin chromophore, aclacinomysins, actinomycin, authrarnycin, azaserine, bleomycins,

cactinomycin, carabicin, caminomycin, carzinophilin, chromomycinis, dactinomycin, daunorubicin, detorubicin, 6-diazo-5-oxo-L-norleucine, doxorubicin, epirubicin, esorubicin, idarubicin, marcellomycin, mitomycin, mitomycin C, mycophenolic acid, nogalamycin, olivomycin, peplomycin, potfiromycin, puromycin, quelamycin, rodorubicin, streptonigrin, streptozocin, tubercidin, ubenimex, zinostatin, zorubicin, methotrexate, 5-fluorouracil (5-FU), denopterin, methotrexate, pteropterin, trimetrexate, fludarabine, 6-mercaptopurine, thiamiprine, thioguanine, ancitabine, azacitidine, 6-azauridine, carmofur, cytarabine, dideoxyuridine, doxifluridine, enocitabine, floxuridine, calusterone, dromostanolone propionate, epitiostanol, mepitiostane, testolactone, aminoglutethimide, mitotane, trilostane, frolinic acid, aceglatone, aldophosphamide glycoside, aminolevulinic acid, eniluracil, amsacrine, bestrabucil, bisantrene, edatraxate, defofamine, demecolcine, diaziquone, elformithine, elliptinium acetate, epothilone, etoglucid, gallium nitrate, hydroxyurea, lentinan, lonidainine, maytansine, ansamitocins, mitoguazone, mitoxantrone, mopidanmol, nitraerine, pentostatin, phenamet, pirarubicin, losoxantrone, podophyllinic acid, 2-ethylhydrazide, procarbazine, PSK polysaccharide complex, razoxane, rhizoxin, sizofuran, spirogermanium, tenuazonic acid, triaziquone; 2,2',2"-trichlorotriethylamine, trichothecene, T-2 toxin, verracurin A, roridin A, anguidine, urethane, vindesine, dacarbazine, mannomustine, mitobronitol, mitolactol, pipobroman, gacytosine, arabinoside, cyclophosphamide, thiotepa, paclitaxel, doxetaxel, chlorambucil, gemcitabine, 6-thioguanine, mercaptopurine, methotrexate, cisplatin, oxaliplatin, carboplatin, vinblastine, platinum, etoposide, ifosfamide, mitoxantrone, vincristine, vinorelbine, novantrone, teniposide, edatrexate, daunomycin, aminopterin, xeloda, ibandronate, irinotecan, RFS 2000, difluoromethylomithine, retinoic acid or capecitabine. In some embodiments, the infectious disease is a viral infection, or a bacterial infection. In some embodiments, the infection is associated with COVID-19 (SARS-CoV-2), SARS-CoV, MERS-CoV, Ebola virus, influenza, cytomegalovirus, variola and group A *Streptococcus*, or sepsis.

[0010] In one aspect, described herein is a method of treating an inflammatory disease, a metabolic disease, an autoimmune disease, or a neurodegenerative disease. The method comprises administering to a subject in need thereof an effective amount of a modulator of macrophage activation; wherein the modulator inhibits a serotonin transporter or receptor, a histamine transporter or receptor, a dopamine transporter or receptor, an adrenoceptor, VEGF, EGF and/or leptin. Numerous embodiments are further provided that can be applied to any aspect of the present invention described herein. For example, in some embodiments, the modulator is Bostunib, Su11274, Alsterpaullone, Alrestatin, Bisantrene, triptolide, lovastatin, QS 11, Regorafenib, Sorafenib, MLN2238, GW-843682X, KW 2449, Axitinib, JTE 013, Purmorphamine, Arcyriaflavin A, Dasatinib, NVP-LDE225, 1-Naphthyl PP1, Selamectin, MGCD-265, podofilox, colchicine, or vinblastine sulfate. In some embodiments, the inflammatory disease, the metabolic disease, or the autoimmune disease is diabetes, obesity, non-alcoholic fatty liver disease (NAFLD), hepatic steatosis, non-alcoholic steatohepatitis, cirrhosis, rheumatoid arthritis (RA), acute respiratory distress syndrome (ARDS), cardiovascular disease, remote tissue injury after ischemia and reperfusion, dermatomyositis, pemphigus, lupus nephritis and resultant glomerulonephritis and vasculitis, cardiopulmonary bypass, cardioplegia-induced coronary endothelial dysfunction, type II membranoproliferative glomerulonephritis, IgA nephropathy, acute renal failure, cryoglobulinemia, antiphospholipid syndrome, Chronic open-angle glaucoma, acute closed angle glaucoma, macular degenerative diseases, age-related macular degeneration (AMD), choroidal neovascularization (CNV), uveitis, diabetic retinopathy, ischemia-related retinopathy, endophthalmitis, intraocular neovascular disease, diabetic macular edema, pathological myopia, von Hippel-Lindau disease, histoplasmosis of the eye, Neuromyelitis Optica (NMO), Central Retinal Vein Occlusion (CRVO), corneal neovascularization, retinal neovascularization, Leber's hereditary optic neuropathy, optic neuritis, Behcet's retinopathy, ischemic optic neuropathy, retinal vasculitis, Anti-Neutrophilic Cytoplasmic Autoantibody vasculitis, Purtscher retinopathy, Sjogren's dry eye disease, dry AMD, sarcoidosis, temporal arteritis, polyarteritis nodosa, multiple sclerosis, hyperacute rejection, hemodialysis, chronic occlusive pulmonary distress syndrome (COPD), asthma, aspiration pneumonia, multiple sclerosis, Guillain-Barre syndrome, Myasthenia Gravis, Bullous Pemphigoid, or myositis. In some embodiments, the neurodegenerative disease is Alzheimer's disease, amyotrophic lateral sclerosis, multiple sclerosis, glaucoma, myotonic dystrophy, Guillain-Barre' syndrome (GBS), Myasthenia Gravis, Bullous Pemphigoid, spinal muscular atrophy, Down syndrome, Parkinson's disease, or Huntington's disease.

[0011] In one aspect, described herein is a method of treating an inflammatory disease, a metabolic disease, an autoimmune disease, or a neurodegenerative disease. The method comprises administering to a subject in need thereof an effective amount of diphenyleneiodonium (DPI). Numerous embodiments are further provided that can be applied to any aspect of the present invention described herein. For example, in some embodiments, the inflammatory disease, the metabolic disease, or the autoimmune disease is diabetes, obesity, Non-alcoholic fatty liver disease (NAFLD), hepatic steatosis, non-alcoholic steatohepatitis, cirrhosis, rheumatoid arthritis (RA), acute respiratory distress syndrome (ARDS), cardiovascular disease, remote tissue injury after ischemia and reperfusion, dermatomyositis, pemphigus, lupus nephritis and resultant glomerulonephritis and vasculitis, cardiopulmonary bypass, cardioplegia-induced coronary endothelial dysfunction, type II membranoproliferative glomerulonephritis, IgA nephropathy, acute renal failure, cryoglobulinemia, antiphospholipid syndrome, Chronic open-angle glaucoma, acute closed angle glaucoma, macular degenerative diseases, age-related macular degeneration (AMD), choroidal neovascularization (CNV), uveitis, diabetic retinopathy, ischemia-related retinopathy, endophthalmitis, intraocular neovascular disease, diabetic macular edema, pathological myopia, von Hippel-Lindau disease, histoplasmosis of the eye, Neuromyelitis Optica (NMO), Central Retinal Vein Occlusion (CRVO), corneal neovascularization, retinal neovascularization, Leber's hereditary optic neuropathy, optic neuritis, Behcet's retinopathy, ischemic optic neuropathy, retinal vasculitis, Anti-Neutrophilic Cytoplasmic Autoantibody vasculitis, Purtscher retinopathy, Sjogren's dry eye disease, dry AMD, sarcoidosis, temporal arteritis, polyarteritis nodosa, multiple sclerosis, hyperacute rejection, hemodialysis, chronic occlusive pulmonary distress syndrome (COPD), asthma, aspiration pneumonia, multiple sclerosis, Guillain-Barre syn-

drome, Myasthenia Gravis, Bullous Pemphigoid, or myositis. In some embodiments, the neurodegenerative disease is Alzheimer's disease, amyotrophic lateral sclerosis, multiple sclerosis, glaucoma, myotonic dystrophy, Guillain-Barre' syndrome (GBS), Myasthenia Gravis, Bullous Pemphigoid, spinal muscular atrophy, Down syndrome, Parkinson's disease, or Huntington's disease.

BRIEF DESCRIPTION OF THE DRAWINGS

[0012] FIGS. **1**A-**1**H show a high throughput screen for compounds that activate human macrophages. FIG. **1**A and FIG. **1**B show that hMDMs were cultured for 24 hours in the presence of LPS, IFNγ, TNFα, IFNγ plus TNFα (I+T), IL-10, IL-4 or IL-13. Shown are examples of cell morphologies of M1-activating macrophages by IFNγ and M2-activating macrophages by IL-4 (FIG. **1**A) and calculated Z-scores for each stimulus (FIG. **1**B) from three independent experiments. Each symbol represents a technical replicate. The Z-score was calculated by T-test to measure the difference of cell morphology between treatment and control. Stimuli had negative Z-scores when induced cells to round morphology and positive scores when induced cells to elongated morphology. FIG. **1**C shows the flowchart of screening and data analysis. Equally mixed human monocytes isolated from fresh blood of 4 healthy donors were cultured in vitro with 50 ng/mL M-CSF for 7 days. hMDMs were trypsinized and plated on 384-well plates (5000 cells/well in 50 μL). Cells were recovered in 10 ng/mL M-CSF for 16 hrs and then treated with compounds for 24 hrs. Cells were washed, fixed and stained with Phalloidin and DAPI. The plates were scanned with a high-content microscope with six-fields per well to quantify the cell number and cell morphology. FIG. **1**D shows composition of compound libraries used in the screen. FIG. **1**E shows examples of cell shape changes induced by two compounds and their corresponding Z-scores as compared to DMSO controls. The cell eccentricity was calculated to measure the cell morphology. The Z-score was calculated by T-test to measure the difference in cell morphologies between each compound and DMSO control. FIG. **1**F shows plot of Z-scores of 4126 compounds and number of cells captured in each well. The dash lines are the cutoffs for M1 activation (left) and M2 activation (right) based on the average of Z-scores from FIG. **1**B. FIG. **1**G shows classification of identified compounds based on their origination and the function of their known targets. FIG. **1**H shows pathway analysis of known targets of identified M1- or M2-activating compounds. Each dot is one specific pathway having protein targets by compounds and dot size refer to the number of compounds. The average Z-score (y-axis) and number of compounds that have protein targets belongs to one specific pathway are plotted. Selected known (black) and novel (gray) pathways associated with macrophage activation are indicated.

[0013] FIGS. **2**A-**2**F show validation of macrophage activation induced by compounds or by ligands of the identified novel pathways. FIGS. **2**A-**2**B show that the morphology changes induced by selected compounds are dosage-dependent. Dosage response was calculated based on the measurement of Z-scores at different concentrations of the compound in a Michaelis-Menten model. Shown are representative dosage response curves of M1-activating (thiostrepton) and M2-activating (bosutinib) compounds (FIG. **2**A). 25 of the 30 tested compounds had typical dosage dependent response (FIG. **2**B). Effective concentration (EC) was defined as the concentration of compounds inducing cell morphology changes to reach the cutoffs of either M1 or M2. EC, fitness (R square) and Max Z-score were calculated by the Michaelis-Menten equation. Data were summarized from 3 independent experiments. FIG. **2**C shows GSEA of transcriptional response to 8 selected compounds and controls (IL-4 and IFNγ). Duplicate hMDM samples were treated with 2 M2-activating and 6 M1-activating compounds as well as IL-4 and IFNγ for 24 hrs. Gene expression levels were measured by RNA-seq separately. GSEA preranked analysis was performed based on the whole genome gene list ranked on gene expression changes using a gene set of 49 transcriptional modules in response to 29 stimuli in hMDMs. bosut.: bosutinib; alster.: alsterpaullone; mocet.: mocetinostat; thios.: thiostrepton; niclo.: niclosamide; chlor.: chlorhexidine; fenb.: fenbendazole; fluvo.: fluvoxamine. FIG. **2**D shows GO enrichment analysis of DEGs induced by each compound and positive controls. The numbers of DEGs that are up and down regulated are indicated. FIG. **2**E shows GSEA of transcriptional response to 6 ligands of the identified novel pathways in FIG. **1**H. dopa.: dopamine; 5HT: serotonin. Duplicate hMDM samples were stimulated with each ligand and analyzed by RNA-seq separately. FIG. **2**F shows GO enrichment analysis of DEGs induced by the ligands and positive controls. The numbers of DEGs that are up and down regulated are indicated.

[0014] FIGS. **3**A-**3**E show reprogramming screen of compounds on differentiated macrophages. FIG. **3**A shows that hMDMs were differentiated into M2 by IL4 plus IL13 and then treated with each of the 127 identified M1-activating compounds at either 5 μM or 10 μM for 24 hrs in the absence of differentiating cytokines. Shown are comparison of Z-scores between 5 μM or 10 μM of compounds. FIG. **3**B shows that hMDMs were differentiated into M1 by IFNγ plus TNFα and then treated with each of the 180 identified M2-activating compounds at either 5 μM or 10 μM for 24 hrs in the absence of differentiating cytokines. Shown are comparison of Z-scores between 5 μM or 10 μM of compounds. FIG. **3**C shows the effective concentration of 40 selected M1- or M2-activating compounds calculated from the dosage assays. EC and fitness of 21 M1-polarizing (triangle) and 19 M2-polarizing compounds (circle) were calculated by the Michaelis-Menten equation and plotted. Data were summarized from 3 independent experiments. FIGS. **3**D-**3**E show that hMDMs were differentiated into either M2 by IL4 plus IL13 or M1 by IFNγ plus TNFα and then treated with 127 M1-activating (FIG. **3**D) or 180 M2-activating (FIG. **3**E) compounds for 24 hrs in the presence of differentiating cytokines. Filled dots showed the overlapping ones with the 37 M1-activating (FIG. **3**A) and 21 M2-activating (FIG. **3**B) compounds.

[0015] FIGS. **4**A-**4**F show reprogramming of differentiated macrophages by selected compounds. FIG. **4**A shows number of DEGs induced by each compound: upregulated genes and down-regulated genes. hMDMs were differentiated into either M2 by IL-4 plus IL-13 or M1 by IFNγ plus TNFα and duplicate samples were then treated with either M1-activating or M2-activating compounds, respectively, at the effective concentrations. Controls include two differentiated M1 and M2 macrophages, M2 macrophages treated with IFNγ and M1 macrophages treated with IL-4. Gene expression in each sample was measured by RNA-seq separately. FIG. **4**B shows hierarchical clustering heatmap

of Pearson correlation coefficients for 7620 DEGs induced by compounds as well as IFNγ and IL-4. FIG. **4**C shows GSEA analysis of transcriptional responses to each compound as compared to IFNγ and IL-4. FIG. **4**D show network of GO enriched terms using BiNGO on top 10% central hubs genes (n=1255) of macrophage activation network. Node color and size represent the FDR values of enriched GO terms. FIGS. **4**E-**4**F shows functional enrichment analysis of DEGs induced by each compound. Shared (FIG. **4**E) and unique pathways (FIG. **4**F) are shown. Compound targets and FDA-approval information are indicated. The order of M1-activating and M2-activating compounds in FIG. **4**E and FIG. **4**F are the same as in FIG. **4**A.

[0016] FIGS. **5**A-**5**E show that thiostrepton induces macrophages into pro-inflammatory state and enhances anti-tumor activity in vitro. FIG. **5**A shows volcano plot showing changes in transcription in hMDMs induced by thiostrepton (n=2). hMDMs were treated with 2.5 μM thiostrepton for 24 hrs followed by RNA-seq. DEGs were identified by edgeR at $P<0.05$ with at least 2 fold-change. Data for genes that were not classified as differentially expressed are plotted in black. Filled dots represent upregulated and down-regulated genes as shown. FIG. **5**B shows GO enrichment analysis of DEGs induced by thiostrepton. FIG. **5**C shows GSEA of transcriptional response to thiostrepton. FIG. **5**D shows that thiostrepton inhibits the development and function of TAMs in vitro. Mouse BMMs were cultured in normal medium with or without 2.5 μM thiostrepton for 24 hrs (group 1), or cultured in B16F10 tumor cell conditioned medium (CM) with or without 2.5 μM thiostrepton for 24 hrs (group 2), or cultured with B16F10 tumor cell CM for 24 hrs first and then treated with 2.5 μM thiostrepton for another 24 hrs (group 3). The transcript levels of the indicated genes were quantified by qPCR. Data were summarized from two independent experiments. FIG. **5**E shows that thiostrepton enhances anti-tumor activities of macrophages. Mouse BMMs were treated with thiostrepton for 24 hrs. Untreated and treated macrophages were co-cultured with equal number of B16F10 melanoma cells for 12 hrs. The number of tumor cells were quantified by flow cytometry after subtracting macrophages from total number of cells. Data were summarized from three independent experiments. ** $P<0.01$ by T-test.

[0017] FIGS. **6**A-**6**F show that thiostrepton exhibits anti-tumor activities through reprogramming tumor-associated macrophages in vivo. FIG. **6**A shows tumor growth curves in B6 mice bearing subcutaneous B16F10 tumors treated I.P. with DMSO, TA99, thiostrepton (300 mg/kg or 150 mg/kg) and thipstrepton plus TA99. Arrows indicate dosing time points. FIG. **6**B shows tumor growth curves in B6 mice bearing subcutaneous B16F10 tumors treated I.P. with TA99, and S.C. with PBS or DMSO or thiostrepton (20 mg/kg) or thiostrepton plus TA99 (n=10-12 mice per group). FIGS. **6**C-**6**D show flow cytometry analysis of TAM ($F4/80^{+}CD11b^{+}Ly6C^{-}Ly6G^{-}$), inflammatory monocytes ($F4/80^{int}CD11b^{+}Ly6C^{+}Ly6G^{-}$) and monocytes ($F4/80^{-}CD11b^{+}Ly6C^{+}Ly6G^{+}$) in the tumors of control, TA99-treated, thiostrepton-treated and thiostrepton plus TA99-treated tumor-bearing mice 18 days after tumor engraftment. Shown are representative F4/80 versus CD11b staining profiles gating on CD45+ cells (FIG. **6**C) and summarized data (FIG. **6**D) from three independent experiments with 3-4 mice per group per experiment. Error bars indicate standard deviation (SD). FIG. **6**E shows immunohistochemistry staining of F4/80 in tumor sections. Scale bar: 100 m. FIG. **6**F shows comparison of gene expression changes induced by thiostrepton in tumor infiltrated macrophages by I.P. (n=4) or S.C. administration (n=2) of thiostrepton or DMSO (n=2). Tumor infiltrated macrophages were sorted from tumor issues based on $CD45^{+}F4/80^{+}CD11b^{+}$ $Gr\text{-}1^{-}$ 18 days after tumor engraftment. I.P.: intraperitoneal injection; S.C.: para-tumor subcutaneous injection. * $P<0.05$ and ** $P<0.01$ by T-test.

[0018] FIGS. **7**A-**7**B show morphology and phenotypes of activated macrophages. FIG. **7**A shows F-actin staining of M1- and M2-like macrophages. hMDMs were induced to become M0 by M-CSF. The resulting macrophages were polarized to M1 by IFNγ or M2 by IL4. Then, M1 macrophages were treated with M2-type compound bosutinib (1 mM) for 24 hrs, and M2 macrophages were treated with M1-type compound thiostrepton (2.5 mM) for 24 hrs. F-actin was stained and images were acquired by fluorescent microscopy with 60× objective. Cell nuclei are stained with DAPI. Representative data were shown from two independent experiments. FIG. **7**B shows CD163, CD206, CD80 and CD86 in hMDM treated with DMSO, or IFNγ or IL4 quantified by flow cytometry. Shown are the representative staining profiles from three independent experiments. The numbers show mean fluorescent intensity (MFI)+/−standard error of the mean (SEM) for n=3 samples per group.

[0019] FIG. **8** shows the top list of proteins that are targeted by M1-activating and M2-activating compounds. Histone deacetylases and VEGF receptors are highlighted gray.

[0020] FIGS. **9**A-**9**C show comparison of the differentially expressed genes induced by selected compounds (FIG. **9**A), ligands for novel pathways (FIG. **9**B), and controls (IL-4 and IFNγ). FIG. **9**C shows changes of the selected M1 markers (CD80 and CD86) and M2 markers (CD206 and CD163) at protein level induced by compound as assayed by flow cytometry. Shown are the changes of the relative mean fluorescence intensity (MFI) to controls. 0.2 refers to 20% MFI increase.

[0021] FIG. **10** shows comparison of EC of 21 M1-activating and 19 M2-activating compounds in the presence or absence of the polarizing cytokines.

[0022] FIGS. **11**A-**11**E show reprogramming of differentiated macrophages by selected compounds. FIG. **11**A shows principal component analysis of global transcriptional response of hMDMs to 17 M1-activating and 17 M2-activating compounds. The samples are the same as those in FIG. **4**A. FIG. **11**B shows functional enrichment analysis of DEGs induced by each compound. Shown is the assembled heatmap and number of up-regulated and down-regulated DEGs (bottom panel). FIG. **11**C shows comparison of relative transcript levels of the selected M1 and M2 genes following compound treatment based on RNA-seq. FIG. **11**D shows comparison of the transcript levels of the selected M1 and M2 genes following compound treatment as measured by quantitative PCR. FIG. **11**E shows comparison of the protein levels of the selected M1 and M2 markers following compound treatment as measured by flow cytometry. Shown are the relative MFI change to controls. 0.2 refers to 20% MFI increase. The order of M1-activating and M2-activating compounds in b-e is the same as in FIG. **4**A.

[0023] FIG. **12** shows macrophage activation network. The network was inferred by ARACNe (Margolin et al. 2006). The top 10% central hub gene network was visual-

ized by Cytoscape (Shannon et al. 2003). The dark marked nodes are transcription factors (regulators). Top 10 central hubs and top 10 central TF hubs are listed.

[0024] FIGS. **13**A-**13**B show that thiostrepton inhibits the development and function of M2-like macrophages in vitro. FIG. **13**A shows mouse BMMs were cultured with B16F10 tumor cell conditioned medium (CM) for 24 hrs first and then treated with 2.5 mM thiostrepton for another 24 hrs (group 3 from FIG. **5**D). Expression of MHCII, CD80, iNOS, Arg1 and CD206 were quantified by flow cytometry. Shown are representative staining profiles of treated (red) and untreated (dark) TAMs from two independent experiments. FIG. **13**B shows that mouse BMMs were not treated or treated with 2.5 mM thiostrepton for 24 hrs in normal medium (group 1), or polarized with IL-4/IL-13 in the absence or presence of 2.5 mM thiostrepton for 24 hrs (group 2), or polarized with lactic acid in the absence or presence of 2.5 mM thiostrepton for 24 hrs (group 4). Alternatively, mouse BMMs were polarized with IL-4/IL-13 (group 3) or lactic acid (group 5) for 24 hrs first and then either not treated or treated with 2.5 mM thiostrepton for another 24 hrs. The transcript levels of the indicated genes were quantified by qPCR. Data are summarized from two independent experiments.

[0025] FIGS. **14**A-**14**C show that thiostrepton activates macrophages in vitro. FIG. **14**A shows that mouse BMMs were treated with thiostrepton for 24 hrs (same as FIG. **5**E). Conditioned medium (CM) was collected and filtered. B16F10 melanoma cells were cultured for 12 hrs with CM or CM heat-inactivated at 95° C. for 5 min. The number of tumor cells were quantified by flow cytometry. Data were summarized from two independent experiments. * P<0.05 by T-test. P values are shown based on t-test. FIGS. **14**B-**14**C show that thiostreption enhances ADCP of macrophages. Mouse BMMs (FIG. **14**B) or hMDM (FIG. **14**C) were treated with 2.5 mM thiostrepton for 24 hrs, then co-cultured with equal number of eFluro670 and anti-CD20 labelled human B-cell lymphoma cells for 2 hrs, and analyzed by flow cytometry. Macrophages that have phagocytosed tumor cells are identified as efluro670+ and CD14+. Shown are representative eFluro670 histograms gating on CD14+ macrophages from three different experiments.

[0026] FIGS. **15**A-**15**B show that thiostrepton activates macrophages in vivo without altering the total number of gut bacterial counts. FIG. **15**A shows flow cytometry analysis of macrophages (F4/80+CD11b+) and monocytes (F4/80−CD11b+) in the bone marrow and spleen of mice 6 days post treatment with either DMSO or thiostrepton by I.P. or S.C. (n=3). Shown are representative F4/80 versus CD11b staining profiles gating on CD45+ cells. I.P.: intraperitoneal injection; S.C.: paratumor subcutaneous injection. FIG. **15**B shows total bacterial counts in the stool sample of mice. Data shown are mean±s.d. n.s., not significant by T-test.

[0027] FIGS. **16**A-**16**D show effect of thiostrepton on macrophages, NK cells and CD8+ T cells in vivo. B6 mice bearing subcutaneous B16F10 tumor were treated as in FIG. **6**. Single cell suspensions were prepared from tumors 18 day after engraftment, stained and analyzed by flow cytometry. FIGS. **16**A-**16**B show representative intracellular staining profiles of Arg1 vs. CD86 gated on F4/80+CD11b+ Gr1− TAMs (FIG. **16**A) and summarized data from n=5 mice per group from two independent experiments (FIG. **16**B). FIG. **16**C shows representative intracellular staining profiles of IFNγ vs. TNFα gated on CD45+ NK1.1+ NK cells (top two rows) and CD45+ CD8a+ T cells (bottom two rows). Samples for T-cell staining were stimulated in vitro by T-cell stimulation cocktail for 4 hrs. FIG. **16**D shows summarized data from n=4~6 mice per group from two independent experiments. * P<0.05 by T-test. Data shown are mean±s.d.

[0028] FIGS. **17**A-**17**D show transcriptional response of TAMs to thiostrepton in vivo. FIG. **17**A shows GO enrichment analysis showing enrichment of certain pathways in the up-regulated and down-regulated genes in TAMs following I.P. administration of thiostrepton or DMSO. GO sets of biological process, number of genes and P-value are shown. Tumor infiltrated macrophages were sorted from tumor tissues based on CD45+F4/80+CD11b+Gr1− 18 days after tumor engraftment. Gene expression levels were measured by RNAseq. FIG. **17**B shows GSEA showing enriched gene sets in TAMs induced by thiostrepton in vivo by I.P. administration (FDR q-value <0.05). FIG. **17**C shows GO enrichment analysis showing enrichment of certain pathways in the up-regulated and down-regulated genes in TAMs induced by S.C. administration of thiostrepton or DMSO. GO sets of biological process, number of genes and P-value are shown. FIG. **17**D shows GSEA showing enriched gene sets in TAMs induced by thiostrepton in vivo by S.C. administration (FDR q-value <0.05). I.P.: intraperitoneal injection; S.C.: paratumor subcutaneous injection.

[0029] FIGS. **18**A-**18**D show that thiostrepton inhibits tumor growth in the bone marrow. NSG mice were grafted with 1×10^7 GMB-luc cells and dosed twice at 14 and 21 days later with 0.5 mg/kg Rituximab (Ritu) and/or 300 mg/kg thiostrepton (Thio). Tumor burden was monitored (FIG. **18**A) and quantified (FIG. **18**B) by imaging the luciferase activity in vivo (n=5~6 mice per group). Data are shown as mean±s.e.m. At day 28 post tumor engraftment, bone marrow cells were analyzed by flow cytometry (FIG. **18**C). Shown are representative F4/80 versus CD11b staining profiles gating on $CD45^+$ cells (top panel), Ly6C versus Ly6G staining profiles gating on $F4/80^+CD11b^+$ cells (bottom panel). MHCII histograms gating on macrophages from FIG. **18**C. FIG. **18**D shows summarized data of MHCII expression in bone marrow macrophages from FIG. **18**C. Data shown are mean±s.d. * P<0.05, ** P<0.01 and *** P<0.001, by T-test.

[0030] FIGS. **19**A-**19**D shows that M1-type compound, cucurbitacin I, also activates macrophages and inhibits tumor growth. FIG. **19**A shows that cucurbitacin I inhibits the development and function of tumor-associated macrophages in vitro induced by IL4/IL13. Mouse BMMs were not treated or treated with 2.5 mM thiostrepton for 24 hours in normal medium (group 1) or in the presence of IL4/IL13 (group 2), or mouse BMMs were polarized with IL4/IL13 for 24 hours and then either not treated or treated with 2.5 mM thiostrepton for 24 hours (group 3). RNA was isolated and the transcript levels of the indicated genes were quantified by PCR. Data, shown as mean±s.d., were summarized from two independent experiments. * P<0.05 and ** P<0.01 by T-test. FIG. **19**B shows B16F10 tumor growth in B6 mice treated i.p. with DMSO, TA99, cucurbitacin I (1 mg/kg) and cucurbitacin I plus TA99 (n=6 mice per group). Data are shown as mean±s.e.m. FIGS. **19**C-**19**D show flow cytometry analysis of TAM ($F4/80^+CD11b^+Ly6C^-Ly6G^-$), inflammatory monocytes ($F4/80^{int}CD11b^+Ly6C^+Ly6G^-$) and monocytes ($F4/80^-CD11b^+Ly6C^+Ly6G^+$) in the tumors of mice treated with DMSO, TA99, cucurbitacin I, and cucurbitacin I plus TA99 18 days after tumor engraftment. Shown are

representative F4/80 versus CD11b staining profiles gating on CD45+ cells and MHCII histograms gating on macrophages from c.

[0031] FIGS. **20**A-**20**F show that DPI stimulates both rapid and sustained increase in glycolysis in macrophages. FIG. **20**A shows glycolysis pathway with involved enzymes and intermediates and TCA cycle with selected intermediates. FIGS. **20**B-**20**C show the short-term effects of DPI on ECAR (FIG. **20**B) and OCR (FIG. **20**C) in ImKCs. ECAR and OCR were measured by Seahorse analyzer in ImKCs for 20 min, then for another 120 min following addition of different concentrations of DPI (5, 50 or 500 nM), and then for another 40 min following addition of rotenone plus antimycin A (Rot/AA) (FIG. **20**B) or 2-deoxylglucose (2-DG) (FIG. **20**C). Shown are representative data of three independent experiments. FIGS. **20**D-**20**E show the long-term effects of DPI on ECAR. ImKCs were seeded and incubated with or without DPI (50 and 500 nM) for 24 hrs. ECAR values were then measured under the basal conditions with sequential addition of 15 mM glucose, 2 μM oligomycin, and 50 mM Rot plus 1 M AA (FIG. **20**D). Specific parameters for glycolysis, glycolytic capacity and glycolytic reserve were calculated and data are presented as the mean±sd (n=18) from three independent experiments (FIG. **20**E). FIG. **20**F shows select metabolite levels. ImKCs were treated with DPI for 6 hrs and select metabolites in the glycolytic pathway and TCA cycle were quantified by LC-MS. Data are presented as the mean±sd (n=4). P values were calculated by student t-test. * P<0.05, ** P<0.01, *** P<0.001, **** P<0.0001.

[0032] FIGS. **21**A-**21**I show DPI stimulates glycolysis through GPR3 and β-arrestin2. FIGS. **21**A-**21**B show DPI-stimulated glycolysis is independent of the NOX activity. Wildtype (WT) and p47phox$^{-/-}$ BMDMs were seeded and incubated without or with DPI (50 and 500 nM) for 24 hrs and ECAR was measured by Seahorse analyzer (FIG. **21**A). WT BMDMs were seeded and incubated without or with DPI (500 nM) in the absence or the presence of NOX inhibitor apocynin (100 μM) for 24 hrs and ECAR was measured by Seahorse analyzer (FIG. **21**B). Data are presented as the mean±sd (n=15) from three independent experiments. FIG. **21**C shows the effect of DPI on glucose uptake in WT and p47phox$^{-/-}$ BMDMs. BMDMs were treated with DMSO or DPI (50 and 500 nM) for 24 hrs in the presence of the fluorescent glucose analog 2-NBDG. The mean fluorescence intensity (MFI) of 2-NBDG in cells was measured by flow cytometry and normalized to DMSO controls of wildtype BMDMs. Data are presented as the mean±sd (n=3). FIG. **21**D shows that DPI-stimulated glycolysis requires GPR3. ImKCs were transfected with siRNA specific for Gpr3 or a scramble siRNA as control. 48 hrs later, transfected ImKCs were seeded and incubated without or with DPI (50 and 500 nM) for 24 hrs and ECAR was measured by Seahorse analyzer. Data are presented as the mean±sd (n=15) from three independent experiments. FIG. **21**E shows that transfected ImKCs were incubated without or with DPI (50 and 500 nM) for 24 hrs in the presence of 2-NBDG to measure the glucose uptake. Data are presented as the mean±sd (n=4). FIG. **21**F shows that ImKCs were incubated with DMSO, DPI (500 nM) or S1P (3 mM) for 24 hrs and ECAR was measured by Seahorse analyzer. Data are presented as the mean±sd (n=12). FIG. **21**G shows that DPI-stimulated glycolysis requires β-arrestin-2. Abbr2$^{-/-}$ ImKC were constructed by CRISPR-Cas9-mediated gene editing. WT and Abbr2$^{-/-}$ ImKCs were seeded and incubated without or with DPI (50 and 500 nM) for 24 hrs and ECAR was measured by Seahorse analyzer. Data are presented as the mean±sd (n=15) from three independent experiments. FIG. **21**H shows that WT andAbbr2$^{-/-}$ ImKCs were incubated without or with DPI (50 and 500 nM) for 24 hrs in the presence of 2-NBDG to measure the glucose uptake. Data are presented as the mean±sd (n=4). FIG. **21**I shows that DPI induces β-arrestin2 translocation to cytoplasm membrane. ImKCs were transfected with Abbr2-GFP fusion gene and stimulated with DMSO, DPI (50 nM), or S1P (3 mM). The GFP signal was captured with a TIRF microscope at indicated time points. Shown are representative data of GFP signal at 0 min and 10 min, and merged signal from three independent experiments. P values were calculated by student t-test. * P<0.05, ** P<0.01, *** P<0.001, **** P<0.0001.

[0033] FIGS. **22**A-**22**E show that DPI stimulates rapid increase in glycolytic activity through the formation of GPR3-β-arrestin2-GAPDH-PKM2 enzymatic super complex. FIG. **22**A shows Co-IP of β-arrestin2 with ERK1/2, enolase, GAPDH, and PKM2. ImKCs were transfected with β-arrestin2 and then treated with or without 50 nM DPI for 6 hrs. Cell lysates were precipitated with anti-β-arrestin2 and the precipitates were analyzed by Western blotting for the indicated proteins. Shown are representative data from one of the three experiments. FIG. **22**B shows that DPI-stimulated glycolysis requires PKM2. BMDMs were prepared from wild-type and Pkm$^{-/-}$ mice, seeded and incubated with or without DPI (50 and 500 nM) for 24 hrs and ECAR was measured by Seahorse analyzer. Data are presented as the mean±sd (n=15) from three independent experiments. FIG. **22**C shows that WT and Pkm$^{-/-}$ BMDMs were seeded and incubated with or without DPI (50 and 500 nM) for 24 hrs in the presence of 2-NBDG to measure the glucose uptake. Data are presented as the mean±sd (n=4). FIGS. **22**D-**22**E show that DPI stimulates enzymatic activities of PKM2 and GAPDH. Wildtype and Abbr2$^{-/-}$ ImKCs were treated with DPI (500 nM) for 6 hrs and the enzymatic activities of PKM2 (FIG. **22**D) and GAPDH (FIG. **22**E) were measured by colorimetric assay kits. Data are presented as the mean±sd (n=6). P values were calculated by student t-test. * P<0.05, ** P<0.01, *** P<0.001, **** P<0.0001.

[0034] FIGS. **23**A-**23**D show that DPI stimulates sustained increase in glycolytic activity through nuclear translocation of PKM2 and transcriptional activation. FIG. **23**A shows that DPI-induced transcription of glycolytic genes requires PKM2. WT and Pkm$^{-/-}$ BMDMs were not treated or treated with DPI (50 and 500 nM) for 24 hrs. The transcript levels of Pkm, Ldha, Hk2 and c-Myc were measured by real-time qPCR. Data were collected from two independent experiments with 3 biological replicates per group. Transcriptional level was normalized to β-actin first and then to DMSO control. Data are presented as the mean±sd. FIG. **23**B shows induction of dimeric PKM2 by DPI. ImKCs were not treated or treated with DPI (50 and 500 nM) for 6 or 12 hrs. Cell lysates were run on native PAGE gel and analyzed by Western blotting. Shown are representative data from two independent experiments. FIG. **23**C shows that DPI induces nuclear translocation of PKM2. ImKCs and human primary KCs were not treated or treated with DPI (50 nM) for 24 hrs, stained with anti-PKM2 and DAPI, followed by confocal imaging. Shown are represen-

tative images from two independent experiments. Enlarged areas are boxed. FIG. **23**D shows that DPI stimulates transactivation of c-Myc. c-Myc luciferase reporter plasmid was transfected into WT and $Pkm^{-/-}$ BMDMs. Transfected cells were not treated or treated with DPI (50 and 500 nM) for 6 hrs and luciferase activities were measured. Data are presented as the mean±sd (n=5). P values were calculated by student t-test. * P<0.05, ** P<0.01, *** P<0.001, **** P<0.0001.

[0035] FIGS. **24**A-**24**H show that DPI inhibits HFD-induced obesity and liver pathogenesis through PKM2 expression in Kupffer cells. FIGS. **24**A-**24**B shows that DPI prevents weight gain in mice fed with HFD. Male B6 mice at 5 weeks of age were fed with HFD or normal chow diet (ND) for a total of 8 weeks. Three weeks after HFD (arrow), half of mice were given DPI in vehicle (2 mg/kg) and the other half were given vehicle alone every five days for a total of 6 doses. The body weight (FIG. **24**A) and food consumption (FIG. **24**B) were monitored weekly. Data are presented as the mean±sd from three independent experiments with 12-15 mice per group. FIG. **24**C shows the weights of eWAT and iWAT of mice after 8 weeks on HFD. Each dot represents one mouse. FIG. **24**D show fast glucose assay. Mice from FIG. **24**A at week 7 plus 3 days were starved overnight (12~16 hrs) with only water. Glucose (1 mg/kg) was injected intraperitoneally and blood glucose levels were monitored at the indicated time. AUC (right panel) were calculated for statistics. FIG. **24**E shows serum levels of AST and ALT. Sera from mice in FIG. **24**A were collected and activities of AST and ALT were measured by colorimetric assay kits (Sigma). FIG. **24**F shows comparison of H&E staining of liver sections from HFD mice treated with vehicle or DPI after 8 weeks on HFD. Shown are representative H&E staining from one mouse per group from FIG. **24**A. Arrows point to lipid droplets. Scale bar: 100 μm. FIGS. **24**G-**24**H show DPI's effect on KC-specific $Pkm^{-/-}$ mice fed with HFD. Male KC-specific $Pkm^{-/-}$ mice at the age of 5 weeks were fed with HFD for a total of 8 weeks. Three weeks after HFD, half of the mice were given DPI in vehicle (2 mg/kg) and the other half were given vehicle every 5 days for a total of 6 doses. Body weights were monitored weekly (FIG. **24**G). Data are presented as the mean±sd from two independent experiments with 6 mice per group. Comparison of H&E staining of liver sections after 8 weeks on HFD. Shown are representative H&E staining from one mouse per group. Arrows in FIG. **24**F and FIG. **24**H point to lipid droplets. Scale bar: 100 μm. P values were calculated by student t-test. * P<0.05, ** P<0.01, *** P<0.001, **** P<0.0001.

[0036] FIGS. **25**A-**25**D show that DPI upregulates glycolysis and suppresses inflammatory responses of Kupffer cells in HFD-fed mice. FIG. **25**A shows comparison of gene expression in KCs isolated from mice fed with ND or HFD. Single cell suspension was prepared from mice from FIG. **24**A after 8 weeks on HFD (6 mice per group), stained with anti-F4/80, anti-CD11b and anti-Gr-1. $F4/80^{+}CD11b^{+}Gr1^{low}$ macrophages were purified by cell sorting followed by RNAseq. Shown are differentially expressed genes among the three groups. FIG. **25**B shows functional enrichment analysis of DEGs based on comparison of KCs from HFD-fed and ND-fed mice or from HFD-fed mice treated with DPI or vehicle. FIG. **25**C shows GSEA of gene expression profiles of KCs either from HFD and ND mice, or from HFD mice treated with DPI or vehicle. Graphs in FIG. **25**B and FIG. **25**C indicate up- and down-regulated pathways as labeled. FIG. **25**D shows macrophage polarization index analysis based on the expression profile in FIG. **25**A with the online software MacSpectrum (see the World Wide Web at macspectrum.uconn.edu). M1-type polarization is expressed as positive scores whereas M2-type polarization is expressed as negative scores.

[0037] FIGS. **26**A-**26**H shows that DPI upregulates glycolysis and suppresses inflammatory responses of Kupffer cells from patients with NAFLD. FIGS. **26**A-**26**D show scRNAseq analysis of the macrophage populations. A total of 5,497 macrophages based on the expressing of CD14 and CD68 (cluster 5, 8 and 12 in FIG. **35**A) were subjected to clustering analysis by tSNE. A total of 7 clusters were identified (FIG. **26**A). Relative proportion of each cluster in each sample was calculated and shown (FIG. **26**B). Each cluster was annotated based on the expression of typical markers as shown by dot plot (FIG. **26**C) and heatmap (FIG. **26**D). FIG. **26**E shows trajectory inference of the liver macrophages by slingshot (Street et al. 2018). FIG. **26**F shows GO enrichment analysis of DEGs between C3 and C1 and C2. FIGS. **26**G-**26**H show comparison of gene expression changes induced by DPI in primary KCs isolated from NAFLD liver biopsies. $CD14^{+}$ KCs were sorted from single cell suspension of NAFLD human liver biopsies (n=2) and treated with DMSO or DPI (500 nM) for 24 hrs, followed by RNAseq to quantify gene expression. Shown are the expression changes of glycolytic genes and DAM markers (FIG. **26**G) and GO enrichment analysis of DEGs induced by DPI in KCs (FIG. **26**H). Graphs in FIG. **26**F and FIG. **26**H indicate up- and down-regulated pathways as labeled.

[0038] FIGS. **27**A-**27**C show that DPI stimulates both rapid and sustained increase in glycolysis in macrophages. FIG. **27**A shows that DPI stimulates transcription of glycolytic genes in human primary macrophages following treatment with 50 nM DPI for 24 hours. Heatmap of transcript levels is based on reanalysis of RNAseq data from Hu et al. 2021. FIG. **27**B shows that DPI stimulates expression of glycolytic enzymes at protein level as measured by Western blotting. Total protein lysates were isolated from either mouse ImKCs with or without DPI treatment for 6 and 12 hrs or human primary macrophages with or without DPI treatment for 12 hrs at the indicated concentrations. Equal amounts of total proteins from whole-cell lysates were subjected to Western blotting analysis. β-actin was used as a loading control. Shown are representative data of two independent experiments. FIG. **27**C shows metabolite analysis in ImKCs. ImKCs were treated with DPI (500 nM) for 24 hrs and the select metabolites were quantified by LC-MS. Shown are representative data of two independent experiments. P values were calculated by student t-test. * P<0.05, ** P<0.01. n.s. not significant.

[0039] FIGS. **28**A-**28**I show that DPI stimulates glycolysis through GPR3 and β-arrestin2. FIGS. **28**A-**28**B show that DPI-stimulated glycolysis is independent of the NOX activity. Wild-type (WT) and $p47phox^{-/-}$ BMDMs were seeded and incubated without or with DPI (50 and 500 nM) for 24 hrs and ECAR was measured by Seahorse analyzer. Specific parameters for glycolytic capacity and glycolytic reserve were calculated and summarized based on two independent experiments. Data are presented as the mean±sd (n=15) from three independent experiments. FIG. **28**C shows Western blotting of GPR3 in ImKCs transfected with scramble or siGpr3. FIGS. **28**D-**28**E show that ImKCs were transfected

with siRNA specific for Gpr3 or scramble siRNA. 48 hours later, transfected ImKCs were seeded and incubated without or with DPI (50 and 500 nM) for 24 hrs and ECAR was measured by Seahorse analyzer. Data are presented as the mean±sd (n=15) from three independent experiments. FIG. **28**F shows Western blotting of β-arrestin2 in wild-type or Abbr2$^{-/-}$ ImKCs. FIGS. **28**G-**28**H show that WT and Abbr2$^{-/-}$ ImKCs were seeded and incubated without or with DPI (50 and 500 nM) for 24 hrs and ECAR was measured by Seahorse analyzer. Data are presented as the mean±sd (n=15) from three independent experiments. FIG. **28**I show that BMDMs were transfected with Arrb2-GFP fusion gene and stimulated with DMSO or DPI (50 nM). The GFP signal was captured with a TIRF microscope at indicated time points. Shown are representative data of GFP signal at 0 min and 10 min, and the merged signal from three independent experiments. P values were calculated by student t-test. * P<0.05, ** P<0.01, *** P<0.001, **** P<0.0001. n.s. not significant.

[0040] FIG. **29**A-**29**D show that DPI stimulates rapid increase in glycolytic activity through the formation of GPR3-β-arrestin-GAPDH-PKM2 enzymatic super complex. FIGS. **29**A-**29**B show comparison of DPI's effect on glycolysis in wild-type and Pkm$^{-/-}$ BMDMs. BMDMs were generated from wildtype and PKM2$^{-/-}$ mice, seeded and incubated with or without DPI (50 and 500 nM) for 24 hrs and ECAR was measured by Seahorse analyzer. Data are presented as the mean±sd (n=15) from three independent experiments. FIGS. **29**C-**29**D show activation of PKM2 and GAPDH enzymatic activity by DPI is inhibited by ERK1/2 inhibitor. ImKCs were treated with DMSO or DPI alone (500 nM) or DPI plus ERK1/2 inhibitor (SCH772984, 1 mM) for 6 hrs and the enzymatic activities of PKM2 (c) and GAPDH (d) were measured by colorimetric assay kits (Biovision). Data are presented as the mean±sd (n=6). P values were calculated by student t-test. * P<0.05, ** P<0.01, *** P<0.001, **** P<0.0001. n.s. not significant.

[0041] FIGS. **30**A-**30**B show that DPI stimulates sustained increase in glycolytic activity through formation of dimeric PKM2. FIG. **30**A shows induction of dimeric PKM2 by DPI. ImKCs were not treated or treated with DPI (50 and 500 nM) for 6 or 12 hrs. Cells were treated with crosslinking agent DSS and lysed. Lysates were run on SDS-PAGE and analyzed by Western blotting. Shown are representative data from two independent experiments. FIG. **30**B shows that phosphorylation of ERK1/2 is inhibited by SCH772984 in the presence of DPI. ImKCs were not treated or treated with DPI (50 and 500 nM) in the presence or the absence of SCH772984 for 12 hrs. Cells were lysed and analyzed for total ERK1/2 and phosphorylated ERK1/2 by Western blotting. Shown are representative data from two independent experiments. P values were calculated by student t-test. * P<0.05, ** P<0.01, *** P<0.001, **** P<0.0001. n.s. not significant.

[0042] FIG. **31** shows that DPI stimulates metabolism of blood glucose in mice. C57BL/6 mice at 10 weeks of age were given a single injection of DPI (2 mg/kg) intraperitoneally. Six hrs later (−360 min), mice were injected intraperitoneally with glucose (1.5 mg/kg). Blood glucose levels were monitored at the indicated time. Data are presented as the mean±sd with 5 mice per group. P values were calculated by student t-test. * P<0.05, ** P<0.01, *** P<0.001.

[0043] FIGS. **32**A-**32**E show that DPI inhibits HFD-induced obesity and liver pathogenesis. FIGS. **32**A-**32**B show that male B6 mice at 5 weeks of age were fed with HFD for a total of 16 weeks. Nine weeks after HFD (arrow), half of the mice were dosed with vehicle and the other half with DPI in vehicle (2 mg/kg) every 5 days with a total of 6 doses. The weight (FIG. **32**A) and food consumption (FIG. **32**B) were monitored weekly. Data are presented as the mean±sd from two independent experiments with 9-10 mice per group. FIG. **32**C shows the weights of eWAT and iWAT after 16 weeks on HFD. FIG. **32**D shows fast glucose assay. At week 15 plus 3 days, mice from FIG. **32**A were starved overnight (12~16 hrs) with only water. Glucose (1 mg/kg) was injected intraperitoneally and blood glucose levels were measured at the indicated time. AUC were calculated for statistics (right panel). FIG. **32**E shows comparison of H&E and trichrome staining of liver sections from HFD mice treated with vehicle or DPI. Shown are representative H&E staining from one mouse per group from a. Scale bar: 100 m. P values were calculated by student t-test. * P<0.05, ** P<0.01, *** P<0.001. n.s. not significant.

[0044] FIG. **33** shows expression of PKM2 and PKM1 in human and mouse Kupffer cells and hepatocytes. scRNAseq data from normal human liver and mouse liver were reanalyzed for expression of PKM2 and PKM1 as well as markers of macrophages (VSIG4 or F4/80) and hepatocytes (APOC3 or Apoc3) using featureplot in Seurat package. In the mouse dataset, the small population of hepatocytes (Apoc3+) is due to the removal of hepatocytes in the process of enriching immune cells for scRNAseq.

[0045] FIGS. **34**A-**34**C show effect of DPI on Kupffer cell-specific Pkm$^{-/-}$ mice on HFD. FIG. **34**A shows fast glucose assay. KC-specific Pkm$^{-/-}$ mice were given HFD for a total of 8 weeks. Three weeks after HFD, half of the mice were given DPI in vehicle (2 mg/kg) and the other half were given vehicle every 5 days for a total of 6 doses. At 7 weeks plus 3 days, mice were starved overnight (12~16 hrs) with only water. Glucose (1 mg/kg) was injected intraperitoneally and blood glucose levels were monitored at the indicated time. FIG. **34**B shows the weights of eWAT and iWAT after 8 weeks on HFD. FIG. **34**C shows serum levels of AST and ALT. Sera from mice were collected at the end of HFD feeding and activities of AST and ALT were measured by colorimetric assay kits (Sigma). Shown are representative data from two independent experiments with 5~6 mice per group. P values were calculated by student t-test. n.s. not significant. * P<0.05.

[0046] FIGS. **35**A-**35**D show Single cell RNAseq analysis of immune cells from biopsies of healthy and NAFLD human livers. A total 47,724 immune cells from 3 healthy and 3 NAFLD human liver biopsies were clustered into 14 clusters by tSNE (FIG. **35**A). Each cluster was annotated based on the expression of typical markers as T and B cells, NK cells, macrophages, neutrophils and dendritic cells as shown by dot plotting (FIG. **35**B). Cell fraction of each cluster (FIG. **35**C) and relative proportion of each cluster in each sample (FIG. **35**D) were calculated and shown.

[0047] FIG. **36** shows GO enrichment analysis of DEGs of different liver macrophage subpopulations. DEGs were identified using the function of FindMarkers in Seurat package between different clusters as indicated with setting min.fct to 0.25 and logfc.threshold to 0.25. Up- and down-regulated DEG were applied to GO ontology enrichment analysis by the online tool DAVID (see the World Wide Web at david.ncifcrf.gov). Shown are the selected top GO terms

and p values based on the significance and redundance. Graphs indicate up- and down-regulated pathways as labeled.

DETAILED DESCRIPTION OF THE INVENTION

[0048] Macrophages are remarkably plastic and in response to different local stimuli can polarize toward multi-dimensional spectrum of phenotypes, including the pro-inflammatory M1-like and the anti-inflammatory M2-like states. Using a high throughput phenotypic screen, ~300 compounds that potently activated primary human macrophages toward either pro-inflammatory (M1-like) or anti-inflammatory (M2-like) state were identified from a library of ~4000 FDA-approved drugs, bioactive compounds and natural products. Among the hits, ~30 were capable of reprogramming M1-like macrophages toward M2-like state and another ~20 were capable of reprogramming M2-like macrophages toward M1-like state. Transcriptional analysis of 34 non-redundant hits on macrophage reprogramming by RNA-seq identified shared pathways through which the selected hits modulate macrophage activation, as well as new unique targets and pathways by which individual compound stimulates macrophage activation. One M1-activating compound, thiostrepton, was further shown to reprogram tumor-associated macrophages toward M1-like state in mice and exhibit potent anti-tumor activity either alone or in combination with an antibody therapeutic. Described herein are new compounds, targets and pathways involved in macrophage activation. The methods described herein provide a valuable resource not only for studying the macrophage biology but also for developing novel therapeutics or repositioning known drugs for treating diseases through modulating macrophage activation.

[0049] Macrophages are a key class of phagocytic cells that readily engulf and degrade dying/dead cells and invading bacteria and viruses. As such, macrophages play an essential role in development, tissue homeostasis and repair, and immunity. Consistently, macrophages are generated during early ontogeny and throughout the adult life. In mammals, the first wave of macrophages is generated from the yolk sac and gives rise to macrophages in the central nervous system, i.e., microglia, for example. The second wave of macrophages is generated from fetal liver and give rise to alveolar macrophages in the lung and Kupffer cells in the liver among others. After birth, macrophages are generated from the bone marrow where hematopoietic stem cells give rise to monocytes, which differentiate into tissue resident macrophages upon migration from blood into specific tissues.

[0050] A remarkable feature of macrophages is their plasticity: the ability to respond to local stimuli to acquire different phenotypes and functions so as to respond to changing physiological needs. Macrophages from different tissues exhibit different phenotypes and functions. For example, Kupffer cells in the liver function in the degradation of toxic and waste products as well as in the maintenance of metabolic homeostasis, whereas alveolar macrophages in the lung function in removal of dust, microorganisms, and surfactants from the respiratory surfaces despite their common origin from fetal liver. Within the same tissue, macrophages are heterogeneous and can change phenotypes and functions in response to changing local tissue environment. For example, macrophages can eliminate antibody-bound tumor cells through Fc receptor-mediated phagocytosis (antibody-dependent cellular phagocytosis or ADCP). However, once adapted to the tumor microenvironment, the tumor-associated macrophages (TAM) suppress anti-tumor immune responses and promote tumor growth and metastasis.

[0051] Macrophage plasticity underlies their ability to be activated toward a spectrum of phenotypes and acquire diverse functions. One extreme is the classically activated pro-inflammatory M1 macrophages and the other extreme is the alternatively activated anti-inflammatory M2 macrophages. By expressing inflammatory cytokines, such as IFNγ and TNFα, and reactive oxygen species, M1 macrophages mediate anti-microbial and anti-tumor responses, but can also cause inflammation and tissue damage if hyper-activated. In contrast, by expressing anti-inflammatory cytokines, such as IL-10, TGFβ and arginase, M2 macrophages mediate tissue repair, but can also mediate fibrosis if dysregulated. While M1 and M2 serves to define the opposite activating states of macrophages in simplistic manner, most macrophages exhibit multi-dimensional spectrum of phenotypes in response to various physiological and pathological signals. By transcriptional profiling of human monocyte-derived macrophages (hMDMs) in response to 29 different stimuli, such as pro- and anti-inflammatory cytokines, 49 gene expression modules that are associated with macrophage activation were identified. Many aspects of macrophage activation/plasticity remain poorly defined. In particular, how small molecules modulate macrophage activation remains to be elucidated.

[0052] Because of their critical function in maintaining tissue homeostasis and repair, dysregulation of macrophage polarization has been implicated in contributing to many human diseases including cancer, fibrosis, obesity, diabetes, and infectious, cardiovascular, inflammatory and neurodegenerative diseases. For example, TAMs are one of the most abundant immune cells present in solid tumors. Clinical and experimental studies have shown that TAMs produce various membranous and soluble factors that enhance tumor cell growth and invasion as well as suppress anti-tumor immune responses to allow cancer cells to escape immune surveillance. TAMs are derived from circulating monocytes in the tumor microenvironment, which progressively skews macrophages into the immunosuppressive state, phenotypically resembling M2-activated macrophages. Reprogramming M2-like TAMs toward M1-like macrophages is associated with expression of a strong anti-tumor activity. In a remarkable synergy, cyclophosphamide-activated macrophages efficiently eliminate leukemia cells in refractory bone marrow microenvironment in combination with monoclonal antibody therapeutics. Repolarizing TAMs toward a pro-inflammatory, anti-tumorigenic M1-like state proves an efficient approach to cancer immunotherapy either alone or in combination with antibody therapeutics. More broadly, as dysregulation of macrophage activation has emerged as a key determinant in many disease development and progression, modulation of macrophage activation could be a fruitful approach for disease intervention.

[0053] Described herein is a high throughput phenotypic screen for small molecules that activate primary human macrophages. By screening a library of 4126 compounds which include FDA-approved drugs, bioactive compounds and natural products, ~300 potently activated M-CSF cultured macrophages toward pro-inflammatory M1-like or

anti-inflammatory M2-like state (or spectrum) were identified. Among the hits, ~30 were capable of reprogramming M2-like macrophages induced by IL4/IL13 toward pro-inflammatory M1-like macrophages and another ~20 were capable of reprogramming M1-like macrophages induced by IFNγ/TNFα toward anti-inflammatory M2-like macrophages. By analyzing the effects of the 34 selected hits on macrophage reprogramming through RNA-seq, we identified new cellular pathways that mediate macrophage activation (or reprogramming). M1-activating compounds thiostrepton and cucurbitacin I were further shown to reprogram TAMs toward M1-like macrophages in mice and exhibit potent anti-tumor activity either alone or in combination with monoclonal antibody therapeutics. The examples herein reveal a remarkable plasticity of macrophage polarization and provides a valuable resource not only for studying the macrophage biology but also for developing novel therapeutics or repositioning known drugs for treating diseases through macrophage reprogramming. Furthermore, the phenotypic screen can be extended to much larger compound libraries and in combination with transcriptional profiling is a powerful approach to elucidate the mechanism of action of small molecule compounds in macrophage polarization for precision disease intervention.

[0054] The high throughput phenotypic screen described herein is based on macrophage cell shape changes in response to compounds. Cell shape change is a valid phenotypic profiling of macrophage activation based on the following considerations. First, cell shape changes are mediated by changes in cytoskeleton dynamics and are known to associate with different states of cell function in general. More specifically, both mouse and human macrophages exhibit dramatically different cell shapes following activation into different phenotypes in vitro: an elongated shape for M2-like macrophages and round shape for M1-like macrophages. Consistently, we showed that known M1-activating stimuli LPS, IFNγ and TNFα induced round shape of differentiated macrophages whereas known M2-activating stimuli IL4, IL13 and IL10 induced elongated cell shape of differentiated macrophages (FIG. **1**). Similarly, GM-CSF-induced round human macrophages and M-CSF-induced elongated human macrophages exhibited M1-like and M2-like phenotypes, respectively, based on cytokine profiles, and the genome-wide gene expression. Second, it has been shown that inducing cytoskeleton changes by extracellular stress or drug paclitaxel lead to macrophage polarization. In the examples herein, we also identified several compounds/drugs that modulate macrophage morphology by directly regulating actin-cytoskeleton, including paclitaxel as well as other M1-activating compounds: cytochalasin-B, fenbendazole, parbendazole, methiazole, and M2-activating compounds: podofilox, colchicine and vinblastine sulfate. Analysis of human macrophage responses to fenbendazole and paclitaxel further confirmed that both drugs activated macrophages toward M1-like phenotype at both the transcriptional and translational level (FIGS. **2**C, **4**, **9**C, and **11**). Third, although we used cell shape change as a high throughput readout in the initial phenotypic screen, we confirmed the effects of over 40 selected compounds on macrophage activation at the whole genomic level by RNA-seq (FIGS. **2** and **4**) and protein expression of typical M1 and M2 markers by flow cytometry (FIG. **11**). As expected, pathway analysis of DEGs identified cell morphogenesis and cytoskeleton organization as major GO terms that are regulated by the compounds (FIG. **4**C). Thus, a cell shape-based phenotypical profiling is a valid approach to screen for small molecule compounds that activate human macrophages. The data in the Examples herein is a first proof-of-concept large scale screen using primary human macrophages. The screen can be extended to much larger compound libraries as the microscopy-based cell shape profiling can be easily scaled up. As further discussed below, the combination of the phenotypic screen and transcriptional analysis could be a powerful approach to identify compounds and their mechanisms of action in macrophage activation for new drug development.

[0055] The data herein identifies compounds, targets and pathways that mediate macrophage activation and sheds new light on the underlying molecular mechanisms. In our library, many compounds have known protein targets. Based on functional pathway enrichment analysis of protein targets of M1- or M2-activating compounds, we identified known pathways, such as cytokine, in macrophage activation. More importantly, we identified new pathways, including leptin, VEGF, EGF and neurotransmitter pathways, which mediate macrophage activation. Although studies have shown these pathways in macrophage function, their effects on macrophage activation and underlying mechanisms are unknown. Our transcriptional analysis of macrophages suggests that the ligands of these pathways activate macrophage by regulating gene expression of both typical M1 and M2 modules. For example, in hMDMs, leptin upregulates the expression of typical M1 modules induced by IFNγ while suppresses the expression of chronic inflammation TPP modules (FIG. **2**). Notably, the ligands of serotonin transporter and receptors, histamine transporter and receptors, dopamine transporter and receptors, and adrenoceptors all stimulated M1-like macrophage activation, shedding light on the cross-talk between neuronal and immune systems and the potential roles of macrophage activation in neurological diseases.

[0056] Macrophages exhibit a multi-dimensional spectrum of phenotypes beyond M1 and M2. Our identification of a diverse panel of macrophage-activating compounds that target GPCRs, enzymes, kinases, nuclear hormone receptors (NHRs), and transporters (FIG. **1**G) adds to the molecular basis of macrophage plasticity and further identifies new pathways in macrophage activation. Our extensive transcriptional analysis with over 40 selected compounds identifies how each compound stimulates macrophage activation through shared mechanisms and unique pathways. All compounds modulated macrophage activation through common pathways such as inflammatory response, immune response, chemokine- and cytokine-mediated signaling pathways. Furthermore, each compound induced unique transcriptional responses of macrophages through their specific cellular targets; and many of these unique pathways are not known to mediate macrophage activation. For example, thiostrepton has been shown to have antiproliferative activity in cancer cells by inhibiting proteasome function or FOXM. In both human and mouse macrophages, thiostrepton upregulated expression of pro-inflammatory genes, as well as genes associated with IFN/NFκB pathway and oxidative-reduction process (FIGS. **5** and **17**). The transcriptional analysis also revealed that most of the identified compounds stimulate macrophage activation through modulating a fraction of M1- or M2-specific gene modules as well as common denominators that are induced by M1- or M2-activating cytokines (FIGS. **4**C, and **4**D). The milder effect is expected as

individual compound only regulates specific signaling pathways through relevant protein targets (FIG. **4**E). These observations further shed light on the nature of macrophage activation. The identified large panel of small molecule compounds and their corresponding targets and pathways are a rich resource for further studying basic macrophage biology.

[0057] The data described herein also provides a rich resource for exploring compounds/targets/pathways for modulating macrophage activation in disease intervention. Reprogramming macrophage has emerged as a significant approach for treating a variety of diseases. Suppression or reprogramming of M2-like TAMs into M1-like macrophages by small molecule compounds is associated with induction of a strong anti-tumor activity alone or in combination with other therapeutics. Similarly, suppression or reprogramming of M1-like macrophages into M2-like state significantly inhibits the progression of inflammatory and autoimmune diseases. In this study, we confirmed M1-activating compounds thiostrepton and cucurbitacin I potently reprogrammed TAMs toward M1-like macrophages and enhanced anti-tumor activity either alone or in combination with an antibody therapeutic (FIGS. **6**, **18**, and **19**), showing that M1-activating compounds can be explored for reprogramming M2-like macrophages for the treatment of cancer and fibrosis where M2-like macrophages play a significant role in disease processes. Similarly, M2-polarizing compounds can be explored for the treatment of inflammatory diseases by suppressing the inflammatory activities of M1-like macrophages. In complex diseases, pathogenic macrophages are known to be heterogeneous including both M1- and M2-like phenotypes, or have a transitional or intermediate phenotype with mixed characteristics of M1-like and M2-like phenotypes, or exhibit a dynamic phenotype during the disease progression. To target the desired macrophage population, it is critical to suppress the expression of signature genes/pathways in the pathogenic macrophages at the correct time window. Our identification of unique pathways modulated by each compound by transcriptional analysis provides a basis for selecting the appropriate compounds to reprogram macrophages for precision disease intervention.

Activation of GPR3-β-Arrestin2-PKM2 Pathway in Kupffer Cells Protects Against Obesity and Liver Pathogenesis Through Enhanced Glycolysis

[0058] Increasing evidence suggests a critical role of macrophages in regulating body weight and obesity associated pathologies. However, the underlying molecular and cellular mechanisms remain to be elucidated. Here, we show that diphenyleneiodonium (DPI), an agonist of G-protein coupled receptor 3 (GPR3), stimulates both rapid and sustained increase in glycolysis at cellular level and protects mice from high fat diet (HFD) induced obesity and liver pathogenesis. Activation of GPR3 by DPI results in a rapid recruitment of β-arrestin2 to the plasma membrane, formation of β-arrestin2-GAPDH-PKM2 super complex, greatly increased enzymatic activities of GAPDH and PKM2, and therefore a rapid increase in glycolytic activities. DPI stimulation also results in the formation of PKM2 dimers, translocation of PKM2 from the cytosol to the nucleus, transactivation of c-Myc, and transcription of glycolytic genes, leading to a sustained increase in glycolysis. In mice, DPI inhibits HFD-induced obesity and liver pathogenesis by enhancing glycolysis and suppressing inflammatory response of Kupffer cells in a PKM2-dependent manner. In patients with non-alcoholic fatty liver disease (NAFLD), single cell RNA sequencing identifies a population of disease-associated macrophages that exhibit reduced expression of glycolytic genes but increased expression of inflammatory genes. DPI stimulates glycolysis and suppresses inflammatory responses of Kupffer cells from NAFLD patients. These findings identify GPR3-β-arrestin2-PKM2 signaling as a critical pathway for metabolic reprogramming of Kupffer cells and activation of this pathway as a potential approach to inhibit the development of obesity and NAFLD.

[0059] Non-alcoholic fatty liver disease (NAFLD) is the most common liver disorder globally and is induced by fat deposition in the liver. NAFLD progresses through a series of stages: from simple steatosis to non-alcoholic steatohepatitis (NASH) to cirrhosis. Although the disease pathogenesis is not well understood, development of NAFLD is highly correlated with obesity and diabetes, and pathogenetically associated with lipid accumulation, inflammation, injury and fibrosis in the liver. As NFLAD is also a metabolic disorder, mechanisms that link metabolism to inflammation offers insights into the pathogenesis and help to identify targets for therapeutic development.

[0060] Kupffer cells (KCs) are the resident macrophages in the liver and the most abundant tissue macrophages in the body. They play a key role in detoxification, pathogen removal and tissue repair and homeostasis, but they can also contribute to the pathogenesis of liver diseases, including NAFLD, as they are involved in the initiation and progression of inflammation and tissue injury. In response to local stimuli, KCs regulate both metabolic and immune functions in the homeostatic liver. Lipids and other metabolites have been shown to not only regulate the expression of genes associated with immune response in human macrophages, but also modulate the activation of KCs in models of fatty liver disease and steatohepatitis. Disease-associated macrophages (DAMs) have been identified by single cell RNA sequencing (scRNAseq) in livers from patients with advanced NAFLD (NASH and cirrhosis) and from mouse models of NASH. DAMs exhibit altered expression of pathways associated with not only inflammation but also metabolism, suggesting that reprogramming dysfunctional macrophages may be a promising strategy to treat NAFLD.

[0061] G protein-coupled receptors (GPCRs) play essential roles in metabolic disorders as they serve as receptors for metabolites and fatty acids. In our screen for compounds that can reprogram macrophages, we found that diphenyleneiodonium (DPI), an agonist of GPR3, upregulates expression of genes involved in glycolysis and lipid metabolism. GPR3 is highly expressed in the brain and has been shown to play important roles in neurological processes. GPR3 is considered as a constitutively active orphan receptor that mediates sustained cAMP production in the absence of a ligand. An important mechanism that regulates GPCR signaling is desensitization, involving the receptor kinases (GRKs) and the β-arrestins. GPR3 stimulates the A3 production by recruiting the scaffold protein β-arrestin2 to regulate γ-secretase activity. Despite these progresses, little is known about the function and mechanism of GPR3 signaling in other cell types, especially in regulating metabolism.

[0062] We have investigated the effect of DPI on metabolic reprogramming of macrophages, the underlying

molecular mechanisms, and physiological effect of DPI on high fat diet (HFD)-induced obesity and pathogenesis. We show: i) DPI induces a rapid switch of cellular metabolism from oxidative phosphorylation (OxPhos) to glycolysis in macrophages by stimulating the formation of β-arrestin2-GAPDH-PKM2 super complex with greatly increased enzymatic activities; ii) DPI also induces a prolonged increase in glycolytic activities by stimulating translocation of PKM2 from cytosol to nucleus, transactivation of c-Myc, and transcription of glycolytic genes; iii) DPI inhibits HFD-induced obesity and liver pathogenesis in mice by stimulating glycolysis and suppressing inflammation in KCs and in a manner that requires PKM2 expression in KCs; and iv) DPI also stimulates glycolysis and suppresses inflammation of KCs from patients with NAFLD. These findings identify that GPR3 to β-arrestin2 to PKM2 and to c-Myc signaling is a critical pathway for metabolic reprogramming of macrophages and activation of this pathway in KCs is an approach for therapeutic interventions of obesity and NAFLD.

[0063] DPI has been reported as an agonist of GPR3 and an inhibitor of NOX. Consistent with previous observation that NOX-deficiency leads to a lower cellular glycolysis, we found that p47phox$^{-/-}$ BMDMs and inhibition of NOX activity by apocynin in macrophages lead to a significantly reduced basal level of glycolytic activity. However, DPI (50 nM) stimulated a similar level of increase in glycolysis in p47phox$^{-/-}$ BMDMs as in wild-type BMDMs, or with or without inhibitor apocynin, showing that DPI stimulates glycolysis independent of NOX activity. In contrast, although GPR3 knockdown also reduces the basal level of glycolytic activities, DPI (50 nM) failed to stimulate any significant increase in glycolysis, suggesting that DPI stimulates glycolysis through activation of GPR3. Similarly, β-arrestin2 and PKM2 are required for mediating the effect of DPI on glycolysis as knockout of these genes in BMDMs abolishes DPI-induced glycolysis. The difference between β-arrestin2 and PKM2 is that the former is required for maintaining a threshold level of basal glycolytic activity while the latter is not required. These genetic analyses identify a signaling pathway involving GPR3, β-arrestin2 and PKM2 in mediating the effect of DPI on glycolysis as well as NOX, GPR3 and β-arrestin2 in maintaining a threshold level of basal cellular glycolysis. As SIP, a putative endogenous ligand of GPR3, also induces a significant increase in glycolysis in macrophages, the identified pathway likely functions in metabolic reprogramming in response to endogenous ligands.

[0064] Consistent with a critical role of β-arrestin2 in GPCR signaling by functioning as a scaffold protein, we show that activation of GPR3 by DPI leads to a rapid recruitment of β-arrestin2 to the plasma membrane (FIG. **21**I), presumably to GPR3. Biochemically, we further show that activation of GPR3 by DPI results in the formation of glycolytic enzyme super complex, including β-arrestin2, enolase, GAPDH and PKM2 (FIG. **22**A), in an ERK1/2-dependent manner (FIG. **30**). The greatly increased enzymatic activities of GAPDH and PKM2 provides a biochemical basis for the rapid increase of glycolytic activities following DPI treatment.

[0065] We found that activation of GPR3 by DPI also promotes the formation of PKM2 dimers in an ERK1/2-dependent manner (FIGS. **23**B and **30**A). ERK1/2-dependent formation of PKM2 dimers is known to translocate from the cytosol to the nucleus and activate transcription of glycolytic genes. Indeed, DPI stimulates PKM2 translocation into the nucleus in both ImKCs and primary human KCs and c-Myc transcription in an PKM2-dependent manner (FIG. **23**C). c-Myc is known to directly activate almost all glycolytic genes through binding the classical E-box sequence. Besides an increased level of transcription, we also show that DPI stimulates c-Myc transactivation activities by reporter gene assay in ImKCs (FIG. **23**D). These findings provide a molecular mechanism by which DPI stimulates a sustained increase of glycolytic activities in macrophages.

[0066] Consistent with the increased glucose consumption through elevated glycolysis, DPI has profound effects on glucose metabolism and on HFD-induced weight gain, lipid deposition and fibrosis in the liver at the organismal level. DPI confers a better glucose tolerance in mice under normal conditions (FIG. **31**). DPI significantly inhibits HFD-induced weight gains without affecting feed intake (FIGS. **24** and **32**). Impressively, DPI treatment of obese mice on HFD every 5 days is able to almost completely eliminate lipid droplet accumulation and fibrosis in the liver (FIGS. **24**F and **32**E), suggesting that DPI's effect on liver pathologies is not completely dependent on body weight reduction. Supporting this notion, KCs from HFD-fed mice with or without DPI treatment differ dramatically in expression of glycolytic and inflammatory genes (FIG. **25**). DPI greatly stimulates expression of genes in glycolysis pathway but suppresses expression of inflammatory genes, showing the effect on liver pathologies is likely a result of both increased glycolysis (and therefore reduced lipid accumulation) and reduced inflammation (fibrosis). Remarkably, knockout of PKM2 specifically in KCs in mice abolishes the effect of DPI on HFD-induced obesity and liver pathogenesis (FIG. **24**G-**24**H), suggesting that metabolic reprogramming of KCs alone is sufficient to protect from obesity and liver pathogenesis.

[0067] Finally, we show the presence of DAMs in the liver of NAFLD patients, which share the same phenotype, including expression of TREM2, CD9, GPNMB, MHCII (HLA-DRB1), C1QA and CLEC10A, as those found in the livers of patients with NASH and cirrhosis. As similar DAMs have been observed in various tissues with diverse pathologies, such as HFD-induced NASH in mice, scar tissues, Alzheimer's disease, and lung fibrosis, DAMs from different diseases may share a common gene expression signature. Our scRNAseq shows that DAMs are inhibited in glycolysis but increased in inflammation as suggested by downregulation of glycolytic genes and upregulation of inflammatory genes (FIG. **26**). Importantly, KCs, including DAMs, from NAFLD patients respond to DPI by upregulating the transcription of glycolytic genes and downregulating the transcription of inflammatory genes (FIG. **26**G-**26**H). As such, reprogramming macrophage metabolism, such as by DPI, is a promising therapeutic approach to treat diverse metabolic diseases.

[0068] In one aspect, described herein is a method of identifying a modulator of macrophage activation. The method comprises contacting a primary macrophage cell with a candidate agent; monitoring or photographing the morphology of the cell contacted with the candidate agent; and optionally comparing the cell's morphology in the presence of the candidate agent with the cell's morphology in the absence of the candidate agent; wherein a change in

morphology in the presence of the candidate agent is indicative of modulation of macrophage activation.

[0069] In another aspect, described herein is a method of treating cancer, fibrosis, or an infectious disease. The method comprises administering to a subject in need thereof an effective amount of a modulator of macrophage activation; wherein the modulator changes the morphology of a macrophage cell from elongated shape to round shape.

[0070] In one aspect, described herein is a method of treating an inflammatory disease, a metabolic disease, an autoimmune disease, or a neurodegenerative disease. The method comprises administering to a subject in need thereof an effective amount of a modulator of macrophage activation; wherein the modulator changes the morphology of a macrophage cell from round shape to elongated shape.

[0071] In another aspect, described herein is a method of treating cancer, fibrosis, or an infectious disease. The method comprises administering to a subject in need thereof an effective amount of a modulator of macrophage activation; wherein the modulator activates a serotonin transporter or receptor, a histamine transporter or receptor, a dopamine transporter or receptor, an adrenoceptor, VEGF, EGF and/or leptin.

[0072] In one aspect, described herein is a method of treating an inflammatory disease, a metabolic disease, an autoimmune disease, or a neurodegenerative disease. The method comprises administering to a subject in need thereof an effective amount of a modulator of macrophage activation; wherein the modulator inhibits a serotonin transporter or receptor, a histamine transporter or receptor, a dopamine transporter or receptor, an adrenoceptor, VEGF, EGF and/or leptin.

[0073] In another aspect, described herein is a method of treating an inflammatory disease, a metabolic disease, an autoimmune disease, or a neurodegenerative disease. The method comprises administering to a subject in need thereof an effective amount of diphenyleneiodonium (DPI).

Definitions

[0074] Unless otherwise defined herein, scientific and technical terms used in this application shall have the meanings that are commonly understood by those of ordinary skill in the art. Generally, nomenclature used in connection with, and techniques of, chemistry, cell and tissue culture, molecular biology, cell and cancer biology, neurobiology, neurochemistry, virology, immunology, microbiology, pharmacology, genetics and protein and nucleic acid chemistry, described herein, are those well-known and commonly used in the art.

[0075] The methods and techniques of the present disclosure are generally performed, unless otherwise indicated, according to conventional methods well known in the art and as described in various general and more specific references that are cited and discussed throughout this specification. See, e.g. "Principles of Neural Science", McGraw-Hill Medical, New York, N.Y. (2000); Motulsky, "Intuitive Biostatistics", Oxford University Press, Inc. (1995); Lodish et al., "Molecular Cell Biology, 4th ed.", W. H. Freeman & Co., New York (2000); Griffiths et al., "Introduction to Genetic Analysis, 7th ed.", W. H. Freeman & Co., N.Y. (1999); and Gilbert et al., "Developmental Biology, 6th ed.", Sinauer Associates, Inc., Sunderland, MA (2000).

[0076] The term "agent" is used herein to denote a chemical compound (such as an organic or inorganic compound, a mixture of chemical compounds), a biological macromolecule (such as a nucleic acid, an antibody, including parts thereof as well as humanized, chimeric and human antibodies and monoclonal antibodies, a protein or portion thereof, e.g., a peptide, a lipid, a carbohydrate), or an extract made from biological materials such as bacteria, plants, fungi, or animal (particularly mammalian) cells or tissues. Agents include, for example, agents whose structure is known, and those whose structure is not known.

[0077] "Adjuvant" or "Adjuvant therapy" broadly refers to an agent that affects an immunological or physiological response in a patient or subject. For example, an adjuvant might increase the presence of an antigen over time or to an area of interest like a tumor, help absorb an antigen presenting cell antigen, activate macrophages and lymphocytes and support the production of cytokines. By changing an immune response, an adjuvant might permit a smaller dose of an immune interacting agent to increase the effectiveness or safety of a particular dose of the immune interacting agent. For example, an adjuvant might prevent T cell exhaustion and thus increase the effectiveness or safety of a particular immune interacting agent.

[0078] The terms "decrease", "reduced", "reduction", or "inhibit" are all used herein to mean a decrease by a statistically significant amount. In some embodiments, "reduce," "reduction" or "decrease" or "inhibit" typically means a decrease by at least 10% as compared to a reference level (e.g., the absence of a given ligand) and can include, for example, a decrease by at least about 10%, at least about 20%, at least about 25%, at least about 30%, at least about 35%, at least about 40%, at least about 45%, at least about 50%, at least about 55%, at least about 60%, at least about 65%, at least about 70%, at least about 75%, at least about 80%, at least about 85%, at least about 90%, at least about 95%, at least about 98%, at least about 99%, or more. As used herein, "reduction" or "inhibition" does not encompass a complete inhibition or reduction as compared to a reference level. "Complete inhibition" is a 100% inhibition as compared to a reference level.

[0079] As used herein, the term "antibody" may refer to both an intact antibody and an antigen binding fragment thereof. Intact antibodies are glycoproteins that include at least two heavy (H) chains and two light (L) chains interconnected by disulfide bonds. Each heavy chain includes a heavy chain variable region (abbreviated herein as VH) and a heavy chain constant region. Each light chain includes a light chain variable region (abbreviated herein as VL) and a light chain constant region. The VH and VL regions can be further subdivided into regions of hypervariability, termed complementarity determining regions (CDR), interspersed with regions that are more conserved, termed framework regions (FR). Each VH and VL is composed of three CDRs and four FRs, arranged from amino-terminus to carboxy-terminus in the following order: FR1, CDR1, FR2, CDR2, FR3, CDR3, FR4. The variable regions of the heavy and light chains contain a binding domain that interacts with an antigen. The term "antibody" includes, for example, monoclonal antibodies, polyclonal antibodies, chimeric antibodies, humanized antibodies, human antibodies, multispecific antibodies (e.g., bispecific antibodies), single-chain antibodies and antigen-binding antibody fragments.

[0080] The terms "antigen binding fragment" and "antigen-binding portion" of an antibody, as used herein, refers to one or more fragments of an antibody that retain the ability to bind to an antigen. Examples of binding fragments encompassed within the term "antigen-binding fragment" of an antibody include Fab, Fab', F(ab')2, Fv, scFv, disulfide linked Fv, Fd, diabodies, single-chain antibodies, NANOBODIES®, isolated CDRH3, and other antibody fragments that retain at least a portion of the variable region of an intact antibody. These antibody fragments can be obtained using conventional recombinant and/or enzymatic techniques and can be screened for antigen binding in the same manner as intact antibodies.

[0081] The terms "increased", "increase" or "enhance" or "activate" are all used herein to generally mean an increase by a statically significant amount; for the avoidance of any doubt, the terms "increased", "increase" or "enhance" or "activate" means an increase of at least 10% as compared to a reference level, for example an increase of at least about 20%, or at least about 30%, or at least about 40%, or at least about 50%, or at least about 60%, or at least about 70%, or at least about 80%, or at least about 90% or up to and including a 100% increase or any increase between 10-100% as compared to a reference level, or at least about a 2-fold, or at least about a 3-fold, or at least about a 4-fold, or at least about a 5-fold or at least about a 10-fold increase, at least about a 20-fold increase, at least about a 50-fold increase, at least about a 100-fold increase, at least about a 1000-fold increase or more as compared to a reference level.

[0082] "Immunotherapy" is treatment that uses a subject's immune system to treat cancer and includes, for example, checkpoint inhibitors, cancer vaccines, cytokines, cell therapy, CAR-T cells, and dendritic cell therapy.

[0083] A "patient," "subject," or "individual" are used interchangeably and refer to either a human or a non-human animal. These terms include mammals, such as humans, primates, livestock animals (including bovines, porcines, etc.), companion animals (e.g., canines, felines, etc.) and rodents (e.g., mice and rats).

[0084] "Treating" a condition or patient refers to taking steps to obtain beneficial or desired results, including clinical results. As used herein, and as well understood in the art, "treatment" is an approach for obtaining beneficial or desired results, including clinical results. Beneficial or desired clinical results can include, but are not limited to, alleviation or amelioration of one or more symptoms or conditions, diminishment of extent of disease, stabilized (i.e. not worsening) state of disease, preventing spread of disease, delay or slowing of disease progression, amelioration or palliation of the disease state, and remission (whether partial or total), whether detectable or undetectable. "Treatment" can also mean prolonging survival as compared to expected survival if not receiving treatment.

[0085] The term "preventing" is art-recognized, and when used in relation to a condition, such as a local recurrence (e.g., pain), a disease such as cancer, a syndrome complex such as heart failure or any other medical condition, is well understood in the art, and includes administration of a composition which reduces the frequency of, or delays the onset of, symptoms of a medical condition in a subject relative to a subject which does not receive the composition. Thus, prevention of cancer includes, for example, reducing the number of detectable cancerous growths in a population of patients receiving a prophylactic treatment relative to an untreated control population, and/or delaying the appearance of detectable cancerous growths in a treated population versus an untreated control population, e.g., by a statistically and/or clinically significant amount.

[0086] "Administering" or "administration of" a substance, a compound or an agent to a subject can be carried out using one of a variety of methods known to those skilled in the art. For example, a compound or an agent can be administered, intravenously, arterially, intradermally, intramuscularly, intraperitoneally, subcutaneously, ocularly, sublingually, orally (by ingestion), intranasally (by inhalation), intraspinally, intracerebrally, and transdermally (by absorption, e.g., through a skin duct). A compound or agent can also appropriately be introduced by rechargeable or biodegradable polymeric devices or other devices, e.g., patches and pumps, or formulations, which provide for the extended, slow or controlled release of the compound or agent. Administering can also be performed, for example, once, a plurality of times, and/or over one or more extended periods.

[0087] Appropriate methods of administering a substance, a compound or an agent to a subject will also depend, for example, on the age and/or the physical condition of the subject and the chemical and biological properties of the compound or agent (e.g., solubility, digestibility, bioavailability, stability and toxicity). In some embodiments, a compound or an agent is administered orally, e.g., to a subject by ingestion. In some embodiments, the orally administered compound or agent is in an extended release or slow release formulation, or administered using a device for such slow or extended release.

[0088] A "therapeutically effective amount" or a "therapeutically effective dose" of a drug or agent is an amount of a drug or an agent that, when administered to a subject will have the intended therapeutic effect. The full therapeutic effect does not necessarily occur by administration of one dose, and may occur only after administration of a series of doses. Thus, a therapeutically effective amount may be administered in one or more administrations. The precise effective amount needed for a subject will depend upon, for example, the subject's size, health and age, and the nature and extent of the condition being treated, such as cancer or MDS. The skilled worker can readily determine the effective amount for a given situation by routine experimentation.

Screening Assays

[0089] The present disclosure provides methods of identifying a modulator of macrophage activation, comprising contacting a primary macrophage cell with a candidate agent; monitoring or photographing the morphology of the cell contacted with the candidate agent; and optionally comparing the cell's morphology in the presence of the candidate agent with the cell's morphology in the absence of the candidate agent; wherein a change in morphology in the presence of the candidate agent is indicative of modulation of macrophage activation.

[0090] As used herein, the term "test compound" or "candidate agent" refers to an agent or collection of agents (e.g., compounds) that are to be screened for their ability to have an effect on the cell. Test compounds can include a wide variety of different compounds, including chemical compounds, mixtures of chemical compounds, e.g., polysaccharides, small organic or inorganic molecules (e.g., molecules having a molecular weight less than 2000 Daltons, less than 1500 Dalton, less than 1000 Daltons, or less than 500

Daltons), biological macromolecules, e.g., peptides, proteins, peptide analogs, and analogs and derivatives thereof, peptidomimetics, nucleic acids, nucleic acid analogs and derivatives, an extract made from biological materials such as bacteria, plants, fungi, or animal cells or tissues, naturally occurring or synthetic compositions.

[0091] Depending upon the particular embodiment being practiced, the test compounds can be provided free in solution, or can be attached to a carrier, or a solid support, e.g., beads. A number of suitable solid supports can be employed for immobilization of the test compounds. Examples of suitable solid supports include agarose, cellulose, dextran (commercially available as, i.e., Sephadex, Sepharose) carboxymethyl cellulose, polystyrene, polyethylene glycol (PEG), filter paper, nitrocellulose, ion exchange resins, plastic films, polyaminemethylvinylether maleic acid copolymer, glass beads, amino acid copolymer, ethylene-maleic acid copolymer, nylon, silk, etc. Additionally, for the methods described herein, test compounds can be screened individually, or in groups. Group screening is particularly useful where hit rates for effective test compounds are expected to be low such that one would not expect more than one positive result for a given group.

[0092] A number of small molecule libraries are known in the art and commercially available. These small molecule libraries can be screened using the screening methods described herein. A chemical library or compound library is a collection of stored chemicals that can be used in conjunction with the methods described herein to screen candidate agents for a particular effect. A chemical library comprises information regarding the chemical structure, purity, quantity, and physiochemical characteristics of each compound. Compound libraries can be obtained commercially, for example, from Enzo Life Sciences™, Aurora Fine Chemicals™, Exclusive Chemistry Ltd.™, ChemDiv, ChemBridge™, TimTec Inc.™, AsisChem™, and Princeton Biomolecular Research™, among others.

[0093] Without limitation, the compounds can be tested at any concentration that can exert an effect on the cells relative to a control over an appropriate time period. In some embodiments, compounds are tested at concentrations in the range of about 0.01 nM to about 100 nM, about 0.1 nM to about 500 microM, about 0.1 microM to about 20 microM, about 0.1 microM to about 10 microM, or about 0.1 microM to about 5 microM.

[0094] The compound screening assay can be used in a high throughput screen. High throughput screening is a process in which libraries of compounds are tested for a given activity. High throughput screening seeks to screen large numbers of compounds rapidly and in parallel. For example, using microtiter plates and automated assay equipment, a laboratory can perform as many as 100,000 assays per day, or more, in parallel.

[0095] The compound screening assays described herein can involve more than one measurement of the cell or reporter function (e.g., measurement of more than one parameter and/or measurement of one or more parameters at multiple points over the course of the assay). Multiple measurements can allow for following the biological activity over incubation time with the test compound. In one embodiment, the reporter function is measured at a plurality of times to allow monitoring of the effects of the test compound at different incubation times.

[0096] The screening assay can be followed by a subsequent assay to further identify whether the identified test compound has properties desirable for the intended use. For example, the screening assay can be followed by a second assay selected from the group consisting of measurement of any of: bioavailability, toxicity, or pharmacokinetics, but is not limited to these methods.

EXAMPLES

[0097] The invention now being generally described, it will be more readily understood by reference to the following examples which are included merely for purposes of illustration of certain aspects and embodiments of the present invention, and are not intended to limit the invention.

Example 1: Experimental Procedures

Human Monocyte-Derived Macrophages and Cell Lines

[0098] Human peripheral blood mononuclear cells (PBMCs) were isolated from fresh blood (Research Blood Components LLC.) by density gradient centrifugation with Ficoll-Paque Plus (GE healthcare) and LeucoSep™ (Greiner Bio-one). Human monocytes were purified from PBMC using the EasySep™ human monocyte isolation kit (Stemcell Technology) according to the manufacture's protocol. For in vitro differentiation of monocytes into human macrophages (M0, primary macrophage), isolated monocytes were cultured in complete RMPI1640 supplemented with 10% FCS (Gibco), 2 mM L-glutamine (Corning) and 1% PenStrep solution (Corning) in the presence of 50 ng/mL recombinant human M-CSF (Peprotech) for 7 days. Tumor cell line B16F10 were purchased from ATCC and cultured in complete DMEM supplemented with 10% FCS, 1% PenStrep solution and 2 mM L-glutamine. Luciferase-expressing human lymphoma B cell line (GMB) were described in Roghanian et al. *Cancer Immunol Res* (2019) and cultured in complete RPMI 1640 containing 10% FCS, 2 mM L-glutamine, 0.55 mM 2-mercaptoethanol (Gibco), 1% non-essential amino acids (Lonza), 1 mM sodium pyruvate (Cellgro) and 1% PenStrep solution.

High Throughput Compound Screening, High-Content Microscope and Image Analysis

[0099] Based on the shape difference of M1 (round) and M2 (elongated) differentiated macrophages, we developed a high throughput method to screen compounds which could modulate macrophage polarization. Human M0 primary macrophages differentiated from monocytes in vitro were seeded using a Multidrop Combi dispenser (Thermo Scientific) at a density of 5,000 cells/well in 50 μL complete RPMI in the presence of 10 ng/mL M-CSF into optical 384-well plates (Cat. 393562, BD Falcon) and cultured for 16 hrs for cell recovery. Around 20% of macrophages in this stage (M0) are elongated. Cells were treated with a library of over 4000 individual compounds or drugs at the final concentration of 20 μM using the CyBi-Well simultaneous pipettor (CyBio). The screening compound library composes of the 2066 bioactive compounds, 320 FDA approved drugs, 440 oncological drugs and 1280 natural compounds from the center for the development of therapeutics in Broad Institute at MIT. After 24 hr incubation, supernatants were removed using the microplate washer (Bioteck) and cells were fixed by adding 50 μL 16% paraformaldehyde (Thermo

Scientific) with the dispenser for 20 minutes. Cells were then washed with 50 μL 1×PBS twice and incubated for 20 minutes with NucBlue and AF746 Phalloidin (Invitrogen) to stain nucleus and cytoskeleton. Cells were then washed with 50 μL 1×PBS twice and maintained in PBS for the image acquirement. Plates were read in the Opera Phenix high content screening system (PerkinElmer) to photograph cells using 20× objective in 2 fluorescent channels (Blue and FarRed). A total of 6 different fields in each well and an average of 1,000 cells were imaged per well. CellProfiler was used to identify each cell by overlapping signals from its nucleus and cytoskeleton, and calculate the eccentricity as the parameter to measure the cell morphology. The Z-score was calculated by T-test to measure the difference of cell morphology between each treatment and control. For each row of the 384-well plate, total 4 wells with first and last two columns treated with the same concentration of DMSO were combined as the control for the other 20 treatment wells in that row. In the meantime, classic M1 and M2 stimuli were added to generate the gold-standard Z-score cutoffs with M1 or M2 activation. Classic M1 stimuli include LPS (100 ng/mL), IFNγ (50 ng/mL, Peprotech), TNFα (50 ng/mL, Peprotech), or IFNγ plus TNFα. Classic M2 stimuli include IL-10 (10 ng/mL, Peprotech), IL-4 (10 ng/mL, Peprotech), or IL-13 (5 ng/mL, Peprotech). The gold-standard Z-scores were used as the cutoffs to identify potent compounds to activate macrophage into M1 or M2 state.

[0100] To further screen to compounds which could reactivate or reprogram differentiated macrophages, potent 127 M1-activating and 180 M2-activating compounds from the first-round screening were cherry-picked up. Human macrophages were seeded into optical 384-well plates. Sixteen hours later, medium in M1 plates were replaced by M1 differentiating medium (complete RPMI with 50 ng/mL IFNγ and 50 ng/mL TNFα) and medium in M2 plates by M2 differentiating medium (complete RPMI with 5 ng/mL IL-4 and 5 ng/mL IL-13). After 24 hrs cell differentiation, M1 plates (M1 macrophages) and M2 plates (M2 macrophages) were treated with M2-activating compounds and M1-activating compounds respectively for 24 hrs. Two independent experiments were performed with or without replacing differentiating medium right before treatment. Cell imaging and analysis were performed as indicated above.

Compound Target and Pathway Analysis

[0101] The identified compounds were classified based on the database from the International Union of Basic and Clinical Pharmacology (IUPHAR) (guidetopharmacology.org). The protein targets of the compounds were text-mined based on the target databases of UPHAR and DrugBank (drugbank.ca). The pathway enrichment analysis of protein targets of compounds was based on the WikiPathways.

Mice, Antibodies and Flow Cytometry

[0102] B6 mice were purchased from the Jackson Laboratory and maintained in the animal facility at the Massachusetts Institute of Technology (MIT). NSG mice were purchased from the Jackson Laboratory and maintained under specific pathogen-free conditions in the animal facilities at MIT. All animal studies and procedures were approved by the Massachusetts Institute of Technology's Committee for Animal Care. Flow cytometry antibodies specific for mouse CD11b (M1/70), F4/80 (BM8), MHC-II (M5/114.15.2), Ly6C (HK1.4), Ly6G (1A8), Gr-1 (RB6-8C5), CD80 (16-10A1), CD86 (GL-1), CD163 (S15049I), CD206 (C068C2), IFNγ (XMG1.2) and TNFα (MP6-XT22) were from Biolegend (USA) and iNOS (CXNFT) as from eBioscience (USA). Flow cytometry antibodies specific for human CD80 (2D10), CD86 (BU63), CD163 (GHI/61) and CD206 (15-2) were fopm Biolegend (USA) and iNOS (4E5) was from Novus Biologicals (USA). Antibody ARG1 (AlexF5) specific for both human and mouse was from eBioscience (USA). B16F10 melanoma specific antibody TA99 for in vivo study was prepared as described. Single cell preparation from different organs, staining of cells with fluorophore-conjugated antibodies and analysis of the stained cells using flow cytometry are as described. Briefly, cells in single cell suspension were incubated with specific antibodies at 4° C. for 20 minutes, washed twice, and resuspended in FACS buffer containing either DAPI. Cells were fixed and permeabilized with Cyto-Fast Fix/Perm buffer set (Biolegend) for intracellular staining according to the manufacture's protocol. Samples were stimulated by the cell stimulation cocktail (eBioscience) for 4 hrs and then fixed/permeabilized for intracellular staining. Cells were run on BD-LSRII, collecting 20,000 to 100,000 live cells per sample. The data were analyzed by FlowJo.

Mouse Tumor Model and Treatment

[0103] For the melanoma model, an inoculum of 1×10^6 B16F10 tumor cells was injected subcutaneously on the flank of 8- to 10-week-old male B6 mice in 100 L sterile PBS. Six days following tumor inoculation, mice were randomized into 4 treatment groups including control (PBS or DMSO), tumor-targeting antibody TA99, compound, compound plus TA99. TA99 was administered at 100 g per dose intraperitoneally (I.P.). The compound was administrated at the indicated dosage by either I.P. or paratumor injection subcutaneously (S.C.). All mice were dosed at day 6 and day 12 post tumor inoculation for a total of 2 treatments. Tumor size was measured as an area (longest dimension×perpendicular dimension) at day 6, day 12 and day 18 post tumor inoculation. Mice were euthanized for analysis at day 18 post tumor inoculation. For the lymphoma model, 1×10^7 GMB cells were injected through tail intravenously in 100 μL sterile PBS into 10- to 12-week-old male NSG mice. Mice were treated two weeks post tumor cell engraftment. Tumor-targeting antibody Rituxumab (InvivoGen) was administered at 10 mg/kg intraperitoneally. The compound was administrated I.P. at the indicated dosage. All mice were dosed at week 2 and week 3 post tumor injection for a total of 2 treatments. Tumor growth and spread was visualized using an IVIS Spectrum-bioluminescent imaging system (PerkinElmer) at week 2, week 3 and week 4 post tumor injection. Mice were euthanized for analysis at week 4 post tumor inoculation.

Histopathology and Immunochemical Staining

[0104] Mice were euthanized and tumor tissues were isolated and fixed with 10% neutral-buffered formalin solution (Sigma-Aldrich) for 24 hours. The tissues were processed with Tissue Processor (Leica Microsystems) and embedded in paraffin. Sections were cut at 5 m thickness, mounted on polylysine-coated slides (Thermo Fisher Scientific), de-waxed, rehydrated, and processed for hematoxylin

and eosin (H&E) staining according to a standard protocol. For immunochemical staining, antigen retrieval was carried out by either microwaving the slides in 0.01 M sodium citric acid buffer (pH 6.0) for 30 min. Sections were then immersed for 1 hour in blocking buffer (3% BSA, 0.2% Triton X-100 in PBS), then incubated in primary antibody in blocking buffer at 4° C. overnight, followed by incubation with secondary antibody conjugated HRP at 4° C. for 1 hour. All lung stained sections were scanned with a high-resolution Leica Aperio Slide Scanner. Images were analyzed by WebScope software.

Mouse Bone Marrow-Derived Macrophages and Tumor-Associated Macrophages

[0105] Mouse bone marrow-derived macrophages (mBMM) were prepared as described previously[54]. Briefly, fresh bone marrow cells were isolated from B6 mice. Cells were plated into 6-well plate with 1×10^6/mL in complete RPMI with 2-mercaptoethanol and cultured for 6 days with fresh medium change every 2 days. mBMMs were differentiated to resemble TAMs in the presence of 10 ng/mL mIL-4 and mIL-13 (Peprotech) or 25 mM lactate acid for 24 hrs or tumor conditioned medium (CM). To prepare CM, 70% confluent B16F10 cultured were replaced with fresh medium and the tumor medium was collected and filtered (0.2 m) 24 hrs later. The mixture of 3 volumes of tumor medium with 1 volume of complete RPMI for mBMM serves as the CM. Expression of Arg, Fizz1 and Vegfa were quantified by qPCR to assess the development of TAMs. Other genes of Tnf, Il1b, Nos2, Cxcl2, Ccl5, Ym1 and Tgfb serve as macrophage activating markers. To assay the tumor growth inhibition, mBMMs (10,000 cells per well in 96 well plate) were treated with thiostrepton for 24 hrs and then cocultured with equal number of B16 melanoma cells in fresh complete RPMI for 12 hrs. The conditioned medium treated or not treated with thiostrepton were collected and filtered. The numbers of B16 melanoma cells were cultured for 12 hrs with conditioned medium or conditioned medium heated at 95° C. for 5 min. Tumor cells were quantified by flow cytometry to determine the macrophage-dependent killing function.

RNA Isolation, RNA Sequencing and Data Analysis

[0106] RNAs were extracted with RNeasy MiniElute kit (Qiagen), converted into cDNA and sequenced using Next-Generation Sequencing (Illumina). RNA-seq data was aligned to the mouse genome (version mm10) and raw counts of each genes of each sample were calculated with bowtie2 2.2.3 and RSEM 1.2.15. Differential expression analysis was performed using the program edgeR at $P<0.05$ with a 2 fold-change. The gene expression level across different samples was normalized and quantified using the function of cpm. Differentially expressed genes were annotated using online functional enrichment analysis tool DAVID (http://david.ncifcrf.gov/). Gene set enrichment analysis were performed with GSEA with FDR q-value<0.05. The heatmap figure was visualized with MeV. To quantify the levels of RNA transcripts, total RNA was extracted from various cells and reverse transcribed by TaqManÂ® Reverse Transcription Reagents Kit (ABI Catalog No. N8080234), followed by amplification with Sybr Green Master Mix (Roche Catalog No. 04707516001) with specific primers (Table 4) and detected by Roche LightCycler 480. The Ct values were normalized with housekeeping gene GAPDH for comparison.

[0107] Table 4 shows primers for qPCR.

TABLE 4

shows primers for qPCR.

mouse Primer	Sequence	SEQ ID NO:
Arg1-F	CATTGGCTTGCGAGACGTAGAC	1
Arg1-R	GCTGAAGGTCTCTTCCATCACC	2
Fizz1-F	CAAGGAACTTCTTGCCAATCCAG	3
Fizz1-R	CCAAGATCCACAGGCAAAGCCA	4
Vegfa-F	CTGCTGTAACGATGAAGCCCTG	5
Vegfa-R	GCTGTAGGAAGCTCATCTCTCC	6
Ym1-F	TACTCACTTCCACAGGAGCAGG	7
Ym1-R	CTCCAGTGTAGCCATCCTTAGG	8
Tgfb-F	TGATACGCCTGAGTGGCTGTCT	9
Tgfb-R	CACAAGAGCAGTGAGCGCTGAA	10
Tnf-F	GGTGCCTATGTCTCAGCCTCTT	11
Tnf-R	GCCATAGAACTGATGAGAGGGAG	12
Il1b-F	ACGGCTGAGTTTCAGTGAGACC	13
Il1b-R	CACTCTGGTAGGTGTAAGGTGC	14
Ccl2-F	GCTACAAGAGGATCACCAGCAG	15
Ccl2-R	GTCTGGACCCATTCCTTCTTGG	16
Ccl5-F	CCTGCTGCTTTGCCTACCTCTC	17
Ccl5-R	ACACACTTGGCGGTTCCTTCGA	18
Cxcl2-F	CATCCAGAGCTTGAGTGTGACG	19
Cxcl2-R	GGCTTCAGGGTCAAGGCAAACT	20
Gapdh-F	AGTATGACTCCACTCACGGC	21
Gapdh-R	GTTCACACCCATCACAAACA	22
Nos2_F	GAGACAGGGAAGTCTGAAGCAC	23
Nos2_w	CCAGCAGTAGTTGCTCCTCTTC	24
human Primer	Sequence	
GAPDH-F	GTCTCCTCTGACTTCAACAGCG	25
GAPDH-R	ACCACCCTGTTGCTGTAGCCAA	26
TNF-F	CTCTTCTGCCTGCTGCACTTTG	27
TNF-R	ATGGGCTACAGGCTTGTCACTC	28
IL1B-F	CCACAGACCTTCCAGGAGAATG	29
IL1B-R	GTGCAGTTCAGTGATCGTACAGG	30
CXCL2-F	GGCAGAAAGCTTGTCTCAACCC	31
CXCL2-R	CTCCTTCAGGAACAGCCACCAA	32

TABLE 4-continued

shows primers for qPCR.		
IL10-F	TCTCCGAGATGCCTTCAGCAGA	33
IL10-R	TCAGACAAGGCTTGGCAACCCA	34
CD86-F	TCATTCCCTGATGTTACGAGC	35
CD86-R	TCTTCCCTCTCCATTGTGTTG	36
CD163-F	GTGTGATGACTCTTGGGACTTG	37
CD163-R	AGGATGACTGACGGGATGAG	38
CD206-F	GACTGATAAGTGGAGGGTGAGG	39
CD206-R	CCAGAGAGGAACCCATTCG	40

Macrophage Activation Network Induced by Compounds

[0108] To determine the central hubs of all stimulation conditions by compounds (refer to FIG. **4**) reflecting the core macrophage activation network, transcriptional interactions between genes were first determined by ARACNe based on the perturbed transcriptional profiles of 34 compounds as well as IFNγ and IL4 controls. The 12549 unique present genes were taken into calculation of mutual information with p-value less than 1e-7. The threshold of the data processing inequality (DPI) theorem from information theory used by ARACNe was set to 0.1 to detect total 400,165 regulatory interactions in the core macrophage activation network. GO enrichment analysis and enrichment map of top 10% central hubs (1255 genes) was performed by BiNGO. The network was visualized by Cytoscape.

Statistic Methods

[0109] Statistical significance was determined with the two-tailed unpaired or paired Student's t-test. The FDRs were computed with q=p*n/i, (p=P value, n=total number of tests, i=sorted rank of P value).

Data Availability

[0110] Raw RNAseq are deposited in the database of Gene Expression Omnibus (GEO) with accession ID: GSE14992 and GSE155551.

Example 2: Phenotypic Screen of Macrophage Activation

[0111] Human monocytes were isolated from peripheral blood mononuclear cells (PBMCs) and differentiated into macrophages in a 7-day culture in the presence of recombinant human M-CSF. The resulting human monocyte-derived macrophages (hMDMs) were stimulated with different known M1-activating stimuli, including lipopolysaccharide (LPS), IFNγ, TNFα, or IFNγ plus TNFα, or M2-activating cytokines, including IL-10, IL-4 or IL-13, for 24 hours. The M1-activated hMDMs were round with punctate F-actin staining whereas M2-activated hMDMs were elongated with filamentous F-actin staining (FIGS. **1**A and **7**A). Expression of known M1 markers including CD80 and CD86 were up-regulated by IFNγ and suppressed by IL-4 while M2 markers CD206 and CD163 were up-regulated by IL-4 and suppressed by IFNγ (FIG. **7**B). The Z-score for each stimulus was calculated to index its activation ability from the distributions of cell shapes between treated wells and untreated wells by T-test of an average of 1000 cells per well. The M1-activated hMDMs had an average of Z-score of −4 whereas the M2-activated hMDMs had an average of Z-score of 6 (FIG. **1**B). M1- and M2-like human and mouse macrophages have distinct morphologies.

[0112] Based on the correlation between cell shape and macrophage activation, we developed a high throughput screen for compounds that activate hMDMs to either M1- or M2-like state (FIG. **1**C). Human monocytes purified from four healthy donors were mixed at equal ratio and differentiated into macrophages with M-CSF. The resulting macrophages were seeded into 384-well plates and cultured overnight in the presence of M-CSF to maintain macrophages at mostly a non-activated stage. Macrophages in each well were then treated with one of 4126 compounds, including 2086 bioactive compounds, 760 FDA-approved drugs, and 1280 natural products (FIG. **1**D), at a final concentration of 20 M for 24 hours. Cell images were taken by high-content scanning microscope and cell shapes were quantified by Cellprofiler (FIG. **1**E). Based on Z-score cutoffs: −4 for M1-activated macrophages and 6 for M2-activated macrophages, 127 and 180 compounds were identified, respectively, to activate human macrophages toward M1-like state (referred to as M1-activating compounds) and M2-like state (referred to as M2-activating compounds) (FIG. **1**F). 98 of 127 (77%) M1-activating and 166 of 180 (92%) M2-activating compounds are FDA-approved drugs (FIG. **1**G). Text-mining identified 119 known protein targets for 80 of the 127 M1-activating compounds and 220 protein targets for 144 of the 180 M2-activating compounds. The targets include G-protein coupled receptors (GPCRs), enzymes, kinases, nuclear hormone receptors (NHRs), and transporters (FIG. **1**G). Many targets of M1- and M2-activating compounds belong to the families of histone deacetylases and VEGF receptors, respectively (FIG. **8**). Some known regulators of macrophage polarization, such as STAT3, FYN, MAP2K1 and CDKs, were rediscovered. Pathways analysis of the protein targets identified known pathways, such as IL-4, IL-1β, and TGFβ pathways, and novel pathways, such as neurotransmitter, leptin, EGF and VEGF signaling pathways, in macrophage activation (FIG. **1**H and Table 1).

[0113] Table 1 shows pathway analysis of proteins targeted by identified compounds.

Pathway Name (Wiki)	Number Compounds	Number Genes Pathway	Compound List	Target List	Number Targets	Average Z-value
GPCRs, Class A Rhodopsin-like	13	261	2-[(4-Phenylpiperazin-1-yl) methyl]-2,3-dihydroimidazo [1,2-c]quinazolin-5(6H)-one; FTY720; Terciprazine; Diphenyleneiodonium	PTGDR; CNR1; HTR2A; HTR1A; DRD2; CNR2; HRH2; PTGIR; CYSLTR1; HTR2C;	19	−5.92

-continued

Pathway Name (Wiki)	Number Compounds	Number Genes Pathway	Compound List	Target List	Number Targets	Average Z-value
			chloride; PIMOZIDE; "WIN 55,212-2 mesylate"; TCB2; FLUOXETINE; Alprostadil; SCH 79797 dihydrochloride; DOXEPIN HYDROCHLORIDE; FPL 55712; CANDESARTAN CILEXTIL	AGTR1; ADRA1A; DRD3; PTGER4; GPR3; PTGER1; HRH1; PTGER2; F2R		
Leptin signaling pathway	12	78	cucurbitacin I; Vemurafenib; niclosamide; Vemurafenib; skepinone-L; SMER 3; niclosamide; SB 202190; IKK 16; Dephostatin; CHIR-99021; API-2	GSK3A; RAF1; MAPK14; IKBKG; MTOR; AKT1; PTPN1; IKBKB; GSK3B; CHUK; STAT3; MAPK1	12	−7.54
B Cell Receptor Signaling Pathway	9	100	Vemurafenib; Vemurafenib; skepinone-L; SB 202190; LFM-A13; IKK 16; Dephostatin; CHIR-99021; API-2	GSK3A; RAF1; MAPK14; PTPN6; IKBKG; BRAF; AKT1; IKBKB; GSK3B; CHUK; MAPK1; BTK	12	−5.82
Notch Signaling Pathway	16	61	cucurbitacin I; MGCD-0103; MS-275; MS-275; MS-275; niclosamide; SMER 3; niclosamide; CI-994; CI-994; PLUMBAGIN; MK-0752; CHIR-99021; CI-994; DAPT; API-2	PSENEN; HDAC1; MTOR; AKT1; APH1A; GSK3B; EP300; HDAC2; PSEN1; STAT3; NCSTN	11	−7.78
BDNF signaling pathway	15	146	cucurbitacin I; Cantharidin; Vemurafenib; FTY720; Ro 08-2750; niclosamide; Vemurafenib; skepinone-L; SMER 3; niclosamide; DEOXYGEDUNIN; SB 202190; "WIN 55,212-2 mesylate"; CHIR-99021; API-2	CNR1; RAF1; MAPK14; NGF; PPP2CA; MTOR; AKT1; NTRK2; GSK3B; STAT3; MAPK1	11	−8.01
IL-4 Signaling Pathway	12	56	cucurbitacin I; niclosamide; skepinone-L; PIMOZIDE; niclosamide; SB 202190; IKK 16; PLUMBAGIN; DOXEPIN HYDROCHLORIDE; Dephostatin; CHIR-99021; API-2	MAPK14; PTPN6; AKT1; IKBKB; EP300; CHUK; HRH1; MAPK11; STAT3; MAPK1	10	−6.90
Kit receptor signaling pathway	13	59	cucurbitacin I; Vemurafenib; niclosamide; Vemurafenib; skepinone-L; SMER 3; niclosamide; SB 202190; LFM-A13; PLUMBAGIN; Dephostatin; CHIR-99021; API-2	RAF1; MAPK14; PTPN6; MTOR; AKT1; EP300; STAT3; MAPK1; BTK	9	−7.34
MAPK Signaling Pathway	9	168	Vemurafenib; Vemurafenib; skepinone-L; SB 202190; IKK16; CMPD-1; CHIR-99021; API-2; PF-3758309	RAF1; MAPK14; PAK1; IKBKG; BRAF; AKT1; IKBKB; MAPKAPK2; MAPK1	9	−5.75
Insulin Signaling	8	160	Vemurafenib; Vemurafenib; skepinone-L; SB 202190; IKK 16; Dephostatin; CHIR-99021; API-2	GSK3A; RAF1; MAPK14; AKT1; PTPN1; IKBKB; GSK3B; MAPK11; MAPK1	9	−5.91
Focal Adhesion	6	191	cytochalasin B; Vemurafenib; Vemurafenib; CHIR-99021; API-2; PF-3758309	RAF1; PAK1; BRAF; AKT1; PAK6; PAK4; GSK3B; ACTG1; MAPK1	9	−9.11
TGF beta Signaling Pathway	16	135	MGCD-0103; MS-275; MS-275; Vemurafenib; MS-275; Vemurafenib; skepinone-L; SMER 3; CI-994; SB 202190; CI-994; WP1130; PLUMBAGIN; CHIR-99021; CI-994; API-2	HDAC1; RAF1; MAPK14; UCHL5; MTOR; AKT1; EP300; MAPK1	8	−7.01

-continued

Pathway Name (Wiki)	Number Compounds	Number Genes Pathway	Compound List	Target List	Number Targets	Average Z-value
SIDS Susceptibility Pathways	11	85	Fluvoxamine maleate; PIMOZIDE; thiostrepton; DEOXYGEDUNIN; AT-DYRK-01; SERTRALINE HYDROCHLORIDE; QX 222; TCB2; FLUOXETINE; PLUMBAGIN; DOXEPIN HYDROCHLORIDE	SCN5A; HTR2A; HTR1A; FOXM1; SLC6A4; MAOA; NTRK2; EP300	8	−6.20
AGE/RAGE pathway	11	66	cucurbitacin I; Vemurafenib; FTY720; niclosamide; Vemurafenib; skepinone-L; niclosamide; SB 202190; IKK 16; CHIR-99021; API-2	PLA2G4A; RAF1; MAPK14; AKT1; IKBKB; CHUK; STAT3; MAPK1	8	−7.98
EGF/EGFR Signaling Pathway	11	162	cucurbitacin I; Vemurafenib; niclosamide; Vemurafenib; skepinone-L; SMER 3; niclosamide; SB 202190; CHIR-99021; API-2; PF-3758309	RAF1; MAPK14; PAK1; MTOR; BRAF; AKT1; STAT3; MAPK1	8	−7.75
IL-5 Signaling Pathway	9	42	cucurbitacin I; Vemurafenib; niclosamide; Vemurafenib; SMER 3; niclosamide; LFM-A13; CHIR-99021; API-2	GSK3A; RAF1; MTOR; AKT1; GSK3B; STAT3; MAPK1; BTK	8	−8.26
TCR Signaling Pathway	8	91	Vemurafenib; Vemurafenib; skepinone-L; SB 202190; IKK 16; CHIR-99021; API-2; PF-3758309	RAF1; MAPK14; PAK1; IKBKG; AKT1; IKBKB; CHUK; MAPK1	8	−5.88
Regulation of Actin Cytoskeleton	6	151	cytochalasin B; Vemurafenib; Vemurafenib; SCH 79797 dihydrochloride; CHIR-99021; PF-3758309	RAF1; PAK1; BRAF; PAK6; PAK4; ACTG1; MAPK1; F2R	8	−9.17
Monoamine GPCRs	6	34	2-[(4-Phenylpiperazin-1-yl)methyl]-2,3-dihydroimidazo[1,2-c]quinazolin-5(6H)-one; Terciprazine; PIMOZIDE; TCB2; FLUOXETINE; DOXEPIN HYDROCHLORIDE	HTR2A; HTR1A; DRD2; HRH2; HTR2C; ADRA1A; DRD3; HRH1	8	−6.32
Androgen receptor signaling pathway	14	89	cucurbitacin I; MGCD-0103; MS-275; MS-275; MS-275; niclosamide; niclosamide; CI-994; CI-994; PLUMBAGIN; CHIR-99021; CI-994; API-2; PF-3758309	HDAC1; KAT2B; AKT1; PAK6; GSK3B; EP300; STAT3	7	−8.11
TWEAK Signaling Pathway	12	42	MGCD-0103; MS-275; MS-275; MS-275; skepinone-L; CI-994; SB 202190; CI-994; IKK 16; CHIR-99021; CI-994; API-2	HDAC1; MAPK14; AKT1; IKBKB; GSK3B; CHUK; MAPK1	7	−7.03
TSH signaling pathway	10	66	cucurbitacin I; Vemurafenib; niclosamide; Vemurafenib; skepinone-L; SMER 3; niclosamide; SB 202190; CHIR-99021; API-2	RAF1; MAPK14; MTOR; BRAF; AKT1; STAT3; MAPK1	7	−8.10
TNF alpha Signaling Pathway	6	93	Cantharidin; Vemurafenib; Vemurafenib; IKK 16; CHIR-99021; API-2	RAF1; PPP2CA; IKBKG; AKT1; IKBKB; CHUK; MAPK1	7	−7.28
IL-1 signaling pathway	6	54	skepinone-L; SB 202190; IKK 16; CMPD-1; CHIR-99021; API-2	MAPK14; IKBKG; AKT1; IKBKB; CHUK; MAPKAPK2; MAPK1	7	−5.06
RANKL/RANK Signaling Pathway	6	55	skepinone-L; SMER 3; SB 202190; IKK 16; CHIR-99021; API-2	MAPK14; IKBKG; MTOR; AKT1; IKBKB; CHUK; MAPK1	7	−5.31

-continued

Pathway Name (Wiki)	Number Compounds	Number Genes Pathway	Compound List	Target List	Number Targets	Average Z-value
Toll-like receptor signaling pathway	5	102	skepinone-L; SB 202190; IKK 16; CHIR-99021; API-2	MAPK14; IKBKG; AKT1; IKBKB; CHUK; MAPK11; MAPK1	7	−5.13
Integrin-mediated Cell Adhesion	5	99	Vemurafenib; Vemurafenib; CHIR-99021; API-2; PF-3758309	RAF1; PAK1; BRAF; AKT1; PAK6; PAK4; MAPK1	7	−6.05
Regulation of toll-like receptor signaling pathway	5	103	skepinone-L; SB 202190; IKK 16; CHIR-99021; API-2	MAPK14; IKBKG; AKT1; IKBKB; CHUK; MAPK11; MAPK1	7	−5.13
Small Ligand GPCRs	3	18	FTY720; "WIN 55,212-2 mesylate"; Alprostadil	PTGDR; CNR1; CNR2; PTGIR; PTGER4; PTGER1; PTGER2	7	−6.01
IL-6 signaling pathway	13	44	cucurbitacin I; MGCD-0103; MS-275; MS-275; MS-275; niclosamide; niclosamide; CI-994; CI-994; PLUMBAGIN; CHIR-99021; CI-994; API-2	HDAC1; AKT1; GSK3B; EP300; STAT3; MAPK1	6	−8.40
Oncostatin M Signaling Pathway	10	64	cucurbitacin I; Vemurafenib; niclosamide; Vemurafenib; skepinone-L; SMER 3; niclosamide; SB 202190; CHIR-99021; API-2	RAF1; MAPK14; MTOR; AKT1; STAT3; MAPK1	6	−8.10
TSLP Signaling Pathway	9	48	cucurbitacin I; niclosamide; skepinone-L; SMER 3; niclosamide; SB 202190; LFM-A13; CHIR-99021; API-2	MAPK14; MTOR; AKT1; STAT3; MAPK1; BTK	6	−7.67
Cell Cycle	9	104	MGCD-0103; MS-275; MS-275; MS-275; CI-994; CI-994; PLUMBAGIN; CHIR-99021; CI-994	HDAC1; CDK1; GSK3B; EP300; HDAC2; HDAC3	6	−7.54
Interleukin-11 Signaling Pathway	8	44	cucurbitacin I; Vemurafenib; niclosamide; Vemurafenib; niclosamide; IKK 16; CHIR-99021; API-2	RAF1; AKT1; IKBKB; CHUK; STAT3; MAPK1	6	−8.49
Senescence and Autophagy	6	106	Vemurafenib; sb 225002; Vemurafenib; skepinone-L; SB 202190; CHIR-99021	RAF1; MAPK14; BRAF; CXCR2; GSK3B; MAPK1	6	−7.28
IL17 signaling pathway	6	31	cucurbitacin I; niclosamide; niclosamide; IKK 16; CHIR-99021; API-2	IKBKG; AKT1; IKBKB; GSK3B; STAT3; MAPK1	6	−8.48
Prostaglandin Synthesis and Regulation	2	31	FTY720; Alprostadil	PTGDR; PLA2G4A; PTGIR; PTGER4; PTGER1; PTGER2	6	−6.44
IL-2 Signaling Pathway	8	40	cucurbitacin I; Vemurafenib; niclosamide; Vemurafenib; SMER 3; niclosamide; CHIR-99021; API-2	RAF1; MTOR; AKT1; STAT3; MAPK1	5	−8.65
IL-3 Signaling Pathway	8	49	cucurbitacin I; Vemurafenib; niclosamide; Vemurafenib; niclosamide; Dephostatin; CHIR-99021; API-2	RAF1; PTPN6; AKT1; STAT3; MAPK1	5	−8.44
GPCRs, Other	7	103	FTY720; PIMOZIDE; "WIN 55,212-2 mesylate"; TCB2; FLUOXETINE; CMPD-1; SCH 79797 dihydrochloride	CNR1; HTR2A; DRD3; GNRHR; F2R	5	−5.54
FSH signaling pathway	7	27	Vemurafenib; Vemurafenib; skepinone-L; SMER 3; SB 202190; CHIR-99021; API-2	RAF1; MAPK14; MTOR; AKT1; MAPK1	5	−6.29
Corticotropin-releasing hormone	6	95	Vemurafenib; Vemurafenib; skepinone-L; SB 202190; CHIR-99021; API-2	MAPK14; BRAF; AKT1; GSK3B; MAPK1	5	−6.29

-continued

Pathway Name (Wiki)	Number Compounds	Number Genes Pathway	Compound List	Target List	Number Targets	Average Z-value
Wnt Signaling Pathway Netpath	3	51	SMER 3; CHIR-99021; API-2	GSK3A; MTOR; AKT1; GSK3B; MAPK1	5	−5.04
Retinoblastoma (RB) in Cancer	11	87	MGCD-0103; MS-275; MS-275; Vemurafenib; MS-275; Vemurafenib; CI-994; CI-994; CHIR-99021; CI-994; Rubitecan	HDAC1; RAF1; CDK1; TOP2A	4	−7.68
Apoptosis-related network due to altered Notch3 in ovarian cancer	10	53	MGCD-0103; MS-275; MS-275; MS-275; CI-994; CI-994; SCH 79797 dihydrochloride; CHIR-99021; CI-994; API-2	HDAC1; AKT1; MAPK1; F2R	4	−7.23
MicroRNAs in cardiomyocyte hypertrophy	9	85	cucurbitacin I; MS-275; MS-275; Vemurafenib; MS-275; niclosamide; Vemurafenib; niclosamide; API-2	RAF1; AKT1; HDAC9; STAT3	4	−10.03
Pathogenic *Escherichia coli* infection	8	58	cytochalasin B; Parbendazole; Paclitaxel; Methiazole; Methiazole; PACLITAXEL; PACLITAXEL; Paclitaxel	TUBA1A; ACTG1; TUBB2C; TUBB1	4	−7.58
Monoamine Transport	8	32	Fluvoxamine maleate; skepinone-L; GBR 12783; SERTRALINE HYDROCHLORIDE; SB 202190; GBR 13069 dihydrochloride; FLUOXETINE; DOXEPIN HYDROCHLORIDE	MAPK14; SLC6A4; SLC6A2; SLC6A3	4	−6.48
Signaling of Hepatocyte Growth Factor Receptor	7	34	cucurbitacin I; Vemurafenib; niclosamide; Vemurafenib; niclosamide; CHIR-99021; PF-3758309	RAF1; PAK1; STAT3; MAPK1	4	−8.98
Serotonin Receptor 2 and ELK-SRF/GATA4 signaling	7	19	Vemurafenib; Terciprazine; Vemurafenib; PIMOZIDE; TCB2; FLUOXETINE; CMPD-1	HTR2A; RAF1; HTR2C; MAPK APK2	4	−6.55
Interferon type I signaling pathways	7	58	cucurbitacin I; niclosamide; skepinone-L; SMER 3; niclosamide; SB 202190; Dephostatin	MAPK14; PTPN6; MTOR; STAT3	4	−8.51
IL-7 Signaling Pathway	5	25	cucurbitacin I; niclosamide; niclosamide; CHIR-99021; API-2	AKT1; GSK3B; STAT3; MAPK1	4	−9.17
MAPK Cascade	5	29	Vemurafenib; Vemurafenib; skepinone-L; SB 202190; CHIR-99021	RAF1; MAPK14; BRAF; MAPK1	4	−6.68
Alpha 6 Beta 4 signaling pathway	5	31	skepinone-L; SMER 3; SB 202190; CHIR-99021; API-2	MAPK14; MTOR; AKT1; MAPK1	4	−5.38
Apoptosis	2	84	IKK 16; API-2	IKBKG; AKT1; IKBKB; CHUK	4	−4.67
G Protein Signaling Pathways	1	92	DIPYRIDAMOLE	PDE8B; PDE7B; PDE8A; PDE4A	4	−4.41
Parkin-Ubiquitin Proteasomal System pathway	7	71	Parbendazole; Paclitaxel; Methiazole; Methiazole; PACLITAXEL; PACLITAXEL; Paclitaxel	TUBA1A; TUBB2C; TUBB1	3	−5.17

-continued

Pathway Name (Wiki)	Number Compounds	Number Genes Pathway	Compound List	Target List	Number Targets	Average Z-value
Cardiac Hypertrophic Response	6	54	MS-275; MS-275; Vemurafenib; MS-275; Vemurafenib; API-2	RAF1; AKT1; HDAC9	3	−8.88
p38 MAPK Signaling Pathway	4	34	FTY720; skepinone-L; SB 202190; CMPD-1	PLA2G4A; MAPK14; MAPKAPK2	3	−6.13
Extracellular vesicle-mediated signaling in recipient cells	4	31	Vemurafenib; Vemurafenib; SMER 3; API-2	RAF1; MTOR; AKT1	3	−6.93
FAS pathway and Stress induction of HSP regulation	3	42	cytochalasin B; CMPD-1; PF-3758309	PAK1; ACTG1; MAPKAPK2	3	−11.15
Integrated Pancreatic Cancer Pathway	3	12	FTY720; PLUMBAGIN; API-2	PLA2G4A; AKT1; EP300	3	−5.69
Signal Transduction of SIP Receptor	3	25	FTY720; CHIR-99021; API-2	S1PR1; AKT1; MAPK1	3	−5.63
Glycogen Metabolism	2	36	Cantharidin; CHIR-99021	GSK3A; PPP2CA; GSK3B	3	−8.64
Nicotine Activity on Dopaminergic Neurons	2	21	PIMOZIDE; RESERPINE	DRD2; DRD3; SLC18A2	3	−5.22
T-Cell Receptor and Co-stimulatory Signaling	2	30	CHIR-99021; API-2	GSK3A; AKT1; GSK3B	3	−4.44
Estrogen signaling pathway	1	27	IKK 16	IKBKG; IKBKB; CHUK	3	−4.98
Serotonin Receptor 2 and STAT3 Signaling	6	4	cucurbitacin I; niclosamide; PIMOZIDE; niclosamide; TCB2; FLUOXETINE	HTR2A; STAT3	2	−8.86
EPO Receptor Signaling	5	27	cucurbitacin I; Vemurafenib; niclosamide; Vemurafenib; niclosamide	RAF1; STAT3	2	−10.82
Serotonin Transporter Activity	5	11	Fluvoxamine maleate; AT-DYRK-01; SERTRALINE HYDROCHLORIDE; FLUOXETINE; DOXEPIN HYDROCHLORIDE	SLC6A4; MAOA	2	−7.01
TFs Regulate miRNAs related to cardiac hypertrophy	4	8	cucurbitacin I; niclosamide; niclosamide; API-2	AKT1; STAT3	2	−10.34
TGF Beta Signaling Pathway	4	54	cucurbitacin I; niclosamide; niclosamide; PLUMBAGIN	EP300; STAT3	2	−10.42
IL-9 Signaling Pathway	4	17	cucurbitacin I; niclosamide; niclosamide; CHIR-99021	STAT3; MAPK1	2	−10.38
Serotonin Receptor 4/6/7 and NR3C Signaling	3	18	Vemurafenib; Vemurafenib; CMPD-1	BRAF; MAPKAPK2	2	−7.28
Oxidative Stress	3	29	skepinone-L; AT-DYRK-01; SB 202190	MAPK14; MAOA	2	−5.76

-continued

Pathway Name (Wiki)	Number Compounds	Number Genes Pathway	Compound List	Target List	Number Targets	Average Z-value
Secretion of Hydrochloric Acid in Parietal Cells	2	4	RABEPRAZOLE SODIUM; DOXEPIN HYDROCHLORIDE	ATP4A; HRH2	2	−5.47
Wnt Signaling Pathway and Pluripotency	2	95	Cantharidin; CHIR-99021	PPP2CA; GSK3B	2	−8.64
Parkinsons Disease Pathway	2	71	skepinone-L; SB 202190	MAPK14; MAPK11	2	−5.89
Dopamine metabolism	2	13	Cantharidin; AT-DYRK-01	PPP2CA; MAOA	2	−9.13
Complement and Coagulation Cascades	2	60	SCH 79797 dihydrochloride; MENADIONE	PROC; F2R	2	−4.50
Peptide GPCRs	2	73	CMPD-1; CANDESARTAN CILEXTIL	AGTR1; GNRHR	2	−4.53
Hypothetical Network for Drug Addiction	2	33	SIB 1757; PIMOZIDE	DRD2; GRM5	2	−7.11
Physiological and Pathological Hypertrophy of the Heart	3	25	cucurbitacin I; niclosamide; niclosamide	STAT3	1	−12.33
TCA Cycle Nutrient Utilization and Invasiveness of Ovarian Cancer	3	5	cucurbitacin I; niclosamide; niclosamide	STAT3	1	−12.33
Adipogenesis	3	131	cucurbitacin I; niclosamide; niclosamide	STAT3	1	−12.33
Bladder Cancer	2	29	Vemurafenib; Vemurafenib	BRAF	1	−8.55
Sphingolipid Metabolism	1	19	NVP 231	CERK	1	−4.79
Calcium Regulation in the Cardiac Cell	1	151	2-[(4-Phenylpiperazin-1-yl)methyl]-2,3-dihydroimidazo[1,2-c]quinazolin-5(6H)-one	ADRA1A	1	−9.21
Gastric cancer network 2	1	31	Rubitecan	TOP2A	1	−4.17
Nucleotide Metabolism	1	19	Mycophenolic acid	IMPDH1	1	−4.54
Fluoropyrimidine Activity	1	33	DIPYRIDAMOLE	SLC29A1	1	−4.41
Heart Development	1	44	CHIR-99021	MAPK1	1	−4.52
ACE Inhibitor Pathway	1	17	CANDESARTAN CILEXTIL	AGTR1	1	−4.32
GPCRs, Class C Metabotropic glutamate, pheromone	1	15	SIB 1757	GRM5	1	−7.89
Arrhythmogenic Right Ventricular Cardiomyopathy	1	74	cytochalasin B	ACTG1	1	−20.00

-continued

Pathway Name (Wiki)	Number Compounds	Number Genes Pathway	Compound List	Target List	Number Targets	Average Z-value
Electron Transport Chain	1	103	DIHYDROROTENONE	NDUFS7	1	−5.14
Integrated Breast Cancer Pathway	1	17	NVP 231	CERK	1	−4.79
G1 to S cell cycle control	1	69	CHIR-99021	CDK1	1	−4.52
Biogenic Amine Synthesis	1	15	AT-DYRK-01	MAOA	1	−5.50
ErbB Signaling Pathway	1	55	PF-3758309	PAK4	1	−4.29
Myometrial Relaxation and Contraction Pathways	1	156	cytochalasin B	ACTG1	1	−20.00
Gastric Cancer Network 1	1	29	Rubitecan	TOP2A	1	−4.17
Striated Muscle Contraction	1	38	cytochalasin B	ACTG1	1	−20.00
PDGF Pathway	1	12	CHIR-99021	MAPK1	1	−4.52
DNA Damage Response (only ATM dependent)	1	61	CHIR-99021	GSK3B	1	−4.52
Oxidative phosphorylation	1	60	DIHYDROROTENONE	NDUFS7	1	−5.14
Ovarian Infertility Genes	1	31	Alprostadil	PTGER2	1	−4.86
Wnt Signaling Pathway	1	66	CHIR-99021	GSK3B	1	−4.52
mRNA Processing	1	127	YK 4-279	DHX9	1	−7.60
Focal Adhesion	44	191	Bosutinib; AT7867; SC-1; Bosutinib; PF-573228; SU11274(PKI-SU11274); Y-27632; VX-680; 1-Naphthyl PP1; MGCD-265; Neratinib; TW-37; Tozasertib; Alsterpaullone; Sunitinib Malate; Vandetanib; Tozasertib VX-680 (MK-0457); Erlotinib; Sunitinib malate; PCI-32765; BMS-536924; AZD2171; RAF265; HA-1077; SP600125; KX2-391; Tivozanib; Erlotinib; Dasatinib; Ki8751; PODOFILOX; AG-013736; Gefitinib; HA-1077; Crizotinib; H 89 dihydrochloride; HA-1077; ABT-737; ABT-199 (GDC-0199); Sorafenib; CAL-101; NVP-ADW742; OSI-906 (Linsitinib); Axitinib	BLK; BCL2; RAF1; TXK; HCK; PIK3CD; KDR; MAPK9; MAP2K2; PTK2; ROCK1; BRAF; AKT2; MAPK8; EGFR; MAP2K1; AKT1; PDGFRB; IGF1R; TNK2; PTK6; GSK3B; PDGFRA; SRC; FYN; AKT3; MET; ERBB2; MAPK1; ROCK2; FLT1	31	12.54
GPCRs, Class A Rhodopsin-like	11	261	AZELASTINE HYDROCHLORIDE; SURAMIN; JTE 013; BNTX maleate; Eltoprazine	HTR2A; HTR1A; OPRD1; MLNR; CHRM2; DRD2; SSTR4; HRH2;	31	8.60

-continued

Pathway Name (Wiki)	Number Compounds	Number Genes Pathway	Compound List	Target List	Number Targets	Average Z-value
			hydrochloride; CV 1808; VINCAMINE; Doxepine HCl; ERYTHROMYCIN STEARATE; "7,4'-DIHYDROXYFLAVONE"; "L-803,087 trifluoroacetate"	ADRA2A; HTR2C; ADRA1A; CHRM4; HTR1B; P2RY2; ADORA2A; OPRK1; P2RY11; P2RY1; CHRM1; ADRA1B; HRH3; HTR2B; ADRA2C; ADRA2B; CHRM5; P2RY13; HRH1; CHRM3; P2RY10; ADRA1D; OPRM1		
EGF/EGFR Signaling Pathway	35	162	Bosutinib; AT7867; SC-1; Bosutinib; PF-573228; KW 2449; Y-27632; VX-680; 1-Naphthyl PP1; Neratinib; Cyt387; Go 6976; Tozasertib; TG-101348; INCB018424; Vandetanib; Tozasertib VX-680 (MK-0457); H-7 dihydrochloride; Erlotinib; sotrastaurin; C-1; RAF265; HA-1077; SP600125; KX2-391; INCB018424; Erlotinib; Dasatinib; AZD1480; Gefitinib; HA-1077; H 89 dihydrochloride; HA-1077; Sorafenib; MLN8237	RAF1; AURKA; ABL1; MAPK9; PRKCA; MAPK3; PRKCD; MAP2K2; PTK2; ROCK1; MAP3K2; RPS6KA3; BRAF; MAPK8; EGFR; MAP2K1; AKT1; PRKCB; JAK2; TNK2; PTK6; JAK1; SRC; RPS6KA5; ERBB2; MAPK1	26	13.80
MAPK Signaling Pathway	28	168	Bosutinib; AT7867; SC-1; Bosutinib; Neratinib; Sunitinib Malate; Vandetanib; H-7 dihydrochloride; Erlotinib; sotrastaurin; Sunitinib malate; C-1; AZD2171; RAF265; SP60012 5; VER155008; Erlotinib; CGP 57380; "Dibutyryl-cAMP, sodium salt"; Gefitinib; HA-1077; H 89 dihydrochloride; HA-1077; Phorbol 12-Myristate 13-Acetate; Sorafenib; APIGENIN; cyclosporine; LY 364947	PPP3CA; TGFBR2; RAF1; MAPK9; MAPK3; PRKCD; PRKACA; MAP2K2; MKNK1; MAP3K2; RPS6KA3; BRAF; AKT2; MAPK8; EGFR; MAP2K1; AKT1; PRKCH; PDGFRB; TGFBR1; MAPK10; FGFR1; RPS6KA5; AKT3; MAPK1; HSPA1A	26	12.36
Insulin Signaling	21	160	Bosutinib; AT7867; SC-1; Bosutinib; Go 6976; Alsterpaullone; Dorsomorphin dihydrochloride; H-7 dihydrochloride; sotrastaurin; B MS-5369 24; C-1; SP600125; OLEANOIC ACID; triptolide; PODOFILOX; H 89 dihydrochloride; Sorafenib; APIGENIN; CAL-101; NVP-ADW742; OSI-906 (Linsitinib)	INSR; PRKAA2; RAF1; PIK3CD; MAPK9; PRKCA; MAPK3; PRKCD; MAP2K2; MAP3K2; RPS6KA3; AKT2; MAPK8; MAP2K1; PTPN1; PRKCQ; AKT1; PRKCH; MAP4K5; IGF1R; GSK3B; MAPK10; PRKAA1; XBP1; RPS6KA5; MAPK1	26	13.46
Leptin signaling pathway	37	78	Bosutinib; AT7867; SC-1; Bosutinib; PF-573228; Y-27632; VX-680; 1-Naphthyl PP1; Neratinib; TW-37; Cyt387; Tozasertib; Alsterpaullone; TG-101348; INCB018424; Vandetanib; Dorsomorphin dihydrochloride; Tozasertib VX-680 (MK-0457); Erlotinib; BMS-536924; HA-1077; SP600125; KX2-391; OLEANOIC ACID; INCB018424; Erlotinib; Dasatinib; PODOFILOX; AZD1480; Gefitinib; HA-1077; H 89 dihydrochloride; HA-	PRKAA2; BCL2L1; RAF1; MAPK3; MAP2K2; PTK2; ROCK1; MAPK8; EGFR; MAP2K1; PTPN1; AKT1; IGF1R; JAK2; GSK3B; JAK1; SRC; PRKAA1; FYN; ERBB2; ROCK2; MAPK1	22	13.15

-continued

Pathway Name (Wiki)	Number Compounds	Number Genes Pathway	Compound List	Target List	Number Targets	Average Z-value
			1077; ABT-737; Sorafenib; NVP-ADW742; OSI-906 (Linsitinib)			
BDNF signaling pathway	27	146	Bosutinib; AT7867; SC-1; Bosutinib; VX-680; 1-Naphthyl PP1; Cyt387; Tozasertib; Alsterpaullone; TG-101348; INCB018424; Vandetanib; Dorsomorphin dihydrochloride; Tozasertib VX-680 (MK-0457); sotrastaurin; C-1; SP600125; KX2-391; INCB018424; Dasatinib; BARBITAL; N9-isopropylolomoucine; AZD1480; H 89 dihydrochloride; SCH727965; Sorafenib; APIGENIN	CDK5; PRKAA2; RAF1; GRIA2; MAPK9; MAPK3; PRKCD; MAP2K2; CSNK2A1; MAP3K2; RPS6KA3; MAPK8; MAP2K1; AKT1; JAK2; GSK3B; MAPK10; SRC; PRKAA1; FYN; RPS6KA5; MAPK1	22	13.68
Oncostatin M Signaling Pathway	29	64	Bosutinib; AT7867; SC-1; Bosutinib; Y-27632; VX-680; 1-Naphthyl PP1; Arcyriaflavin A; Cyt387; Go 6976; Tozasertib; TG-101348; INCB018424; Vandetanib; Tozasertib VX-680 (MK-0457); H-7 dihydrochloride; sotrastaurin; C-1; CDK9 inhibitor 14; SP600125; KX2-391; INCB018424; Dasatinib; N9-isopropylolomoucine; AZD1480; (−)-Epigallocatechin Gallate; H 89 dihydrochloride; SCH727965; Sorafenib	RAF1; PRKCE; MAPK9; PRKCA; MAPK3; PRKCD; MAP2K2; MAPK8; MAP2K1; AKT1; PRKCH; PRKCB; JAK2; JAK3; TYK2; JAK1; SRC; SERPINE1; CDK2; MAPK1	20	14.00
Regulation of Actin Cytoskeleton	23	151	Bosutinib; SC-1; Bosutinib; PF-573228; Y-27632; Neratinib; Sunitinib Malate; Vandetanib; Erlotinib; Sunitinib malate; AZD2171; RAF265; HA-1077; Erlotinib; Ki8751; Gefitinib; HA-1077; H 89 dihydrochloride; HA-1077; VINCAMINE; Doxepine HCl; Sorafenib; CAL-101	CHRM2; RAF1; PIK3CD; MAPK3; MAP2K2; PTK2; ROCK1; CHRM4; BRAF; EGFR; MAP2K1; PDGFRB; CHRM1; PDGFRA; CHRM5; FGFR1; CHRM3; ROCK2; MAPK1	19	12.92
Monoamine GPCRs	4	34	AZELASTINE HYDROCHLORIDE; Eltoprazine hydrochloride; VINCAMINE; Doxepine HCl	HTR2A; HTR1A; CHRM2; DRD2; HRH2; ADRA2A; HTR2C; ADRA1A; CHRM4; HTR1B; CHRM1; ADRA1B; HTR2B; ADRA2C; ADRA2B; CHRM5; HRH1; CHRM3; ADRA1D	19	9.17
Cell Cycle	18	104	Bosutinib; Bosutinib; KW 2449; 1-Naphthyl PP1; Arcyriaflavin A; apicidin; Alsterpaullone; CD K9 inhibitor 14; Dasatinib; N9-isopropylolomoucine; MK-1775; KU-55933; rigosertib; (−)-Epigallocatechin Gallate; SCH727965; Belinostat; APIGENIN; Pandacostat	HDAC1; HDAC6; HDAC4; PLK1; CDK4; CDK1; ABL1; CDK6; HDAC5; EP300; WEE1; GSK3B; HDAC8; ATM; HDAC2; CDK2; HDAC7; HDAC3	18	12.54
Calcium Regulation in the	15	151	Bosutinib; Bosutinib; Y-27632; Go 6976; H-7 dihydrochloride; sotrastaurin;	ADCY5; ADCY2; CHRM2; PRKCE; PRKCA; ADRA1A;	18	12.27

-continued

Pathway Name (Wiki)	Number Compounds	Number Genes Pathway	Compound List	Target List	Number Targets	Average Z-value
Cardiac Cell			C-1; "Dibutyryl-cAMP, sodium salt"; HA-1077; H 89 dihydrochloride; HA-1077; Phorbol 12-Myristate 13-Acetate; VINCAMINE; Doxepine HCl; COLFORSIN	PRKCD; PRKACA; CHRM4; PRKCQ; PRKCH; CHRM1; ADRA1B; PRKD1; CHRM5; CAMK2G; CHRM3; ADRA1D		
Kit receptor signaling pathway	33	59	Bosutinib; AT7867; SC-1; Bosutinib; VX-680; 1-Naphthyl PP1; TW-37; Cyt387; Go 6976; Tozasertib; Sunitinib Malate; TG-101348; INCB018424; Vandetanib; Tozasertib VX-680 (MK-0457); H-7 dihydrochloride; sotrastaurin; Sunitinib malate; PCI-32765; C-1; AZD2171; SP600125; KX2-391; INCB018424; Dasatinib; AG-013736; AZD1480; (−)-Epigallocatechin Gallate; H 89 dihydrochloride; ABT-737; ABT-199 (GDC-0199); Sorafenib; NVP-ADW742	BCL2; KIT; RAF1; LYN; PRKCA; MAPK3; MAP2K2; RPS6KA3; MAPK8; MAP2K1; AKT1; JAK2; EP300; SRC; FYN; MAPK1; BTK	17	13.04
IL-3 Signaling Pathway	30	49	Bosutinib; AT7867; SC-1; Bosutinib; VX-680; 1-Naphthyl PP1; TW-37; Cyt387; Tozasertib; TG-101348; INCB018424; Vandetanib; Tozasertib VX-680 (MK-0457); H-7 dihydrochloride; C-1; SP600125; KX2-391; INCB018424; Dasatinib; ER 27319 maleate; "Dibutyryl-cAMP, sodium salt"; AZD1480; HA-1077; H 89 dihydrochloride; HA-1077; Phorbol 12-Myristate 13-Acetate; ABT-737; ABT-199 (GDC-0199); Sorafenib; CAL-101	SYK; BCL2; BCL2L1; RAF1; LYN; HCK; PIK3CD; MAPK3; PRKACA; MAPK8; MAP2K1; AKT1; JAK2; JAK1; SRC; FYN; MAPK1	17	12.90
TGF beta Signaling Pathway	26	135	Bosutinib; AT7867; SC-1; Bosutinib; PF-573228; SU11274(PKI-SU11274); Y-27632; VX-680; 1-Naphthyl PP1; apicidin; Tozasertib; Vandetanib; Tozasertib VX-680 (MK-0457); HA-1077; SP600125; KX2-391; Dasatinib; (−)-Epigallocatechin Gallate; HA-1077; Crizotinib; H 89 dihydrochloride; HA-1077; Belinostat; Sorafenib; LY 364947; Pandacostat	HDAC1; TGFBR2; RAF1; MAPK9; MAPK3; MAP2K2; PTK2; ROCK1; MAPK8; MAP2K1; AKT1; TGFBR1; EP300; SRC; MET; SIK1; MAPK1	17	14.40
B Cell Receptor Signaling Pathway	17	100	Bosutinib; AT7867; SC-1; Bosutinib; VX-680; 1-Naphthyl PP1; Tozasertib; Alsterpaullone; Tozasertib VX-680 (MK-0457); sotrastaurin; PCI-32765; C-1; RAF265; SP600125; ER 27319 maleate; H 89 dihydrochloride; Sorafenib	SYK; LCK; BLK; RAF1; LYN; MAPK9; MAPK3; PRKCD; MAP2K2; BRAF; MAPK8; MAP2K1; AKT1; GSK3B; FYN; MAPK1; BTK	17	16.07
AGE/RAGE pathway	34	66	Bosutinib; AT7867; SC-1; Bosutinib; Y-27632; VX-680; 1-Naphthyl PP1; Neratinib; Cyt387; Go 6976; Tozasertib; TG-101348; INCB018424; Vandetanib; Tozasertib VX-680 (MK-0457); H-7	INSR; RAF1; MAPK9; PRKCA; MAPK3; PRKCD; ROCK1; MAPK8; EGFR; MAP2K1; AKT1; PRKCB; JAK2; MMP7; SRC; MAPK1	16	13.16

-continued

Pathway Name (Wiki)	Number Compounds	Number Genes Pathway	Compound List	Target List	Number Targets	Average Z-value
			dihydrochloride; Erlotinib; sotrastaurin; BMS-536924; C-1; HA-1077; SP600125; KX2-391; INCB018424; Erlotinib; Dasatinib; AZD1480; Gefitinib; (−)-Epigallocatechin Gallate; HA-1077; H 89 dihydrochloride; HA-1077; Sorafenib; OSI-906 (Linsitinib)			
Corticotropin-releasing hormone	19	95	Bosutinib; AT7867; SC-1; Bosutinib; PF-573228; TW-37; Go 6976; Alsterpaullone; Dorsomorphin dihydrochloride; H-7 dihydrochloride; sotrastaurin; C-1; RAF265; SP600125; ETHOSUXIMIDE; H 89 dihydrochloride; ABT-737; ABT-199 (GDC-0199); Sorafenib	BCL2; PRKAA2; MAPK9; PRKCA; MAPK3; PRKCD; PTK2; BRAF; MAPK8; MAP2K1; PRKCQ; AKT1; PRKCB; GSK3B; CACNA1H; MAPK1	16	15.28
TSLP Signaling Pathway	19	48	Bosutinib; AT7867; SC-1; Bosutinib; VX-680; 1-Naphthyl PP1; Cyt387; Tozasertib; TG-101348; INCB018424; Vandetanib; Tozasertib VX-680 (MK-0457); PCI-32765; SP600125; KX2-391; INCB018424; Dasatinib; AZD1480; H 89 dihydrochloride	LCK; LYN; HCK; MAPK9; MAPK3; MAP2K2; MAPK8; MAP2K1; AKT1; JAK2; JAK1; SRC; FYN; MAPK1; BTK	15	15.70
Integrin-mediated Cell Adhesion	21	99	Bosutinib; AT7867; SC-1; Bosutinib; PF-573228; Y-27632; VX-680; 1-Naphthyl PP1; Tozasertib; Vandetanib; Tozasertib VX-680 (MK-0457); RAF265; HA-1077; SP600125; KX2-391; Dasatinib; HA-1077; H 89 dihydrochloride; HA-1077; Sorafenib; APIGENIN	RAF1; MAP2K2; PTK2; ROCK1; BRAF; AKT2; MAP2K1; AKT1; MAPK10; SRC; FYN; AKT3; ROCK2; MAPK1	14	15.44
IL-6 signaling pathway	19	44	Bosutinib; AT7867; SC-1; Bosutinib; TW-37; apicidin; Cyt387; Alsterpaullone; TG-101348; INCB018424; sotrastaurin; C-1; INCB018424; AZD1480; (−)-Epigallocatechin Gallate; H 89 dihydrochloride; ABT-737; Belinostat; Pandacostat	HDAC1; BCL2L1; HCK; MAPK3; PRKCD; MAP2K2; MAP2K1; AKT1; JAK2; EP300; TYK2; GSK3B; JAK1; MAPK1	14	14.59
TSH signaling pathway	25	66	Bosutinib; AT7867; SC-1; Bosutinib; VX-680; 1-Naphthyl PP1; Arcyriaflavin A; Cyt387; Tozasertib; TG-101348; INCB018424; Vandetanib; Tozasertib VX-680 (MK-0457); RAF265; CDK9 inhibitor 14; KX2-391; INCB018424; Dasatinib; N9-isopropylolomoucine; AZD1480; H 89 dihydrochloride; SCH727965; Zardaverine; Sorafenib; COLFORSIN	PDE4D; ADCY2; RAF1; CDK4; MAPK3; BRAF; MAP2K1; AKT1; JAK2; JAK1; SRC; CDK2; MAPK1	13	13.92
IL-5 Signaling Pathway	19	42	Bosutinib; AT7867; SC-1; Bosutinib; Ro 31-8220 mesylate; TW-37; Cyt387; Alsterpaullone; TG-101348; INCB018424; PCI-32765; INCB018424; ER 27319 maleate; AZD1480; H 89 dihydrochloride; ABT-737; ABT-199 (GDC-0199); Sorafenib; APIGENIN	SYK; BCL2; RAF1; LYN; MAPK3; MAP2K2; PIM1; MAP2K1; AKT1; JAK2; GSK3B; MAPK1; BTK	13	14.53

-continued

Pathway Name (Wiki)	Number Compounds	Number Genes Pathway	Compound List	Target List	Number Targets	Average Z-value
TCR Signaling Pathway	15	91	Bosutinib; AT7867; SC-1; Bosutinib; VX-680; 1-Naphthyl PP1; Tozasertib; Tozasertib VX-680 (MK-0457); sotrastaurin; C-1; SP600125; BNTX maleate; H 89 dihydrochloride; Sorafenib; "7,4'-DIHYDROXYFLAVONE"	LCK; RAF1; MAPK9; MAPK3; PRKCD; MAP2K2; MAPK8; MAP2K1; PRKCQ; AKT1; FYN; MAPK1; OPRM1	13	16.54
Androgen receptor signaling pathway	27	89	Bosutinib; AT7867; Bosutinib; PF-573228; Y-27632; VX-680; 1-Naphthyl PP1; Neratinib; apicidin; Tozasertib; Alsterpaullone; Vandetanib; Salermide; Tozasertib VX-680 (M K-0457); Erlotinib; HA-1077; KX2-391; Erlotinib; Dasatinib; Gefitinib; (−)-Epigallocatechin Gallate; HA-1077; H 89 dihydrochloride; HA-1077; Belinostat; Retinoic acid; Pandacostat	HDAC1; KAT2B; PTK2; ROCK1; EGFR; AKT1; SIRT1; EP300; GSK3B; SRC; ROCK2; NR2C2	12	13.58
Senescence and Autophagy	26	106	Bosutinib; SC-1; Bosutinib; VX-680; 1-Naphthyl PP1; Arcyriaflavin A; TW-37; Tozasertib; Alsterpaullone; Vandetanib; Tozasertib VX-680 (MK-0457); BMS-536924; RAF265; CDK9 inhibitor 14; KX2-391; Dasatinib; PODOFILOX; N9-isopropylolomoucine; (−)-Epigallocatechin Gallate; ABT-737; SCH727965; ABT-199 (GDC-0199); Sorafenib; APIGENIN; NVP-ADW742; OSI-906 (Linsitinib)	BCL2; RAF1; CDK4; BRAF; MAP2K1; CDK6; IGF1R; GSK3B; SRC; SERPINE1; CDK2; MAPK1	12	12.45
Interleukin-11 Signaling Pathway	21	44	Bosutinib; AT7867; SC-1; Bosutinib; VX-680; 1-Naphthyl PP1; TW-37; Cyt387; Tozasertib; TG-101348; INCB018424; Vandetanib; Tozasertib VX-680 (MK-0457); KX2-391; INCB018424; Dasatinib; AZD1480; H 89 dihydrochloride; ABT-737; ABT-199 (GDC-0199); Sorafenib	BCL2; RAF1; MAPK3; MAP2K2; MAP2K1; AKT1; JAK2; TYK2; JAK1; SRC; FYN; MAPK1	12	14.86
IL-2 Signaling Pathway	19	40	Bosutinib; AT7867; SC-1; Bosutinib; VX-680; 1-Naphthyl PP1; TW-37; Cyt387; Tozasertib; TG-101348; INCB018424; Tozasertib VX-680 (MK-0457); INCB018424; ER 27319 maleate; AZD1480; H 89 dihydrochloride; ABT-737; ABT-199 (GDC-0199); Sorafenib	SYK; LCK; BCL2; RAF1; MAPK3; MAP2K2; MAP2K1; AKT1; JAK3; JAK1; FYN; MAPK1	12	15.29
G Protein Signaling Pathways	14	92	Y-27632; Triazolothiadiazine; Go 6976; H-7 dihydrochloride; sotrastaurin; C-1; "Dibutyryl-cAMP, sodium salt"; HA-1077; H 89 dihydrochloride; HA-1077; Phorbol 12-Myristate 13-Acetate; Zardaverine; cyclosporine; COLFORSIN	ADCY5; PPP3CA; PDE4D; ADCY2; PRKCE; PRKCA; PRKCD; PRKACA; PRKCQ; PRKCH; PRKD1; PDE4A	12	9.68
MicroRNAs in cardiomyocyte hypertrophy	12	85	AT7867; Y-27632; CDK9 inhibitor 14; HA-1077; HA-1077; H 89 dihydrochloride; HA-	RAF1; HDAC4; PIK3CD; ROCK1; CDK9; AKT2; HDAC9; AKT1;	12	10.76

-continued

Pathway Name (Wiki)	Number Compounds	Number Genes Pathway	Compound List	Target List	Number Targets	Average Z-value
			1077; SCH727965; Belinostat; Sorafenib; CAL-101; Pandacostat	HDAC5; CDK7; HDAC7; ROCK2		
Retinoblastoma (RB) in Cancer	22	87	Bosutinib; Bosutinib; KW 2449; 1-Naphthyl PP1; Arcyriaflavin A; apicidin; Daunorubicin; Alsterpaullone; AZD7762; CDK9 inhibitor 14; Dasatinib; PODOFILOX; N9-isopropylolomoucine; Bisantrene dihydrochloride; MK-1775; SCH727965; Belinostat; Doxorubicin; Sorafenib; APIGENIN; Pandacostat; Axitinib	HDAC1; RAF1; CDK1; CDK4; PLK4; ABL1; TOP2A; CDK6; WEE1; CHEK1; CDK2	11	12.00
SIDS Susceptibility Pathways	18	85	Sunitinib Malate; TG-101348; Vandetanib; H-7 dihydrochloride; Sunitinib malate; C-1; BARBITAL; "Dibutyryl-cAMP, sodium salt"; Eltoprazine hydrochloride; (−)-Epigallocatechin Gallate; HA-1077; H 89 dihydrochloride; HA-1077; Phorbol 12-Myristate 13-Acetate; UB 165 fumarate; Doxepine HCl; ERYTHROMYCIN STEARATE; Sorafenib	HTR2A; HTR1A; CHRM2; GABRA1; SLC6A4; PRKACA; CHRNA4; KCNH2; CHRNB2; EP300; RET	11	8.59
RANKL/RANK Signaling Pathway	15	55	Bosutinib; AT7867; SC-1; Bosutinib; PF-573228; VX-680; 1-Naphthyl PP1; Tozasertib; Vandetanib; Tozasertib VX-680 (MK-0457); SP600125; KX2-391; Dasatinib; ER 27319 maleate; H 89 dihydrochloride	SYK; LYN; MAPK9; MAPK3; PTK2; AKT2; MAPK8; MAP2K1; AKT1; SRC; MAPK1	11	17.73
Myometrial Relaxation and Contraction Pathways	14	156	Bosutinib; Bosutinib; Y-27632; Go 6976; H-7 dihydrochloride; sotrastaurin; C-1; "Dibutyryl-cAMP, sodium salt"; HA-1077; H 89 dihydrochloride; HA-1077; Phorbol 12-Myristate 13-Acetate; Zardaverine; COLFORSIN	ADCY5; PDE4D; ADCY2; PRKCE; PRKCA; PRKCD; PRKACA; PRKCQ; PRKCH; PRKD1; CAMK2G	11	12.63
Wnt Signaling Pathway and Pluripotency	10	95	Y-27632; Go 6976; Alsterpaullone; H-7 dihydrochloride; sotrastaurin; C-1; SP600125; (−)-Epigallocatechin Gallate; Retinoic acid; APIGENIN	PPARD; PRKCE; MAPK9; PRKCA; PRKCD; PRKCQ; PRKCH; MMP7; GSK3B; PRKD1; MAPK10	11	10.68
Toll-like receptor signaling pathway	8	102	Bosutinib; AT7867; SC-1; Bosutinib; SP600125; H 89 dihydrochloride; APIGENIN; CAL-101	PIK3CD; MAPK9; MAPK3; MAP2K2; AKT2; MAPK8; MAP2K1; AKT1; MAPK10; AKT3; MAPK1	11	19.88
Regulation of toll-like receptor signaling pathway	8	103	Bosutinib; AT7867; SC-1; Bosutinib; SP600125; H 89 dihydrochloride; APIGENIN; CAL-101	PIK3CD; MAPK9; MAPK3; MAP2K2; AKT2; MAPK8; MAP2K1; AKT1; MAPK10; AKT3; MAPK1	11	19.88
Pathogenic *Escherichia coli* infection	18	58	Bosutinib; Bosutinib; KW 2449; Y-27632; 1-Naphthyl PP1; Go 6976; H-7 dihydrochloride; sotrastaurin;	ABL1; PRKCA; TUBA1A; ROCK1; TUBA4A; TUBB; TUBA1B; FYN;	10	13.21

-continued

Pathway Name (Wiki)	Number Compounds	Number Genes Pathway	Compound List	Target List	Number Targets	Average Z-value
			C-1; HA-1077; Dasatinib; Colchicine; Vinbiastine sulfate; PODOFILOX; COLCHICINE; HA-1077; H 89 dihydrochloride; HA-1077	TUBB1; ROCK2		
IL-7 Signaling Pathway	14	25	Bosutinib; AT7867; SC-1; Bosutinib; 1-Naphthyl PP1; TW-37; Cyt387; Alsterpaullone; TG-101348; INCB018424; INCB018424; AZD1480; H 89 dihydrochloride; ABT-737	BCL2L1; MAPK3; MAP2K2; MAP2K1; AKT1; JAK3; GSK3B; JAK1; FYN; MAPK1	10	17.09
IL-4 Signaling Pathway	12	56	AT7867; SC-1; AZELASTINE HYDROCHLORIDE; Cyt387; TG-101348; INCB018424; INCB018424; AZD1480; (−)-Epigallocatechin Gallate; H 89 dihydrochloride; Doxepine HCl; CAL-101	PIK3CD; MAPK3; AKT1; JAK2; JAK3; EP300; TYK2; JAK1; HRH1; MAPK1	10	13.46
Wnt Signaling Pathway Netpath	11	51	AT7867; SC-1; Go 6976; Alsterpaullone; Vandetanib; H-7 dihydrochloride; sotrastaurin; C-1; SP600125; H 89 dihydrochloride; APIGENIN	TEK; MAPK9; PRKCA; MAPK8; CDK6; AKT1; PRKCB; GSK3B; MAPK1	9	14.30
TNF alpha Signaling Pathway	9	93	AT7867; SC-1; TW-37; SP600125; rigosertib; H 89 dihydrochloride; ABT-737; Sorafenib; APIGENIN	BCL2L1; RAF1; PLK1; MAPK9; MAPK3; CSNK2A1; MAPK8; AKT1; MAPK1	9	13.71
Wnt Signaling Pathway	8	66	Y-27632; Go 6976; Alsterpaullone; H-7 dihydrochloride; sotrastaurin; C-1; SP600125; APIGENIN	PRKCE; MAPK9; PRKCA; PRKCD; PRKCQ; PRKCH; GSK3B; PRKD1; MAPK10	9	11.58
Cardiac Hypertrophic Response	7	54	AT7867; CDK9 inhibitor 14; H 89 dihydrochloride; SCH727965; Belinostat; Sorafenib; Pandacostat	RAF1; HDAC4; CDK9; AKT2; HDAC9; AKT1; HDAC5; CDK7; HDAC7	9	11.34
GPCRs, Other	6	103	AZELASTINE HYDROCHLORIDE; SURAMIN; Purmorphamine; NVP-LDE225; CV 1808; Doxepine HCl	HTR2A; CHRM2; HRH4; ADORA2A; P2RY11; SMO; P2RY13; CHRM3; ADRA1D	9	9.64
Notch Signaling Pathway	21	61	Bosutinib; AT7867; Bosutinib; VX-680; 1-Naphthyl PP1; apicidin; Cyt387; Tozasertib; Alsterpaullone; TG-101348; INCB018424; Vandetanib; Tozasertib VX-680 (MK-0457); KX2-391; INCB018424; Dasatinib; AZD1480; (−)-Epigallocatechin Gallate; H 89 dihydrochloride; Belinostat; Pandacostat	HDAC1; LCK; AKT1; JAK2; EP300; GSK3B; SRC; HDAC2	8	14.04
Signaling of Hepatocyte Growth Factor Receptor	13	34	Bosutinib; SC-1; Bosutinib; PF-573228; VX-680; 1-Naphthyl PP1; Tozasertib; Vandetanib; Tozasertib VX-680 (MK-0457); SP600125; KX2-391; Dasatinib; Sorafenib	RAF1; MAPK3; MAP2K2; PTK2; MAPK8; MAP2K1; SRC; MAPK1	8	17.05
Nuclear Receptors in Lipid Metabolism and Toxicity	10	33	TTNPB; AM-580; PODOPHYLLIN ACETATE; Erlotinib; 4-(4-octylphenyl)benzoate; TTNPB; NP-009852; NP-009832; FLAVONE; ERYTHROMYCIN STEARATE; Retinoic acid	ABCB1; PPARD; NR1I2; RARG; RARA; RARB; CYP3A4; CYP2C9	8	8.26

-continued

Pathway Name (Wiki)	Number Compounds	Number Genes Pathway	Compound List	Target List	Number Targets	Average Z-value
TWEAK Signaling Pathway	8	42	AT7867; SC-1; apicidin; Alsterpaullone; SP600125; H 89 dihydrochloride; Belinostat; Pandacostat	HDAC1; MAPK9; MAPK3; AKT2; MAPK8; AKT1; GSK3B; MAPK1	8	15.15
MAPK Cascade	7	29	Bosutinib; SC-1; Bosutinib; RAF265; SP600125; Sorafenib; APIGENIN	RAF1; MAPK3; MAP2K2; MAP3K2; BRAF; MAP2K1; MAPK10; MAPK1	8	18.11
Nuclear Receptors	6	38	TTNPB; AM-580; Erlotinib; 4-(4-octylphenyl)benzoate; TTNPB; Retinoic acid	PPARD; NR1I2; RARG; RARA; RARB; RXRA; RXRB; NR2C2	8	8.64
IL-1 signaling pathway	6	54	Bosutinib; AT7867; SC-1; Bosutinib; SP600125; H 89 dihydrochloride	MAPK9; MAPK3; MAP2K2; MAP3K2; MAPK8; MAP2K1; AKT1; MAPK1	8	24.34
FSH signaling pathway	21	27	Bosutinib; AT7867; SC-1; Bosutinib; VX-680; 1-Naphthyl PP1; Go 6976; Tozasertib; Vandetanib; Tozasertib VX-680 (MK-0457); H-7 dihydrochloride; sotrastaurin; C-1; KX2-391; Dasatinib; "Dibutyryl-cAMP, sodium salt"; HA-1077; H 89 dihydrochloride; HA-1077; Phorbol 12-Myristate 13-Acetate; Sorafenib	RAF1; PRKCA; MAPK3; PRKACA; AKT1; SRC; MAPK1	7	14.54
Alpha 6 Beta 4 signaling pathway	17	31	Bosutinib; AT7867; SC-1; Bosutinib; PF-573228; VX-680; 1-Naphthyl PP1; Go 6976; Tozasertib; Vandetanib; Tozasertib VX-680 (MK-0457); H-7 dihydrochloride; sotrastaurin; C-1; KX2-391; Dasatinib; H 89 dihydrochloride	PRKCA; MAPK3; PRKCD; PTK2; AKT1; SRC; MAPK1	7	17.19
Nicotine Activity on Dopaminergic Neurons	15	21	Alsterpaullone; H-7 dihydrochloride; C-1; BARBITAL; "Dibutyryl-cAMP, sodium salt"; N9-isopropylolomoucine; HA-1077; H 89 dihydrochloride; HA-1077; Phorbol 12-Myristate 13-Acetate; UB 165 fumarate; SCH727965; Doxepine HCl; APIGENIN; COLFORSIN	ADCY2; CDK5; DRD2; PRKACA; CHRNA4; CHRNB2; CHRNA3	7	8.03
miRs in Muscle Cell Differentiation	10	18	Y-27632; Go 6976; H-7 dihydrochloride; sotrastaurin; C-1; "Dibutyryl-cAMP, sodium salt"; HA-1077; H 89 dihydrochloride; HA-1077; Phorbol 12-Myristate 13-Acetate	PRKCE; PRKCA; PRKCD; PRKACA; PRKCQ; PRKCH; PRKD1	7	10.02
TGF Beta Signaling Pathway	9	54	SC-1; Cyt387; TG-101348; INCB018424; SP600125; INCB018424; AZD1480; (−)-Epigallocatechin Gallate; LY 364947	TGFBR2; MAPK9; MAPK3; TGFBR1; EP300; JAK1; SERPINE1	7	11.85
G1 to S cell cycle control	8	69	Arcyriaflavin A; Alsterpaullone; CDK9 inhibitor 14; N9-isopropylolomoucine; MK-1775; KU-55933; SCH727965; APIGENIN	CDK4; CDK1; CDK6; WEE1; CDK7; ATM; CDK2	7	9.35

-continued

Pathway Name (Wiki)	Number Compounds	Number Genes Pathway	Compound List	Target List	Number Targets	Average Z-value
Serotonin Receptor 2 and ELK-SRF/GATA4 signaling	6	19	Bosutinib; SC-1; Bosutinib; Eltoprazine hydrochloride; Doxepine HCl; Sorafenib	HTR2A; RAF1; HTR2C; MAPK3; MAP2K2; MAP2K1; HTR2B	7	19.12
Parkin-Ubiquitin Proteasomal System pathway	5	71	VER155008; Colchicine; Vinblastine sulfate; PODOFILOX; COLCHICINE	TUBA1A; TUBA4A; TUBB; HSPA1B; TUBA1B; TUBB1; HSPA1A	7	8.51
Apoptosis	11	84	AT7867; TW-37; BMS-536924; SP600125; PODOFILOX; H 89 dihydrochloride; ABT-737; ABT-199 (GDC-0199); APIGENIN; NVP-ADW742; OSI-906 (Linsitinib)	BCL2; BCL2L1; BCL2L2; AKT1; IGF1R; MAPK10	6	10.65
IL17 signaling pathway	9	31	AT7867; SC-1; Cyt387; Alsterpaullone; TG-101348; INCB018424; INCB018424; AZD1480; H 89 dihydrochloride	MAPK3; AKT1; JAK2; GSK3B; JAK1; MAPK1	6	15.37
Extracellular vesicle-mediated signaling in recipient cells	9	31	AT7867; Neratinib; Vandetanib; Erlotinib; Erlotinib; Gefitinib; H 89 dihydrochloride; Sorafenib; LY 364947	TGFBR2; RAF1; EGFR; AKT1; TGFBR1; ERBB2	6	12.01
IL-9 Signaling Pathway	8	17	Bosutinib; SC-1; Bosutinib; Cyt387; TG-101348; INCB018424; INCB018424; AZD1480	MAPK3; MAP2K2; MAP2K1; JAK3; JAK1; MAPK1	6	18.38
ErbB Signaling Pathway	16	55	Bosutinib; AT7867; Bosutinib; VX-680; 1-Naphthyl PP1; Neratinib; Go 6976; Tozasertib; Vandetanib; Tozasertib VX-680 (MK-0457); H-7 dihydrochloride; sotrastaurin; C-1; KX2-391; Erlotinib; Dasatinib	ERBB4; PRKCA; SRC; AKT3; ERBB2	5	15.95
Apoptosis-related network due to altered Notch3 in ovarian cancer	12	53	Bosutinib; AT7867; SC-1; Bosutinib; PF-573228; KW 2449; 1-Naphthyl PP1; apicidin; Dasatinib; H 89 dihydrochloride; Belinostat; Pandacostat	HDAC1; ABL1; PTK2; AKT1; MAPK1	5	19.29
G13 Signaling Pathway	10	38	Bosutinib; Bosutinib; Y-27632; HA-1077; SP600125; HA-1077; H 89 dihydrochloride; HA-1077; APIGENIN; CAL-101	PIK3CD; ROCK1; TNK2; MAPK10; ROCK2	5	13.72
Interferon type I signaling pathways	10	58	Bosutinib; Bosutinib; 1-Naphthyl PP1; Cyt387; TG-101348; INCB018424; INCB018424; AZD 1480; H 89 dihydrochloride; CAL-101	PIK3CD; TYK2; JAK1; FYN; RPS6KA5	5	14.75
Endochondral Ossification	9	66	Dorsomorphin dihydrochloride; Sunitinib malate; BMS-536924; PODOFILOX; Belinostat; Sorafenib; NVP-ADW742; Pandacostat; OSI-906 (Linsitinib)	HDAC4; DDR2; IGF1R; BMPR1A; FGFR1	5	8.01
Serotonin Receptor 4/6/7 and NR3C Signaling	6	18	Bosutinib; SC-1; Bosutinib; RAF265; H 89 dihydrochloride; Sorafenib	MAPK3; MAP2K2; BRAF; MAP2K1; RPS6KA5	5	19.57

-continued

Pathway Name (Wiki)	Number Compounds	Number Genes Pathway	Compound List	Target List	Number Targets	Average Z-value
Adipogenesis	6	131	TTNPB; AM-580; TTNPB; (−)-Epigallocatechin Gallate; Stem Regenin 1; Retinoic acid	AHR; PPARD; RARA; RXRA; SERPINE1	5	8.26
Monoamine Transport	5	32	AZELASTINE HYDROCHLORIDE; OXOLINIC ACID; AMINOBENZTROPINE; CV 1808; Doxepine HCl	SLC6A4; SLC6A2; ADORA2A; HRH3; SLC6A3	5	11.54
Signal Transduction of SIP Receptor	3	25	AT7867; SC-1; H 89 dihydrochloride	MAPK3; AKT2; AKT1; AKT3; MAPK1	5	24.11
Aryl Hydrocarbon Receptor	14	43	Arcyriaflavin A; Neratinib; Sunitinib Malate; TG-101348; Vandetanib; Erlotinib; Sunitinib malate; CDK9 inhibitor 14; Erlotinib; N9-isopropylolomoucine; Gefitinib; StemRegenin 1; SCH727965; Sorafenib	AHR; EGFR; RET; CDK2	4	10.09
Bladder Cancer	9	29	Arcyriaflavin A; Neratinib; Vandetanib; Erlotinib; RAF265; CDK9 inhibitor 14; Erlotinib; Gefitinib; Sorafenib	CDK4; BRAF; EGFR; ERBB2	4	10.50
T-Cell Receptor and Co-stimulatory Signaling	9	30	Bosutinib; AT7867; Bosutinib; VX-680; 1-Naphthyl PP1; Tozasertib; Alsterpaullone; Tozasertib VX-680 (MK-0457); H 89 dihydrochloride	LCK; AKT1; GSK3B; FYN	4	19.74
Type II interferon signaling (IFNG)	8	41	Cyt387; TG-101348; INCB018424; sotrastaurin; C-1; INCB018424; "7-DESACETOXY-6,7-DEHYDROGEDUNIN"; AZD1480	EIF2AK2; PRKCD; JAK2; JAK1	4	10.25
Constitutive Androstane Receptor Pathway	5	20	PODOPHYLLIN ACETATE; NP-009852; NP-009832; FLAVONE; ERYTHROMYCIN STEARATE; Retinoic acid	ABCB1; RXRA; CYP3A4; CYP2C9	4	7.52
DNA Damage Response (only ATM dependent)	4	61	Alsterpaullone; SP600125; APIGENIN; CAL-101	PIK3CD; MAPK9; GSK3B; MAPK10	4	8.85
Peptide GPCRs	3	73	BNTX maleate; "7,4'-DIHYDROXYFLAVONE"; "L-803,087 trifluoroacetate"	OPRD1; SSTR4; OPRK1; OPRM1	4	7.39
EPO Receptor Signaling	15	27	Bosutinib; Bosutinib; VX-680; 1-Naphthyl PP1; Cyt387; Tozasertib; TG-101348; INCB018424; Vandetanib; Tozasertib VX-680 (MK-0457); KX2-391; INCB018424; Dasatinib; AZD1480; Sorafenib	RAF1; JAK2; SRC	3	14.17
miRNAs involved in DNA damage response	7	15	Bosutinib; Bosutinib; KW 2449; 1-Naphthyl PP1; Dasatinib; KU-55933; APIGENIN	ABL1; CDK6; ATM	3	17.68
Integrated Pancreatic Cancer Pathway	7	12	AT7867; Sunitinib Malate; Sunitinib malate; AZD2171; Ki8751; (−)-Epigallocatechin Gallate; H 89 dihydrochloride	AKT1; EP300; PDGFRA	3	12.95
Amyotrophic lateral sclerosis (ALS)	4	34	TW-37; ABT-737; ABT-199 (GDC-0199); cyclosporine	PPP3CA; BCL2; BCL2L1	3	8.38

-continued

Pathway Name (Wiki)	Number Compounds	Number Genes Pathway	Compound List	Target List	Number Targets	Average Z-value
Ovarian Infertility Genes	4	31	Arcyriaflavin A; Dorsomorphin dihydrochloride; CDK9 inhibitor 14; KU-55933	CDK4; ATM; BMPR1B	3	11.00
Fluoropyrimidine Activity	3	33	Ko-143; Acyclovir; zebularine	CDA; ABCG2; TK1	3	7.74
p38 MAPK Signaling Pathway	3	34	CGP57380; H89 dihydrochloride; LY 364947	MKNK1; TGFBR1; RPS6KA5	3	7.42
Eicosanoid Synthesis	3	19	SURAMIN; valdecoxib; Cilastatin sodium	PLA2G2A; DPEP1; PTGS2	3	9.43
Drug Induction of Bile Acid Pathway	3	17	PODOPHYLLIN ACETATE; Erlotinib; ERYTHROMYCIN STEARATE	ABCB1; NR1I2; CYP3A4	3	8.35
Nucleotide GPCRs	2	11	SURAMIN; CV 1808	P2RY2; ADORA2A; P2RY1	3	9.28
Glycolysis and Gluconeogenesis	1	48	LONIDAMINE	HK3; HK2; HK1	3	6.13
TCA Cycle Nutrient Utilization and Invasiveness of Ovarian Cancer	10	5	Neratinib; Cyt387; TG-101348; INCB018424; Vandetanib; Erlotinib; INCB018424; Erlotinib; AZD1480; Gefitinib	EGFR; JAK1	2	10.60
Gastric cancer network 2	9	31	Neratinib; Daunorubicin; Vandetanib; Erlotinib; Erlotinib; PODOFILOX; Bisantrene dihydrochloride; Gefitinib; Doxorubicin	TOP2A; EGFR	2	9.81
Gastric Cancer Network 1	9	29	KW 2449; VX-680; Tozasertib; Daunorubicin; Tozasertib VX-680 (MK-0457); PODOFILOX; Bisantrene dihydrochloride; Doxorubicin; MLN8237	AURKA; TOP2A	2	11.59
Cholesterol Biosynthesis	7	15	Cerivastatin; Cerivastatin; TIOCONAZOLE; Pitavastatin calcium; ERYTHROMYCIN STEARATE; lovastatin; fluvastatin	HMGCR; CYP51A1	2	8.06
Serotonin Receptor 2 and STAT3 Signaling	6	4	Cyt387; TG-101348; INCB018424; INCB018424; AZD1480; Doxepine HCl	HTR2A; JAK2	2	10.06
Type III interferon signaling	5	10	Cyt387; TG-101348; INCB018424; INCB018424; AZD1480	TYK2; JAK1	2	10.70
Osteoblast Signaling	5	17	Sunitinib Malate; Sunitinib malate; AZD2171; Ki8751; Sorafenib	PDGFRB; PDGFRA	2	9.48
FAS pathway and Stress induction of HSP regulation	4	42	TW-37; SP600125; ABT-737; ABT-199 (GDC-0199)	BCL2; MAPK8	2	9.24
Tryptophan metabolism	3	46	PODOPHYLLIN ACETATE; ERYTHROMYCIN STEARATE; tetraethylthiuram disulfide	CYP3A4; ALDH2	2	7.49
Irinotecan Pathway	3	14	Ko-143; PODOPHYLLIN ACETATE; ERYTHROMYCIN STEARATE	ABCG2; CYP3A4	2	8.50
Fatty Acid Omega Oxidation	3	15	PODOPHYLLIN ACETATE; ERYTHROMYCIN STEARATE; tetraethylthiuram disulfide	CYP3A4; ALDH2	2	7.49

-continued

Pathway Name (Wiki)	Number Compounds	Number Genes Pathway	Compound List	Target List	Number Targets	Average Z-value
Farnesoid X Receptor Pathway	3	19	PODOPHYLLIN ACETATE; ERYTHROMYCIN STEARATE; Retinoic acid	RXRA; CYP3A4	2	7.63
Selenium Micronutrient Network	3	86	BMS-536924; ERYTHROMYCIN STEARATE; OSI-906 (Linsitinib)	INSR; ALB	2	7.78
Apoptosis Modulation by HSP70	3	18	SP600125; VER155008; APIGENIN	MAPK10; HSPA1A	2	8.57
Folate Metabolism	3	67	BMS-536924; ERYTHROMYCIN STEARATE; OSI-906 (Linsitinib)	INSR; ALB	2	7.78
Liver X Receptor Pathway	3	10	PODOPHYLLIN ACETATE; ERYTHROMYCIN STEARATE; Retinoic acid	RXRA; CYP3A4	2	7.63
Vitamin B12 Metabolism	3	52	BMS-536924; ERYTHROMYCIN STEARATE; OSI-906 (Linsitinib)	INSR; ALB	2	7.78
Secretion of Hydrochloric Acid in Parietal Cells	2	4	AZELASTINE HYDROCHLORIDE; Doxepine HCl	HRH2; CHRM1	2	11.02
Apoptosis Modulation and Signaling	2	13	Go 6976; VER155008	PRKD1; HSPA1A	2	11.09
Heart Development	2	44	SC-1; Dorsomorphin dihydrochloride	BMPR1A; MAPK1	2	20.40
TFs Regulate miRNAs related to cardiac hypertrophy	2	8	AT7867; H 89 dihydrochloride	AKT2; AKT1	2	21.31
Nicotine Activity on Chromaffin Cells	2	4	ETHOSUXIMIDE; UB 165 fumarate	CACNA1G; CHRNA3	2	8.15
Codeine and Morphine Metabolism	2	8	PODOPHYLLIN ACETATE; ERYTHROMYCIN STEARATE	ABCB1; CYP3A4	2	8.02
Hypothetical Network for Drug Addiction	2	33	BARBITAL; Doxepine HCl	DRD2; GRIA2	2	7.75
Vitamin D Metabolism	1	10	Retinoic acid	RXRA; RXRB	2	6.86
PDGF Pathway	1	12	SC-1	MAPK3; MAPK1	2	25.00
Dopamine metabolism	7	13	H-7 dihydrochloride; C-1; "Dibutyryl-cAMP, sodium salt"; HA-1077; H 89 dihydrochloride; HA-1077; Phorbol 12-Myristate 13-Acetate	PRKACA	1	8.23
Statin Pathway	5	29	Cerivastatin; Cerivastatin; Pitavastatin calcium; lovastatin; fluvastatin	HMGCR	1	8.12
TP53 Network	5	13	Bosutinib; Bosutinib; KW 2449; 1-Naphthyl PP1; Dasatinib	ABL1	1	21.90
ID signaling pathway	4	16	Arcyriaflavin A; CDK9 inhibitor 14; N9-isopropylolomoucine; SCH727965	CDK2	1	10.10
DNA Replication	4	41	Arcyriaflavin A; CDK9 inhibitor 14; N9-isopropylolomoucine; SCH727965	CDK2	1	10.10
Inflammatory Response Pathway	3	30	VX-680; Tozasertib; Tozasertib VX-680 (MK-0457)	LCK	1	13.99

-continued

Pathway Name (Wiki)	Number Compounds	Number Genes Pathway	Compound List	Target List	Number Targets	Average Z-value
Influenza A virus infection	3	12	TW-37; ABT-737; ABT-199 (GDC-0199)	BCL2	1	9.05
Ectoderm Differentiation	2	10	Ro 31-8220 mesylate; APIGENIN	PIM1	1	10.67
Oxidative Stress	2	29	SP600125; APIGENIN	MAPK10	1	8.26
Arachidonate Epoxygenase/ Epoxide Hydrolase	2	5	NP-009852; NP-009832; FLAVONE	CYP2C9	1	7.36
Hedgehog Signaling Pathway	2	16	Purmorphamine; NVP-LDE225	SMO	1	8.61
Mitochondrial Gene Expression	1	19	cyclosporine	PPP3CA	1	6.35
Spinal Cord Injury	1	4	valdecoxib	PTGS2	1	8.60
Proteasome Degradation	1	61	MLN2238	PSMB5	1	7.13
ACE Inhibitor Pathway	1	17	PERINDOPRIL ERBUMINE	ACE	1	7.27
Cytoplasmic Ribosomal Proteins	1	88	H 89 dihydrochloride	RPS6KA3	1	7.14
Parkinsons Disease Pathway	1	71	LRRK2-IN-1	LRRK2	1	8.88
Matrix Metalloproteinases	1	30	(−)-Epigallocatechin Gallate	MMP7	1	7.36
Electron Transport Chain	1	103	oligomycin A	ATP6	1	7.16
Glycogen Metabolism	1	36	Alsterpaullone	GSK3B	1	12.55
Blood Clotting Cascade	1	25	(−)-Epigallocatechin Gallate	SERPINE1	1	7.36
SREBF and miR33 in cholesterol and lipid homeostasis	1	4	Dorsomorphin dihydrochloride	PRKAA1	1	11.09
Integrated Breast Cancer Pathway	1	17	CDK9 inhibitor 14	CDK7	1	9.91
Complement and Coagulation Cascades	1	60	(−)-Epigallocatechin Gallate	SERPINE1	1	7.36
Translation Factors	1	50	7-DESACETOXY-6,7-DEHYDROGEDUNIN	EIF2AK2	1	7.92
Oxidative phosphorylation	1	60	oligomycin A	ATP6	1	7.16
Eukaryotic Transcription Initiation	1	41	CDK9 inhibitor 14	CDK7	1	9.91
Prostaglandin Synthesis and Regulation	1	31	valdecoxib	PTGS2	1	8.60
Serotonin Transporter Activity	1	11	Doxepine HCl	SLC6A4	1	6.87

Example 3: Validation of Selected Compounds and Pathways

[0114] To validate the effect of identified compounds on macrophage activation, we assayed dosage responses of the commercially available top list of compounds to determine their effective concentration (EC) on cell shape change. 20 of 23 selected M1-activating and 4 of 6 M2-activating compounds showed strong dosage effects with an EC below 10 M (FIGS. **2**A-**2**B and Table 2). We performed RNA-seq analysis with 6 M1-activating (mocetinostat, thiostrepton, niclosamide, chlorhexidine, fenbendazole and fluvoxamine) and 2 M2-activating (bosutinib and alsterpaullone) compounds to determine if they activate macrophages at the transcriptional level. Fresh hMDMs were treated with compounds at the EC for 24 hours, followed by RNA-seq. The compounds induced diverse transcriptional responses with variable number of differentially expressed genes (DEG) to similar degrees as those induced by IL-4 or IFNγ (FIG. **9**A). To explore the functional differences of hMDMs induced by compounds, gene set enrichment analysis (GSEA) of transcriptional responses to each compound was compared to previously identified 49 gene expression modules in response to 29 different stimuli in hMDMs. Similar to IFNγ, the six M1-activating compounds up-regulated the gene expression of typical M1 modules (module #7, #8) induced by IFNγ, as well as chronic inflammation TPP modules (module #30, #32) induced by TNFα/PGE2/P3C (FIG. **2**C). The M1-activating compounds also down-regulated the modules (#26, #27) similarly as LPS. The two M2-activating compounds down-regulated the gene expression of typical M1 modules although they did not upregulate the gene expression modules (module #15) induced by IL-4 (FIG. **2**C). Consistently, all M1-activating compound upregulated expression of classical M1 markers CD80 and CD86 and down-regulated expression of classical M2 markers CD163 and CD206. Both M2-activating compounds down-regulated M1 markers (FIG. **9**C). Moreover, based on function enrichment analysis of the DEGs, all 8 compounds induced consensus pathways related to inflammatory response, chemotaxis/chemokine-mediated signaling and response to IFNγ and TNFα (FIG. **2**D). These results suggest that select compounds modulate macrophage activation at the transcriptional levels.

[0115] We also analyzed transcriptional responses of hMDMs to ligands of novel pathways, including serotonin (5HT), dopamine, VEGF, EGF and leptin by RNA-seq. Each ligand induced diverse transcriptional response (FIG. **9**B). In particular, 5HT, VEGF, EGF and leptin up-regulated the gene expression of typical M1 modules (#7, #8) but down-regulated the gene expression of the TPP modules (#30, #32) (FIG. **2**E). In contrast, dopamine down-regulated the gene expression of typical M1 modules but up-regulated the TPP modules (FIG. **2**E), suggesting these ligands regulate different aspects of macrophage activation. Function enrichment analysis of the DEGs identified induction of pathways related to inflammatory response, chemotaxis/chemokine-mediated signaling and wound healing by these ligands (FIG. **2**F). Taken together, these results suggest that the compounds as well as upstream signals of their protein targets modulate macrophage activation.

[0116] Table 2 shows dosage information of selected compounds on M0 macrophages.

Compound	EC	R square	Max absolute Z-value	Category
Taxol	0.10459189	0.416	−6.68139	M1
Cucurbitacin I	0.34174063	0.6048	−4.808	M1
Chlorhexidine	1.62736296	0.7308	−13.45	M1
Fenbendazole	0.4703644	0.8408	−12.37	M1
Thiostrepton	3.93691593	0.542	−12.75	M1
Diphenyleneiodonium chloride	0.67677365	0.4593	−8.509	M1
LE135	0.41887689	0.5289	−8.912	M1
Fluvoxamine	10.6420447	0.8318	−7.38	M1
Niclosamide	0.79658547	0.8077	−8.929	M1
MS275	1.04687704	0.5386	−7.993	M1
Mocetinostat	0.45359214	0.7105	−15.14	M1
Pimozide	1.17941118	0.2042	−8.006	M1
NP-010176	4.03386043	0.5479	−8.156	M1
HMN214	0.10382862	0.6514	−12.51	M1
Celastrol	0.79618903	0.4416	−4.485	M1
Cantharidin	0.17983226	0.2334	−31.36	M1
NVP 231	2.24851869	0.8661	−22.37	M1
FTY720	2.94456442	0.8244	−11.58	M1
Evodiamine	0.3969275	0.9413	−26.36	M1
Penfluridol	2.52355815	0.8439	−4.873	M1
Bostunib	0.09135798	0.3168	23.5	M2
Su11274	0.72193028	0.9476	17.8	M2
Alsterpaullone	0.3076402	0.4391	13.9	M2
ALRESTATIN	3.66821661	0.8352	15.05	M2

Example 4: Reprogramming Screen of Compounds on Polarized Macrophages

[0117] To investigate whether the identified compounds could reprogram or reactivate macrophages after M1- or M2-like differentiation, we rescreened the hits on M1- or M2-activated macrophages. hMDMs were activated into M2-like macrophages by IL-4 plus IL-13 or M1-like macrophages by IFNγ plus TNFα. After removing the differentiating cytokines, M2-like macrophages were treated with each of the 166 M1-activating compounds and M1-like macrophages were treated with each of the 180 M2-activating compounds at a final concentration of either 5 μM and 10 μM. 24 hours later, cell images were taken and cell shapes were quantified. Based on the same Z-score cutoff, 37 M1-activating and 21 M2-activating compounds were identified to induce cell shape changes at the concentration of both 5 μM and 10 μM (FIGS. **3**A-**3**B). Dosage responses were carried out with 40 commercial available compounds (21 M1-activating and 19 M2-activating) on polarized macrophages. 17 of the M1-activating (81%) and 18 of the M2-activating (95%) compounds had typical dosage dependent response with an EC below 10 μM, and induced statistical significant changes of cell shape (FIG. **3**C and Table 3).

[0118] We also rescreened the hits on differentiated macrophages in the presence of differentiating cytokines: either IL-4 plus IL-13 or IFNγ plus TNFα. Surprisingly, more compounds exhibited significant effects on cell shape changes in the presence of these cytokines (67 M1- and 55 M2-activating) than in absence of these cytokines (46 M1- and 25 M2-activating) at the same compound concentration of 5 μM (FIGS. **3**D-**3**E). Consistently, 28 of the 37 M1-activating and 18 of the 21 M2-activating compounds were identified again to induce significant cell shape change at the concentration of 5 μM. In the dosage response assay, the ECs of many M1-activating compounds were lower in the presence of cytokines than in the absence of cytokines (FIG. **10**).

Thus, the presence of differentiating cytokines makes macrophages more sensitive to reprogramming.

[0119] Table 3 shows dosage information of selected compounds on differentiated macrophages

Compounds	EC	R-square	Category
Bisantrene dihydrochloride	1.984795322	0.737	M2
triptolide	0.061894009	0.2428	M2
lovastatin	0.442115573	0.3319	M2
QS 11	0.261082221	0.7666	M2
Regorafenib	2.882594235	0.7596	M2
Sorafenib	0.794071491	0.7332	M2
MLN2238	3.461032864	0.3362	M2
GW-843682X	0.897347267	0.5783	M2
KW 2449	2.16025641	0.8979	M2
Axitinib	0.591495199	0.9957	M2
JTE 013	0.938113208	0.6378	M2
Purmorphamine	2.345142857	0.8143	M2
Arcyriaflavin A	1.342190889	0.6374	M2
Dasatinib	0.761950413	0.6968	M2
NVP-LDE225	2.76599809	0.6752	M2
1-Naphthyl PP1	2.072231834	0.8623	M2
SELAMECTIN	15	0	M2
MGCD-265	0.911173577	0.8933	M2
Bosutinib	0.164371173	0.523	M2
Cantharidin	0.158610234	0.9764	M1
Cucurbitacin I	1.759105431	0.53	M1
Alprostadil	0.056193353	0.1288	M1
HMN-214	1.482432432	0.3942	M1
WP1130	15	0.05	M1
MS275	0.81097561	0.181	M1
SMER3	0.093980962	0.4302	M1
SCH 79797 dihydrochloride	0.219379028	0.7105	M1
NVP 231	5.744680851	0.4822	M1
Prulifloxacin	15	0	M1
FTY720	0.131265421	0.262	M1
DIHYDROCELASTRYL DIACETATE	15	0.03	M1
Diphenyleneiodonium chloride	0.336300175	0.2451	M1
Penfluridol	0.169426434	0.7956	M1
thiostrepton	0.407871889	0.3882	M1
Evodiamine	0.679884726	0.949	M1
MITOXANTRONE HYDROCHLORIDE	0.559348161	0.5764	M1
Quinolinium	8.365292011	0.1839	M1
Fenbendazole	0.649293564	0.7447	M1
Niclosamide	1.12595217	0.3178	M1
Taxol	0.128848	0.1359	M1

Example 5: Shared and Unique Effects of Identified Compounds on Macrophage Transcription

[0120] To broadly validate the identified compounds on macrophage activation (reprogramming) and to shed light on how the compounds activate macrophages, we selected 17 M1- and 17 M2-activating compounds with ECs below 5 μM and performed transcriptional profiling by RNA-seq. M2-like macrophages induced by IL-4 plus IL-13 were treated with each of the 17 M1-activating compounds at its ECs for 24 hours. Similarly, M1-like macrophages induced by IFNγ plus TNFα were treated with each of the 17 M2-activating compounds at its ECs for 24 hours. Different compounds up-regulated and down-regulated different number of genes (FIG. **4**A), and a total of 7247 genes exhibited at least a two-fold change after exposure to at least one compound. Hierarchical clustering of Pearson's correlations of DEGs induced by compounds as well as by IFNγ and IL-4 showed that all 17 M1-activating compounds clustered together with IFNγ and all 17 M2-activating compounds clustered together with IL-4 (FIG. **4**). Principal component analysis (PCA) of global transcriptional response showed that M1-like macrophages, M2-like macrophages treated with IFNγ, M1-like macrophages treated with IL-4, and M1-like macrophages treated with M2-activating compounds grouped together, whereas M2-like macrophages and M2-like macrophages treated with M1-activating compounds grouped together (FIG. **11**A). Although most compounds as well as IL-4 moderately modulated the global gene expression, GSEA of transcriptional functional modules showed that all M1-activating compounds clustered together and up-regulated typical M1 modules (#7, #8) and the TPP modules (#30, #32) (FIG. **4**C). All M2-activating compounds clustered together and down-regulated the typical M1 modules (#7, #8) and the TPP modules (#30, #32). The modules (#26, #27), which are down-regulated by LPS, were also down-regulated by M1-activating compounds but up-regulated by M2-activating compounds. Moreover, expression of typical M1 markers CD80 and CD86 was up-regulated by M1-activating compounds and suppressed by M2-activating compounds while expression of the M2 markers CD206 and CD163 was up-regulated by M2-activating compounds and suppressed by M1-activating compounds (FIG. **11**C). These results were further validated at transcriptional level by qPCR and at protein level by flow cytometry (FIGS. **11**D-**11**E).

[0121] To investigate the common denominators of macrophage activation, a reverse engineering regulatory network was assembled by ARACNe based on mutual information between each gene pair computed from the compound-perturbing expression profiles. Top 10% central hub genes inferred from the network (n=1255 most interconnected genes) collectively participated in 98,048 interactions. Most of top central hub genes or regulators, such as GBP1, FAM26F, STAT1, have been shown to play essential roles in macrophage activation and function (FIG. **12**). We performed GO enrichment analysis of these hub genes with visualization of GO enrichment networks by BiNGO. This GO-term network identified functional clusters associated with macrophage activation, including not only previously identified clusters of immune response, leukocyte or lymphocyte activation, catabolic and metabolic process, but also new clusters of stress response, cell migration, protein transport, secretion, cell proliferation, ion homeostasis, phosphorylation and signaling, as well as tissue remodeling and wound healing (FIG. **4**D). Moreover, function enrichment analysis of DEGs showed that different compounds not only modulated gene expression in the common immune response pathways and chemotaxis/chemokine-mediated signaling pathway but perturbed specific (unique) pathways (FIGS. **4**E-**4**F and **11**B). Consistently, these unique pathways perturbed by compounds were primarily through their putative targets. For example, M1-activating compound MS275 inhibits HDACs (histone deacetylase), which perturbed the pathway of chromatin assembly. M2-activating compound bisantrene inhibits TOP2A (topoisomerase II), which perturbed the pathway of DNA topological change (FIG. **4**F). These data suggest that the identified compounds reprogram the differentiated macrophages through modulating the expression of genes associated with macrophage activation as well as specific pathways unique to each compound.

Example 6: Induction of Macrophages to Proinflammatory State by Thiostrepton

[0122] To determine if the identified compounds activate macrophages in disease setting in vivo, we selected thiostrepton, a natural cyclic oligopeptide and an approved veterinary antibiotic for treating skin infection, and tested it to activate macrophages to M1-like state. Similar to other thiopeptide antibiotics, thiostrepton inhibits the ribosome function of bacterial protein synthesis. Recently, thiostrepton was shown to exhibit antiproliferative activity in human cancer cells through inhibiting proteasome and/or FOXM1 transcription factor. Following treatment of hMDMs with 2.5 μM thiostrepton for 24 hours, hMDMs were polarized to express proinflammatory cytokines TNFα and IL-1β and down-regulate the M2 chemokine CCL24 (FIG. **5**A). Functional enrichment analysis of the DEGs showed that IFN/NFκB pathway, TNF-mediated pathway, oxidative-reduction process, protein polyubiquitination and cellular response to LPS were upregulated, while DNA replication, cell cycle and cell matrix adhesion were down-regulated (FIG. **5**B). GSEA analysis showed pathways of TNFα signaling via NFκB and ROS were upregulated while pathways of E2F target and mitotic spindle were down-regulated (FIG. **5**C). These results show that thiostrepton regulates the expression of genes associated with proteasome and DNA replication in hMDMs.

[0123] To determine the effect of thiostrepton on TAM in vitro, mouse bone marrow macrophages (BMMs) were cultured in the conditioned medium (CM) of B16F10 tumor cells in the absence or presence of thiostrepton for 24 hrs. Alternatively, BMMs were cultured in the conditioned medium for 24 hrs first and then treated with thiostrepton for another 24 hrs. The expression of selected genes associated with macrophage polarization was assayed by qPCR. Thiostrepton inhibited the expression of TAM/M2-associated genes Arg1, Fizz1, Vegfa, Ym1 and Tgfb but up-regulated the expression of M1-associated genes Tnf, Il1b, Cxcl2 and Nos2 (FIG. **5**D). The effect of thiostrepton was observed whether thiostrepton was added into the conditioned medium culture or BMMs were differentiated into TAM first (Compare groups 2 and 3 in FIG. **5**D). Consistently, flow cytometry analysis revealed up-regulation of MHCII, CD80 and iNOS but down-regulation of ARG1 (FIG. **13**A). Similarly, we examined the effect of thiostrepton on IL-4/IL-13 and lactic acid-polarized BMMs. As shown in FIG. **13**B, thiostrepton inhibited the expression of Arg1, Fizz1, Ym1 and Tgfb but elevated expression of Tnf, Il1b, Cxcl2 and Ccl5 whether thiostrepton was added together with cytokines or lactic acid or after BMM polarization.

[0124] To examine whether thiostrepton-activating macrophages or conditioned medium have effects on tumor cell growth, BMMs were treated with thiostrepton for 24 hrs. Equal numbers of primed BMMs and melanoma cells (B16F10) were co-cultured for 12 hrs. Significantly more melanoma cells were lost in the presence of thiostrepton-treated macrophages as compared to the untreated macrophages in a dose-dependent manner (FIG. **5**E). Similarly, more melanoma cells were lost in the conditioned medium from thiostrepton-treated macrophages than conditioned medium from untreated macrophages or heat-inactivated thiostrepton-treated conditioned medium (FIG. **14**A). To determine whether thiostreption-activated macrophages exhibit enhanced ADCP, thiostreption-activated macrophages were co-cultured with equal number of human B lymphoma cells (GMB) labeled with eFluro670 dye and anti-CD20 for 2 hrs. Thiostrepton elevated ADCP of both human and mouse macrophages (FIGS. **14**B-**14**C). These data show that thiostrepton activates and reprograms macrophages toward a pro-inflammatory state and enhances their tumor-killing activity in vitro.

Example 7: Reprogramming TAMs for Enhanced Anti-Tumor Activity In Vivo by Thiostrepton

[0125] Next, we examined whether thiostrepon has anti-tumor effect in vivo through activating macrophages. B16F10 melanoma cells were injected subcutaneously into syngeneic C57BL/6 mice. 6 and 12 days later, tumor-bearing mice were treated with either vehicle (DMSO), melanoma specific antibody TA99, thiostrepton, or combination of TA99 and thiostrepton by intraperitoneal injection (I.P.). In a dosage-dependent manner (150 or 300 mg/kg), thiostrepton strongly suppressed the tumor growth alone and additively with TA99 (FIG. **6**A). Since thiostrepton inhibits cell proliferation and is an antibiotic, to exclude its systematic effects on immune cells and on gut microbiome, tumor-bearing mice were treated by para-tumor subcutaneous injection (S.C.) with a lower dose of thiostrepton (20 mg/kg). This local treatment also suppressed the tumor growth and exhibited additive effects with TA99 (FIG. **6**B). Flow cytometry analysis of single cell suspensions of dissected tumors at day 18 post tumor engraftment showed elevated levels of macrophages and monocytes in mice given thiostrepton or thiostrepton plus TA99 as compared to mice given vehicle or TA99 (FIGS. **6**C-**6**D). Consistently, more abundant macrophages were stained positive for F4/80 by immunochemistry in tumor sections from mice treated with thiostrepton or thiostrepton plus TA99 than mice treated with vehicle or T99 (FIG. **6**E). In non-tumor bearing mice, intraperitoneal administration of thiopstrepton led to increased numbers of macrophages in the spleen and bone marrow while subcutaneous administration did not have significant effects on macrophage numbers (FIG. **15**A). In both dosing strategies, thiostrepton did not change the total bacterial counts in the gut (FIG. **15**B). Moreover, flow cytometry analysis of TAM revealed elevated levels of iNOS and CD86 and decreased levels of Arg1 in mice given thiostrepton or thiostrepton plus TA99 as compared to mice given vehicle or TA99 (FIGS. **16**A-**16**B). Interestingly, an increased number of $TNF\alpha^+$ $IFN\gamma^+$ NK cells (but not $CD8^+$ T cells) was found in tumors in mice given thiostrepton or thiostrepton plus TA99 as compared to mice given vehicle or TA99 (FIG. **16**C).

[0126] To investigate whether tumor-infiltrated macrophages were reprogrammed, we purified TAMs from B16F10 melanoma tumors from mice dosed with thiostrepton or vehicle by I.P. or S.C. at day 18 post tumor engraftment and performed RNA-seq. GSEA and functional enrichment analysis showed that thiostrepton up-regulated the expression of genes associated with inflammatory response and ROS and down-regulated the expression of genes associated with mitotic division in TAMs from mice treated with thiostrepton by both I.P. and S.C. (FIG. **17**). The expression of the pro-inflammatory cytokines, including Tnf, Il1b, Cxcl1 and Cxcl2, were also significantly upregulated (FIG. **6**F), consistent with the results from thiostrepton treatment of hMDMs in vitro (FIG. **5**A).

[0127] To further confirm the anti-tumor effects of thiostrepton in vivo, we injected i.v. luciferase-expressing

human B lymphoma cells into NSG mice. Tumor-bearing mice were treated with rituximab (anti-CD20), thiostrepton or both at 2 and 3 weeks post tumor engraftment. Quantification of tumor burden by luciferase imaging showed that thiostrepton alone or together with rituximab significantly reduced the tumor burden in the bone marrow (FIGS. **18**A-**18**B). Consistently, higher percentages of F4/80$^+$ CD11b$^+$ macrophages with higher expression of MHCII were found in the bone marrow of mice treated with thiostrepton than mice given vehicle or rituximab whereas the frequencies of Ly6G$^+$ neutrophils were lower (FIGS. **18**C-**18**D). Moreover, another M1-activating compound, cucurbitacin I, also inhibited B16F10 growth by activating macrophages both in vitro and in vivo (FIG. **19**). Taken together, M1-activating compounds could reprogram TAMs into pro-inflammatory macrophages to inhibit tumor growth in vivo.

Example 8: Material and Methods

Mice, Antibodies, Cell Lines and Plasmids

[0128] C57BL/6 (B6) mice, p47phox$^{-/-}$, Clec4f-Cre mice were purchased from the Jackson Laboratory and maintained in the animal facility at the Massachusetts Institute of Technology (MIT). PKM^{flox} mice were described in the previous publication. Antibodies specific for CD11b (M1/70), F4/80 (BM8), MHC-II (M5/114.15.2), CD45.2 (104), CD9 (MZ3) for flow cytometry were from Biolegend. Anti-GPR3 (#SC390276) was from Santa Cruz Biotechnology. Anti-β-arrestin2 (#4674), Glycolysis Antibody Sampler Kit (#8337), anti-Myc and anti-FLAG were from Cell Signaling Technology. Anti-PKM2 (#1C11C7) was from Abcam. β-Arrestin2 CRISPR plasmids (sc432139) was from Santa Cruz Biotechnology. pCMV-β-arrestin2-GFP (PS10010), pCMV6-Flag-myc-barrestin2 (PS100001) and Arrb2 mouse siRNA Oligo Duplex (Locus ID 216869) were from Origene. Immortalized Kupffer cell line (ABI-TC192D, AcceGen), human primary KCs (ABC-TC3646, AcceGen), THP-1 (ATCC TIB-202) and 293T (CRL-3216) were cultured following vendor instructions (37° C., 5% CO_2). Transfection of ImKCs with siRNAs was accomplished using Lipofectamine™ 2000 (Thermo Fisher Scientific) according to the manufacturer's instruction. Apocynin (PHL83252) was from Sigma.

Bone Marrow Derived Macrophages (BMDMs)

[0129] Mouse BMDMs were prepared. Fresh bone marrow cells were isolated from B6 mice, plated onto a six-well plate with 1×10^6/mL in complete RPMI with 2-mercaptoethanol and 20% L929 supernatants which were obtained by culturing L-929 cells for 6 days with medium change every 2 days.

Co-Immunoprecipitation, Western Blotting and Native PAGE

[0130] 293T cells were transfected with FLAG-tagged β-arrestin2, using TransIT®-LT1 Transfection Reagent (Mirus). Thirty-six hours after transfection, the cells were lysed using cold Lysis Buffer containing 20 mM Tris-HCl (pH 7.4), 150 mM NaCl, 0.1% NP-40, 10% glycerol, proteinase inhibitor (Roche Catalog No. 11836153001), and phosphatase inhibitors (Roche Catalog No. 04906845001). The clear supernatants from the lysate were incubated with M2-magnetic beads conjugated with anti-FLAG antibody (Sigma Catalog No. M8823) for 2 hours at 4° C. Then the beads were washed twice and eluted by the 3×FLAG peptides (Sigma Catalog No. F4799) as described in the Sigma manual for Western blotting.

[0131] Proteins were extracted from cells with RIPA buffer. Protein concentration was quantified by BCA Protein Assay Kit (Pierce Biotechnology). Samples containing 20 μg total protein were resolved on a 10% SDS-PAGE gel and electro-transferred onto a PVDF membrane (Millipore Corporation). The membrane was blocked in 5% (w/v) fat-free milk in PBST (PBS containing 0.1% Tween-20). The blot was hybridized overnight with primary antibodies: anti-pSRC (D49G4, Cell Signaling Technology, 1:1000) and pSIK1/2/3 (#ab199474, Abcam, 1:1000) according to the recommended dilution in 5% fat-free milk. The blot was washed twice in PBST and then incubated with anti-Rabbit HRP-conjugated secondary antibody (Cell Signaling Technology, 1:2000) in 5% fat-free milk. The membrane was washed twice in PBST and subjected to protein detection by ECL Plus Western Blotting Detection System (GE Healthcare) before being exposed to a Kodak BioMax XAR film. The membrane was stripped and reblotted with the anti-β-tubulin (D49G4, Cell Signaling Technology) for protein loading control.

[0132] Protein was extracted from cells in 1× Native PAGE sample buffer (ThermoFisher) containing 1% digitonin followed by 20 min spin at 12,000×g to pellet debris. Protein extracts were analyzed using NativePAGE Novex System (ThermoFisher) and subsequently transferred to PVDF membrane, fixed, and blotted for native proteins.

Metabolite Profiling

[0133] ImKCs were treated with DPI (#81050, Cayman) at 50 or 500 nM for 6 hrs or 24 hrs. Cells were washed once in ice-cold 0.9% NaCl and lysates were extracted in 80% methanol solution containing internal standards for LC/MS by scraping on dry ice followed by 10-minute mixing with vortex in 4° C. Following lysate extraction, debris were removed by high-speed centrifugation and supernatant was dried using speedvac. Samples were analyzed by LC/MS on QExactive Orbitrap instruments (Thermo Scientific) in Whitehead Institute metabolite profiling core facility. Data analysis was performed using the in-house software described previously (Lewis et al., 2014).

β-arrestin2 Nuclear Translocation Assay

[0134] BMDMs or ImKCs were cotransfected with plasmids encoding FLAG-GPR3-GFP or β-arrestin2-RFP. Twenty-four hours after transfection, cells were reseeded into a 24-well glass-bottom plate (Nest, Shanghai, China) and treated with DPI (50 nM), S1P (3 mM), or vehicle control (0.3% DMSO) for the indicated duration. The fluorescent signals of membrane-bound receptor or β-arrestin2 were collected as live images using a total internal reflection fluorescence (TIRF) microscope (Olympus).

Oxygen Consumption, Glucose Stress Assay, Glucose Consumption and Lactate Production

[0135] OCR and ECAR were measured in isolated tissues or cultured ImKCs using the Seahorse XFe Extracellular Flux Analyzer (Agilent). For tissue respiration assays, 1.0 mg adipose tissue was dissected from inguinal WAT depots by using a surgical biopsy instrument (Integra Miltex Standard Biopsy Punches, Thermo Fisher) and placed into XF96

Islet Capture Microplates and pre-incubated with XF assay medium with pH value at 7.4. XF assay medium supplemented with 1 mM sodium pyruvate, 2 mM GlutaMax™-I, and 25 mM glucose. Isolated MDMs or Kupffer cells were subjected to a mitochondrial stress test by adding oligomycin (2 μM) followed by carbonyl cyanide 4-(trifluoromethoxy), phenylhydrazone (FCCP, 5 μM), and antimycin (1 μM). For glucose stress assay and ECAR measurement, XF assay medium was supplemented only with GlutaMax™-I. Tissue or cells were subjected to a glucose stress test by adding highly concentrated glucose (for tissue, 25 mM; for cells, 10 mM), followed by adding oligomycin (5 μM), FCCP (5 μM), and 2-DG (50 mM). Cells were seeded in culture dishes, and the medium was changed after 6 hours with serum-free DMEM. Cells were incubated for 12-16 hours, and the culture medium was then collected for measurement of glucose and lactate concentrations. Glucose levels were determined using a glucose (GO) assay kit (Sigma). Glucose consumption was the difference in glucose concentration when compared with DMEM. Lactate levels were determined using a lactate assay kit (Eton Bioscience).

Immunofluorescence and Microscope

[0136] BMDMs or Kupffer Cells were fixed and incubated with primary antibodies, and then labeled with Alexa Fluor dye-conjugated secondary antibodies and counterstained with Hoechst 33342 according to standard protocols. Cells were examined using a deconvolution microscope (Zeiss) with a 63-A oil immersion objective. Axio Vision software from Zeiss was used to deconvolute Z-series images.

PKM and GAPDH Enzymatic Activity

[0137] The enzymatic activities of PKM and GAPDH were measured using the pyruvate kinase activity assay kit (Biovision, #K709) and GAPDH activity assay kit (Biovision, #K680) according to the manufacturer's protocols, respectively.

Myc Luciferase Assay

[0138] The c-Myc activity was assessed using the Myc Reporter kit (BPS Biosciences) and the Dual-Luciferase Reporter System (Promega) according to the manufacturers' instructions. Briefly, 100 μL (1.5×10^5 cells/mL) control and Kupffer cells were seeded into 96-well plates. After overnight incubation, when cells reached ~50% confluency, 1 μL of Reporter A (60 ng/μL) in the Myc Reporter kit was transfected into cells using Turbofectin 8.0. After 48 hours, cells were lysed in 25 μL Passive Lysis Buffer (provided in the Dual-Luciferase Reporter kit). 20 μL of cell lysate was transferred to 96-well plates and placed in a 96-well microplate luminometer (GloMax-Multi, Promega). 100 μL Luciferase Assay Reagent II and 100 μL Stop & Glo Reagent (both provided in the Dual-Luciferase Reporter kit) were sequentially injected, and firefly and *Renilla* luciferase activities were automatically measured. c-Myc activities were determined by the ratios of firefly to *Renilla* luciferase activities.

HFD-Induced NAFLD Mouse Model and Treatment

[0139] C57BL/6 mice at 5 weeks of age (body weight=23-25 g) were randomly assigned to three groups: 5 mice were fed with a normal chow diet for 16 weeks and then injected with saline once every 5 days for 4 weeks; 10 mice were fed with HFD (60 kcal % fat) for 16 weeks to induce obesity and hepatosteatosis and then divided into two groups: HFD+vehicle (HFD) group (n=5) was injected with the vehicle (PEG3000) and HFD+DPI group (n=5) was injected with DPI in vehicle (2 mg/kg) i.p. every 5 days for 4 weeks.

Histopathology and Immunochemical Staining

[0140] Liver samples fixed in 10% buffered formalin were embedded in paraffin, sliced (2 μm sections), and stained with hematoxylin and eosin (H&E). Histological examination for morphological changes was performed in a blinded manner. Liver sections were scored according to the criteria of the NAFLD activity score (NAS).

Glucose Tolerance Test (GTT)

[0141] The GTT were performed in mice 19 weeks after feeding with HFD or NC. For GTT, mice were fasted overnight, followed by an intraperitoneal injection of 1 g/kg glucose. For the ITT, mice were fasted for 6 hours, followed by an intraperitoneal injection of 0.75 units/kg insulin. Blood was obtained from the tail vein before (0 min) and after (15, 30, 60, 90 and 120 min) the injection of glucose or insulin. Glucose levels were measured using an automatic glucometer (Roche Diagnostics, Rotkreuz, Switzerland).

Human Liver Immune Cell Isolation and Kupffer Cell Isolation

[0142] Human liver biopsies were obtained from livers procured from deceased donors deemed unacceptable for liver transplantation. Samples were collected with appropriate institutional ethics approval from The First Affiliated Hospital of Jilin University. All experiments were performed in accordance with the relevant guidelines and regulations. In addition, written informed consent was obtained from each subject. During organ retrieval, donor liver grafts were perfused in situ with cold (HTK) solution (Methapharm) to thoroughly flush out circulating cells, leaving only tissue resident cells that are then used to prepare a single-cell suspension to isolate immune cells. The unused liver caudate lobe post liver transplantation was collected and flushed with HBS+EGTA at 4° C. to remove any non-liver resident cells. Single-cell isolation from the resected caudate lobe was performed with a modified two-step collagenase procedure (MacFarland et al. 2017 ACnano). Single cell suspension was stained with anti-CD45 to sort all immune cells for scRNAseq or anti-CD14 to sort KCs for in vitro treatment by flow cytometry (BD Aria).

RNA Isolation, Sequencing, and Data Analysis

[0143] Mouse livers were dissected and digested with Collagenase IV (Roche). Single cell suspension was stained with anti-F4/80, anti-CD11b and anti-Gr-1. $F4/80^{+}CD11b^{+}Gr1^{low}$ macrophages were sorted by flow cytometry (BD Aria). RNAs were extracted with RNeasy MinElute Kit (Qiagen), converted into cDNA and sequenced using Next-Generation Sequencing (Illumina). RNA-seq data were aligned to the human genome (version hg19) and raw counts of each genes of each sample were calculated with bowtie2 2.2.3 (Langmead et al. 2009) and RSEM 1.2.15 (Li et al. 2011). Differential expression analysis was performed using the program edgeR at $P<0.05$ with a two-fold change (Robinson et al. 2010). The gene expression level across different samples was normalized and quantified using the

function of cpm. DEGs were annotated using online functional enrichment analysis tool DAVID (Huang et al. 2007).

Single Cell RNAseq and Computational Analysis

[0144] Sorted CD45$^+$ cells were resuspended and washed in 0.05% RNase-free BSA in PBS for single-cell library preparation with 10× Chromium Next GEM Single Cell 3' Kit (10×Genomics according to the manufacturer's instructions. The single-cell cDNA libraries were sequenced by NexSeq500 (Illumina). Raw sequences were demultiplexed, aligned, filtered, barcode counting, unique molecular identifier (UMI) counting with Cell Ranger software v3.1 (10× Genomics) to digitalize the expression of each gene for each cell. The analysis was performed using the Seurat 3.0 package. We first processed each individual data set separately prior to combining data from multiple samples. The outlier cells with extreme low number (<500) or high number (>5,000) of gene features as doublets, or low total UMI (<1,000) and high mitochondrial ratio (>15%) from each data set were removed. Subsequently, samples were combined based on the identified anchors for the following integrated analysis. We ran principal component analysis (PCA) and used the first 15 principal components (PCs) to perform tSNE clustering. We checked well-defined marker genes for each cluster to identify potential cell populations, such as T cells (CD3E, CD8A, CD4, CD69, IL7R), B and plasma cells (CD19, MS4A1, SDC1), DC (CD11C, CLEC9A), NK cells (CD56, CD16, GZMB). For macrophage analysis, CD14 and CD68 positive clusters were selected for subsequent analyses. We repeated PCA, tSNE clustering on the integrated data sets of macrophages. Differential expression analysis was performed to identify the genes significantly upregulated in each cluster compared with all other cells. For gene sets representing specific cellular functions or pathways, we performed functional enrichment analysis with the biological process of Gene Ontology by the online tool DAVID.

Statistic Methods

[0145] Statistical significance was determined with the two-sided unpaired or paired Student's t test. The FDRs were computed with q=P×n/i, where P=P value, n=total number of tests, and i=sorted rank of P value.

Example 9: DPI Stimulates Both Rapid and Sustained Increase in Glycolysis in Macrophages

[0146] DPI stimulates transcription of many genes in the glycolysis pathway in human primary macrophages (FIG. **20**A and FIG. **27**A). We confirmed the upregulation of hexokinase (HK), glyceraldehyde-3-phosphate dehydrogenase (GAPDH), lactate dehydrogenase A (LDHA) and enolase at the protein level in both human primary macrophages and an immortalized line of mouse Kupffer cells (ImKCs) in an DPI dose- and treatment time-dependent manner (FIG. **27**B). To investigate the effect of DPI on cellular metabolism, we measured cellular activities in glycolysis and oxidative phosphorylation (OxPhos) by assaying extracellular acidification rate (ECAR) and oxygen consumption rate (OCR), respectively, in ImKCs in the absence or the presence of 5, 50 and 500 nM DPI. In a dose-dependent manner, DPI stimulated an immediate increase in ECAR and a concomitant decrease in OCR (FIGS. **20**B-**20**C). The DPI-stimulated increase in glycolysis was sensitive to glucose, oligomycin, and rotenone plus antimycin A, and was associated with significant increase in glycolytic capacity and reserve (FIGS. **20**D-**20**E). The effects of DPI on glycolysis and OxPhos were confirmed by quantifying the levels of the major intermediates in the glycolysis pathway and the tricarboxylic acid (TCA) cycle in ImKCs 6 hours after DPI treatment. As shown in FIG. **20**F, in a DPI dose-dependent manner, glucose level decreased significantly while the levels of intermediates in the glycolysis pathway, including glucose 6-phosphate (G6P), fructose 1,6-bisphosphare (F1, 6BP), glyceraldehyde 3-phosphate (G3P), pyruvate, and lactate increased significantly. In contrast, the levels of TCA cycle intermediates, including acetyl-CoA, citrate, α-ketoglutarate (α-KG), succinate, fumarate and malate, all decreased in a DPI dose-dependent manner. Similar changes in the levels of glucose, glycolysis and TCA cycle intermediates were also seen 24 hours after DPI treatment (FIG. **27**C). These results show that DPI regulates cellular metabolism dynamically at two levels: rapid stimulation of glycolysis with concomitant inhibition of OxPhos and sustained stimulation of glycolysis by upregulating transcription and expression of genes in the glycolysis pathway.

Example 10: DPI Stimulates Glycolysis Through GPR3 and β-Arrestin2

[0147] DPI is an agonist of GPR3 and an inhibitor of GAPDH oxidase (NOX). We first determined the requirement of NOX in DPI-stimulated glycolysis. Bone marrow derived macrophages (BMDMs) were prepared from p47phox$^{-/-}$ mice, which do not have any functional NOX activity as p47phox is the organizer of phagocyte NAPDH oxidase (NOX2). Compared to wild-type (WT) BMDMs, p47phox$^{-/-}$ BMDMs had a significantly lower basal level of glycolysis, glycolytic capacity and glycolytic reserve (FIGS. **21**A-**21**C and FIGS. **28**A-**28**B). However, DPI stimulated similar levels of increase in glycolysis, glycolytic capacity and glucose consumption in a dose-dependent manner in both wild-type and p47phox$^{-/-}$ BMDMs. Similarly, DPI stimulated similar increase in glycolysis in ImKCs when NOX activity was pharmacologically inhibited by apocynin, a NOX specific inhibitor (FIG. **21**B). These data show that DPI-stimulated glycolysis is independent of NOX activity.

[0148] To determine the requirement of GPR3, we knocked down GPR3 by siRNA (siGpr3) in ImKCs. Although GPR3 knockdown was about 70% (FIG. **28**C), the basal level of glycolysis and glycolytic capacity were significantly decreased in siGpr3 ImKCs as compared to ImKCs transfected with scramble siRNA (FIG. **21**D). Importantly, at 50 nM, DPI did not stimulate any increase in glycolysis, glycolytic capacity and glucose consumption in siGpr3 ImKCs as compared to controls (FIGS. **21**D-**21**E and FIGS. **28**D-**28**E). However, at 500 nM, DPI stimulated a significant increase in glycolysis and glycolytic capacity in siGpr3 ImKCs, but the magnitude of increase was significantly lower than that in scramble siRNA transfected ImKCs, probably due to the partial knockout of GPR3 by siRNA or stimulation of other proteins by DPI. Moreover, sphingosine-1-phosphate (S1P), a reported endogenous ligand of GPR3, also stimulated a significant increase in glycolysis in ImKCs, although the magnitude of increase was much lower than that stimulated by 50 nM DPI (FIG. **21**F), showing that activation of GPR3 by an endogenous ligand also stimulates glycolysis in macrophages.

[0149] β-arrestin2, encoded by Arrb2, has been reported to bind to GPR3 and is required for GPR3 signaling. To investigate the requirement of 0-arrestin2 in DPI-stimulated glycolysis, we constructed Arrb2$^{-/-}$ ImKCs using CRISPR-Cas9 mediated gene editing (FIG. **28**F). The same as siGpr3 ImKCs, the basal level of glycolysis and glycolytic capacity were significantly decreased in Arrb2$^{-/-}$ ImKCs as compared to parental ImKCs (FIGS. **21**G-**21**H and FIGS. **28**G-**28**H), and at 50 nM, DPI did not stimulate any increase in glycolysis and glycolytic capacity in Abbr2$^{-/-}$ ImKCs. Moreover, DPI, but not S1P, stimulated translocation of β-arrestin2 from cytosol to the plasma membrane in 10 min in both ImKCs and BMDMs (FIG. **21**I and FIG. **28**I).

[0150] Together, these results show that DPI-stimulated glycolysis is dependent on GPR3 and β-arrestin2 and that activation of GPR3 by DPI leads to rapid trafficking of 0-arrestin2 to the plasma membrane.

Example 11: DPI Stimulates Rapid Increase in Glycolytic Activity Through the Formation of GPR3-β-Arrestin2-GAPDH-PKM2 Super Enzymatic Complex

[0151] How does DPI stimulate a rapid increase in glycolytic activity? We investigated the interaction between β-arrestin2 and metabolic enzymes, including PKM2 and GAPDH. To investigate this mechanism, we treated ImKCs with or without DPI for 6 hours and immunoprecipitated β-arrestin2 followed by Western blotting analysis. ERK1/2, enolase, GAPDH and PKM2 co-precipitated with β-arrestin2 (FIG. **22**A). Notably, significantly higher levels of GAPDH and PKM2 co-precipitated with β-arrestin2 following DPI treatment, suggesting that DPI promotes interactions between β-arrestin2 and GAPDH and PKM2. To determine the requirement of PKM2 in DPI-induced glycolysis, we treated BMDMs from wild-type and Pkm$^{-/-}$ mice with DPI and measured glycolytic activity. The same as siGpr3 ImKCs and Arrb2$^{-/-}$ ImKCs, 50 nM DPI did not stimulate any increase in glycolysis, glycolytic capacity and glucose consumption of Pkm$^{-/-}$ BMDMs (FIGS. **22**B-**22**C and FIGS. **29**A-**29**B). We also measured the enzymatic activity of PKM2 and GAPDH in parental and Arrb2$^{-/-}$ ImKCs in the absence or the presence of 50 nM DPI. As shown in FIGS. **22**D-**22**E, DPI stimulated an immediate increase in PKM2 and GAPDH enzymatic activities in an β-arrestin2-dependent manner. Moreover, DPI's effect on PKM2 and GAPDH enzymatic activities were abolished when phosphorylation of ERK1/2 was inhibited by aapocynin (FIG. **29**C). Thus, DPI stimulates the formation of GPR3-β-arrestin2-GAPDH-PKM2 complex, leading to enhanced enzymatic activities of PKM2 and GAPDH, and providing a mechanistic explanation for the observed rapid increase in glycolytic activity following DPI treatment.

Example 12: DPI Stimulates Sustained Increase in Glycolytic Activity Through Nuclear Translocation of PKM2 and Transcriptional Activation

[0152] How does DPI stimulate transcription of genes in the glycolysis pathway? PKM2 is known to be present in monomeric, dimeric and tetrameric forms. While the tetrameric form exhibits glycolytic enzymatic activity, the dimeric form can translocate into the nucleus and function as a transcriptional cofactor to activate expression of c-Myc, which, in turn, can directly activate the transcription of almost all glycolytic genes through binding the classical E-box sequence. To test this mechanism, we first determined if PKM2 is required for DPI-induced transcription of glycolytic genes. BMDMs were prepared from wild-type and Pkm$^{-/-}$ mice, incubated with or without 50 and 500 nM DPI for 24 hours, and the transcript levels of key glycolytic genes were quantified by RT-PCR. In a dose-dependent manner, DPI stimulated the transcription of Pkm, Ldha and Hk2 in the wild-type but not in Pkm$^{-/-}$ BMDMs (FIG. **23**A), suggesting PKM2 is required for mediating DPI-stimulated transcription of glycolytic genes.

[0153] Next, we determined if DPI induces formation of dimeric PKM2 and nuclear translocation. ImKCs were treated with 50 or 500 nM DPI for 6 or 12 hours, lysed and analyzed directly by Native PAGE gel, followed by anti-PKM2 Western blotting. While PKM2 was found in monomeric and tetrameric forms without DPI treatment, dimeric form was induced following DPI treatment in a dose-dependent manner (FIG. **23**B). Induction of dimeric PKM2 by DPI was further confirmed by DSS crosslinking followed by Western blotting and abolished by inhibition of ERK1/2 with SCH772984 (FIGS. **30**A-**30**B), consistent with the previous reports. To further determine PKM2 nuclear translocation following DPI treatment, both ImKCs and human primary KCs were not treated or treated with DPI for 24 hours and then stained with anti-PKM2. Without DPI treatment, anti-PKM2 fluorescent signals were localized in the cytosol, whereas with DPI treatment, significant amount of anti-PKM2 fluorescent signals was detected in the nucleus (FIG. **23**C), suggesting translocation of PKM2 from cytosol into the nucleus following DPI treatment.

[0154] We also determined if c-Myc is induced by DPI in a PKM2-dependent manner. As shown in FIG. **23**A, in a dose-dependent manner, DPI stimulated the transcription of c-Myc in wild-type but not Pkm$^{-/-}$ BMDMs. To determine whether DPI activates c-Myc transcriptional activity, we performed c-Myc luciferase reporter assays in the parental ImKCs and Pkm$^{-/-}$ ImKCs. Luciferase activity was induced by DPI only in parental ImKCs not in Pkm$^{-/-}$ ImKCs (FIG. **23**D), showing that DPI activates c-Myc transcriptional activity in PKM2-dependent manner.

[0155] Taken together, these results show that DPI stimulates sustained increase in glycolytic activity through nuclear translocation of PKM2, transcriptional activation of c-Myc, and transcription of glycolytic genes.

Example 13: DPI Inhibits HFD-Induced Obesity and Liver Pathogenesis Through PKM2 Expression in Kupffer Cells

[0156] To explore the in vivo consequence of DPI on glycolysis, we examined fast glucose response in DPI pretreated mice. C57BL/6 (B6) mice were injected intraperitoneally (i.p.) with 2 mg/kg DPI and 6 hours later mice were injected i.p. with 1.5 mg/kg glucose. Blood glucose levels were measured before DPI injection, 6 hours after DPI injection and at different time points after glucose injection. As shown in FIG. **31**, mice had the same levels of blood glucose before DPI injection. 6 hours after DPI injection, DPI treated mice had a significantly lower level of blood glucose and maintained significantly lower levels of glucose 15 and 30 min after glucose injection, suggesting DPI stimulates an increased metabolic rate of blood glucose. We further examined whether DPI inhibits high fat diet (HFD) induced obesity and liver pathogenesis. B6 mice at 5 weeks

of age were fed with HFD for a total of 8 weeks. Three weeks after the start on HFD when mice had exhibited significant weight gain, a portion of the mice were given vehicle (PEG3000) and the rest of the mice were given DPI (2 mg/kg) in vehicle i.p. every five days. Among the HFD-fed mice, DPI treatment immediately and significantly reduced the weight gain as compared to vehicle treated group (FIG. **24**A) without affecting the weekly food intake (FIG. **24**B). Consistently, DPI-treated mice had significantly lower levels of iWAT after 8 weeks on HFD (FIG. **24**C). Notably, DPI-treated HFD mice gained weight at similar rate as mice fed with normal diet (ND) (FIG. **24**A), suggesting that DPI inhibits weight gain due to extra fat uptake but not the normal growth. Glucose tolerance test showed that the DPI-treated HFD mice displayed a significant increase in glucose tolerance compared to the vehicle-treated HFD mice (FIG. **24**D). DPI treatment also significantly reduced the lipid deposition in the liver as compared to vehicle-treated HFD mice (FIG. **23**E). Consistently, the concentrations of serum ALT and AST in HFD-fed mice were significantly higher than in normal diet-fed mice (FIG. **23**F). DPI administration significantly reduced the HFD-induced elevation of serum AST and ALT.

[0157] We also examined the effect of DPI on hepatic steatosis. B6 mice were fed with HFD for 16 weeks. Nine weeks after HFD when mice became obese, DPI (2 mg/kg) was given once every 5 days for a total of 10 doses. DPI also significantly reduced the weight gain without affecting the weekly food intake (FIGS. **24**A-**24**B). The weight of iWAT was significantly lower in DPI-treated group than in vehicle-treated group (FIG. **31**C). Similarly, the DPI-treated HFD mice displayed an increased glucose tolerance and had reduced lipid droplet, steatosis and collagen deposition in the liver (FIGS. **31**D-**31**E). Together, these results show that DPI inhibits HFD-induced obesity, lipid deposition and hepatic steatosis in mice.

[0158] To investigate the cell types in the liver that mediate DPI's effect, we analyzed the expression of PKM2 in different cell types in the livers using known single cell RNAseq data. In both human and mice, PKM2 was highly expressed in Kupffer cells and intermediately expressed in other immune cells, while PKM1 (PKLR) was exclusively expressed in APOC3' hepatocytes (FIG. **25**). To directly test whether PKM2 expression in Kupffer cells mediate the effect of DPI, we constructed KC-specific PKM2 knockout ($Pkm^{-/-}$) mice by crossing Clec4f-Cre mice with PKM2 floxed ($Pkm^{f/f}$) mice. KC-specific $Pkm^{-/-}$ mice were fed with HFD for 8 weeks starting at 5 weeks of age. Three weeks after HFD, half of the mice were given vehicle and the other half was given DPI (2 mg/kg) i.p. every 5 days. As shown in FIGS. **24**I-**24**J, DPI did not reduce the HFD-induced body-weight gain and lipid droplet deposition in the livers of KC-specific $Pkm^{-/-}$ mice. Similarly, KC-specific $Pkm^{-/-}$ mice with or without DPI treatment had similar glucose tolerance, serum AST and ALT levels, except that DPI treated mice has a significantly lower level of iWAT (FIG. **33**). These results show that DPI inhibits HFD-induced obesity and liver pathogenesis is dependent on PKM2 expression in Kupffer cells.

Example 14: DPI Upregulates Glycolysis and Suppresses Inflammatory Responses of Kupffer Cells in HFD-Fed Mice

[0159] To further investigate the effects of DPI on Kupffer cells in vivo, we purified KCs from vehicle- or DPI-treated HFD-fed mice and age-matched mice on the normal diet, and performed RNA-seq. GSEA and functional enrichment analysis showed that upregulation of genes associated with immune and inflammatory responses in KCs from mice fed with HFD or ND (FIGS. **25**A-**25**C). Expression of genes involved in inflammation were significantly suppressed in KCs from HFD mice following DPI treatment. In contrast, expression of many other genes that was down-regulated in KCs from HFD mice were significantly upregulated after DPI treatment (FIG. **25**A). Interestingly, expression of genes involved in glycolysis, oxidative phosphorylation and fatty acid metabolism was downregulated in KCs of HFD mice, whereas expression of these genes was upregulated in KCs from HFD mice after DPI treatment (FIGS. **25**A-**25**C). Macrophage polarization index (MPI) analysis showed that KCs were polarized to M1 in HFD-fed mice but to M2 in mice on normal diet, while KCs were reprogrammed to an intermediated phenotype in DPI-treated HFD mice (FIG. **25**D). These results suggest that DPI upregulates glycolysis and suppresses inflammatory responses of KCs in HFD-fed mice.

Example 15: DPI Upregulates Glycolysis and Suppresses Inflammatory Responses of Kupffer Cells from Patients with NAFLD

[0160] Single cell RNAseq analysis of liver cells from NASH and cirrhosis patients has identified $TREM2^{+}$ disease-associated macrophages (DAMs) in the liver that have lower expression of metabolic genes. To determine whether the DAMs are also present in patients with NFALD, we performed scRNAseq of immune cells from liver biopsies of 3 healthy donors and 3 NFALD patients. Fourteen cell clusters were identified, including naïve $CD8^{+}$ T cells, resident memory $CD8^{+}$ (T_{RM}) cells, $CD4^{+}$ T cells, B and plasma cells, $CD56^{low}$ and $CD56^{hi}$ NK cells, macrophages or KCs, neutrophils and proliferating cells (FIG. **35**). Three liver macrophage populations (LM1, LM2, LM3) were identified and further analyzed. As shown in FIGS. **26**A-**26**E, LMs were reclassified into 7 clusters, which could be annotated. Cluster 1 (C1) and C2 were resident KCs as they expressed MNDA and FCN1. C1 differed from C2 by expressing higher levels of inflammatory genes (FIG. **36**) whereas C2 expressed higher levels of glycolytic genes, including PGAM1, PKM, GAPDH and ENO1 (FIG. **26**C). C0, C3 and C4 all expressed MHC-II (HLA-DRB1, etc.). C4 was like dendritic cells as some cells expressed CD1C. C3 resembled to DAMs by expressing C1QA, APOE, TREM2, CD9, GPNMB and CLEC10A, as well as complement genes (C1QA, etc.). C3 was the only elevated LM population in NFALD, with upregulated pathways of antigen processing and presentation, monocyte chemotaxis, response to wounding and down-regulated pathways of immune response, glycolysis, phagocytosis (FIG. **26**F), as observed in advanced NASH and cirrhosis. Based on the trajectory inference (FIG. **26**E) and enriched GO ontology pathways (FIG. **26**F and FIG. **36**), C0 was likely the intermediate or differentiating LM or KCs between resident KCs (C1 and C2) and DAMs (C3) by co-expressing multiple genes, including CD163, LIPA, CCL3, CCL4 and CXCL3 (FIG. **26**C). C5 expressed high levels of myeloid checkpoint receptors LIRB1 and LIRB2. C6 was likely the KCs phagocytosing red blood cells by co-expressing hemoglobin mRNAs (HBD and HBA2) (FIG. **26**C and FIG. **36**).

[0161] To directly examine the effect of DPI on human Kupffer cells from NFALD patients, we purified KCs from two NFALD patients and performed the transcriptional analysis by RNA-seq following DPI treatment ex vivo for 24 hours. The same as human MDMs and mouse ImKCs, the expression of glycolytic genes was upregulated by DPI whereas the expression of DAM markers, including APOE, CLEC10A, TREM2 and C1QA, was downregulated (FIG. **26**G). Functional enrichment analysis showed that DPI-treated KCs not only upregulated the expression of glycolytic genes but also suppressed the expression of genes associated with chemokine-mediated signaling, chemotaxis and inflammatory response (FIG. **26**H). These results show that DPI also upregulates glycolysis and suppresses inflammatory responses of Kupffer cells from patients with NAFLD.

INCORPORATION BY REFERENCE

[0162] All publications and patents mentioned herein are hereby incorporated by reference in their entirety as if each individual publication or patent was specifically and individually indicated to be incorporated by reference. In case of conflict, the present application, including any definitions herein, will control.

EQUIVALENTS

[0163] While specific embodiments of the subject invention have been discussed, the above specification is illustrative and not restrictive. Many variations of the invention will become apparent to those skilled in the art upon review of this specification and the claims below. The full scope of the invention should be determined by reference to the claims, along with their full scope of equivalents, and the specification, along with such variations.

SEQUENCE LISTING

```
Sequence total quantity: 40
SEQ ID NO: 1            moltype = DNA  length = 22
FEATURE                 Location/Qualifiers
source                  1..22
                        mol_type = other DNA
                        organism = synthetic construct
SEQUENCE: 1
cattggcttg cgagacgtag ac                                            22

SEQ ID NO: 2            moltype = DNA  length = 22
FEATURE                 Location/Qualifiers
source                  1..22
                        mol_type = other DNA
                        organism = synthetic construct
SEQUENCE: 2
gctgaaggtc tcttccatca cc                                            22

SEQ ID NO: 3            moltype = DNA  length = 23
FEATURE                 Location/Qualifiers
source                  1..23
                        mol_type = other DNA
                        organism = synthetic construct
SEQUENCE: 3
caaggaactt cttgccaatc cag                                           23

SEQ ID NO: 4            moltype = DNA  length = 22
FEATURE                 Location/Qualifiers
source                  1..22
                        mol_type = other DNA
                        organism = synthetic construct
SEQUENCE: 4
ccaagatcca caggcaaagc ca                                            22

SEQ ID NO: 5            moltype = DNA  length = 22
FEATURE                 Location/Qualifiers
source                  1..22
                        mol_type = other DNA
                        organism = synthetic construct
SEQUENCE: 5
ctgctgtaac gatgaagccc tg                                            22

SEQ ID NO: 6            moltype = DNA  length = 22
FEATURE                 Location/Qualifiers
source                  1..22
                        mol_type = other DNA
                        organism = synthetic construct
SEQUENCE: 6
gctgtaggaa gctcatctct cc                                            22

SEQ ID NO: 7            moltype = DNA  length = 22
```

-continued

```
FEATURE                 Location/Qualifiers
source                  1..22
                        mol_type = other DNA
                        organism = synthetic construct
SEQUENCE: 7
tactcacttc cacaggagca gg                                            22

SEQ ID NO: 8            moltype = DNA  length = 22
FEATURE                 Location/Qualifiers
source                  1..22
                        mol_type = other DNA
                        organism = synthetic construct
SEQUENCE: 8
ctccagtgta gccatcctta gg                                            22

SEQ ID NO: 9            moltype = DNA  length = 22
FEATURE                 Location/Qualifiers
source                  1..22
                        mol_type = other DNA
                        organism = synthetic construct
SEQUENCE: 9
tgatacgcct gagtggctgt ct                                            22

SEQ ID NO: 10           moltype = DNA  length = 22
FEATURE                 Location/Qualifiers
source                  1..22
                        mol_type = other DNA
                        organism = synthetic construct
SEQUENCE: 10
cacaagagca gtgagcgctg aa                                            22

SEQ ID NO: 11           moltype = DNA  length = 22
FEATURE                 Location/Qualifiers
source                  1..22
                        mol_type = other DNA
                        organism = synthetic construct
SEQUENCE: 11
ggtgcctatg tctcagcctc tt                                            22

SEQ ID NO: 12           moltype = DNA  length = 23
FEATURE                 Location/Qualifiers
source                  1..23
                        mol_type = other DNA
                        organism = synthetic construct
SEQUENCE: 12
gccatagaac tgatgagagg gag                                           23

SEQ ID NO: 13           moltype = DNA  length = 22
FEATURE                 Location/Qualifiers
source                  1..22
                        mol_type = other DNA
                        organism = synthetic construct
SEQUENCE: 13
acggctgagt ttcagtgaga cc                                            22

SEQ ID NO: 14           moltype = DNA  length = 22
FEATURE                 Location/Qualifiers
source                  1..22
                        mol_type = other DNA
                        organism = synthetic construct
SEQUENCE: 14
cactctggta ggtgtaaggt gc                                            22

SEQ ID NO: 15           moltype = DNA  length = 22
FEATURE                 Location/Qualifiers
source                  1..22
                        mol_type = other DNA
                        organism = synthetic construct
SEQUENCE: 15
gctacaagag gatcaccagc ag                                            22

SEQ ID NO: 16           moltype = DNA  length = 22
FEATURE                 Location/Qualifiers
source                  1..22
                        mol_type = other DNA
                        organism = synthetic construct
```

-continued

```
SEQUENCE: 16
gtctggaccc attccttctt gg                                          22

SEQ ID NO: 17          moltype = DNA  length = 22
FEATURE                Location/Qualifiers
source                 1..22
                       mol_type = other DNA
                       organism = synthetic construct
SEQUENCE: 17
cctgctgctt tgcctacctc tc                                          22

SEQ ID NO: 18          moltype = DNA  length = 22
FEATURE                Location/Qualifiers
source                 1..22
                       mol_type = other DNA
                       organism = synthetic construct
SEQUENCE: 18
acacacttgg cggttccttc ga                                          22

SEQ ID NO: 19          moltype = DNA  length = 22
FEATURE                Location/Qualifiers
source                 1..22
                       mol_type = other DNA
                       organism = synthetic construct
SEQUENCE: 19
catccagagc ttgagtgtga cg                                          22

SEQ ID NO: 20          moltype = DNA  length = 22
FEATURE                Location/Qualifiers
source                 1..22
                       mol_type = other DNA
                       organism = synthetic construct
SEQUENCE: 20
ggcttcaggg tcaaggcaaa ct                                          22

SEQ ID NO: 21          moltype = DNA  length = 20
FEATURE                Location/Qualifiers
source                 1..20
                       mol_type = other DNA
                       organism = synthetic construct
SEQUENCE: 21
agtatgactc cactcacggc                                             20

SEQ ID NO: 22          moltype = DNA  length = 20
FEATURE                Location/Qualifiers
source                 1..20
                       mol_type = other DNA
                       organism = synthetic construct
SEQUENCE: 22
gttcacaccc atcacaaaca                                             20

SEQ ID NO: 23          moltype = DNA  length = 22
FEATURE                Location/Qualifiers
source                 1..22
                       mol_type = other DNA
                       organism = synthetic construct
SEQUENCE: 23
gagacaggga agtctgaagc ac                                          22

SEQ ID NO: 24          moltype = DNA  length = 22
FEATURE                Location/Qualifiers
source                 1..22
                       mol_type = other DNA
                       organism = synthetic construct
SEQUENCE: 24
ccagcagtag ttgctcctct tc                                          22

SEQ ID NO: 25          moltype = DNA  length = 22
FEATURE                Location/Qualifiers
source                 1..22
                       mol_type = other DNA
                       organism = synthetic construct
SEQUENCE: 25
gtctcctctg acttcaacag cg                                          22

SEQ ID NO: 26          moltype = DNA  length = 22
```

-continued

```
FEATURE                 Location/Qualifiers
source                  1..22
                        mol_type = other DNA
                        organism = synthetic construct
SEQUENCE: 26
accaccctgt tgctgtagcc aa                                            22

SEQ ID NO: 27           moltype = DNA  length = 22
FEATURE                 Location/Qualifiers
source                  1..22
                        mol_type = other DNA
                        organism = synthetic construct
SEQUENCE: 27
ctcttctgcc tgctgcactt tg                                            22

SEQ ID NO: 28           moltype = DNA  length = 22
FEATURE                 Location/Qualifiers
source                  1..22
                        mol_type = other DNA
                        organism = synthetic construct
SEQUENCE: 28
atgggctaca ggcttgtcac tc                                            22

SEQ ID NO: 29           moltype = DNA  length = 22
FEATURE                 Location/Qualifiers
source                  1..22
                        mol_type = other DNA
                        organism = synthetic construct
SEQUENCE: 29
ccacagacct tccaggagaa tg                                            22

SEQ ID NO: 30           moltype = DNA  length = 23
FEATURE                 Location/Qualifiers
source                  1..23
                        mol_type = other DNA
                        organism = synthetic construct
SEQUENCE: 30
gtgcagttca gtgatcgtac agg                                           23

SEQ ID NO: 31           moltype = DNA  length = 22
FEATURE                 Location/Qualifiers
source                  1..22
                        mol_type = other DNA
                        organism = synthetic construct
SEQUENCE: 31
ggcagaaagc ttgtctcaac cc                                            22

SEQ ID NO: 32           moltype = DNA  length = 22
FEATURE                 Location/Qualifiers
source                  1..22
                        mol_type = other DNA
                        organism = synthetic construct
SEQUENCE: 32
ctccttcagg aacagccacc aa                                            22

SEQ ID NO: 33           moltype = DNA  length = 22
FEATURE                 Location/Qualifiers
source                  1..22
                        mol_type = other DNA
                        organism = synthetic construct
SEQUENCE: 33
tctccgagat gccttcagca ga                                            22

SEQ ID NO: 34           moltype = DNA  length = 22
FEATURE                 Location/Qualifiers
source                  1..22
                        mol_type = other DNA
                        organism = synthetic construct
SEQUENCE: 34
tcagacaagg cttggcaacc ca                                            22

SEQ ID NO: 35           moltype = DNA  length = 21
FEATURE                 Location/Qualifiers
source                  1..21
                        mol_type = other DNA
                        organism = synthetic construct
```

-continued

```
SEQUENCE: 35
tcattccctg atgttacgag c                                          21

SEQ ID NO: 36          moltype = DNA  length = 21
FEATURE                Location/Qualifiers
source                 1..21
                       mol_type = other DNA
                       organism = synthetic construct
SEQUENCE: 36
tcttccctct ccattgtgtt g                                          21

SEQ ID NO: 37          moltype = DNA  length = 22
FEATURE                Location/Qualifiers
source                 1..22
                       mol_type = other DNA
                       organism = synthetic construct
SEQUENCE: 37
gtgtgatgac tcttgggact tg                                         22

SEQ ID NO: 38          moltype = DNA  length = 20
FEATURE                Location/Qualifiers
source                 1..20
                       mol_type = other DNA
                       organism = synthetic construct
SEQUENCE: 38
aggatgactg acgggatgag                                            20

SEQ ID NO: 39          moltype = DNA  length = 22
FEATURE                Location/Qualifiers
source                 1..22
                       mol_type = other DNA
                       organism = synthetic construct
SEQUENCE: 39
gactgataag tggagggtga gg                                         22

SEQ ID NO: 40          moltype = DNA  length = 19
FEATURE                Location/Qualifiers
source                 1..19
                       mol_type = other DNA
                       organism = synthetic construct
SEQUENCE: 40
ccagagagga acccattcg                                             19
```

1. A method of identifying a modulator of macrophage activation, comprising:

contacting a primary macrophage cell with a candidate agent;

monitoring or photographing the morphology of the cell contacted with the candidate agent; and

optionally comparing the cell's morphology in the presence of the candidate agent with the cell's morphology in the absence of the candidate agent; wherein a change in morphology in the presence of the candidate agent is indicative of modulation of macrophage activation.

2. The method of claim **1**, wherein the primary macrophage cell is a bone marrow-derived macrophage or a monocyte-derived macrophage.

3.-**6**. (canceled)

7. The method of claim **1**, wherein the morphology of the cell is changed from elongated shape to round shape.

8. The method of claim **7**, wherein the modulator activates a M1-like macrophage.

9. The method of claim **7**, wherein the modulator deactivates a M2-like macrophage.

10. The method of claim **7**, wherein the modulator changes a tumor-associated macrophage (TAM) to M1-like macrophage.

11. The method of claim **7**, wherein the modulator changes a M2-like macrophage to a M1-like macrophage.

12. The method of claim **7**, wherein the modulator changes a M-CSF macrophage to a M1-like macrophage.

13. The method of claim **7**, wherein the modulator changes a GM-CSF macrophage to a M1-like macrophage.

14. The method of claim **7**, wherein the modulator changes a primary macrophage to a M1-like macrophage.

15. The method of claim **7**, wherein the modulator induces LPS, IFNγ or TNFα.

16. The method of claim **7**, wherein the modulator activates a serotonin transporter or receptor, a histamine transporter or receptor, a dopamine transporter or receptor, an adrenoceptor, VEGF, EGF and/or leptin.

17. The method of claim **7**, wherein the modulator is a M1-activating compound.

18. The method of claim **7**, wherein the modulator is cytochalasin-B, fenbendazole, parbendazole, methiazole, alprostadil, FTY720, penfluridol, taxol, smer-3, cantharidin, SCH79797, mitoxantrone, niclosamide, MS275, HMN-214, DPI, thiostrepton, evodiamine, cucurbitacin-I, NVP 231, Chlorhexidine, Diphenyleneiodonium, LE135, Fluvoxamine, Mocetinostat, Pimozide, NP-010176, Celastrol, FTY720, WP1130, Prulifloxacin, dihydrocelastryl diacetate, or Quinolinium.

19. The method of claim **8**, wherein the M1-like macrophage mediates a pro-inflammatory response, an anti-microbial response, and/or an anti-tumor response.

20.-**23**. (canceled)

24. The method of claim **1**, wherein the morphology of the cell is changed from round shape to elongated shape.

25. The method of claim **24**, wherein the modulator activates a M2-like macrophage.

26.-**33**. (canceled)

34. The method of claim **24**, wherein the modulator is Bostunib, Su11274, Alsterpaullone, Alrestatin, Bisantrene, triptolide, lovastatin, QS 11, Regorafenib, Sorafenib, MLN2238, GW-843682X, KW 2449, Axitinib, JTE 013, Purmorphamine, Arcyriaflavin A, Dasatinib, NVP-LDE225, 1-Naphthyl PP1, Selamectin, MGCD-265, podofilox, colchicine, or vinblastine sulfate.

35.-**38**. (canceled)

39. A method of treating cancer, fibrosis, or an infectious disease, comprising administering to a subject in need thereof an effective amount of a modulator of macrophage activation; wherein the modulator changes the morphology of a macrophage cell from elongated shape to round shape or the modulator activates a serotonin transporter or receptor, a histamine transporter or receptor, a dopamine transporter or receptor, an adrenoceptor, VEGF, EGF and/or leptin, or the modulator is KW 2449.

40.-**62**. (canceled)

63. A method of treating an inflammatory disease, a metabolic disease, an autoimmune disease, or a neurodegenerative disease, comprising administering to a subject in need thereof an effective amount of a modulator of macrophage activation; wherein the modulator changes the morphology of a macrophage cell from round shape to elongated shape, the modulator inhibits a serotonin transporter or receptor, a histamine transporter or receptor, a dopamine transporter or receptor, an adrenoceptor, VEGF, EGF and/or leptin, or the modulator is KW 2449.

64.-**96**. (canceled)

* * * * *